IN THE UNITED STATES PATENT AND TRADEMARK OFFICE

Applicant	:	Fraser, et al.
App. No	:	10/614,648
Filed	:	July 7, 2003
For	:	SYSTEMS AND METHODS FOR TREATING PATIENTS WITH PROCESSED LIPOASPIRATE CELLS
Examiner	:	Lankford, Leon B.
Art Unit	:	1651
Conf #	:	7640

DECLARATION UNDER 35 U.S.C. 1.131

Mail Stop Amendment
Commissioner for Patents
P.O. Box 1450
Alexandria, VA 22313-1450

Dear Sir:

I, John K Fraser, Ph.D., declare and state as follows:

1. I am one of the named inventors on the above-captioned patent application, and am familiar with its contents. I am currently Principal Scientist at Cytori Therapeutics, Inc., ("Cytori") the assignee of the above-captioned application. Cytori develops adipose derived stem and regenerative cell based therapies. In particular, Cytori is dedicated to providing patients with new options for reconstructive and cosmetic surgery. I have been associated with Cytori since 2001.

2. I received a Ph.D. from the University of Otago, New Zealand in 1988 and have worked in the field of stem cell therapy since then. Through the course of my career, I have published at least 34 articles in peer-reviewed scientific journals. I am also a named inventor on at least 22 U.S. Patents and Patent Applications. A copy of my curriculum vitae is attached hereto as **Exhibit A**.

3. I am familiar with the above-captioned application as well as the Office Action dated October 9, 2007.

4. More than one million women worldwide are diagnosed with breast cancer annually, including more than 370,000 women in Europe and more than 240,000 in the United States. A growing percentage of these women are eligible for partial versus full mastectomies. However, partial mastectomy often results in irregular tissue loss in the breast for which these women have few, if any, reconstructive options. One of Cytori's primary corporate goals is the development of tissue implants that are suitable for reconstructing breast tissue in these patients. In order to be suitable for these patients, however, it is imperative that the tissue implant be retained in the body over time. Ideally, the implant should also have the characteristics of native soft tissue. Furthermore, the implant should be made of a material that is either approved for human use or would pose only minimal regulatory concerns.

5. As of the effective filing date of the instant application, those in the field of cosmetic and reconstructive surgery widely recognized the need for a tissue implant meeting the criteria above that was suitable for patients undergoing partial mastectomy. At the time, however, many in the field acknowledged that existing approaches for tissue implants generally were "unsatisfactory in outcome and presented unsolved problems."[1] For example, although silicone and water-filled breast implants are generally soft and stable in the body (at least in the absence of capsular contraction, leakage, or other complication), they are synthetic and generally preformed and typically do not address the needs of partial mastectomy patients who generally experience irregular tissue loss (making a preformed silicone implant unsuitable). Accordingly, as of the effective filing date of the instant application, a suitable tissue implant for patients with a partial mastectomy, i.e., one that provides the characteristics of native soft tissue, is retained in the body over time and poses only minimal regulatory concerns, remained an unmet need.

6. Another one of Cytori's corporate goals is the development of tissue implants that are suitable for cosmetic applications generally, including breast augmentation and repair of soft tissue defects. As of the effective filing date of the instant application, those in the field of cosmetic surgery for breast augmentation and other soft tissue defects recognized the need for a tissue implant meeting the criteria above, i.e., one that provides the characteristics of native soft tissue, is retained in the body over time and poses only minimal regulatory concerns. Towards that end, investigators in the field have tried various techniques. Some of the techniques even employed adipogenic cells. However, the results were less than favorable. Exemplary studies are described in the journal articles listed in **Table 1**, annexed hereto as **Exhibit B**, wherein a mixture of adipose progenitor cells isolated from intact, non-disaggregated adipose tissue, and an acellular lattice were used. Although the investigators reported that the implantation of adipogenic cells on such a matrix or scaffold lead to the formation of tissue that resembled adipose tissue *in vivo,* the tissue was not stable and the volume of the implant declined rapidly over time. Accordingly, as of the effective filing date of the instant application, a suitable tissue implant for cosmetic and soft tissue repair that provides the characteristics of native soft tissue, is

[1] Masuda,T., Furue,M. & Matsuda,T. Photocured, styrenated gelatin-based microspheres for de novo adipogenesis through corelease of basic fibroblast growth factor, insulin, and insulin-like growth factor I. *Tissue Eng* **10**, 523-535 (2004).

retained in the body over time and poses only minimal regulatory concerns remained an unmet need despite the efforts of these investigators.

7. Other techniques at the time of the effective filing date of the instant application involved seeding cells within Matrigel or on biocompatible lattices such as polymeric materials (e.g., glycolic acid, lactic acid, propyl fumarate, etc.). These approaches have since been shown to be incapable of producing a long-lasting soft tissue filler, as indicated in the references provided in **Table 1**. For example, Patrick et al.[2] used cultured preadipocytes seeded on a polylactide disk and, in what the authors described as a short-term *in vivo* study, demonstrated the presence of adipocytes four weeks following implantation. However, when the same group evaluated long term retention of the tissue[3] they reported that the amount of adipose tissue peaked at two months was substantially reduced (to approximately 40% of peak level) by three months, and was totally absent at all time points between five and twelve months. Thus, while these authors could generate adipose tissue with their implant in the short-term, they were unable to retain this tissue in the long term, i.e., at or beyond five months. This is particularly important because the vast majority of studies evaluating adipose tissue generation and retention generally do not evaluate any time point after two months (*see*, **Table 1**). Those studies that have evaluated longer time points show either loss of the graft,[4] substantial reduction in the volume of the implant [5], or techniques that are not suitable for the clinic[6]. For example, Schoeller et. al.[6] detected adipose tissue-like tissue 12 months after placing a preadipocyte/fibrin glue mixture in a surgically created intramuscular capsule. Specifically, they created a capsule by temporarily implanting a silicone block into the muscle, removing the block and filling the resulting capsule with the mixture. This approach fails in the clinic however because it involves multiple surgical procedures which are clearly not suitable for repair of a soft tissue defect. Torio-Padron et al.[7] have also demonstrated the presence of detectable adipose tissue-like tissue twelve months after subcutaneous implantation of preadipocytes in a fibrin glue. However, the volume of this material was considerably reduced such that at 3-4 weeks after implantation only 50% of the original volume of implanted material was present. This is consistent with the findings of Cho et al.[8] who also used a fibrin glue/preadipocyte mixture and found 10-30% retention of volume at

---

[2] Patrick,C.W., Jr., Chauvin,P.B., Hobley,J. & Reece,G.P. Preadipocyte seeded PLGA scaffolds for adipose tissue engineering. *Tissue Eng* **5**, 139-51 (1999).

[3] Patrick,C.W., Jr., Zheng,B., Johnston,C. & Reece,G.P. Long-term implantation of preadipocyte-seeded PLGA scaffolds. *Tissue Eng* **8**, 283-293 (2002).

[4] *Id.*

[5] Torio-Padron,N., Baerlecken,N., Momeni,A., Stark,G.B. & Borges,J. Engineering of adipose tissue by injection of human preadipocytes in fibrin. *Aesthetic Plast Surg* **31**, 285-293 (2007).

[6] Schoeller,T. *et al.* Histomorphologic and volumetric analysis of implanted autologous preadipocyte cultures suspended in fibrin glue: a potential new source for tissue augmentation. *Aesthetic Plast Surg* **25**, 57-63 (2001).

[7] Torio-Padron, supra.

[8] Cho,S.W. *et al.* Engineering of volume-stable adipose tissues. *Biomaterials* **26**, 3577-3585 (2005).

six weeks. A later study by the same group found that the volume could be retained at six weeks by implanting the fibrin glue/preadipocyte/growth factor combination within a rigid protective structure[9]. However, the authors of this study did not evaluate later time points or the impact of removing the rigid structure once the implant had formed. Furthermore, implantation of a rigid structure is clearly inconsistent with repair of a soft tissue defect.

8. The exception to the trend of reduced volume over time is found in studies by groups that have applied vascular surgical techniques to provide a dedicated blood supply to the developing graft. In these studies Matrigel (an extract derived from the Engelbreth-Holm-Swarm mouse tumor cell line) was supplemented with basic Fibroblast Growth Factor (bFGF) and implanted into a silicone sheath placed around the superficial inferior epigastric vessels (or a tied off femoral vessel)[10, 11] that had been surgically exposed such that they were now feeding the implant. Host-derived cells invade the implant and form adipose tissue that was stable to at least four months[12]. However, this approach has a number of disadvantages compared to the mixtures claimed in the instant application. First, Matrigel is an extract derived from a mouse tumor cell line and is not approved for human use. Supplementation with recombinant bFGF (a necessary part of robust adipose tissue generation in this model) is costly and comes with additional regulatory concerns. Furthermore, while this approach generates a volume-stable implant it also applies a semi-rigid silicone dome that becomes filled with adipose. It is also limited to areas in which an adjacent blood supply can be essentially high-jacked to feed the implant. Therefore, while this approach offers the advantage of retention of adipose tissue, it is largely not applicable in the clinic and fails to provide a flexible alternative to the needs of cosmetic and reconstructive surgery. In particular, this approach requires vascular surgical intervention, which is not an available option in many instances.

9. The Katz reference (U.S. Patent No. 6,777,231) is characteristic of the studies as of the effective filing date of the instant application, such as those listed in **Table 1.** Katz teaches that it is most desirable to completely isolate stem cells from other components present in intact, non-disaggregated, adipose tissue such as adipocytes, red blood cells, stromal cells, etc. as well as extracellular matrix material. Katz describes seeding the isolated cells on an acellular lattice, such as those described in the references in **Table 1**. (*See,* Katz at Col. 10, line 27 - Col. 11, line 36).

---

[9] Cho,S.W. *et al.* Enhancement of adipose tissue formation by implantation of adipogenic-differentiated preadipocytes. *Biochem Biophys Res Commun* **345**, 588-594 (2006).

[10] Cronin,K.J. *et al.* New murine model of spontaneous autologous tissue engineering, combining an arteriovenous pedicle with matrix materials. *Plast Reconstr Surg* **113**, 260-269 (2004).

[11] Walton,R.L., Beahm,E.K. & Wu,L. De novo adipose formation in a vascularized engineered construct. *Microsurgery* **24**, 378-384 (2004).

[12] Walton,R.L., supra.

10. The Peterson reference (U.S. Patent No. 6,200,606) is also characteristic of the state of the art as of the effective filing date of the instant application. Peterson relates to the isolation of stem cells from various sources, including adipose tissue. Peterson emphasizes that in order to isolate stem cells from adipose tissue, the tissue must be processed and completely disaggregated to produce cell suspensions. Peterson also discusses combining isolated stem cells with a biocompatible carrier material or a prosthetic device. (*See,* Peterson at Col. 11, line 29-Col. 12, line 30). The biocompatible carrier material and prosthetic devices enumerated in the Peterson reference are similar to or identical to the carriers described in the references listed in **Table 1**.

11. In short, published studies demonstrate that the neither the compositions alone nor the combination of the compositions and the carriers or support materials described in Katz and Peterson are suitable for use as tissue implants for cosmetic or reconstructive surgery.

12. In contrast to the methods described in Katz, Peterson, and the references set forth in **Table 1**, Cytori has developed a tissue implant that comprises a mixture of a concentrated cell population comprising adipose-derived stem cells and unprocessed adipose tissue that comprises intact, non-disaggregated, tissue fragments. This mixture is the subject of the instant patent application.

13. The mixture provided in the present patent application addresses the unmet need in the field for a suitable tissue implant that provides the characteristics of native soft tissue, is retained in the body over time and poses only minimal regulatory concerns. The mixture in the present patent application also provides an unexpected improvement over the approaches taught by Katz, Peterson and the studies described in the references listed in **Table 1**, which stress the importance of utilizing purified stem cells for seeding onto a support material. For instance, Example 1 of the instant specification demonstrates the unexpected benefits of using mixtures of concentrated adipose-derived stem cells and unprocessed adipose tissue. Specifically, Example 1 describes a set of experiments that led to the surprising discovery that graft weight and vascularity of fat implants can be improved by mixing unprocessed adipose tissue and isolated preparations of adipose-derived cells comprising stem cells and progenitor cells.

14. The results of the studies in Example 1 of the instant specification were confirmed in a human clinical trial. Briefly, twenty-one (21) female patients aged from 29 to 59 (mean 46.9) years underwent 25 stem cell augmented reconstructions at the Department of Breast Surgery, Kyushu Central Hospital, Fukuoka, Japan. All patients previously received breast conservation therapy ("BCT") for breast cancer. Subsequent to the surgical treatment, 19 patients also received radiation therapy in doses ranging between 50 - 60 Gy (mean 53 Gy). All patients were deemed free of any local recurrence or distant metastasis for $\geq$ 13 months following BCT. The volume of autologous adipose derived stem cell-enhanced fat transplant for each patient was determined by clinical evaluation including assessment of the volume defect at the time of screening, the severity of radiation damage present and an assessment of residual scarring and fibrosis in the affected breast.

15. Under general anesthesia, adipose tissue (approximately twice the estimated volume to be used for reconstruction) was harvested by lipoaspiration using standard tumescent technique. Aspirated adipose tissue was divided into two equal portions; one portion, referred to as "Fat A", was reserved for processing in the cell processing system described in the instant patent application to extract, wash and concentrate adipose derived stem cells; the other portion, "Fat B", was used as the primary filler material. Concurrent to the processing of "Fat A", "Fat B" was irrigated to remove any blood, and the remaining adipose tissue, which had been fragmented into numerous 2 - 5 mm fragments by the lipoaspiration procedure, was enriched with concentrated adipose-derived stem cells out of the cell processing device by gentle mixing immediately prior to the autologous transplantation procedure.

16. After local anesthesia around the recipient site on the breast, three 2 mm incisions were made at strategically selected areas, and the autologous adipose derived stem and regenerative cell (ADRC) enhanced fat graft was injected in 0.1 – 0.2 cc aliquots using a 2.5 cc syringe with a 14-gauge needle. Areas of BCT post operative scarring and radiation fibrosis were incised by multiple 14-gauge needle passes. This resulted both in releasing subcutaneous fibrotic areas and in creating physical spaces to receive the autologous ADRC-enhanced fat graft. After the best possible cosmetic result was achieved, each incision was closed with 6-0 nylon suture.

17. Follow-up was performed at one week, 1, 3, and 6 months after treatment. Data collected at each follow-up visit included clinical examination of the transplantation site(s), photography for historical comparison, a patient questionnaire to measure the outcome from the patient's perspective, and an assessment of breast tissue thickness using t-mode ultrasound.

18. The tissue thickness measurement (TTM) was done using the SSA-700A Aplio (Toshiba, Japan) ultrasound machine at 3 and 6 months post-procedure. TTM were taken at the most prominent area of the scar where the autologous ADRC-enhanced fat transplant was performed using 2-D ultrasound. TTM represents the change in tissue thickness between the skin surface and the pectoralis major muscle surface from baseline to follow up. There was a statistically significant improvement in mean TTM at 1 month compared to baseline ($p < 0.05$, t-test). There was no significant loss of benefit from 1 month to final measurement (p = NS), which ranged from two to eighteen months (mean, 11 months). Patient satisfaction measured by self assessment was 79%. The results are presented in graphical form below.

19. In short, the clinical data provide objective evidence that the mixtures claimed in the instant patent application solved the long felt problem of providing a tissue implant that retains its volume and shape over time, while providing the characteristics of soft tissue, that are also acceptable for human use.

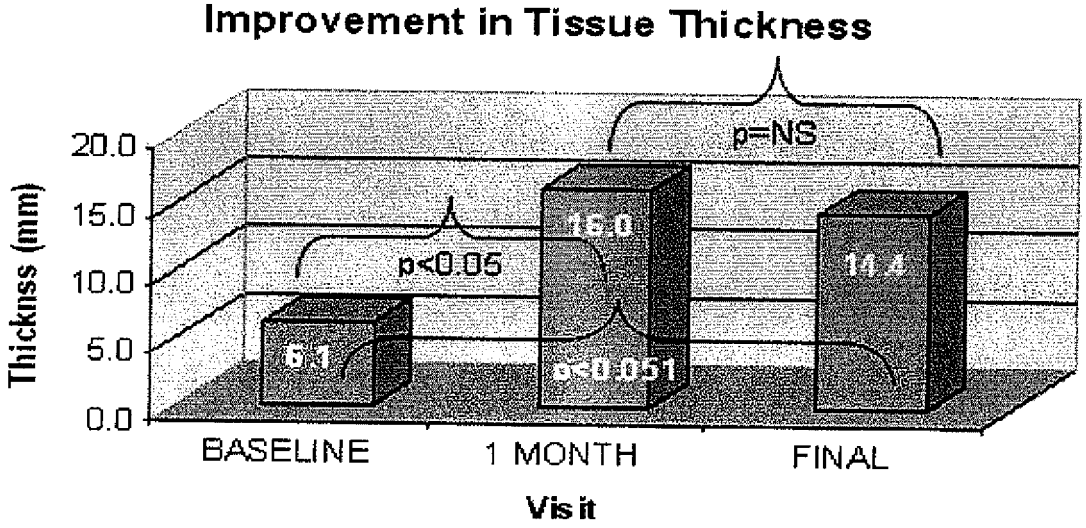

20. A 2004 study by Masuda et al. reports that the addition of isolated, cultured adipogenic cells to fragmented omentum (adipose tissue) resulted in improved graft retention at twelve weeks, when compared to implantations of fragmented omentum tissues alone[13] While the mixtures claimed in the instant application use fresh stem cells, which obviate the need and regulatory concerns regarding cell culture posed by the Masuda composition, this later-published study provides further confirmatory evidence that that addition of a population of cells comprising preadipocytes (*e.g.*, adipose-derived stem cells) to unprocessed omentum (or adipose) tissue, improves graft retention.

21. I hereby declare that all statements made herein of my own knowledge are true and that all statements made on information or belief are believed to be true, and further that these statements were made with the knowledge that willful false statements and the like so made are punishable by fine or imprisonment, or both, under Section 1001 of Title 18 of the United States Code and that such willful statements may jeopardize the validity of the application or any patent issued thereon.

By: _____ Date: 04/04/08
J. Fraser

[13] Masuda,T., Furue,M. & Matsuda,T. Novel strategy for soft tissue augmentation based on transplantation of fragmented omentum and preadipocytes. *Tissue Eng* **10**, 1672-1683 (2004).

EXHIBIT A

CURRICULUM VITAE

John K. Fraser, Ph.D.
E-MAIL: Jfraser@CytoriTx.com
TEL. 858-875-5262

PRESENT POSITION

12/06-Present Principal Scientist: Cytori Therapeutics Inc

PREVIOUS EMPLOYMENT

7/05-12/06	Consultant. John K. Fraser Consulting: Clients include Cytori Therapeutics Inc, NIH, American Institute of Biological Sciences
11/02-7/05	Vice President Research and Technology, Macropore Biosurgery Inc (now Cytori Therapeutics Inc.)
08/01-11/02	Chief Scientific Officer, StemSource Inc (merged with Macropore 11/02)
08/95-07/03	Director, UCLA Umbilical Cord Blood Bank, Division of Hematology-Oncology, Department of Medicine, UCLA School of Medicine, Los Angeles, CA
7/94-7/96	Co-Director, Bone Marrow and Stem Cell Transplant Laboratory, Division of Hematology-Oncology, Department of Medicine, UCLA School of Medicine, Los Angeles, CA.
7/01-07/03	Adjunct Associate Professor, Division of Hematology-Oncology, Department of Medicine, UCLA School of Medicine, Los Angeles, CA.
7/94-7/01	Assistant Professor in Residence, Division of Hematology-Oncology, Department of Medicine, UCLA School of Medicine, Los Angeles, CA.
05/92-07/94	Assistant Research Biologist, Division of Hematology-Oncology, Department of Medicine, UCLA School of Medicine, Los Angeles, CA.

EDUCATION

1988-1992	University of California, Los Angeles **Post-Doctoral Fellowship (Hematology-Oncology)**
1979-1981	Victoria University of Wellington, New Zealand **BSc (Biochemistry and Physiology)**
1982-1988	University of Otago, New Zealand **PhD (Hematology)**

OTHER RELEVANT EXPERIENCE

2/02-07/03	Vice Chair, UCLA Medical Institutional Review Board #1 (M-IRB #1)
07/96-02/02	Member, UCLA Medical Institutional Review Board #1 (M-IRB #1)

NIH Review Committees

5/98, 5/00	Member, NHLBI Special Emphasis Cord Blood Review Panel; "Sibling Donor Cord Blood Banking and Transplantation"
6/01 and 12/05	Member, NCI Site Visit Review Team; "Optimizing Stem Cell Transplant"
3/03	Member NIH-NHLBI Special Emphasis Panel: Stem Cell Biology and Cell-Based Therapies of Heart, Lung, Blood and Sleep Disorders

PEER-REVIEWED PUBLICATIONS

1. Fraser,J.K., Wulur,I., Alfonso,Z., Zhu,M. & Wheeler,E.S. Differences in stem and progenitor cell yield in different subcutaneous adipose tissue depots. *Cytotherapy* **9**, 459-467 (2007).
2. Fraser,J.K., Wulur,I., Alfonso,Z. & Hedrick,M.H. Fat tissue: an underappreciated source of stem cells for biotechnology. *Trends Biotechnol* **24**, 150-154 (2006).
3. Fraser,J.K. *et al.* Plasticity of human adipose stem cells toward endothelial cells and cardiomyocytes. *Nat Clin Pract Cardiovasc Med* **3 Suppl 1**, S33-S37 (2006).
4. Kurtzberg,J. *et al.* Results of the cord blood transplantation (COBLT) study unrelated donor banking program. *Transfusion* **45**, 842-855 (2005).
5. Strem,B.M. *et al.* Expression of cardiomyocytic markers on adipose tissue-derived cells in a murine model of acute myocardial injury. *Cytotherapy* **7** , 282-291 (2005).
6. Strem,B.M. *et al.* Multipotential differentiation of adipose tissue-derived stem cells. *Keio J Med* **54**, 132-141 (2005).
7. Fraser,J.K., Schreiber,R.E., Zuk,P.A. & Hedrick,M.H. Adult stem cell therapy for the heart. *Int J Biochem. Cell Biol* **36**, 658-666 (2004).
8. Lendeckel,S. *et al.* Autologous stem cells (adipose) and fibrin glue used to treat widespread traumatic calvarial defects: case report. *J Craniomaxillofac. Surg* **32**, 370-373 (2004).
9. De Ugarte,D.A. *et al.* Differential expression of stem cell mobilization-associated molecules on multi-lineage cells from adipose tissue and bone marrow. *Immunol. Lett.* **89**, 267-270 (2003).
10. De Ugarte,D.A. *et al.* Comparison of multi-lineage cells from human adipose tissue and bone marrow. *Cells Tissues Organs* **174**, 101-109 (2003).
11. Fraser,J.K. Adipose tissue: challenging the marrow monopoly. *Cytotherapy* **4**, 509-10 (2002).
12. Kim,S.K. *et al.* Ex vivo expansion and clonality of CD34+ selected cells from bone marrow and cord blood in a serum-free media. *Mol Cells* **14**, 367-73 (2002).
13. Zuk,P.A. *et al.* Human adipose tissue is a source of multipotent stem cells. *Mol Biol Cell* **13**, 4279-95 (2002).
14. Ryu,K.H. *et al.* Apoptosis and megakaryocytic differentiation during ex vivo expansion of human cord blood CD34+ cells using thrombopoietin. *Br. J Haematol.* **113**, 470-478 (2001).
15. Ziegner,U.H. *et al.* Unrelated umbilical cord stem cell transplantation for X-linked immunodeficiencies. *J Pediatr.* **138**, 570-573 (2001).
16. Fuller,J.F. *et al.* Characterization of HOX gene expression during myelopoiesis: role of HOX A5 in lineage commitment and maturation. *Blood* **93**, 3391-3400 (1999).
17. Walker,L. *et al.* The Notch/Jagged pathway inhibits proliferation of human hematopoietic progenitors in vitro. *Stem Cells* **17**, 162-171 (1999).
18. Fraser,J.K. *et al.* Cord Blood Transplantation Study (COBLT): cord blood bank standard operating procedures [see comments]. *J Hematother* **7**, 521-61 (1998).
19. Koka,P.S. *et al.* Human immunodeficiency virus inhibits multilineage hematopoiesis in vivo. *J Virol.* **72**, 5121-5127 (1998).
20. Fraser,J.K., Sugarman,J., McCurdy,P.R., Martin,N.L. & Ammann,A.J. Scientific, logistical, and ethical issues related to creation of a stem cell repository for use in experimental trials of gene therapy for AIDS. *Aids Res Hum Retroviruses* **13**, 905-7 (1997).
21. Rettig,M.B. *et al.* Kaposi's sarcoma-associated herpesvirus infection of bone marrow dendritic cells from multiple myeloma patients [see comments]. *Science* **276**, 1851-4 (1997).
22. Feuer,G. *et al.* Human T-cell leukemia virus infection of human hematopoietic progenitor cells: maintenance of virus infection during differentiation in vitro in vivo. *J Virol* **70**, 4038-44 (1996).

23. Fraser,J.K., Lill,M.C. & Figlin,R.A. The biology of the cytokine sequence cascade. *Semin Oncol* 2-8 (1996).
24. Fraser,J.K., Tran,S., Nimer,S.D. & Gasson,J.C. Characterization of nuclear factors that bind to a critical positive regulatory element of the human granulocyte-macrophage colony-stimulating factor promoter. *Blood* **84**, 2523-30 (1994).
25. Fraser,J.K. *et al.* Characterization of a cell-type-restricted negative regulatory activity of the human granulocyte-macrophage colony-stimulating factor gene. *Mol Cell Biol* **14**, 2213-21 (1994).
26. Lill,M. *et al.* Ex vivo production and expansion of functional myeloid cells from CD34 selected hematopoietic progenitor cells. *Stem Cells* **12**, 626-637 (1994).
27. Sakamoto,K.M., Fraser,J.K., Lee,H.J., Lehman,E. & Gasson,J.C. Granulocyte-macrophage colony-stimulating factor and interleukin-3 signaling pathways converge on the CREB-binding site in the human egr-1 promoter. *Mol Cell Biol* **14**, 5975-85 (1994).
28. Gasson,J.C., Fraser,J.K. & Nimer,S.D. Human granulocyte-macrophage colony-stimulating factor (GM-CSF): regulation of expression. *Prog. Clin Biol Res* **338**, 27-41 (1990).
29. Nimer,S., Fraser,J., Richards,J., Lynch,M. & Gasson,J. The repeated sequence CATT(A/T) is required for granulocyte-macrophage colony-stimulating factor promoter activity. *Mol Cell Biol* **10**, 6084-6088 (1990).
30. Fraser,J.K., Tan,A.S., Lin,F.K. & Berridge,M.V. Expression of specific high-affinity binding sites for erythropoietin on rat and mouse megakaryocytes. *Exp Hematol.* **17**, 10-16 (1989).
31. McCaffery,P.J., Fraser,J.K., Lin,F.K. & Berridge,M.V. Subunit structure of the erythropoietin receptor. *J Biol Chem* **264**, 10507-10512 (1989).
32. Fraser,J.K., Nicholls,J., Coffey,C., Lin,F.K. & Berridge,M.V. Down-modulation of high-affinity receptors for erythropoietin on murine erythroblasts by interleukin 3. *Exp Hematol.* **16**, 769-773 (1988).
33. Fraser,J.K., Lin,F.K. & Berridge,M.V. Expression of high affinity receptors for erythropoietin on human bone marrow cells and on the human erythroleukemic cell line, HEL. *Exp Hematol.* **16**, 836-842 (1988).
34. Fraser,J.K. & Berridge,M.V. Induction of B-lymphocyte antigens on the chronic myeloid leukemic cell line K562 using sodium butyrate. *Exp Hematol.* **15**, 406-413 (1987).

EXHIBIT B

Table 1
Summary of Published Studies of Adipose Tissue Implants Using Scaffolds or Collagen

Reference	Model	Longest Time Evaluated
Patrick,C.W., Jr., Zheng,B., Johnston,C. & Reece,G.P. Long-term implantation of preadipocyte-seeded PLGA scaffolds. *Tissue Eng* **8**, 283-293 (2002).	Polylactide scaffold with cultured preradipocytes	12 months
Tabata,Y. *et al.* De novo formation of adipose tissue by controlled release of basic fibroblast growth factor. *Tissue Eng* **6**, 279-289 (2000).	Matrigel and bFGF (no donor cells)	6 weeks
Kimura,Y., Ozeki,M., Inamoto,T. & Tabata,Y. Adipose tissue engineering based on human preadipocytes combined with gelatin microspheres containing basic fibroblast growth factor. *Biomaterials* **24**, 2513-2521 (2003).	bFGF collagen sponge plus preadipocytes	6 weeks
Hemmrich,K. *et al.* Implantation of preadipocyte-loaded hyaluronic acid-based scaffolds into nude mice to evaluate potential for soft tissue engineering. *Biomaterials* **26**, 7025-7037 (2005).	Preadipocytes ion hyaluronic scaffolds	12 weeks
von Heimburg, D. *et al.* Human preadipocytes seeded on freeze-dried collagen scaffolds investigated in vitro and in vivo. *Biomaterials* **22**, 429-38 (2001).	Preadipocytes on freeze-dried collagen	8 weeks
Masuda,T., Furue,M. & Matsuda,T. Photocured, styrenated gelatin-based microspheres for de novo adipogenesis through corelease of basic fibroblast growth factor, insulin, and insulin-like growth factor I. *Tissue Eng* **10**, 523-535 (2004)	Multiple growth factors in gelatin beads (no cells)	4 weeks
Walton,R.L., Beahm,E.K. & Wu,L. De novo adipose formation in a vascularized engineered construct. *Microsurgery* **24**, 378-384 (2004).	Matrigel plus bFGF on a vascular pedicle	16 weeks

Reference	Model	Longest Time Evaluated
Cronin,K.J. *et al.* New murine model of spontaneous autologous tissue engineering, combining an arteriovenous pedicle with matrix materials. *Plast Reconstr Surg* **113**, 260-269 (2004).	Scaffold on a vascular pedicle	6 weeks
Cho,S.W. *et al.* Engineering of volume-stable adipose tissues. *Biomaterials* **26**, 3577-3585 (2005).	Preadipocytes in fibrin glue within a polylactide shell	6 weeks
Masuda,T., Furue,M. & Matsuda,T. Novel strategy for soft tissue augmentation based on transplantation of fragmented omentum and preadipocytes. *Tissue Eng* **10**, 1672-1683 (2004).	Fragmented omentum (adipose) with and without preadipocytes	12 weeks
Alhadlaq,A., Tang,M. & Mao,J.J. Engineered adipose tissue from human mesenchymal stem cells maintains predefined shape and dimension: implications in soft tissue augmentation and reconstruction. *Tissue Eng* **11**, 556-566 (2005).	Culture differentiated MSC on a hydrogel	4 weeks
Choi,Y.S., Park,S.N. & Suh,H. Adipose tissue engineering using mesenchymal stem cells attached to injectable PLGA spheres. *Biomaterials* **26**, 5855-5863 (2005).	Cultured MSC on polylactide spheres	2 weeks
Cho,S.W. *et al.* Enhancement of adipose tissue formation by implantation of adipogenic-differentiated preadipocytes. *Biochem Biophys Res Commun* **345**, 588-594 (2006).	Preadipocytes in fibrin glue with or without bFGF	6 weeks
Choi,Y.S. *et al.* Adipogenic differentiation of adipose tissue derived adult stem cells in nude mouse. *Biochem Biophys Res Commun* **345**, 631-637 (2006).	ADSC and PLGA	8 weeks
Clavijo-Alvarez,J.A. *et al.* A novel perfluoroelastomer seeded with adipose-derived stem cells for soft-tissue repair. *Plast Reconstr Surg* **118**, 1132-1142 (2006).	Fluoropolymer with ADSC	30days

Reference	Model	Longest Time Evaluated
Hong,L., Peptan,I.A., Colpan,A. & Daw,J.L. Adipose tissue engineering by human adipose-derived stromal cells. *Cells Tissues Organs* **183**, 133-140 (2006).	Gelatin sponge with ADSC	4 weeks
Wu,X., Black,L., Santacana-Laffitte,G. & Patrick,C.W., Jr. Preparation and assessment of glutaraldehyde-crosslinked collagen-chitosan hydrogels for adipose tissue engineering. *J Biomed Mater Res A* **81**, 59-65 (2007).	glutaraldehyde-crosslinked collagen-chitosan hydrogels and preadipocytes	14 days
Stosich,M.S. & Mao,J.J. Adipose tissue engineering from human adult stem cells: clinical implications in plastic and reconstructive surgery. *Plast Reconstr Surg* **119**, 71-83 (2007).	Hydrogel or collagen with MSC	4 weeks
Torio-Padron,N., Baerlecken,N., Momeni,A., Stark,G.B. & Borges,J. Engineering of adipose tissue by injection of human preadipocytes in fibrin. *Aesthetic Plast Surg* **31**, 285-293 (2007).	Fibrin glue with cultured preadipocytes	12 months
Schoeller,T. *et al.* Histomorphologic and volumetric analysis of implanted autologous preadipocyte cultures suspended in fibrin glue: a potential new source for tissue augmentation. *Aesthetic Plast Surg* **25**, 57-63 (2001).	Fibrin glue with cultured preadipocytes in a surgically-created intramuscular pouch	12 months

TISSUE ENGINEERING
Volume 8, Number 2, 2002
© Mary Ann Liebert, Inc.

Long-Term Implantation of Preadipocyte-Seeded PLGA Scaffolds

C.W. PATRICK, Jr., Ph.D., B. ZHENG, M.D., C. JOHNSTON, H.T. (ASCP), and G.P. REECE, M.D.

ABSTRACT

Studies were performed in a long-term effort to develop clinically translatable, tissue engineered adipose constructs for reconstructive, correctional, and cosmetic indications. Rat preadipocytes were harvested, isolated, expanded *ex vivo*, and seeded within PLGA scaffolds. Preadipocyte-seeded and acellular (control) scaffolds were implanted for 1–12 months. Explanted scaffolds were stained with osmium tetroxide, processed, and counterstained using H&E. Quantitative histomorphometric analysis was performed on all tissue sections to determine the amount of adipose tissue formed. Analyses revealed maximum adipose formation at 2 months, followed by a decrease at 3 months, and complete absence of adipose and PLGA at 5–12 months. These results extend a previous short-term study (*Tissue Engineering* 1999;5:134) and demonstrate that adipose tissue can be formed *in vivo* using tissue engineering strategies. However, the long-term maintenance of adipose tissue remains elusive.

INTRODUCTION

THE APPLICATION OF TISSUE ENGINEERING to the development of adipose tissue constructs has captured the interests of numerous investigators over the past two years.[1–8] This is due in part to the realization that there are many reconstructive, correctional, and cosmetic indications for patient-specific adipose constructs.[4] In a previous qualitative study, we demonstrated adipose tissue formation within preadipocyte (PA)–seeded PLGA scaffolds implanted for 2 and 5 weeks.[3] Many questions were raised at the conclusion of this initial study. One such question is whether adipose tissue that forms within PLGA scaffolds remains over long periods of time and whether it remains after its supporting polymer scaffold entirely degrades. This question merits consideration based on the longstanding observation that transplanted mature fat resorbs over time. This present study is a continuation and elaboration of the former. Specifically, PAs are seeded within PLGA scaffolds and implanted for 1–12 months. Adipose formation is quantitatively assessed by coupling histology with microscopy and image analysis.

University of Texas Center for Biomedical Engineering and Laboratory of Reparative Biology and Bioengineering, Department of Plastic Surgery, University of Texas M. D. Anderson Cancer Center, Houston, Texas.

MATERIALS AND METHODS

Adipose harvest and in vivo culture

The methods for harvesting and culturing the PAs were previously described.[3,9] Briefly, PAs were isolated from epididymal fat pads of male, 250 g, 70–80-day-old Lewis rats (Harlan) via enzymatic digestion. Rats were euthanized with CO_2 asphyxiation and the shaved harvest site was scrubbed with Betadyne followed by alcohol wash. Within 5 min of death, epididymal adipose tissue was aseptically harvested and placed in 4°C saline solution supplemented with 500 U/mL penicillin and 500 μg/mL streptomycin (Gibco). Using a dissecting microscope, connective tissues and tissue containing blood vessels were resected from the fat. This minimizes fibroblast contamination of *ex vivo* cultures. Harvested tissue was finely minced with a scalpel and enzymatically digested in Ca^{+2}/Mg^{+2}-free saline supplemented with 2% (w/v) type I collagenase (Sigma Chemical Co.) and 5% (w/v) bovine serum albumin (BSA) for 20 min at 37°C on a shaker. For four fat pads, 5 mL of dissociation medium is required. The digested tissue was filtered through a 250-μm mesh followed by a 90-μm nylon mesh to separate undigested debris and capillary fragments from PAs. The filtered cell suspension was centrifuged, and the resulting pellet of PAs was then plated at 10^4 cells/cm^2 onto plastic culture flasks. PAs were cultured in Dulbecco's Modified Eagle's Medium (DMEM) supplemented with 10% fetal bovine serum (FBS), 100 U/mL penicillin, and 100 μg/mL streptomycin. During cell expansion, the PAs were passed prior to confluency since contact inhibition initiates adipocyte differentiation and ceases PA proliferation.[10–15] The 1° passage yields approximately 1.5×10^6 PAs/fat pad.

Polymer fabrication and seeding

PLGA is employed as a model polymer. PLGA foam fabrication and seeding were conducted as previously described.[3] Fabrication of 2.5-mm-thick, 12-mm-diameter, and 90% porosity polymer disks were prepared by a particulate-leaching technique. Briefly, 5 g of solid 75:25 PLGA (Birmingham Polymers Inc.) polymer were dissolved in 80 mL of dichloromethane (Fisher Scientific) to form a solution. Sieved NaCl crystals (Fisher) at a NaCl:PLGA weight fraction of 1:9 were evenly dispersed over a 150-mm Pyrex petri dish (Fisher) with a Teflon lining (Cole-Parmer Instrument Co.). The PLGA/dichloromethane solution was then gently poured over the NaCl crystals. Sieved NaCl crystal size distribution was measured with quantitative microscopy and found to be 135–633 μm. Dichloromethane was evaporated under vacuum, leaving a polymer/NaCl composite 2.5-mm thick. The composite was removed from the Teflon-lined petri dish, and 12-mm-diameter disks were cut using a plug cutter and drill press. The NaCl crystals were then leached from the composite disks by immersion in 800 mL of DI water for 48 h (water changed every 8 h) to yield porous disks. Disks were lyophilized and stored in a vacuum dessicator until use.

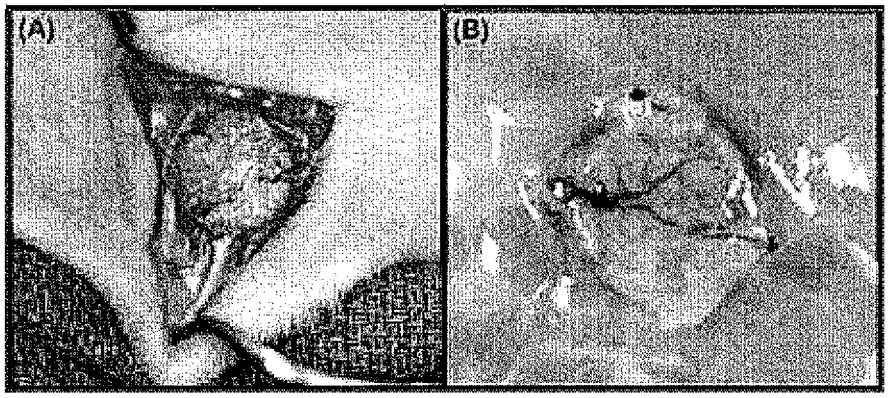

FIG. 1. (A) Example of preadipocyte-seeded disk transplantation. (B) Example of disk harvest (1 month).

Prior to seeding, the test materials were prewetted and sterilized with absolute ethanol for 30 min followed by two sterile saline washes at 20 min/wash and a DMEM wash for 20 min. A 20-μL suspension of PAs (10^5 cells/mL) was injected onto each disk under sterile conditions. Prewetting permits the cell suspension to readily flow throughout the materials. Following 3 h for cell attachment, 24-well culture plates containing one disk/well were filled with 1.5 mL of medium/well. Before transporting the cell-seeded constructs to the operating room, DMEM media was removed and replaced with complete L-15 media, and the constructs were placed in a mobile 37°C warmer. The use of L-15 precludes the need for 5% CO_2 for pH control.

In vivo implantation

Seeded disks were implanted on the back musculature of Lewis rats under anesthesia (0.2 mL/100 gbw intramuscular injection of premixed solution composed of 64 mg/mL ketamine HCl, 3.6 mg/mL xylazine, and 0.07 mg/mL atropine sulfate).[3,9] An isogenic strain is required to avoid an immune response to seeded PAs. The University of Texas M.D. Anderson Cancer Center Animal Care and Use Committee has approved the implantation of PA seeded disks. After shaving the back, two longitudinal incisions (~2 cm each) were made through the skin of the dorsal midline. Individual "pockets" for each disk were prepared between the cutaneous trunci and back muscles of both flanks by careful dissection. Disks were inserted

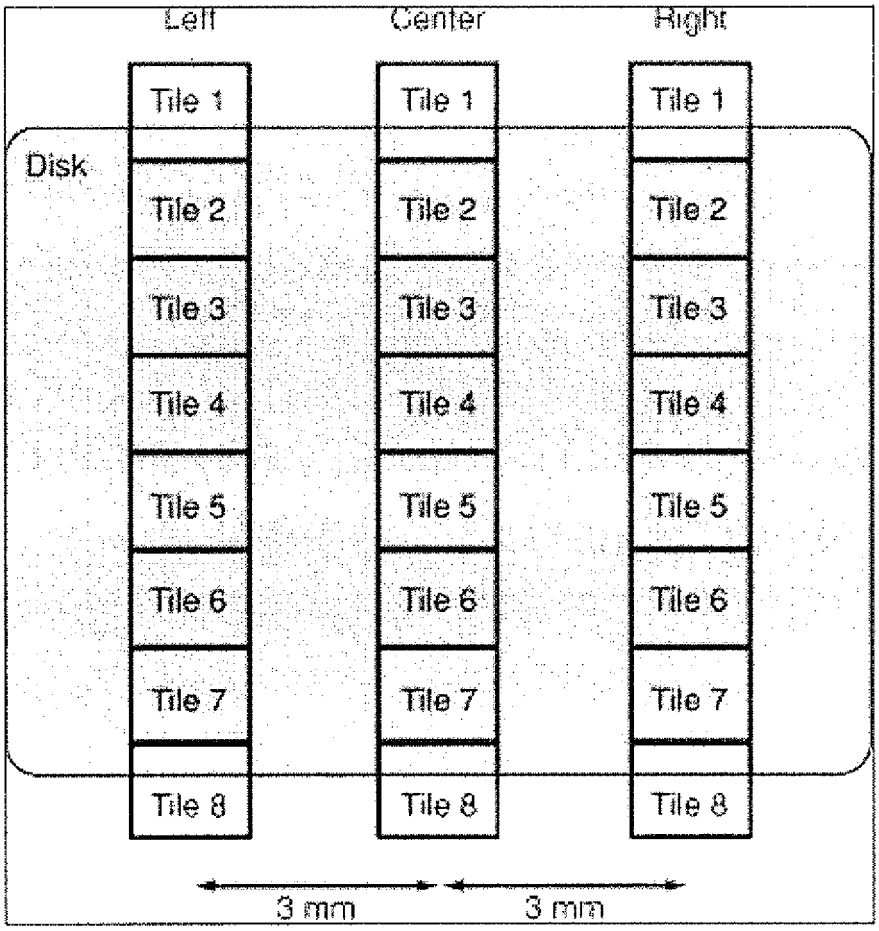

FIG. 2. Illustration depicting image analysis strategy. Three full-thickness images were acquired for each histological section of seeded/control PLGA disks—a center image and left/right images 3 mm from the center. Each full-thickness image was constructed by tiling eight individual 640 × 480 pixel images.

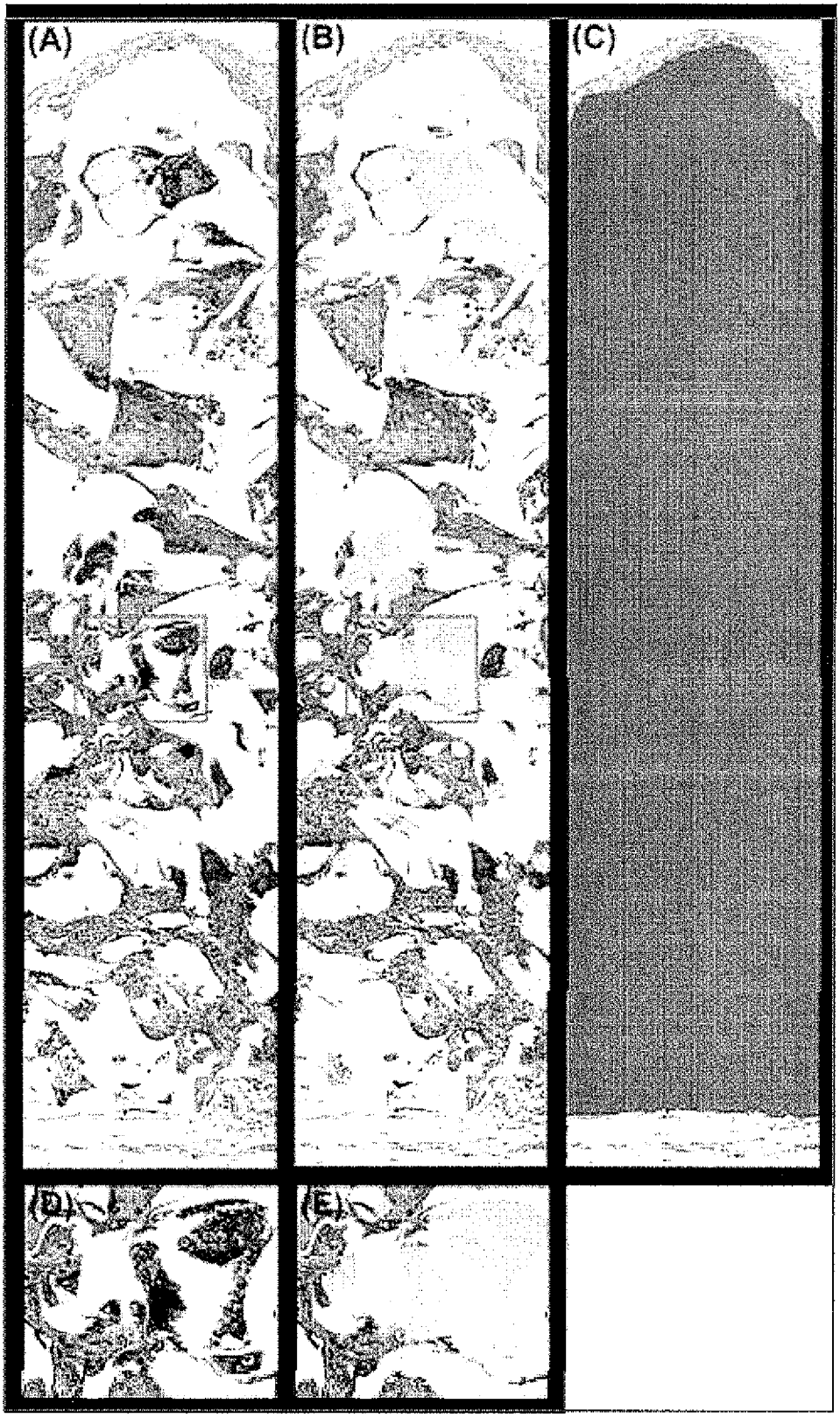
(A)
(B)
(C)
(D)
(E)

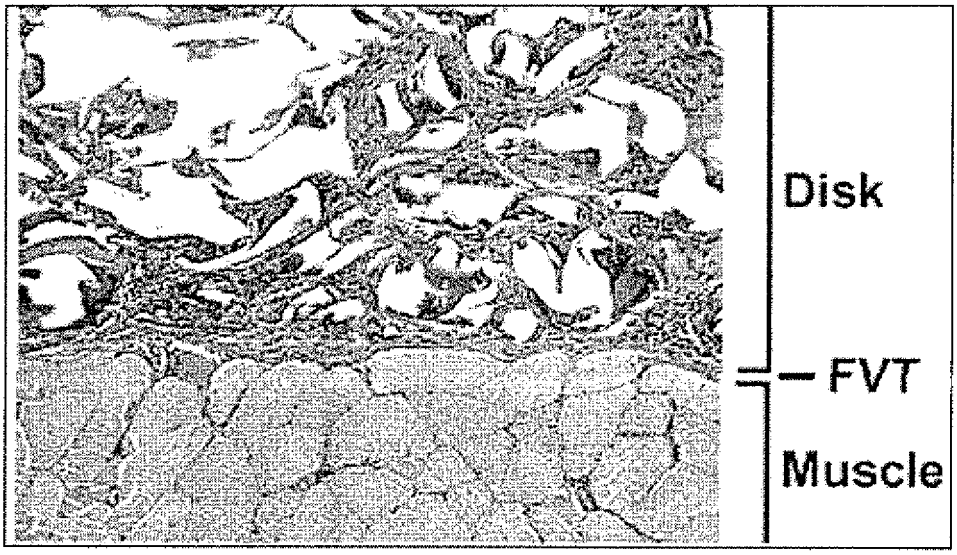

FIG. 4. Representative histology (H&E) depicting the interface between PLGA disks and skeletal muscle beds of the rat. There is no void space or fascia present at the interface, only a thin layer of fibrovascular tissue (FVT). The entire PLGA disk thickness is not shown. Original magnification, ×100.

into each pocket and sutured in place with 5-0 suture (Ethicon), as shown in Figure 1A. Two disks were placed on each side of the incision (four disks per rat) and the incisions closed with 4-0 suture (Ethicon) (Fig. 1B). Animals were housed individually and fed standard rat chow. The disks were left *in vivo* 1, 2, 3, 5, 7, 9, and 12 months. After the elapsed time, the rats were euthanized with CO_2 and the disks harvested. Immediately after harvest, the disks were placed in 10% neutral buffered formalin (Fisher) for future histology.

For this study, a total of 42 rats were used at 6 rats/time period. Each rat was implanted with four disks. Two disks were seeded with PAs, and two disks were implanted without seeding to serve as acellular controls. A total of 84 seeded and 84 acellular disks were used in this study.

Histology

An osmium tetroxide (OsO_4) paraffin procedure was used to demonstrate fat within half of the harvested *in vivo* disks.[3] The remaining half of the disks were frozen for storage and future analyses. Routine staining outlines only "ghost" cells since histological processing with organic solvents and alcohols extract lipid from cells. OsO_4 chemically combines with fat, blackening it in the process. Fat that combines OsO_4 is insoluble in alcohol and xylene, and the tissue can be processed for paraffin embedding and counterstained. After staining with OsO_4, disks were processed for paraffin embedding using standard procedures, except that Histosolve (Shandon) was substituted for xylene. Sections 4 μm thick were cut on a microtome (Leica), placed on slides, counterstained with H&E, and coverslipped to view fibrovascular tissue. Sections were analyzed using brightfield microscopy.

Determination of adipose tissue

High magnification images of histology slides were acquired using an inverted microscope (Olympus), color CCD camera (Olympus), computer-controlled XYZ stage (Ludl Electronic Products), IPLab software

FIG. 3. Illustration depicting routing of full-thickness image tiling and segmentation. (**A,D**) Osmium tetroxide–labeled adipose tissue. (**B,E**) Segmented adipose tissue area (light gray) of A and E, respectively. (**C**) Segmented disk area (dark gray) of A. D and E are higher magnification images of areas denoted by box in A and B, respectively.

(Scanalytics), and a PowerPC (Apple). Images were acquired at a resolution of 0.61 pixels/μm using a 20×, 0.40 NA objective (Olympus). A depiction of the image analysis strategy is shown in Figure 2. Three full-thickness images were acquired automatically from each slide: at the center, ~3 mm right of the center, and ~3 mm left of the center. Image acquisition consisted of digitally tiling eight 640 × 480 pixel images for each full thickness image. Hence, each image was 640 × 3,840 pixels or 390 μm × 2,342 μm (Fig. 3A,D). Next, using image segmentation, the user selected areas of adipose tissue formation (i.e., OsO_4-stained regions) consisting of mature adipocytes or lipid-filled differentiating PAs (Fig. 3B,E). The total scaffold area was determined (Fig. 3C). Data are presented as percent of adipose tissue, defined as follows:

$$\% \text{ Adipose Formation} = 100 \cdot \left(\frac{\Sigma \text{ Left, Center, Right Adipose Area}}{\Sigma \text{ Left, Center, Right Scaffold Area}} \right)$$

Data from center, left, and right full thickness images were pooled, resulting in one value for each slide rather than three.

RESULTS

There were no complications due to surgery or postoperative recovery from anesthesia. Scaffold harvest was unremarkable with no hematomas or seromas. Scaffolds remained intact and appeared to be well-vascularized based on gross inspection (Fig. 1B). As shown in Figure 4, the PLGA disks were sutured in di-

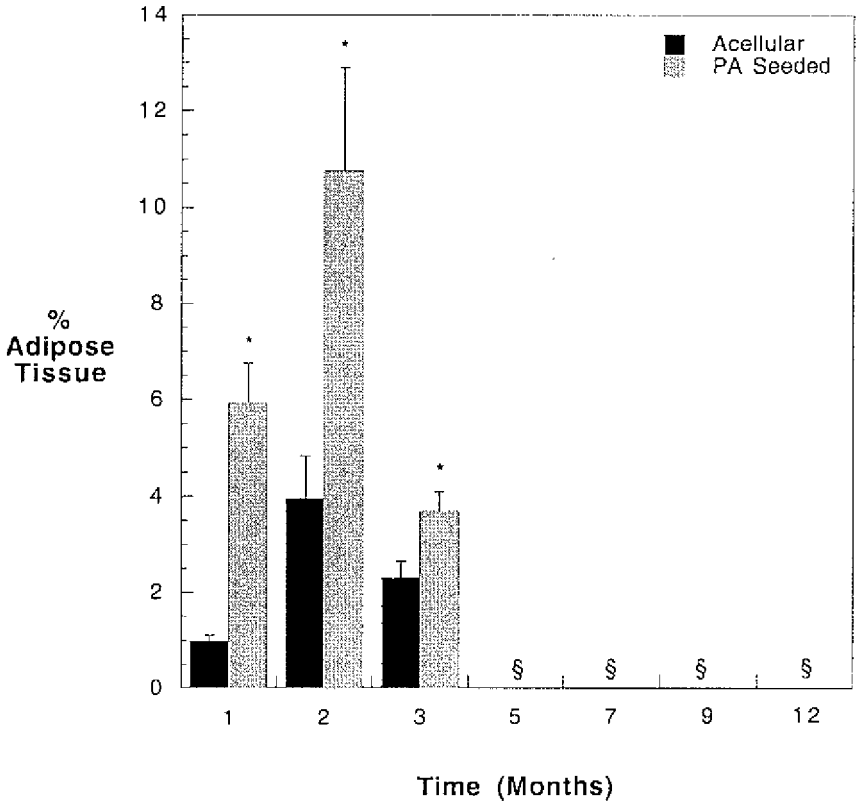

FIG. 5. Percent adipose tissue formation in acellular and preadipocyte (PA)–seeded scaffolds versus implantation time. Data are mean ± SEM of $n = 6$. *Statistical difference in adipose tissue presence between acellular and PA seeded scaffolds ($p \leq 0.05$). §Rats with entirely resorbed PLGA scaffolds and no adipose tissue.

rect apposition to muscle, with no void space or fascia present. Hence, barriers to scaffold revascularization were minimized.

Figure 5 demonstrates the percent adipose formation within the acellular and PA seeded PLGA scaffolds. For months 1–3, PA-seeded scaffolds demonstrated statistically more adipose tissue than their acellular controls. Adipose tissue formation appears to peak at 10.7% at 2 months followed by a decrease. PLGA scaffolds were entirely degraded by 5 months. No PLGA scaffold or fat tissue was present in rats harvested at 5–12 months. The absence of PLGA at ≥5 months is in keeping with the 75:25 copolymer's approximate degradation kinetics of 4–5 months. Exact degradation kinetics is dependent on scaffold geometry, porosity, and molecular weight.

A thin layer of adipose tissue was observed within the fibrovascular tissue (i.e., foreign body capsule) around, but outside both acellular and PA-seeded disks (Fig. 6). The thin layer of adipose tissue was highly vascular and is presumably formed from resident PAs recruited to the foreign body capsule. This observation was noted in the former short-term study[3] and with proprietary cell-seeded and acellular polymers from Johnson & Johnson Corporate Biomaterials Center (data not shown). There was no difference in the layer characteristics at implantation times of 1, 2, and 3 months or between acellular and PA-seeded disks.

Histologically, the amount of all tissue (fibrovascular and adipose combined) decreased between 1 and 3 months as the PLGA degraded (Fig. 7). Without polymer support, the tissue at 3 months formed threads of connecting tissue (Fig. 4C,D). The amount of macrophage infiltration qualitatively decreased with time as well as between 1 and 3 months (Fig. 8). Macrophage presence was localized to polymer–tissue interfaces.

DISCUSSION

This long-term study expanded the results observed with a previous short-term study that demonstrated adipose formation within PA-seeded PLGA scaffolds after 2 and 5 weeks of transplantation.[3] This study addresses the issue of long-term maintenance of adipose formation within a model polymer-cell system. Based on the animal model utilized, one concludes that PA-seeded PLGA scaffolds permit increasing adipose formation that peaks at approximately 2 months and decreases dramatically thereafter. It is encouraging to demonstrate viable adipose tissue formation within PA-seeded PLGA scaffolds for up to 2 months. However, the exact microenvironment required for long-term maintenance remains elusive.

There are several possible explanations for the resorption observed in this long-term study. One explanation may be related to the anatomical site of transplantation. Epididymal PAs were seeded within PLGA

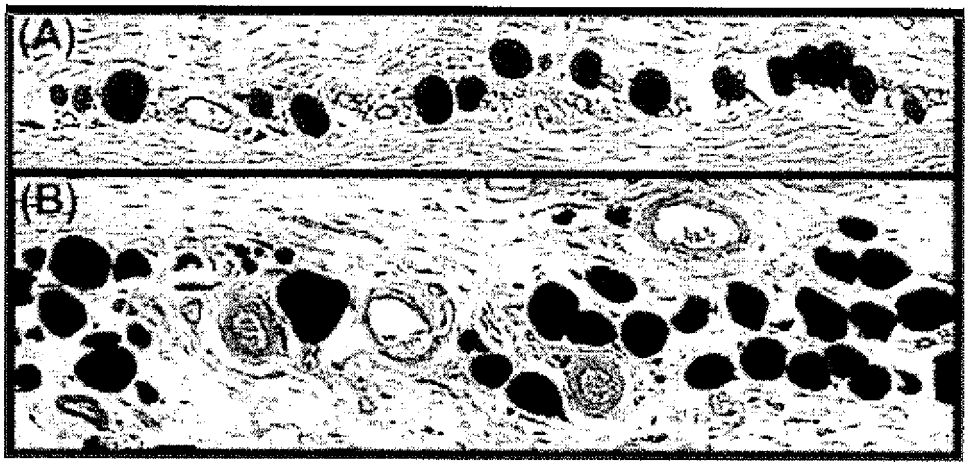

FIG. 6. Representative histology (OsO_4 and H&E) of thin layer of vascular adipose tissue observed outside acellular (A) and PA-seeded (B) disks. There were no differences in perivascular adipose formation between acellular and PA-seeded disks. Original magnification, ×100.

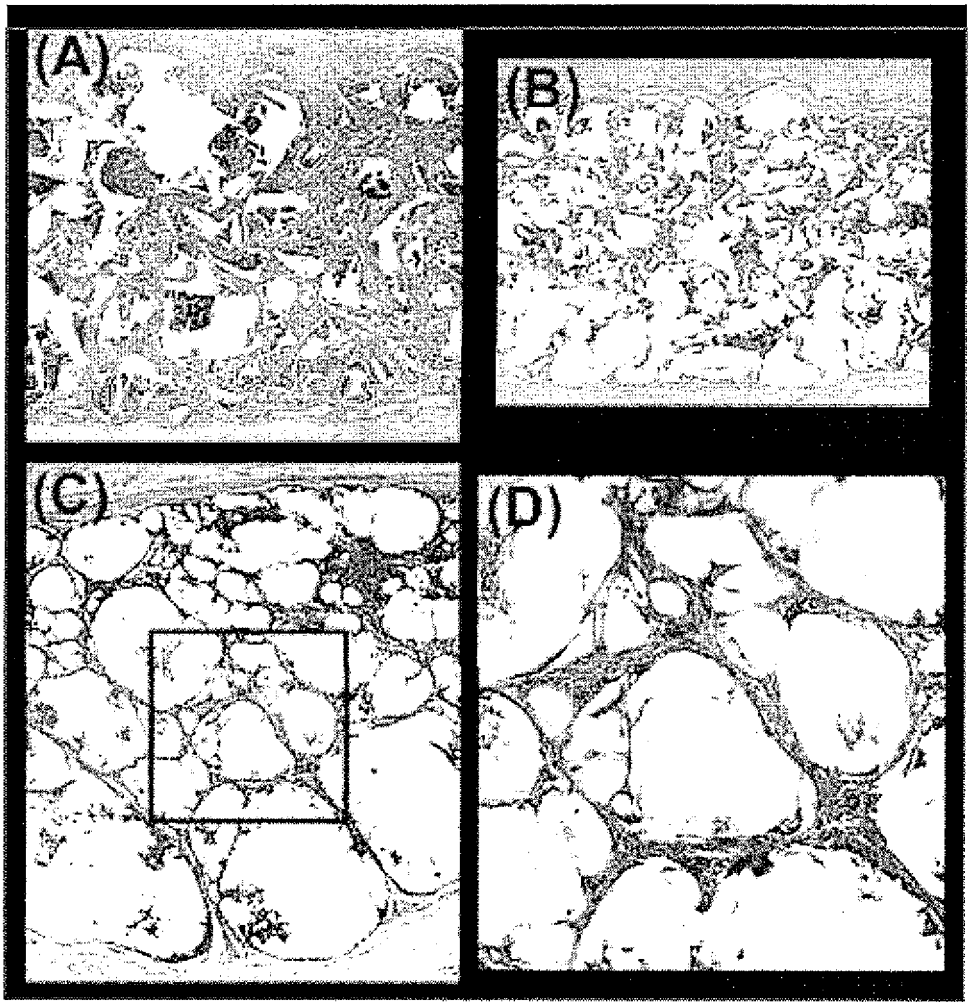

FIG. 7. Representative images (OsO_4 and H&E) depicting extent of tissue presence at 1 month (A), 2 months (B), and 3 months (C,D). D is higher magnification of area denoted in C. Original magnification, ×40 (A–C), ×200 (D).

scaffolds and transplanted to the dorsal subcutaneous region of the rat between two muscle beds, namely the panniculus carnosus (cutaneous trunci) muscle and skeletal muscles of the back. The thin layer of fascia separating the muscle beds was removed prior to construct implantation. Rats typically possess very little subcutaneous adipose tissue. Hence, the microenvironment present in the current model may not support long-term maintenance of adipose tissue. This may be a limitation of the animal model employed. Research is currently being conducted on characterizing a porcine model which has the potential of being a more amenable subcutaneous adipose model. Further, adipose tissue physiology (i.e., rate of replication, capacity for differentiation) is dependent on anatomical location.[16–19] That is, there are site-specific characteristics intrinsic to the PAs that result in regional variations in properties of adipose tissue. Thus, a subcutaneous microenvironment may not optimally support epididymal PAs.

Another explanation for the resorption observed may be the degree of vascularization. It has been known for decades that adequate vascular supply is essential for generation and maintenance of adipose tissue. ECM components secreted by microvascular endothelial cells have been shown to directly stimulate PA differentiation and replication.[20] When avascular constructs are transplanted *in vivo*, the angiogenesis response observed is that of a wound healing cascade. During the late stages of wound healing, there is significant vascular remodeling and involution. The regression of the neovascularization would intuitively re-

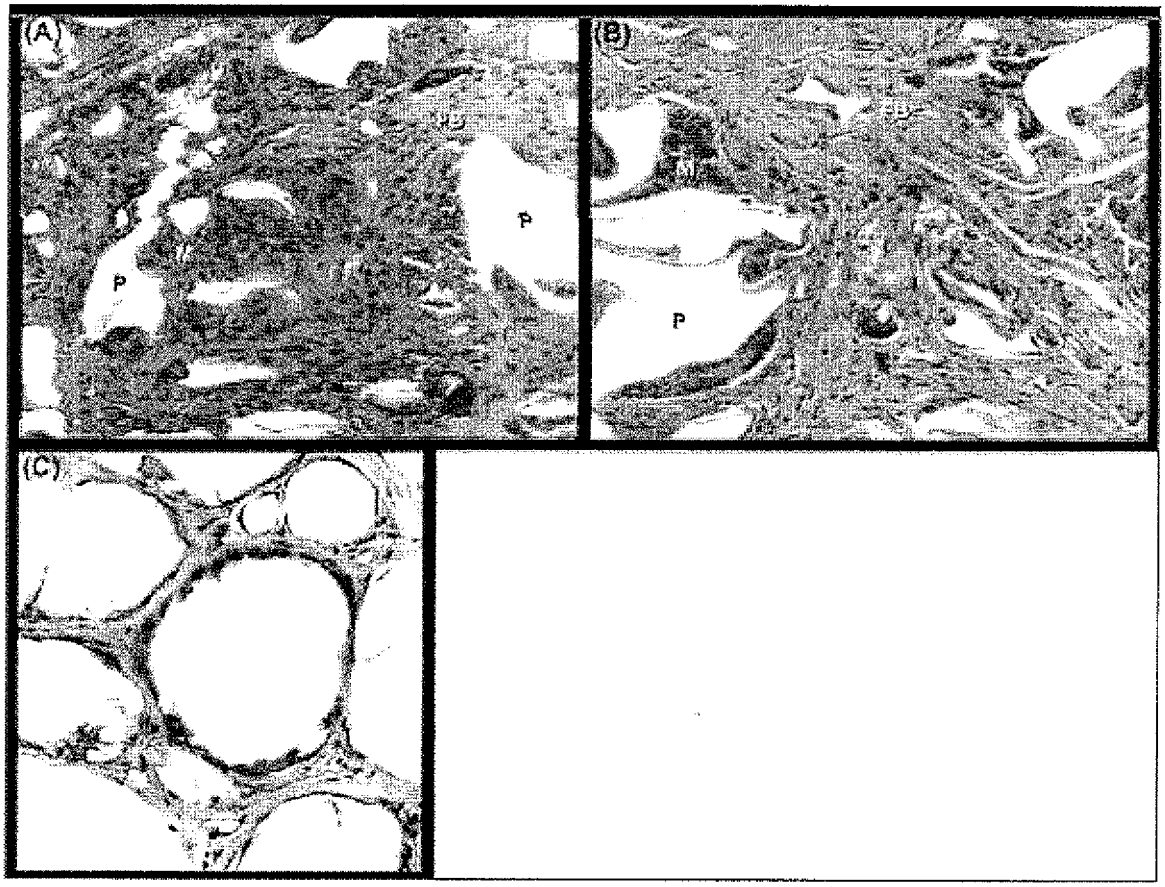

FIG. 8. Representative images (OsO_4 and H&E) depicting extent of macrophage infiltration at 1 month (**A**), 2 months (**B**), and 3 months (**C**). FB, fibroblasts; M, macrophages; P, polymer. Original magnification, ×400.

sult in a concomitant decrease in adipose volume. Moreover, as the amount of PLGA scaffold decreases with time, the influx of macrophages will decrease, as was observed in this study (Fig. 8). Likewise, the level of macrophage-secreted angiogenic factors will decrease resulting in regression of neovascularization. The exact level of vascularization was not determined in this study due to the fact that reagents required for CD31 staining of endothelial cells[21] dissolve the PLGA scaffold. However, gross examination of explants and qualitative examination of H&E-stained sections demonstrate numerous vessels at all time periods.

Long-term maintenance of adipose formation may require a specific, continued support structure. Anatomically, adipose tissue is held together by a network of ECMs (primarily collagen I) and is typically located in a defined anatomical space (e.g., the breast skin envelope for mammary adipose or between dermis and muscle for subcutaneous adipose). Although exact PLGA degradation was not assessed in this study, it is intriguing to note that the absence of adipose tissue corresponded to the absence of PLGA scaffold at time points ≥5 months. Further, at 3 months, the tissue within the disks formed thin interconnecting threads (Fig. 7C,D). One could speculate that the tissue was losing its support structure by 3 months. The use of 75:25 PLGA as a model polymer may limit the current model due to its relatively short degradation time. Using a biomaterial that degrades more slowly may allow adipose tissue to become more mature and maintain its presence longer than 2–3 months.

Finally, the resorption may be related to the lack of a continued, specific microenvironment. The microenvironment of PA regenerative proliferation and differentiation needs to be maintained at the site of transplantation. Several investigators have demonstrated the recruitment of endogenous PAs and *de novo*

adipose formation when the unique microenvironment consisting of Matrigel and bFGF are created in small animal models.[7,22,23] In this present study and others, we have observed formation of *de novo* adipose tissue within the fibrovascular capsule surrounding implanted acellular and PA-seeded biodegradable polymers (Fig. 6). The adipose tissue forms a thin layer parallel to the polymer surface and is surrounded by copious blood vessels (Fig. 6). Although speculative, endogenous PAs may recruit to the highly vascular regions and/or be attracted by factors released by early macrophage invasion.

The apparent resorption of adipose tissue with extended periods is not a new problem. Numerous strategies have been attempted to prevent adipose resorption following grafting, including using small diameter grafts and growth factors. The results of this study illustrate that the long-term maintenance of engineered adipose tissue is not a trivial task. In addition, results of this study suggest that a different combination of cell source, biomaterial, and animal model may lead to more mature adipose tissue for the study of long-term fat maintenance.

ACKNOWLEDGMENTS

We thank the following individuals from University of Texas' Laboratory of Reparative Biology and Bioengineering for their technical assistance with the *in vivo* study: Kristen Dempsey, Cynthia Frye, Gary Klaussen, Shannon Scott, and May Wu. This study was supported in part by a U.S. Army grant (DAMD17-99-1-9268), Cancer Fighter's of Houston grant, and a National Institutes of Health grant (CA16672).

REFERENCES

1. Lee, K.Y., Halberstadt, C.R., Holder, W.D., et al. Breast reconstruction. In: Lanza, R.P., Langer, R., Vacanti, J., eds. Principles of Tissue Engineering. San Diego: Academic Press, 2000, pp. 409–423.
2. Patrick, Jr., C.W., Chauvin, P.B., and Robb, G.L. Tissue engineered adipose. In: Patrick Jr., C.W., Mikos, A.G., McIntire, L.V., eds. Frontiers in Tissue Engineering. Oxford: Elsevier Science, 1998, pp. 369–382.
3. Patrick, Jr., C.W., Chauvin, P.B., and Reece, G.P. Preadipocyte seeded PLGA scaffolds for adipose tissue engineering. Tissue Eng. **5,** 139, 1999.
4. Patrick, Jr., C.W. Adipose tissue engineering: the future of breast and soft tissue reconstruction following tumor resection. Semin. Surg. Oncol. **19,** 302, 2000.
5. Kral, J.G., and Crandall, D.L. Development of a human adipocyte synthetic polymer scaffold. Plast. Reconstr. Surg. **104,** 1732, 1999.
6. Yuksel, E., Weinfeld, A.B., Cleek, R., et al. *De novo* adipose tissue generation through long-term, local delivery of insulin and insulin-like growth factor-1 by PLGA/PEG microspheres in an *in vivo* rat model: a novel concept and capability. Plast. Reconstr. Surg. **105,** 1721, 2000.
7. Beahm, E., Wu, L., and Walton, R.L. Lipogenesis in a vascularized engineered construct. Presented at the American Society of Reconstructive Microsurgeons, San Diego, 2000.
8. Patrick, Jr., C.W. Tissue engineering strategies for soft tissue repair. Anat. Rec. **263,** 361–366, 2001.
9. Patrick Jr., C.W., Wu, X., Johnston, C., et al. Epithelial cell culture—breast. In: Atala, A., and Lanza, R., eds. Methods in Tissue Engineering. San Diego: Academic Press, 2001, pp. 143–154.
10. Ailhaud, G., Amri, E.Z., Bardon, S., et al. The adipocyte: relationships between proliferation and adipose cell differentiation. Am. Rev. Respir. Dis. **142,** S57, 1990.
11. Butterwith, S.C. Molecular events in adipocyte development. Pharmac. Ther. **61,** 399, 1994.
12. Cornelius, P., MacDougald, O.A., and Lane, M.D. Regulation of adipocyte development. Annu. Rev. Nutr. **14,** 99, 1994.
13. MacDougald, O.A., and Lane, M.D. Transcriptional regulation of gene expression during adipocyte differentiation. Annu. Rev. Biochem. **64,** 345, 1995.
14. Ntambi, J.M., and Kim, Y.-C. Adipocyte differentiation and gene expression. J. Nutr. **130,** 3122S, 2000.
15. Smas, C.M., and SookSul, H.S. Control of adipocyte differentiation. Biochem. J. **309,** 697, 1995.
16. Djian, P., Roncari, D.A.K., and Hollenberg, C.H. Influence of anatomic site and age on the replication and differentiation of rat adipocyte precursors in culture. J. Clin. Invest. **72,** 1200, 1983.
17. Hauner, H., and Entenmann, G. Regional variation of adipose differentiation in cultured stromal-vascular cells from the abdominal and femoral adipose tissue of obese women. Int. J. Obesity **15,** 121, 1991.

18. Kirkland, J.L., Hollenberg, C.H., Kindler, S., et al. Effects of age and anatomic site on preadipocyte number in rat fat depots. J. Gerontol. **49,** B31, 1994.
19. Kirkland, J.L., Hollenberg, C.H., and Gillon, W.S. Effects of fat depot site on differentiation-dependent gene expression in rat preadipocytes. Int. J. Obesity Rel. Metab. Disord. **20,** Suppl 3, S102, 1996.
20. Varzaneh, F.E., Shillabeer, G., Wong, K.L., et al. Extracellular matrix components secreted by microvascular endothelial cells stimulate preadipocyte differentiation *in vitro.* Metabolism **43,** 906, 1994.
21. King, T.W., Johnston, C., and Patrick Jr., C.W. Quantification of vascular density using a semi-automated technique for immuno-stained specimens. Anal. Quant. Cytol. Histol. **24,** 39–48, 2002.
22. Kawaguchi, N., Toriyama, K., Nicodemou-Lena, E., et al. *De novo* adipogenesis in mice at the site of injection of basement membrane and basic fibroblast growth factor. Cell Biol. **95,** 1062, 1998.
23. Tabata, Y., Miyao, M., Inamoto, T., et al. *De novo* formation of adipose tissue by controlled release of basic fibroblast growth factor. Tissue Eng. **6,** 279, 2000.

Address reprint requests to:
Charles W. Patrick, Jr., Ph.D.
Department of Plastic Surgery
University of Texas M. D. Anderson Cancer Center
1515 Holcombe Blvd., Box 443
Houston, TX 77030

E-mail: cpatrick@mdanderson.org

This article has been cited by:

1. Filip Stillaert , Michael Findlay , Jason Palmer , Rejhan Idrizi , Shirley Cheang , Aurora Messina , Keren Abberton , Wayne Morrison , Erik W. Thompson . 2007. Host Rather than Graft Origin of Matrigel-Induced Adipose Tissue in the Murine Tissue-Engineering Chamber. *Tissue Engineering* **13**:9, 2291-2300. [Abstract] [PDF] [PDF Plus]
2. Juergen H. Dolderer , Keren M. Abberton , Erik W. Thompson , John L. Slavin , Geoffrey W. Stevens , Anthony J. Penington , Wayne A. Morrison . 2007. Spontaneous Large Volume Adipose Tissue Generation from a Vascularized Pedicled Fat Flap Inside a Chamber Space. *Tissue Engineering* **13**:4, 673-681. [Abstract] [PDF] [PDF Plus]
3. Nestor Torio-Padron, Niklas Baerlecken, Arash Momeni, G. Bjoern Stark, Joerg Borges. 2007. Engineering of Adipose Tissue by Injection of Human Preadipocytes in Fibrin. *Aesthetic Plastic Surgery* **31**:3, 285. [CrossRef]
4. Xuemei Wu, Lindsay Black, Guido Santacana-Laffitte, Charles W. Patrick,. 2007. Preparation and assessment of glutaraldehyde-crosslinked collagen–chitosan hydrogels for adipose tissue engineering. *Journal of Biomedical Materials Research Part A* **81a**:1, 59. [CrossRef]
5. G P L Thomas, K Hemmrich, K M Abberton, D McCombe, A J Penington, E W Thompson, W A Morrison. 2007. Zymosan-induced inflammation stimulates neo-adipogenesis. *International Journal of Obesity* . [CrossRef]
6. K. Hemmrich , M. Meersch , U. Wiesemann , J. Salber , D. Klee , Th. Gries , N. Pallua . 2006. Polyesteramide-Derived Nonwovens as Innovative Degradable Matrices Support Preadipocyte Adhesion, Proliferation, and Differentiation. *Tissue Engineering* **12**:12, 3557-3565. [Abstract] [PDF] [PDF Plus]
7. Aditya V. Vashi , Keren M. Abberton , Gregory P. Thomas , Wayne A. Morrison , Andrea J. O'Connor , Justin J. Cooper-White , Erik W. Thompson . 2006. Adipose Tissue Engineering Based on the Controlled Release of Fibroblast Growth Factor-2 in a Collagen Matrix. *Tissue Engineering* **12**:11, 3035-3043. [Abstract] [PDF] [PDF Plus]
8. John L. Kelly , Michael W. Findlay , Kenneth R. Knight , Anthony Penington , Erik W. Thompson , Aurora Messina , Wayne A. Morrison . 2006. Contact with Existing Adipose Tissue Is Inductive for Adipogenesis in Matrigel. *Tissue Engineering* **12**:7, 2041-2047. [Abstract] [PDF] [PDF Plus]
9. Eileen Gentleman , Eric A. Nauman , Glen A. Livesay , Kay C. Dee . 2006. Collagen Composite Biomaterials Resist Contraction While Allowing Development of Adipocytic Soft Tissue In Vitro . *Tissue Engineering* **12**:6, 1639-1649. [Abstract] [PDF] [PDF Plus]
10. Yosuke Hiraoka , Hiroyasu Yamashiro , Kaori Yasuda , Yu Kimura , Takashi Inamoto , Yasuhiko Tabata . 2006. In Situ Regeneration of Adipose Tissue in Rat Fat Pad by Combining a Collagen Scaffold with Gelatin Microspheres Containing Basic Fibroblast Growth Factor. *Tissue Engineering* **12**:6, 1475-1487. [Abstract] [PDF] [PDF Plus]
11. Karsten Hemmrich, Dennis von Heimburg. 2006. Biomaterials for adipose tissue engineering. *Expert Review of Medical Devices* **3**:5, 635. [CrossRef]
12. Julio A. Clavijo-Alvarez, J Peter Rubin, Jennifer Bennett, Vu T. Nguyen, Jason Dudas, Christopher Underwood, Kacey G. Marra. 2006. A Novel Perfluoroelastomer Seeded with Adipose-Derived Stem Cells for Soft-Tissue Repair. *Plastic and Reconstructive Surgery* **118**:5, 1132. [CrossRef]

13. Timothy A. Moseley, Min Zhu, Marc H. Hedrick. 2006. Adipose-Derived Stem and Progenitor Cells as Fillers in Plastic and Reconstructive Surgery. *Plastic and Reconstructive Surgery* **118**:suppl, 121S. [CrossRef]

14. CYNTHIA A. FRYE, CHARLES W. PATRICK. 2006. THREE-DIMENSIONAL ADIPOSE TISSUE MODEL USING LOW SHEAR BIOREACTORS. *In Vitro Cellular & Developmental Biology - Animal* **42**:5, 109. [CrossRef]

15. Karsten Hemmrich, Melanie Meersch, Dennis von Heimburg, Norbert Pallua. 2006. Applicability of the Dyes CFSE, CM-DiI and PKH26 for Tracking of Human Preadipocytes to Evaluate Adipose Tissue Engineering. *Cells Tissues Organs* **184**:3-4, 117. [CrossRef]

16. Markus Neubauer , Michael Hacker , Petra Bauer-Kreisel , Barbara Weiser , Claudia Fischbach , Michaela B Schulz , Achim Goepferich , Torsten Blunk . 2005. Adipose Tissue Engineering Based on Mesenchymal Stem Cells and Basic Fibroblast Growth Factor in Vitro . *Tissue Engineering* 11:11-12, 1840-1851. [Abstract] [PDF] [PDF Plus]

17. Xihai Kang , Yubing Xie , Douglas A. Kniss . 2005. Adipose Tissue Model Using Three-Dimensional Cultivation of Preadipocytes Seeded onto Fibrous Polymer Scaffolds. *Tissue Engineering* 11:3-4, 458-468. [Abstract] [PDF] [PDF Plus]

18. Liu Hong, Ioana Peptan, Paul Clark, Jeremy J. Mao. 2005. Ex Vivo Adipose Tissue Engineering by Human Marrow Stromal Cell Seeded Gelatin Sponge. *Annals of Biomedical Engineering* 33:4, 511. [CrossRef]

19. Sunil S. Tholpady, Chongdee Aojanepong, Ramon Llull, Jae-Ho Jeong, Aaron C. Mason, J W. Futrell, Roy C. Ogle, Adam J. Katz. 2005. The Cellular Plasticity of Human Adipocytes. *Annals of Plastic Surgery* **54**:6, 651. [CrossRef]

20. Teiichi Masuda , Masutaka Furue , Takehisa Matsuda . 2004. Photocured, Styrenated Gelatin-Based Microspheres for de Novo Adipogenesis through Corelease of Basic Fibroblast Growth Factor, Insulin, and Insulin-Like Growth Factor I. *Tissue Engineering* 10:3-4, 523-535. [Abstract] [PDF] [PDF Plus]

21. Kevin C. Hicok , Tracey V. du Laney , Yang Sheng Zhou , Yuan-Di C. Halvorsen , Daron C. Hitt , Lyndon F. Cooper , Jeffrey M. Gimble . 2004. Human Adipose-Derived Adult Stem Cells Produce Osteoid in Vivo. *Tissue Engineering* 10:3-4, 371-380. [Abstract] [PDF] [PDF Plus]

22. Bradley R. Ringeisen , Heungsoo Kim , Jason A. Barron , David B. Krizman , Douglas B. Chrisey , Shawna Jackman , R.Y.C. Auyeung , Barry J. Spargo . 2004. Laser Printing of Pluripotent Embryonal Carcinoma Cells. *Tissue Engineering* 10:3-4, 483-491. [Abstract] [PDF] [PDF Plus]

23. Claudia Fischbach , Jochen Seufert , Harald Staiger , Michael Hacker , Markus Neubauer , Achim Göpferich , Torsten Blunk . 2004. Three-Dimensional in Vitro Model of Adipogenesis: Comparison of Culture Conditions. *Tissue Engineering* 10:1-2, 215-229. [Abstract] [PDF] [PDF Plus]

24. Charles W. Patrick. 2004. BREAST TISSUE ENGINEERING. *Annual Review of Biomedical Engineering* 6:1, 109. [CrossRef]

25. Jeffrey M Gimble. 2003. Adipose tissue-derived therapeutics. *Expert Opinion on Biological Therapy* 3:5, 705. [CrossRef]

TISSUE ENGINEERING
Volume 6, Number 3, 2000
Mary Ann Liebert, Inc.

De Novo Formation of Adipose Tissue by Controlled Release of Basic Fibroblast Growth Factor

YASUHIKO TABATA, Ph.D.,[1] MANABU MIYAO, B.S.,[1]
TAKASHI INAMOTO, M.D., Ph.D.,[2] TOSHIHIRO ISHII, B.S.,[3]
YOSHIAKI HIRANO, Ph.D.,[3] YOSHIO YAMAOKI, PR.D., M.D.,[4]
and YOSHITO IKADA, Ph.D., D.Med.Sci.[1]

ABSTRACT

***De novo* adipogenesis at the implanted site of a basement membrane extract (Matrigel) was induced through controlled release of basic fibroblast growth factor (bFGF). bFGF was incorporated into biodegradable gelatin microspheres for its controlled release. When the mixture of Matrigel and bFGF-incorporated gelatin microspheres was implanted subcutaneously into the back of mice, a clearly visible fat pad was formed at the implanted site 6 weeks later. Histologic examination revealed that the *de novo* formation of adipose tissue accompanied with angiogenesis was observed in the implanted Matrigel at bFGF doses of 0.01, 0.1, and 1 μg/site, the lower and higher doses being less effective. The *de novo* formation induced by the bFGF-incorporated microspheres was significantly higher than that induced by free bFGF of the same dose. The mRNA of a lipogenesis marker protein, glycerophosphate dehydrogenase, was detected in the formed adipose tissues, biochemically indicating *de novo* adipogenesis. Free bFGF, the bFGF-incorporated gelatin microspheres, or Marigel alone and bFGF-free gelatin microspheres with or without Matrigel did not induce formation of adipose tissue. This *de novo* adipogenesis by mixture of Matrigel and the bFGF-incorporated gelatin microspheres will provide a new idea for tissue engineering of adipose tissue.**

INTRODUCTION

AUTOGRAFTING OF FAT PADS has a long history in plastic and reconstructive surgery for augmentation of lost soft tissues.[1] It has been reported that autologous adipose tissues, such as fat grafts of a few millimeters in size and semiliquid, were transplanted to depressed regions or scars in the breast and facial areas.[2,3] Despite the enthusiasm for such the free-fat autografting, however, researchers have been disappointed by progressive absorption of the tissue graft with time.[4–8] In the examination by microscopy of free-fat autografts removed, necrotic adipocytes were observed and replaced by host fibrous tissue in most areas whereas the transplanted fat cells were hardly proliferated.

It is generally recognized from recent research in cell biology that adipocyte linkage derives from mul-

[1]Institute for Frontier Medical Sciences, Kyoto University, Kyoto 606-8507, Japan.
[2]College of Medical Technology, Kyoto University, Kyoto 606-8507, Japan.
[3]Department of Applied Chemistry, Osaka Institute of Technology, Osaka 535-8585, Japan.
[4]Department of Gastroenterological Surgery, Graduate School of Medicine, Kyoto 606-8501, Japan.

tipotential mesenchymal stem cells with the capacity to differentiate into mesodermal cells, *e.g.*, osteocytes, chondrocytes, adipocytes, and myocytes.[9] These stem cells are morphologically and biochemically converted to matured adipocytes (fat cells) by way of adipose precursor cells. Among the precursor cells are preadipocytes, which have committed or determined to become fat cells and are included in interstitial cells having fibroblast-like morphology.[10]

There are two possible ways based on tissue engineering to induce *de novo* adipogenesis. One method is to carry the preadipocytes in a body site to be induced. It is reported that a preadipocyte cell line induced formation of fat tissue after subcutaneous injection to nude mice.[11] Patrick *et al.* have demonstrated that formation of adipose tissue in the rat subcutis by use of porous discs of poly(lactic-co-glycolic) acid seeded with autologously isolated preadipocytes.[12] The other method is to induce formation of adipose tissue from preadipocytes originally existing in the body. If one can provide a microenvironment suitable for cell proliferation and differentiation, *de novo* formation of adipose tissue can be expected without exogenous adipocytes being transplanted. Recently, Kawaguchi *et al.* have demonstrated that *de novo* adipogenesis in the mouse subcutis could be achieved only by injection of the simple mixture of basic fibroblast growth factor (bFGF) and an extract of basement membrane protein (Matrigel).[13] It is reported that mixing with Matrigel enabled bFGF to promote the vascular response.[14] Thus, it seems reasonable to suppose that such development of a vascular supply is essential for generation and maintainance of the adipose tissue.

It is known that some growth factors promote vascularization. Among the growth factors used to induce capillary formation are acidic FGF, bFGF, platelet-derived growth factor, and vascular endothelial growth factor.[15–18] However, if these growth factors are applied in solution form, one cannot always exhibit their full angiogenic capability because of their *in vivo* short half-life periods. This implies that controlled release of growth factors is needed for effective vascularization. Recently, we have succeeded in releasing biologically active bFGF from a biodegradable hydrogel composed of "acidic" gelatin, which is able to form a polyion complex with "basic" bFGF.[19] *In vivo* experiments revealed that the time profile of bFGF retention in the gelatin hydrogels was in good accordance with that of their degradation.[20] This indicates that the bFGF molecule ionically interacting with the acidic gelatin is released from the hydrogel as the cross-linked gelatin became water soluble with *in vivo* degradation. bFGF-incorporated gelatin hydrogels of disc and microsphere types showed an enhanced angiogenetic effect, in marked contrast to free bFGF.[19,20–23]

The objective of the present study was to investigate the effect of gelatin microspheres for bFGF release on *de novo* formation of adipose tissue in Matrigel. Following subcutaneous implantation of Matrigel mixed with the bFGF-incorporated gelatin microspheres into the backs of mice, *de novo* adipogenesis was evaluated in terms of histologic and biochemical viewpoints and compared with that of Matrigel mixed with bFGF in solution form. We examine the effect of bFGF dose on the formation of adipose tissue.

MATERIALS AND METHODS

Materials

An aqueous solution of human recombinant bFGF with an isoelectric point (IEP) of 9.6 (10 mg/mL) was kindly supplied by Kaken Pharmaceutical Co., Ltd. (Tokyo, Japan). A gelatin sample with an IEP of 5.0 (Nitta Gelatin Co., Osaka, Japan) was extracted from bovine bone (type I collagen) with an alkaline process. Matrigel® basement membrane matrix of growth factor reduced type (Matrigel, Lot# 911947, Becton Dickinson Labware, Bedford, MA) was used here to minimize the effect of growth factor as much as possible. Glutaraldehyde (GA), glycine, and other chemicals were purchased from Wako Pure Chemical Industries (Osaka, Japan) and used without further purification.

Preparation of bFGF-incorporated gelatin microspheres

Gelatin microspheres were prepared through GA crosslinking of gelatin aqueous solution in an emulsion state as reported previously.[23] Immediately after mixing 25 μL of GA aqueous solution (25 wt%) with 10

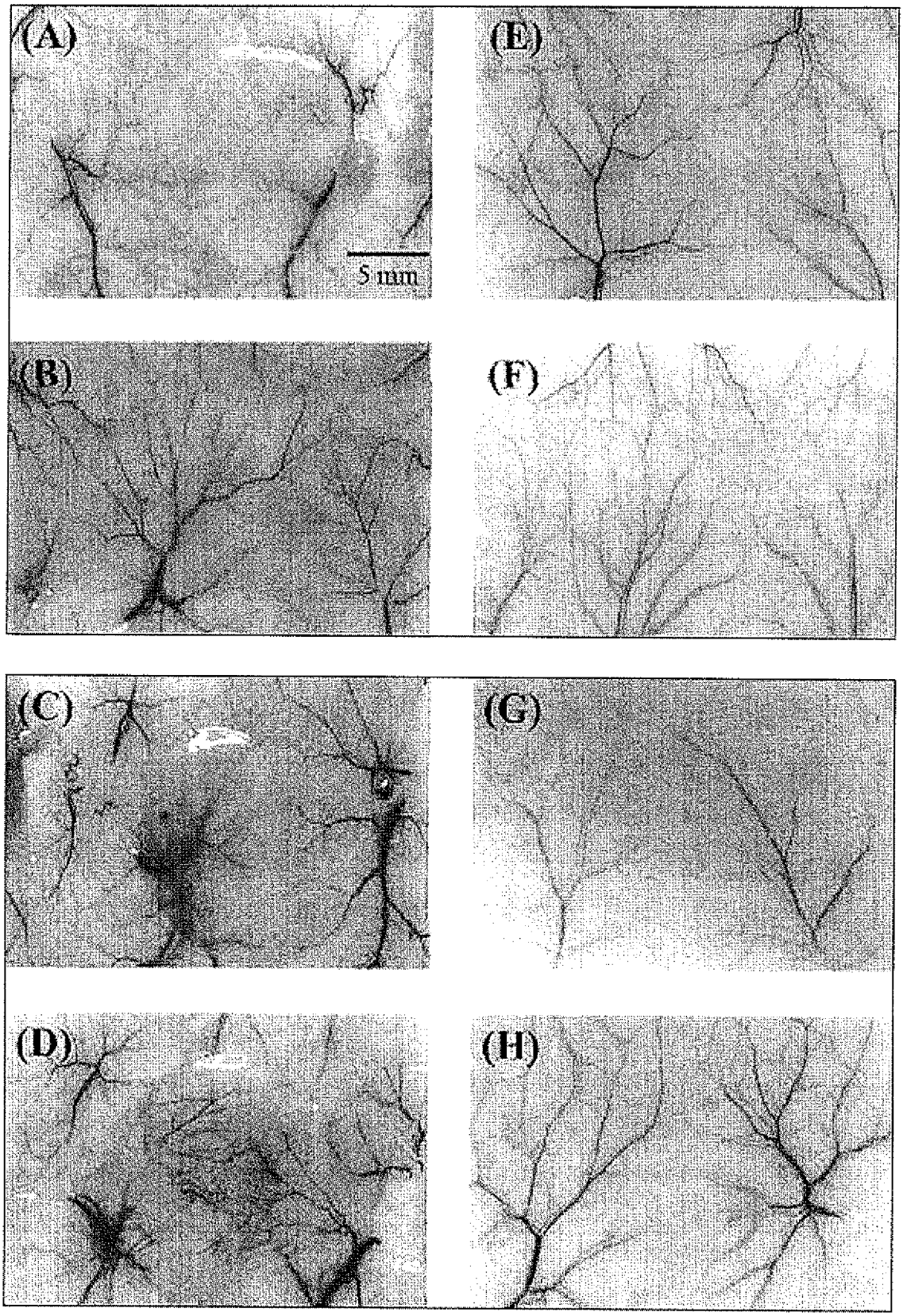

FIG. 1. Tissue appearance of mouse subcutis 6 weeks after treatment of PBS (A,E), bFGF-free, empty gelatin microspheres (B,F), 0.1 μg of free bFGF (C,G), and gelatin microspheres incorporating 0.1 μg of bFGF (D,H) with (A–D) or without Matrigel (E–H).

mL of 10 wt% gelatin aqueous solution preheated at 40°C, the mixed aqueous solution was added dropwise to 375 mL of olive oil with stirring at 420 rpm and 40°C to obtain a W/O emulsion. Stirring was continued for 24 h at 25°C to chemically crosslink the gelatin. After addition of 100 mL of acetone to the reaction mixture, the resulting microspheres were collected by centrifugation (4°C, 3000 rpm, 5 min) and washed five times with acetone by centrifugation. The washed microspheres were placed in 100 mL of 100 mM glycine aqueous solution containing Tween 80 (0.1 wt%), followed by agitation at 37°C for 1 h to block residual aldehyde groups of unreacted GA. Then, the crosslinked microspheres were twice washed with double-distilled water (DDW) by centrifugation, freeze-dried, and sterilized with ethylene oxide gas. The water content of the gelatin microspheres was 95 vol%, when calculated from the microsphere volume before and after swelling in phosphate-buffered saline solution (PBS, pH 7.4) for 24 h at 37°C. The microsphere diameter was measured by viewing at least 100 microspheres with a light microscope and found to range from 60 to 130 μm in the state of PBS swelling.

The original bFGF solution was diluted with DDW to adjust the solution concentration. The aqueous solution containing 0.001, 0.01, 0.1, 1.0, and 10 μg of bFGF (10 μL) as dropped onto 2 mg of freeze-dried gelatin microspheres for impregnation of bFGF into the microspheres. The bFGF solution was completely sorbed into the microspheres by swelling at 25°C for 1 h, because the solution volume was less than that theoretically required for the equilibrated swelling of microspheres. Similarly, empty gelatin microspheres without bFGF were prepared using DDW as the solution to add.

An animal experiment revealed that the gelatin microspheres used were degraded with time in the back subcutis of mice and disappeared 3 weeks later.[23] No influence of bFGF incorporation on the time profile microsphere degradation was observed. In this release system, because the bFGF release is governed by microsphere biodegradation,[20] bFGF is released from the microspheres over 3 weeks.

In vivo *experiments*

The gelatin microspheres (2 mg) swollen with aqueous solution with or without bFGF were homogeneously mixed with 100 μL of Matrigel precooled on ice. The mixture was left for 1 h at 37°C to allow Matrigel to form a hydrogel. As controls, 10 μL of aqueous solutions containing 0.001, 0.01, 0.1, 1.0, and 10 μg of bFGF and PBS were similarly mixed with Matrigel.

Under anesthesia, the mixture of Matrigel with bFGF-incorporated gelatin microspheres or other agents was carefully implanted into the back subcutis of female BALB/c mice (6 weeks old; Shimizu Laboratory Supply, Kyoto, Japan) 1.5 cm apart from the tail root at the body center. The materials used for Matrigel mixing were PBS, empty gelatin microspheres, five doses of free bFGF, and gelatin microspheres incorporating five doses of bFGF. In addition, the similar experiment was performed for the above 12 groups in the absence of Matrigel; PBS, empty gelatin microspheres, free bFGF, and gelatin microspheres incorporating bFGF alone were injected subcutaneously. Each experimental group was composed of 6 mice. The samples were carefully implanted or injected into the subcutaneous site free of originally existing adipose tissue. At 6 weeks post-treatment, the mice were sacrificed by an overdose injection of anesthetic and the skin including the implanted or injected site (2×2 cm^2) was carefully taken off for the subsequent biological examinations. Photographs of the skin flaps were taken to record tissue appearance around the treated site.

De novo formation of adipose tissue at the implanted or injected site was assessed in terms of histologic and biochemical parameters. Of the six skin flaps, three flaps were randomly selected for histological evaluation. The skin flaps were cut at the central portion of implanted or injected site by a scalpel. One cut of the skin was fixed with 10% neutralized formalin solution, embedded in paraffin, and sectioned (2 mm in thickness), followed by staining with hematoxylin and eosin (HE). The other skin cut was embedded in O.C.T. compound, TISSUE-TEK® (4583, Miles Inc., Elkhart, IN), cryosectioned, and stained with Sudan III. Photomicrographs of three cross sections from 3 different mice were taken at different magnifications

FIG. 2. Histologic sections of mouse subcutis 6 weeks after implantation of Matrigel mixed with 0 (**A**), 0.001 (**B**), 0.01 (**C**), 0.1 (**D**), 1.0 (**E**), and 10 μg (**F**) of free bFGF or gelatin microspheres incorporating 0 (**G**), 0.001 (**H**), 0.01 (**I**), 0.1 (**J**), 1.0 (**K**), and 10 μg (**L**) of bFGF. (Magnification: ×100, HE staining.)

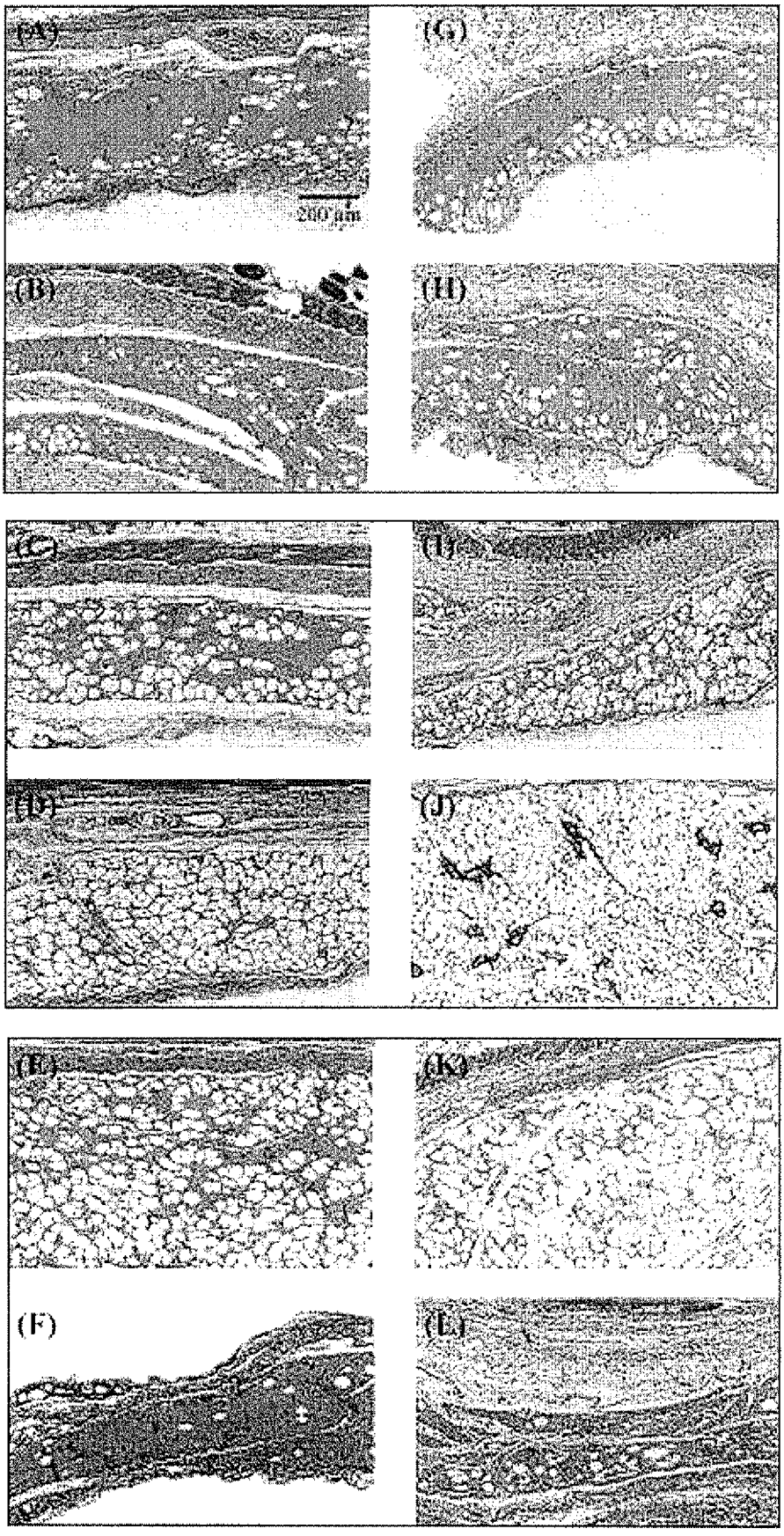
(A)
200 μm
(G)
(B)
(H)
(C)
(I)
(D)
(J)
(E)
(K)
(F)
(L)

to evaluate histologically the *de novo* formation of adipose tissue and vascularization. The ratio of the Sudan III-stained tissue area to the whole area of Matrigel implants was measured to express it as the percent adipose tissue. The residual three skin flaps were used to confirm *de novo* adipogenesis by reverse transcription and polymerase chain reaction (RT-PCR) of glycerophosphate dehydrogenase (GPDH) mRNA.

RT-PCR detection of GPDH mRNA in adipose tissue formed de novo

Total RNA was extracted from the tissue mass formed with TRIZOL reagent (Life Technology, GIBCO BRL Products Inc., Rockville, MD). Briefly, 6 weeks after co-implantation of Matrigel with PBS, 0.1 and 1.0 μg of free bFGF, and gelatin microspheres incorporating 0.1 and 1.0 μg of bFGF, the tissue mass formed in the mouse subcutis was carefully collected without contamination of the surrounding tissue. After being minced by a scissors, the tissue was lysed for 7 min at 25°C with TRIZOL reagent. The total RNA was precipitated conventionally with isopropyl alcohol and 70% ethyl alcohol in DDW from the tissue lysate and dried under vacuum.

The prepared total RNA was reverse transcribed to cDNA by First-Strand cDNA Synthesis Kit (Code #27-9261-01, Amersham Pharmacia Biotech Ltd., Tokyo, Japan). DDW containing 5 μg of total RNA (8 μL) was heated at 65°C for 10 min and cooled on ice for 2 min. The RNA solution was mixed on ice with 7 μL of a reverse transcription reaction mixture, which composes of 5 μL of the Bulk First-Strand Reaction Mix, 1 μL of 0.2 μg/μL pd$(N)_6$ primer, and 1 μL of 200 mM dithiothreitol, followed by incubation at 37°C for 60 min and then quickly cooled down on ice.

Oligonucleotides of mouse GPDH primers were purchased from Takara Shuzo Co. Ltd. (Shiga, Japan) and these sequences were as follows: 5′-CTGTGGGGCCTTGAAGAATA-3′ (GPDH, up-stream, sense) and 5′-CCAAGATCGTGGGTAGCAAT-3′ (GPDH, down-stream, antisense). The sense and antisense primers were dissolved in 100 μL of DDW at respective concentrations of 4 μM to prepare a mixed primer solution. The PCR reaction solution was prepared by mixing on ice 81.5 μL of DDW and 18.5 μL of TaKaRa Ex Taq™ reagent (TakaRa Biochemicals, Takara Shuzo Co. Ltd, Shiga, Japan) which contains 8 μL of dNTP Mixture (2.5 mM each), 0.5 μL of 5 U/μL TaKaRa Ex Taq™, 10 μL of 10 × Ex Taq™ Buffer. Then, 1 μL of the prepared cDNA solution was mixed with 2 μL of the mixed primer solution and 7 μL of the PCR solution. The solution mixture was heated at 94°C for 5 min and then subjected to 40 cycles of PCR. One cycle of PCR consisted of 15 s at 94°C, 15 s at 43°C, and 15 s at 72°C.

After the PCR, the amplified products were fractionated by sodium dodecyl sulfate—4.8% polyacrylamide gel electrophoresis (SDS-PAGE) in 90 mM Tris-borate, 2 mM EDTA (pH 8.0). Amplified products were detected by staining with SYBR™ Green I (TaKaRa Biochemicals, Takara Shuzo Co. Ltd) at room temperature for 30 min.

Statistical analysis

All of the data were analyzed by Fisher's LSD test for multiple comparison, and the statistical significance was accepted at $p < 0.05$. Experimental results were expressed as the means ± the standard deviation of the mean.

RESULTS

De novo *formation of adipose tissue and vascularization following treatment of bFGF with or without Matrigel*

Figure 1 shows the tissue appearance of mouse subcutis 6 weeks after treatment with PBS, bFGF-free empty gelatin microspheres, free bFGF, and gelatin microspheres incorporating bFGF with or without Matrigel. When Matrigel was not co-implanted, the appearance of subcutaneous tissue injected with bFGF in the microspheres-incorporated or free form was similar to that of control, PBS-treated mice. A similar result was observed at different bFGF doses (data not shown). Empty microspheres did not affect the tissue appearance. Gelatin microspheres were completely degraded in the tissue, irrespective of the bFGF incorporation. On the contrary, the tissue appearance was greatly influenced by the presence of Matrigel. When bFGF was mixed together with Matrigel for implantion, capillaries were newly formed at the implanted site

of matrigel, although the capillary number was larger for gelatin microspheres incorporating bFGF than for free bFGF. Empty gelatin microspheres did not contribute to vascularization, and the tissue appearance was similar to that of Matrigel alone. The volume of tissue mass formed by co-implantation of Matrigel with bFGF was large compared with that of other implantation groups.

Influence of bFGF dose on the de novo *formation of adipose tissue*

Figure 2 shows the histological sections of mouse subcutis 6 weeks after implantation with the mixture of Matrigel and different amounts of bFGF. Apparently, co-implantation of bFGF formed *de novo* adipose tissue in the implanted site of Matrigel. When the bFGF dose was 0.01, 0.1, or 1.0 μg, gelatin microspheres incorporating bFGF induced ectopic formation of adipose tissue accompanied by capillary formation to a significantly greater extent than that of free bFGF at the same dose. Less formation of adipose tissue was observed at bFGF doses of 0.001 and 10 μg. Especially, 10 μg of bFGF induced inflammatory reaction in the Matrigel implanted site, irrespective of the dosage form of bFGF. No *de novo* formation of adipose tissue was observed at the Matrigel implanted site together with PBS or empty microspheres.

Figure 3 shows lipid staining of subcutaneous sites implanted with the mixture of Matrigel and PBS, empty gelatin microspheres, free bFGF, or gelatin microspheres incorporating bFGF 6 weeks post-implantation. When the histologic sections were stained with Sudan III, matured adipocytes were stained in the tissue mass formed by co-implantation of Matrigel with gelatin microspheres incorporating 0.1 μg of bFGF. A fewer number of stained cells was found in the implant containing a mixture of Matrigel and the same dose of free bFGF. Only a few adipocytes were stained in the tissue mass formed by implantation of Matrigel alone or its mixture with empty gelatin microspheres.

Figure 4 shows the dependence of *do novo* adipogenesis on the bFGF dose. Adipogenesis was assessed by determining the area percentage of Sudan III-stained adipose tissue to the total tissue on histologic sections 6 weeks after co-implantation of Matrigel with bFGF in the incorporated or free form gelatin micro

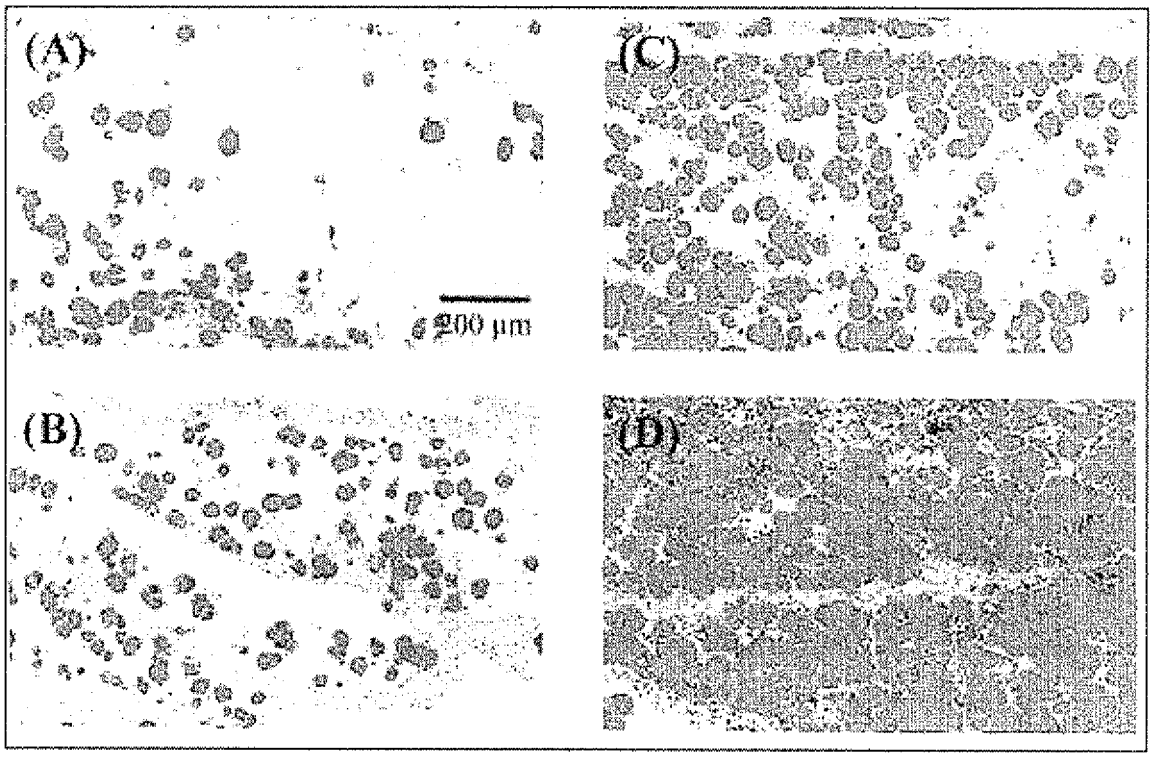

FIG. 3. Lipid staining of mouse subcutis 6 weeks after implantation of Matrigel mixed with PBS (A), bFGF-free, empty gelatin microspheres (B), 0.1 μg of free bFGF (C), and gelatin microspheres incorporating 0.1 μg of bFGF (D). (Magnification: ×100, Sudan III staining.)

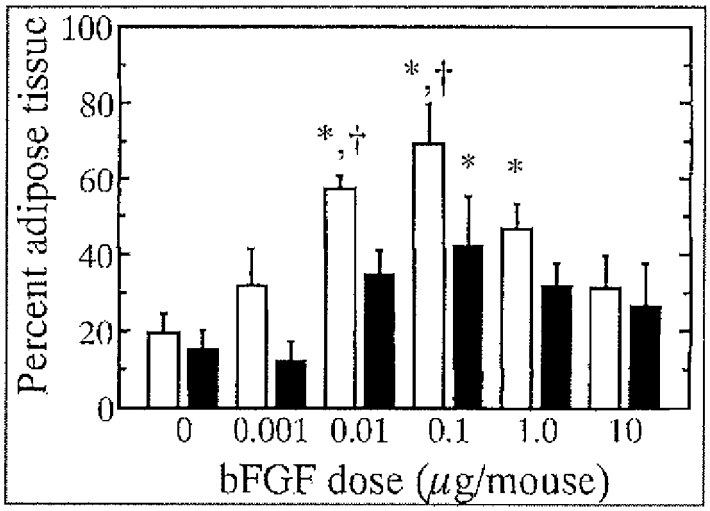

FIG. 4. Effect of bFGF dose on *de novo* adipogenesis 6 weeks after co-implantation of Matrigel with gelatin microspheres incorporating bFGF (□) and free bFGF (■). *, $p < 0.05$ significance against the group implanted with Matrigel mixed with PBS. †, $p < 0.05$ significance against the group implanted with Matrigel mixed with free bFGF at the corresponding dose.

spheres. When gelatin microspheres incorporating 0.01, 0.1, and 1 μg of bFGF were co-implanted with Matrigel, the percent adipose tissue was significantly higher than that of Matrigel alone. On the contrary, for free bFGF, the percent adipose tissue was significantly enhanced at only a dose of 0.1 μg, in contrast to other doses. The highest or lowest dose of bFGF did not enhance adipogenesis and the percent adipose tissue was similar to that of Matrigel alone for both dosage forms of bFGF.

GPDH detection

Figure 5 shows expression of GPDH mRNA products in the tissue mass formed by co-implantation of Matrigel with gelatin microspheres incorporating bFGF or free bFGF. Amplified products of GPDH were not observed when the mixture of Matrigel and PBS was implanted. Co-implantation of Matrigel with gelatin microspheres incorporating 0.1 and 1.0 μg of bFGF induced GPDH mRNA expression, whereas weaker expression was observed for the mixture of Matrigel and 0.1 μg of free bFGF.

DISCUSSION

The hyperplastic formation of adipose tissue in aged animals by feeding with a high carbohydrate or high-fat diet has been investigated intensively. It has been demonstrated in many experiments on rodents that adipose precursor cells possess the potential ability to generate new adipose tissues. The fat depots of mice express large amount of early markers of adipocyte differentiation.[24] A significant population of stromal vascular cells from subcutaneous fat tissues of elderly men and women has been shown to differentiate *in vitro* into adipocytes.[25] Taken together, all of the results suggest that proliferation and differentiation of adipose precursor cells can be promoted depending on their microenvironment. It is recognized that adipocytes and their precursor cells represent only less than one-half of the total cells in adipose tissue; the remaining cells are various blood cells, endothelial cells, and precytes. This tissue cellularity indicates that development of a vascular supply is essential for the generation of maintenance of adipose tissue. What is the microenvironment that allows adipose precursor cells to proliferate and differentiate into matured adipocytes? The present study clearly indicates that such a microenvironment can be provided by implantation of Matrigel together with the release system of bFGF. There will be several reasons to be considered

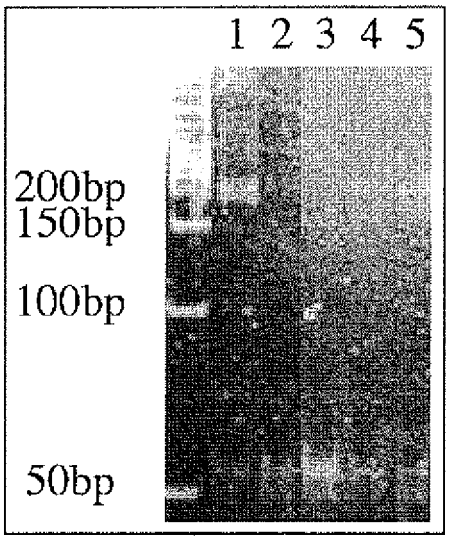

FIG. 5. Expression of GPDH mRNA products of mouse subcutis 6 weeks after implantation of Matrigel mixed with PBS (lane 1), 0.1 μg of free bFGF (lane 2), 1.0 μg of free bFGF (lane 3), and gelatin microspheres incorporating 0.1 (lane 4) or 1.0 μg of bFGF (lane 5).

for the bFGF effect on induced adipogenesis. First, it is possible that the controlled release of bFGF-induced neovascularization, resulting in efficient proliferation and maturation of adipose precursor cells, migrated in the vascularized Matrigel. Second, there is the possibility that bFGF has a direct adipogenic effect. Sheep preadipocytes have been reported to differentiate in a culture medium containing bFGF.[26] It is likely that bFGF increases the number of preadipocytes and the rate of adipocyte differentiation, resulting in enhanced *de novo* adipogenesis.

During the terminal differentiation, adipocytes exhibit marked increases in *de novo* lipogenesis.[27] It is well recognized that the activity level of several proteins and/or mRNA increases with lipogenesis. Among them, GPDH has been used as a representative lipogenesis marker, and the level of activity increase corresponds well with that of preadipocyte differentiation.[27–31] As seen in Fig. 5, it was demonstrated biochemically that the tissue mass formed by the mixture of Matrigel and the gelatin microspheres incorporating bFGF was composed of matured adipocytes.

One promising way to enhance *in vivo* vascularization effectively is to achieve the controlled release of bFGF over an extended period of time. From this point, gelatin microspheres are superior to Matrigel. Significant vascularization was demonstrated to be induced through controlled release of biologically active bFGF from gelatin hydrogel microspheres, in marked contrast to bFGF administered in the solution form.[19,21–23] Histologic examinations revealed that mixing the bFGF-incorporated gelatin microspheres induced neovascularization in Matrigel to a greater extent than free bFGF mixing (Fig. 3). We can be fairly certain that such greater vascularization was one key contributing to significant pronounced formation of adipose tissue (Figs. 4 and 5). Matrigel itself functions to induce angiogenic activity of bFGF to some extent,[14] but the efficacy is not as high as that of the gelatin microspheres. In addition, the adipogenic effect of bFGF should be considered. The bFGF dose dependence indicates that there is an optimal concentration range of bFGF for adipogenesis. It is conceivable that a low dose of bFGF is not enough to exert its angiogenic or adipogenic effect, even though the bioactive protein is released from the gelatin microspheres. Conversely, when the bFGF dose is too high, in addition to the two effects of bFGF, the activity to accelerate infiltration of fibrous tissues into Matrigel will become pronounced. Although adipocyte precursor cells are present in the infiltrated tissue, it is highly possible that the infiltrated fibrous tissue occupies the space in Matrigel necessary for *de novo* formation of adipose tissue.

Another animal experiment revealed that, in place of Matrigel, type I collagen extracted from bovine bone was co-injected subcutaneously into mice together with or without gelatin microspheres incorporat-

ing bFGF. However, none of these treatments induced *de novo* adipogenesis (unpublished data). It is reported that Matrigel enhanced attachment and spreading of predipocytes.[32] These findings indicate that there remains a possibility that Matrigel has additional functions, such as supporting the cell proliferation and differentiation of adipose precursor cells. In an effort to identify adipogenic components of Matrigel, a similar study with implants composed of laminin, type IV collagen, and glycosaminoglycan is currently under way.

ACKNOWLEDGMENT

This work was supported by a grant of "Research for the Future" Program from the Japan Society for the Promotion of Science (JSPS-RFTF96I00203).

REFERENCES

1. Billing, E., and May, J.W. Historical review and present status of free fat graft autotransplantatio n in plastic and reconstructive surgery. Plast. Reconst. Surg. **83,** 368, 1989.
2. Hartram, C.R., Scheflan, M., and Black, P.W. Breast reconstruction with a transverse abdominal island flap. Plast. Reconstr. Surg. **69,** 216, 1982.
3. Ellenbogen, R. Free autogenous pearl fat grafts in the face—a preliminary report of a rediscovered technique. Ann. Plast. Surg. **16,** 179, 1986.
4. Peer, L.A. The neglected "free fat graft," its behavior and clinical use. Plast. Reconstr. Surg. **11,** 40, 1956.
5. Smahel, J. Failure of adipose tissue to heal in the capsule preformed by a silicone implant. Chir. Plast. **8,** 109, 1985.
6. Smahel, J. Experimental implantation of adipose tissue fragments. Br.J. Plast. Surg. **42,** 207, 1989.
7. Ersek, R.A. Transplantation of purified autologous fat: a 3-year follow-up is disappointing. Plast. Reconstr. Surg. **87,** 219, 1991.
8. Fagrell, D., Eneström, S., Berggren, A., and Kniola, B. Fat clinder transplantation: An experimental comparative study of three different kinds of fat transplants. Plast. Reconstr. Surg. **98,** 90, 1996.
9. Caplan, A.I. Mesenchymal stem cells. J. Orthop. Res. **9,** 641, 1991.
10. Ailhaund, G., Grimaldi, P., and Negrel, R. Cellular amd molecular aspects of adipose tissue development. Annu. Rev. Nutr. **12,** 207, 1992.
11. Green, H., and Kehinde, O. Formation of normally differentiated subcutaneous fat pads by an established preadipose cell line. J. Cell Physiol. **101,** 169, 1979.
12. Patrick, C.W., Chauvin, P.B., Hobley, J., and Reece, G.P., Preadipocytes seeded PLGA scaffolds for adipose tissue engineering. Tissue Eng. **5,** 139, 1999.
13. Kawaguchi, N., Toriyama, K., Nicodemou-Lena, E., Inou, K., Torri, S., and Kitagawa, Y. De novo adipogenesis in mice at the site of injection of basement membrane and basic fibroblast growth factor. Proc. Natl. Acad. Sci. USA **95,** 1062, 1998.
14. Passaniti, A., Taylor, R.M., Pili, R., Guo, Y., Long, P.V., Haney, J.A., Pauly, R.R., Grant, D.S., and Martin, G.R. A simple, quantitative method for assessing angiogenesis and antiangiogenetic agents using reconstituted basement membrane, heparin, and fibroblast growth factor. Lab. Invest. **67,** 519, 1992.
15. Wang, J.W., and Aspenberg, P. Basic fibroblast growth factor promotes bone ingrowth in porous hydroxyapatite. Clin. Orthop. Rel. Res. **333,** 252, 1996.
16. Andrade, S.P., Machado, R.D.P., Teixeira, A.S., Belo, A.V. Tarso, and Beraldo, W.T. Sponge-induced angiogenesis in mice and the pharmacological reactivity of the neovasculature quantitated by a fluorimetric method. Microvasc. Res. **54,** 253, 1997.
17. Nimni, M.E. Polypeptide growth factors: targeted delivery systems. Biomaterials **18,** 1201, 1997.
18. Ahrendt, G., Chickering, D.E., and Ranieri, J.P. Angiogenetic growth factors: a review for tissue engineering. Tissue Eng. **4,** 117, 1998.
19. Tabata, Y., and Ikada, Y. Protein release from gelatin matrices. Adv. Drug Delivery Rev. **31,** 187, 1998.
20. Tabata, Y., Nagano, A., and Ikada, Y., Biodegradation of hydrogel carrier incorporating fibroblast growth factor. Tissue Eng. **5,** 127, 1999.
21. Tabata, Y., Hijikata, S., and Ikada, Y. Enhanced vascularization and tissue granulation by fibroblast growth factor impregnated in gelatin hydrogels. J. Controlled Release **31,** 189, 1994.

22. Tabata, Y., and Ikada, Y. Potentiated in vivo biological activity of basic fibroblast growth factor by incorporation into polymer hydrogel microsphere. 4th Japan Int. SAMPE Symp. **4,** 577, 1995.
23. Tabata, Y., Hijikata, S., Muniruzzaman, MD., and Ikada, Y. Neovascularization effect of biodegradable gelatin microspheres incorporating basic fibroblast growth factor. J. Biomater. Sci. Polymer Edn. **10,** 79, 1999.
24. Ailhaud, G. Extracellular factors, signalling pathways and differentiation of adipose precursor cells. Curr. Opin. Cell Biol. **2,** 1043, 1990.
25. Hauner, H., Entenmann, G., Wabitsch, M., Gaillard, D., Ailhaud, G., Negrel, R., and Preiffer, E.F. Promoting effect of glucocorticoids on the differentiation of human adipocytes precursor cells cultured in a chemically defined medium. J. Clin. Invest. **84,** 1663, 1989.
26. Broad, T.E., and Ham, R.G. Growth and adipose differentiation of sheep preadipocyte fibroblasts in serum-free medium. Eur. J. Biochem. **135,** 33, 1983.
27. Smas, C.M., and Sul, H.S. Control of adipocyte differentiation. Biochem, J. **309,** 697, 1995.
28. Pairault, J., and Green, H. A study of the adipose conversion of suspended 3T3 cells by using glycerophosphate dehydrogenase as differentiation marker. Proc. Natl. Acad. Sci. USA **76,** 5138, 1979.
29. Hauner, H., and Löffler, G. Adipose tissue development: The role of precursor cells and adipogenic factors. Klin. Wochenschr. **65,** 803, 1987.
30. Wiederer, O., and Löffler, G. Humoral regulation of the differentiation of rat adipocyte precursor cells in primary culture. J. Lipid Res. **28,** 649, 1987.
31. Entenmann, G., and Hauner, H. Relationship between replication and differentiation in cultured human adipocyte precursor cells. Am. J. Physiol. **270,** 1011, 1996.
32. Hauner, H., Rohrig, K., and Petruschke, T. Effects of epidermal growth factor (EGF), platelet-derived growth factor (PDGF) fibroblast growth factor (FGF) on human adipocyte development and function. Eur. J. Clin. Invest. **25,** 90, 1995.

Address reprint requests to:
Dr. Yasuhiko Tabata
Institute for Frontier Medical Sciences
53 Kawara-cho Shogoin, Sokyo-ku
Kyoto 606-8507, Japan

E-mail: yasuhiko@frontier.kyoto-u.ac.jp

This article has been cited by:

1. Filip Stillaert , Michael Findlay , Jason Palmer , Rejhan Idrizi , Shirley Cheang , Aurora Messina , Keren Abberton , Wayne Morrison , Erik W. Thompson . 2007. Host Rather than Graft Origin of Matrigel-Induced Adipose Tissue in the Murine Tissue-Engineering Chamber. *Tissue Engineering* 13:9, 2291-2300. [Abstract] [PDF] [PDF Plus]
2. Matthew R. Kaufman, Timothy A. Miller, Catherine Huang, Jason Roostaien, Kristy L. Wasson, Rebekah K. Ashley, James P. Bradley. 2007. Autologous Fat Transfer for Facial Recontouring: Is There Science behind the Art?. *Plastic and Reconstructive Surgery* 119:7, 2287. [CrossRef]
3. Sanna-Mari Niemel??, Susanna Miettinen, Yrj?? Konttinen, Timo Waris, Minna Kellom??ki, Nureddin A. Ashammakhi, Timo Ylikomi. 2007. Fat Tissue. *Journal of Craniofacial Surgery* 18:2, 325. [CrossRef]
4. Shinichi Ohta, Norihisa Nitta, Akinaga Sonoda, Ayumi Seko, Toyohiko Tanaka, Ryutaro Takazakura, Akira Furukawa, Masashi Takahashi, Tsutomu Sakamoto, Yasuhiko Tabata. 2007. Embolization Materials Made of Gelatin: Comparison Between Gelpart and Gelatin Microspheres. *CardioVascular and Interventional Radiology* . [CrossRef]
5. Shin-Tai Chen, Reinhard Gysin, Sonia Kapur, David J. Baylink, K.-H. William Lau. 2007. Modifications of the fibroblast growth factor-2 gene led to a marked enhancement in secretion and stability of the recombinant fibroblast growth factor-2 protein. *Journal of Cellular Biochemistry* 100:6, 1493. [CrossRef]
6. Aditya V. Vashi , Keren M. Abberton , Gregory P. Thomas , Wayne A. Morrison , Andrea J. O'Connor , Justin J. Cooper-White , Erik W. Thompson . 2006. Adipose Tissue Engineering Based on the Controlled Release of Fibroblast Growth Factor-2 in a Collagen Matrix. *Tissue Engineering* 12:11, 3035-3043. [Abstract] [PDF] [PDF Plus]
7. Yosuke Hiraoka , Hiroyasu Yamashiro , Kaori Yasuda , Yu Kimura , Takashi Inamoto , Yasuhiko Tabata . 2006. In Situ Regeneration of Adipose Tissue in Rat Fat Pad by Combining a Collagen Scaffold with Gelatin Microspheres Containing Basic Fibroblast Growth Factor. *Tissue Engineering* 12:6, 1475-1487. [Abstract] [PDF] [PDF Plus]
8. Karsten Hemmrich, Dennis von Heimburg. 2006. Biomaterials for adipose tissue engineering. *Expert Review of Medical Devices* 3:5, 635. [CrossRef]
9. Markus Neubauer , Michael Hacker , Petra Bauer-Kreisel , Barbara Weiser , Claudia Fischbach , Michaela B Schulz , Achim Goepferich , Torsten Blunk . 2005. Adipose Tissue Engineering Based on Mesenchymal Stem Cells and Basic Fibroblast Growth Factor in Vitro . *Tissue Engineering* 11:11-12, 1840-1851. [Abstract] [PDF] [PDF Plus]
10. Xihai Kang , Yubing Xie , Douglas A. Kniss . 2005. Adipose Tissue Model Using Three-Dimensional Cultivation of Preadipocytes Seeded onto Fibrous Polymer Scaffolds. *Tissue Engineering* 11:3-4, 458-468. [Abstract] [PDF] [PDF Plus]
11. Oneida Arosarena. 2005. Tissue engineering. *Current Opinion in Otolaryngology & Head and Neck Surgery* 13:4, 233. [CrossRef]
12. Teiichi Masuda , Masutaka Furue , Takehisa Matsuda . 2004. Novel Strategy for Soft Tissue Augmentation Based on Transplantation of Fragmented Omentum and Preadipocytes. *Tissue Engineering* 10:11-12, 1672-1683. [Abstract] [PDF] [PDF Plus]
13. Teiichi Masuda , Masutaka Furue , Takehisa Matsuda . 2004. Photocured, Styrenated Gelatin-Based Microspheres for de Novo Adipogenesis through Corelease of Basic Fibroblast Growth Factor,

Insulin, and Insulin-Like Growth Factor I. *Tissue Engineering* 10:3-4, 523-535. [Abstract] [PDF] [PDF Plus]

14. Claudia Fischbach , Jochen Seufert , Harald Staiger , Michael Hacker , Markus Neubauer , Achim Göpferich , Torsten Blunk . 2004. Three-Dimensional in Vitro Model of Adipogenesis: Comparison of Culture Conditions. *Tissue Engineering* 10:1-2, 215-229. [Abstract] [PDF] [PDF Plus]
15. Charles W. Patrick. 2004. BREAST TISSUE ENGINEERING. *Annual Review of Biomedical Engineering* 6:1, 109. [CrossRef]
16. Yasuhiko Tabata. 2004. Tissue regeneration based on tissue engineering technology. *Congenital Anomalies* 44:3, 111. [CrossRef]
17. Robert L. Walton, Elisabeth K. Beahm, Liza Wu. 2004. De novo adipose formation in a vascularized engineered construct. *Microsurgery* 24:5, 378. [CrossRef]
18. Kevin J. Cronin, Aurora Messina, Kenneth R. Knight, Justin J. Cooper-White, Geoffrey W. Stevens, Anthony J. Penington, Wayne A. Morrison. 2004. New Murine Model of Spontaneous Autologous Tissue Engineering, Combining an Arteriovenous Pedicle with Matrix Materials. *Plastic and Reconstructive Surgery* 113:1, 260. [CrossRef]
19. Hiroyasu Yamashiro , Takashi Inamoto , Michio Yagi , Masaya Ueno , Hironori Kato , Megumi Takeuchi , Shin-Ichi Miyatake , Yasuhiko Tabata , Yoshio Yamaoka . 2003. Efficient Proliferation and Adipose Differentiation of Human Adipose Tissue-Derived Vascular Stromal Cells Transfected with Basic Fibroblast Growth Factor Gene. *Tissue Engineering* 9:5, 881-892. [Abstract] [PDF] [PDF Plus]
20. Yasuhiko Tabata . 2003. Tissue Regeneration Based on Growth Factor Release. *Tissue Engineering* 9:supplement 1, 5-15. [Abstract] [PDF] [PDF Plus]
21. Taka Nakahara , Tatsuo Nakamura , Eizaburo Kobayashi , Masatoshi Inoue , Keiji Shigeno , Yasuhiko Tabata , Kazuhiro Eto , Yasuhiko Shimizu . 2003. Novel Approach to Regeneration of Periodontal Tissues Based on in Situ Tissue Engineering: Effects of Controlled Release of Basic Fibroblast Growth Factor from a Sandwich Membrane. *Tissue Engineering* 9:1, 153-162. [Abstract] [PDF] [PDF Plus]
22. Naofumi Chinen, Masao Tanihara, Miyako Nakagawa, Keiko Shinozaki, Eriko Yamamoto, Yutaka Mizushima, Yasuo Suzuki. 2003. Action of microparticles of heparin and alginate crosslinked gel when used as injectable artificial matrices to stabilize basic fibroblast growth factor and induce angiogenesis by controlling its release. *Journal of Biomedical Materials Research* 67a:1, 61. [CrossRef]
23. Jeffrey M Gimble. 2003. Adipose tissue-derived therapeutics. *Expert Opinion on Biological Therapy* 3:5, 705. [CrossRef]
24. Hong Song , Kim C. O'Connor , Kyriakos D. Papadopoulos , David A. Jansen . 2002. Differentiation Kinetics of in Vitro 3T3-L1 Preadipocyte Cultures. *Tissue Engineering* 8:6, 1071-1081. [Abstract] [PDF] [PDF Plus]
25. Yu Kimura , Makoto Ozeki , Takashi Inamoto , Yasuhiko Tabata . 2002. Time Course of de Novo Adipogenesis in Matrigel by Gelatin Microspheres Incorporating Basic Fibroblast Growth Factor. *Tissue Engineering* 8:4, 603-613. [Abstract] [PDF] [PDF Plus]
26. C. W. Patrick Jr. , B. Zheng , C. Johnston , G. P. Reece . 2002. Long-Term Implantation of Preadipocyte-Seeded PLGA Scaffolds. *Tissue Engineering* 8:2, 283-293. [Abstract] [PDF] [PDF Plus]
27. Steven R. Smith, Eric Ravussin. 2002. Emerging paradigms for understanding fatness and diabetes risk. *Current Diabetes Reports* 2:3, 223. [CrossRef]

28. Shuji Toda, Norimasa Koike, Hajime Sugihara. 2001. Thyrocyte integration, and thyroid folliculogenesis and tissue regeneration: Perspective for thyroid tissue engineering. *Pathology International* 51:6, 403. [CrossRef]

Available online at www.sciencedirect.com
SCIENCE DIRECT®
Biomaterials 24 (2003) 2513–2521
Biomaterials
www.elsevier.com/locate/biomaterials

Adipose tissue engineering based on human preadipocytes combined with gelatin microspheres containing basic fibroblast growth factor

Yu Kimura[a], Makoto Ozeki[a], Takashi Inamoto[b], Yasuhiko Tabata[a,*]

[a] *Institute for Frontier Medical Sciences, Kyoto University, 53 Kawara-cho Shogoin, Sakyo-ku, Kyoto 606-8507, Japan*
[b] *College of Medical Technology, Kyoto University, 53 Kawara-cho Shogoin, Sakyo-ku, Kyoto 606-8507, Japan*

Received 28 September 2002; accepted 17 January 2003

Abstract

Gelatin microspheres containing basic fibroblast growth factor (bFGF) were prepared for the controlled release of bFGF. Co-implantation with the gelatin microspheres enabled preadipocytes to induce adipose tissue formation at the implanted site. Preadipocytes isolated from human fat tissue were suspended with the gelatin microspheres containing bFGF and incorporated into a collagen sponge of cell scaffold. Following subcutaneous implantation of the collagen sponge incorporating human preadipocytes, and gelatin microspheres containing 1 μg of bFGF into the back of nude mice, adipose tissue was formed at the implanted site of collagen sponge within 6 weeks postoperatively although the extent depended on the number of preadipocytes transplanted and the bFGF dose. The formation of adipose tissue was significant compared with the implantation of collagen sponge incorporating human preadipocytes and 1 μg of free bFGF. The area of adipose tissue newly formed was increased with the number of preadipocytes transplanted until to 1.0×10^5 cells/site and thereafter leveled off. The maximum area was observed at the bFGF dose of 1 μg/site. The area was significantly smaller at the bFGF dose of 0.5 μg/site or larger than 1 μg/site. Immunohistochemical examination indicated that the adipose tissue newly formed was composed of human matured adipocytes. No adipogenesis was observed at the implanted site of collagen sponge incorporating either gelatin microspheres containing bFGF or human preadipocytes and the mixed gelatin microspheres containing bFGF and human preadipocytes. We conclude that combination of gelatin microspheres containing bFGF and preadipocytes with the collagen sponge is essential to achieve tissue engineering of fat tissue.
© 2003 Elsevier Science Ltd. All rights reserved.

Keywords: Adipose tissue engineering; Human preadipocytes; bFGF release; Gelatin microspheres; A collagen sponge

1. Introduction

In plastic and reconstructive surgery for augmentation of lost soft tissues [1], autologous transplantation of fat grafts of a few millimeters size and semiliquid has been clinically performed for depressed regions or scars in the breast and facial areas [2,3]. However, this treatment often meets some problems, such as the absorption and fibrosis of tissues grafted [4–7]. Thus, if it is possible to artificially induce formation of adipose tissue at such a defect site, this will be a promising substitute for the tissue graft.

Recently, tissue engineering has been being noticed as a newly emerging biomedical technology to repair or regenerate a body defect by combining cells of high proliferation and differentiation potential with an artificial matrix of cells scaffold and growth factor [8]. This tissue engineering technology is also applicable for regeneration of fat tissue, and some trials have been reported on adipose tissue engineering [9–12]. There are two possible strategies based on tissue engineering to induce adipogenesis. The first strategy is to make use of cells that are potential for proliferation and differentiation to form adipose tissue. The cells are brought into a body site where formation of adipose tissues is expected. For example, it is reported that a preadipocyte cell line induced formation of fat tissue at the site of subcutaneous injection to nude mice [13]. Patrick et al., have succeeded in forming adipose tissue in the rat subcutis by use of porous scaffold of poly(lactic-co-glycolic acid) pre-seeded with autologously isolated preadipocytes [10,14]. Adipose tissue engineering by use of collagen

*Corresponding author. Tel.: +81-75-751-4121; fax: +81-75-751-4646.
E-mail address: yasuhiko@frontier.kyoto-u.ac.jp (Y. Tabata).

0142-9612/03/$ - see front matter © 2003 Elsevier Science Ltd. All rights reserved.
doi:10.1016/S0142-9612(03)00049-8

scaffold combined with human preadipocytes has been reported [15,16]. This is the first report of adipogenesis by use of human cells, which confirmed the possibility of fat tissue engineering for human trial. The second way is to induce in vivo formation of adipose tissue based on precursor or stem cells, like preadipocytes, originally existing in the body. If it is possible to provide a local environment suitable for the proliferation and differentiation of such cells, formation of adipose tissue will be expected without exogenous transplantation of cells necessary for adipogenesis. It has been demonstrated that adipogenesis in the mouse subcutis could be achieved only by injection of the simple mixture of basic fibroblast growth factor (bFGF) and an extract of basement membrane extract (Matrigel) [17]. Mixing with Matrigel enabled bFGF to promote the angiogenetic response [18], which is essential for generation and maintenance of the adipose tissue. We have demonstrated that the controlled release from gelatin hydrogels [19–23] enabled bFGF to significantly enhance the angiogenetic effect in vivo. Following subcutaneous implantation of Matrigel combined with this system of bFGF release into the mouse back, significantly higher adipogenesis at the implanted site was observed than implantation of the mixed Matrigel and free bFGF [24,25]. These findings experimentally confirmed that it was possible to induce adipogenesis by giving transplanted preadipocytes a local environmental field suitable to tissue regeneration in the body. However, since the Matrigel scaffold of the regeneration environment is a mouse-derived material, it is practically impossible to apply it to human.

The present study was undertaken to investigate whether or not a collagen sponge functions as the scaffold for formation of adipose tissue based on gelatin microspheres for bFGF release. Preadipocytes, a precursor of fat cells, were prepared from human fat tissue isolated in breast surgery. Following subcutaneous implantation of collagen sponge incorporating human preadipocytes and the gelatin microspheres containing bFGF into the back of nude mice, adipogenesis was evaluated from the viewpoint of histological area occupied by adipose tissue newly formed and compared with that of collagen sponge incorporating with preadipocytes plus bFGF in the solution form. We examined the effect of the number of preadipocytes transplanted and the bFGF dose on the formation of adipose tissue.

2. Materials and methods

2.1. Materials

An aqueous solution of human recombinant bFGF with an isoelectric point (IEP) of 9.6 (10 mg/ml) was kindly supplied by Kaken Pharmaceutical Co., Ltd., Tokyo, Japan. A gelatin sample with an IEP of 5.0 (Nitta Gelatin Co., Osaka, Japan) was prepared through an alkaline process of type I collagen obtained from bovine bone. It is found that the "acidic" gelatin complexes with the "basic" bFGF mainly due to their electrostatic interaction [26,27]. The freeze-dried sponge sheet ($80 \times 60\,mm^2$, 3-mm thickness) of pigskin type I collagen was kindly supplied by Gunze Co., Ltd., Kyoto, Japan. The sponge sheet was prepared by the dehydrothermal (140°C, 6 h) and the subsequent glutaraldehyde (GA) crosslinking (0.2 wt%, 4°C, 12 h) of collagen. The porosity and pore size of sponge were 90% and 60–100 μm. The collagen sheet was cut by scissors to prepare square sheets ($5 \times 5\,mm^2$) for in vivo experiments. GA, glycine, and other chemicals were purchased from Wako Pure Chemical Industries, Osaka, Japan and used without further purification.

2.2. Isolation and culture of human preadipocytes

Human preadipocytes were primarily isolated from human adipose tissues that were obtained in the reduction mammaplastic surgery of breast cancer patients with informed consent at Kyoto University Hospital. The adipose tissue was washed with phosphate-buffered saline solution (PBS, pH 7.4) to carefully remove blood cells, then minced, and digested by 520 U/ml collagenase (Nitta Gelatin, Osaka, Japan) in a water bath at 37°C for 60 min under shaking. The digested was suspended in Medium 199 containing 10 vol% fetal calf serum (FCS), followed by centrifugation (200*g*, 5 min at 4°C) to remove the supernatant. After washing twice with the medium, the cells obtained were cultured in a cell-culture flask ($75\,cm^2$, CORNING 430720, 1×10^3 cells/cm^2) in the medium containing 0.1 μg/ml of bFGF at 37°C and 5% CO_2–95% air atmosphere pressure. The cells were expanded by two times subculturing and subjected to in vivo experiments. The cell morphology was fibroblast-like. When cultured in the presence of 50 nM of insulin, 100 nM of dexamethasone, 10 μg/ml of transferrin, and 200 pM of triiodethyronine for 14 days, the cells accumulated fat droplets inside. This suggests that the cells isolated had an inherent nature to differentiate into matured adipocytes.

2.3. Preparation of gelatin microspheres containing bFGF

Gelatin microspheres were prepared through GA crosslinking of gelatin aqueous solution in an emulsion state as reported previously [28]. Immediately after mixing 25 μl of GA aqueous solution (25 wt%) with 10 ml of 10 wt% gelatin aqueous solution preheated at 40°C, the mixed aqueous solution was dropwise added to 375 ml of olive oil under stirring at 420 rpm and 40°C

to obtain a W/O emulsion. Stirring was continued for 24 h at 25°C to allow the gelatin to chemically crosslink. After addition of 100 ml of acetone to the reaction mixture, the resulting microspheres were collected by centrifugation (4°C, 3000 rpm, 5 min) and washed five times with acetone by centrifugation. The washed microspheres were placed in 100 ml of 100 mM glycine aqueous solution containing Tween 80 (0.1 wt%), followed by agitation at 37°C for 1 h to block the residual aldehyde groups of unreacted GA. Then, the crosslinked microspheres were twice washed with double-distilled water (DDW) by centrifugation, freeze-dried, and sterilized with ethylene oxide gas. The water content of the gelatin microspheres was 95 vol%, when calculated from the microsphere volume before and after swelling in PBS for 24 h at 37°C. The microsphere diameter was measured by viewing at least 100 microspheres with a light microscope and found to range from 60 to 130 μm in the state of PBS swelling.

The original bFGF solution was diluted with DDW to adjust the bFGF concentrations at 10, 20, 100, 200, and 1000 μg/ml. The aqueous solution of bFGF (50 μl) was dropped onto 2 mg of freeze-dried gelatin microspheres, followed by leaving at 25°C for 1 h for impregnation of bFGF into the microspheres. The bFGF solution was completely absorbed into the microspheres through the impregnation process because the solution volume was much less than that theoretically required for the equilibrated swelling of microspheres.

A series of study [19–23] indicated that bFGF was released from the gelatin hydrogel microspheres of release carrier not by simple diffusion, but by the water-solubilization of bFGF accompanied with hydrogel degradation. bFGF is immobilized into the hydrogel microspheres based on the electrostatic complexation between the basic bFGF and acidic gelatin molecules. The complexed bFGF is not released from the hydrogels unless they are degraded in vivo to form water-soluble gelatin fragments. Animal experiments revealed that the time profile of in vivo retention was in good accordance with that of in vivo hydrogel degradation [23]. When evaluated in terms of angiogenesis, the biological activity of bFGF released from gelatin hydrogels could be detected and lasted for longer time periods as the degradation time period of hydrogels was prolonged [29]. The gelatin microspheres containing bFGF used here were degraded with time in the back subcutis of mice to completely disappear 3 weeks later. Based on the mechanism of bFGF release from this hydrogel system, the gelatin microspheres achieve the controlled release of biologically active bFGF over 3 weeks.

2.4. *In vivo experiments*

The gelatin microspheres (2 mg) swollen with the bFGF aqueous solution were mixed with the suspension of human preadipocytes at cell densities of 2×10^4, 5×10^4, 1×10^5, and 5×10^5 cells/50 μl culture medium. As control, 10 μl of aqueous solutions containing 1 μg of bFGF was similarly mixed with 1×10^5 cells of human preadipocytes. The mixed suspension was dropped on the freeze-dried collagen sponge sheet ($5 \times 5\,mm^2$, 3-mm thickness) for the impregnation, followed by incubation for 3 h under the same conditions as described above for the collagen sponge incorporating human preadipocytes and gelatin microspheres containing bFGF.

Under anesthesia, the collagen sponge incorporating human preadipocytes and gelatin microspheres containing bFGF was carefully implanted into the back subcutis of female BALB/c nude mice, 6 weeks of age (Shimizu Laboratory Supply, Kyoto, Japan), 1.5 cm distance away from the tail root at the body center. As controls, mice received implantation of the collagen sponge incorporating human preadipocytes and free bFGF, or the mixture of two components selected from the sponge, the microspheres containing bFGF, and human preadipocytes. All the animal experiments were performed according to the Guidelines of Animal Experiment of Kyoto University (1985). Each experimental group was composed of six mice.

The mice, 6 weeks after implantation, were sacrificed by an overdose injection of anesthetic and the skin including the implanted site ($2 \times 2\,cm^2$) was carefully taken off for the subsequent biological examinations. The adipose tissues at the implantation site were assessed in terms of histological examination. The skin specimen was fixed with 10% neutralized formalin solution, embedded in paraffin, and sectioned (2 μm in thickness) at the portion of implanted site as central as possible, followed by staining with hematoxylin and eosin (HE). Microphotographs of six cross-sections from six different mice were taken at a similar magnification to histologically evaluate the formation of adipose tissue and angiogenesis. The same area of interest (three portions/cross-section, $0.8 \times 0.5\,mm^2$) was randomly selected and the area occupied by matured adipocytes at the implanted site for every portion was measured by a computer program of NIH image analysis to express as the area of adipose tissue.

2.5. *Immunohistological evaluation of fat tissue newly formed following implantation of a collagen sponge incorporating human preadipocytes and gelatin microspheres containing bFGF*

Deparaffined cross-sections of 4 μm thickness were rehydrated with PBS and incubated with mouse anti-human vimentin antibody (1:20 dilution) in a moist chamber for 24 h at 4°C. Then, the sections were rinsed with PBS three times and incubated with a second antibody-biotin conjugated rabbit anti-mouse IgG + IgA + IgM antibody (Histofine SAB-PO(M) kit, Nichirei

Co., Tokyo, Japan) for 10 min at room temperature. After washing with PBS three times, the sections were incubated with peroxidase-conjugated streptoavidin solution (Histofine) for 5 min at room temperature. Following extensive washing, the sections were exposed to peroxidase substrate DAB (3,3′-diaminobendine, Sigma) for 5 min at room temperature, then rinsed and counter-stained with hematoxylin. The section was viewed to assess the human-specific cellularity in the tissue.

2.6. Statistical analysis

All the data were analyzed by Fisher's LSD test for multiple comparison and the statistical significance was accepted at $p < 0.05$. Experimental results were expressed as the mean + standard deviation of the mean (SD).

3. Results

3.1. Formation of adipose tissue and vascularization following implantation of collagen sponges incorporating human preadipocytes gelatin microspheres containing bFGF

Fig. 1 shows the tissue appearance of mouse subcutis 6 weeks after implantation of collagen sponge incorporating human preadipocytes and gelatin microspheres containing bFGF or other materials. When the collagen sponge was implanted being incorporated with preadipocytes and gelatin microspheres containing bFGF, new formation of tissue mass was found at the implanted site, while many blood vessels were distributed in the tissue formed. The similar change in tissue appearance was observed at the collagen sponge incorporating preadipocytes and free bFGF although the formation of blood vessels was less. Upon implanting with the collagen sponge incorporating either gelatin microspheres containing bFGF or preadipocytes and the mixture of preadipocytes and gelatin microspheres containing bFGF, such a change of tissue appearance was not observed at the implanted site.

Fig. 2 shows the histological sections of the implanted site 6 weeks after implantation. Matured adipocytes accumulating lipid inside were observed in the tissue mass formed 6 weeks after implantation of collagen sponge incorporating human preadipocytes and gelatin microspheres containing bFGF, whereas the sponge incorporating human preadipocytes and free bFGF was less effective. For every combination of two from three components, the collagen sponge, gelatin microspheres containing bFGF, and human preadipocytes, no formation of fat tissue was observed.

Fig. 3 shows the area of adipose tissue newly formed in the mouse subcutis 6 weeks after implantation. The area of adipose tissue newly formed was large by the implantation of the collagen sponge incorporating the combination of human preadipocytes with gelatin microspheres containing bFGF compared with that of the combination with free bFGF. On the contrary, for other control groups, the area of adipose tissue was not detected.

3.2. Influence of the number of human preadipocytes transplanted and the bFGF dose on the formation of adipose tissue

Fig. 4 shows the influence of the preadipocytes number on the area of adipose tissue newly formed 6 weeks after implantation of the collagen sponge, human preadipocytes, and gelatin microspheres containing bFGF. The area increased with an increase in the number of human preadipocytes transplanted up to 1×10^5 cells/site and thereafter leveled off.

Fig. 5 shows the histological sections of the implanted site 6 weeks after implantation of collagen sponges incorporating human preadipocytes and gelatin microspheres containing different doses of bFGF. Irrespective of the bFGF dose, the new formation of adipose tissue was observed by use of gelatin microspheres containing bFGF. Among them, the maximum adipogenesis was achieved at the bFGF dose of 1 μg. Fig. 6 shows effect of the bFGF dose on the area of adipose tissue newly formed 6 weeks after implantation. The area formed was significantly larger at the implanted site of collagen sponge incorporating human preadipocytes and gelatin microspheres containing 1 μg of bFGF than that of other bFGF doses. The co-implantation of gelatin microspheres containing 50 μg of bFGF induced inflammatory reaction in and around the implanted site.

3.3. Immunohistology of fat tissue regenerated by a collagen sponge incorporating human preadipocytes and gelatin microspheres containing bFGF

Fig. 7 shows the immunohistological section of adipose tissue newly formed by a collagen sponge incorporating human preadipocytes and gelatin microspheres containing bFGF. Apparently, the adipose tissue newly formed was throughout stained by the anti-human vimentin antibody, in contrast to the surrounding adipose tissues.

4. Discussion

The hyperplastic formation of adipose tissue in aged animals by feeding with a high carbohydrate or high fat diet has intensively been investigated. It has been recognized in the recent cell biology that adipocyte linkage derives from multipotential mesenchymal stem

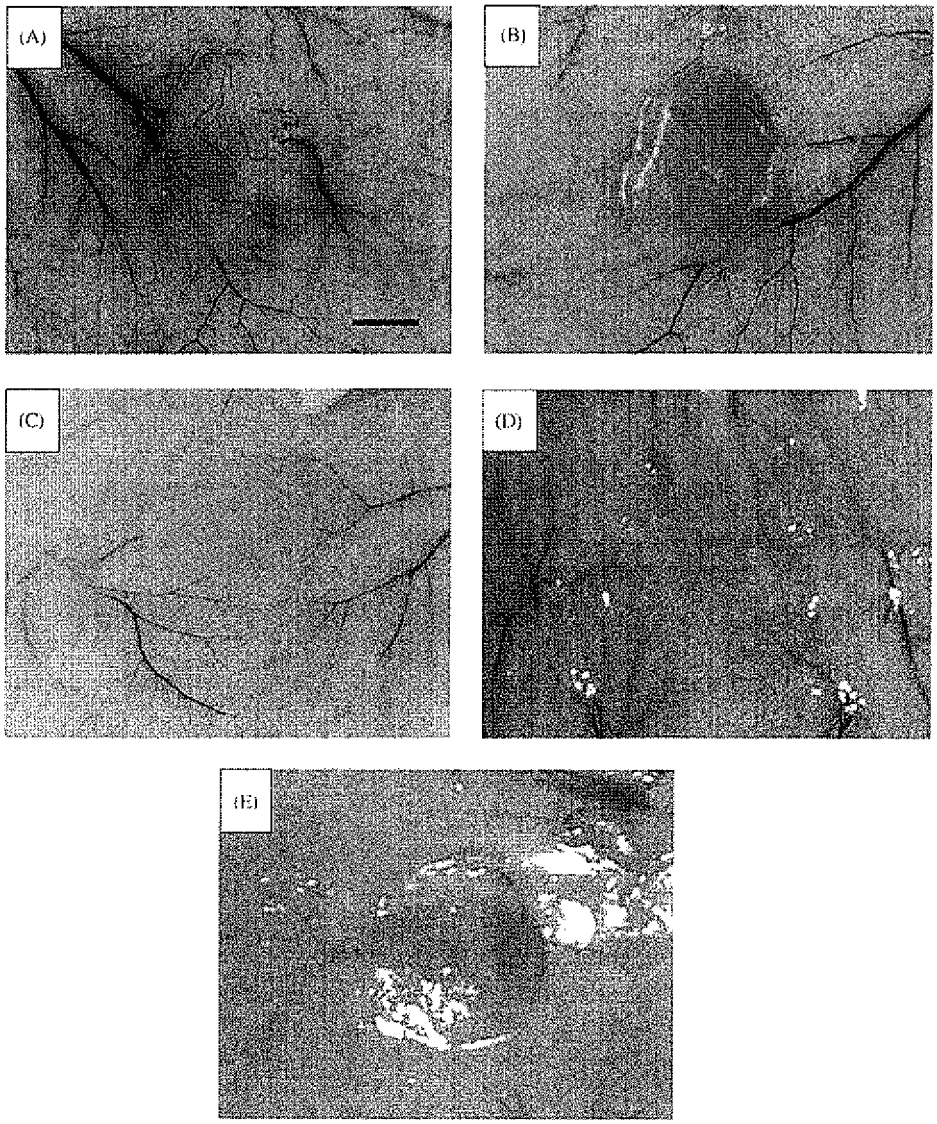

Fig. 1. Tissue appearance of mouse subcutis 6 weeks after implantation of a collagen sponge incorporating human preadipocytes and gelatin microspheres containing 1 μg of bFGF (A), a collagen sponge incorporating human preadipocytes and 10 μg of free bFGF (B), a collagen sponge incorporating human preadipocytes (C), a mixture human of preadipocytes and gelatin microspheres containing 1 μg of bFGF (D), and A collagen sponge incorporating gelatin microspheres containing 1 μg of bFGF (E). Bar = 3 mm. The number of preadipocytes transplanted is 1×10^5 cells/site.

cells with differentiation capacity [30]. The stem cells are morphologically and biochemically converted to matured adipocytes (fat cells) by way of adipose precursor cells [31,32]. Among the precursor cells are preadipocytes that have committed or determined to become fat cells and are included in interstitial cells having fibroblast-like morphology [33]. In addition, it has been demonstrated that the proliferation and differentiation of the precursor cells can be promoted depending on the microenvironment [13,34]. It is well recognized that the number of adipocytes and their precursor cells is only less than half that of total cells present in the adipose tissue and the remaining cells are vascular-related cells, like various blood cells, endothelial cells, and pericytes [12]. This tissue cellularity indicates that development of a vascular supply is essential for the generation and maintenance of adipose tissue. What is the local environment that allows adipose precursor cells to proliferate and differentiate into matured adipocytes? The present study clearly indicates that such an environment can be provided by implantation of the collagen sponge together with the release system of bFGF. There will be several reasons to be considered for the bFGF effect on induced adipogenesis. First, it is possible that the controlled release of bFGF induced angiogenesis, resulting in efficient proliferation and maturation of adipose precursor cells migrated in the in advance angiogenesis-induced scaffold because of

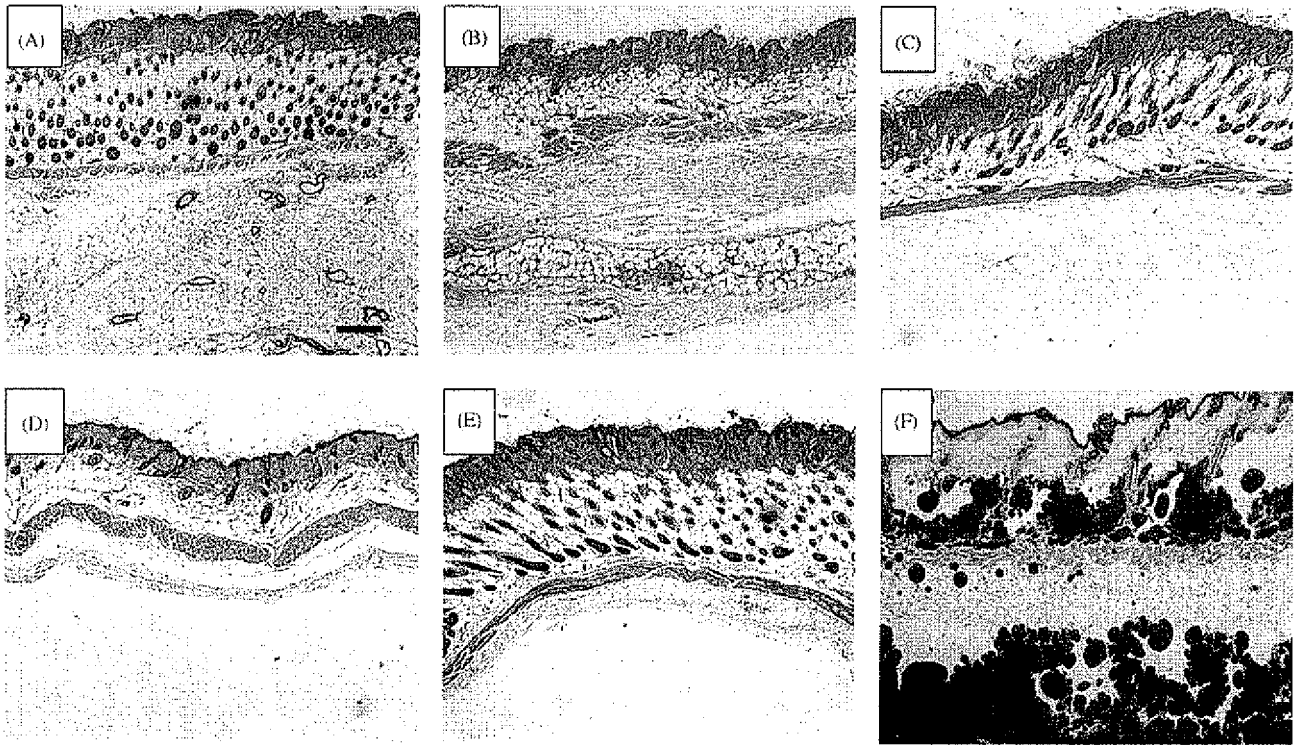

Fig. 2. Formation of adipose tissue in the mouse subcutis 6 weeks after implantation of a collagen sponge incorporating human preadipocytes and gelatin microspheres containing 1 μg of bFGF (A), a collagen sponge incorporating human preadipocytes and 10 μg of free bFGF (B), a collagen sponge incorporating human preadipocytes (C), a mixture of human preadipocytes and gelatin microspheres containing 1 μg of bFGF (D), and a collagen sponge incorporating gelatin microspheres containing 1 μg of bFGF (E) (magnification × 100, HE staining). (F) A Sudan III-stained section of group (A). The gelatin microspheres containing bFGF were completely degraded to disappear from the implanted site. Bar = 300 μm. The number of preadipocytes transplanted is 1×10^5 cells/site.

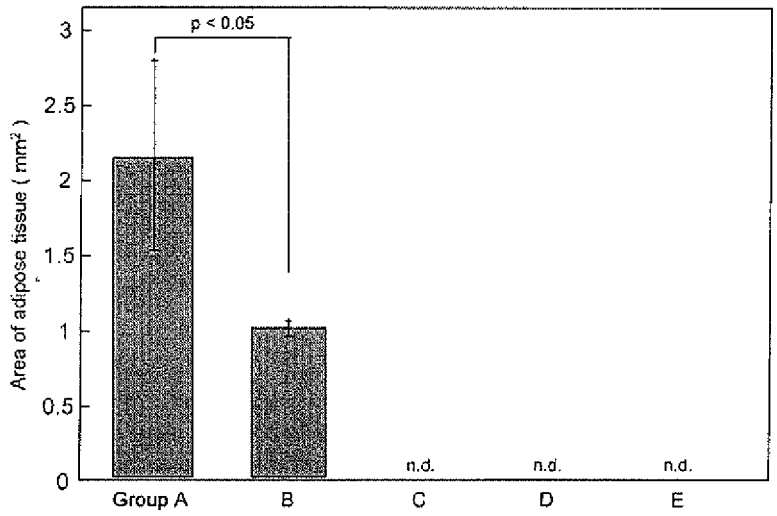

Fig. 3. The area of adipose tissue newly formed at the implanted site of mouse subcutis 6 weeks after implantation of a collagen sponge incorporating 1×10^5 human preadipocytes and gelatin microspheres containing 1 μg of bFGF (A), a collagen sponge incorporating human preadipocytes and 10 μg of free bFGF (B), a collagen sponge incorporating gelatin microspheres containing 1 μg of bFGF (C), a collagen sponge incorporating human preadipocytes (D), and a mixture of human preadipocytes and gelatin microspheres containing 1 μg of bFGF (E) (n.d.: not detected).

good supply of oxygen and nutrients to the cells. Indeed, the previous study indicated that such an angiogenesis-induced environment for tissue regeneration could be artificially created by implantation of Matrigel together with the release system of bFGF [24,25]. bFGF itself acts on the preadipocytes to accelerate their

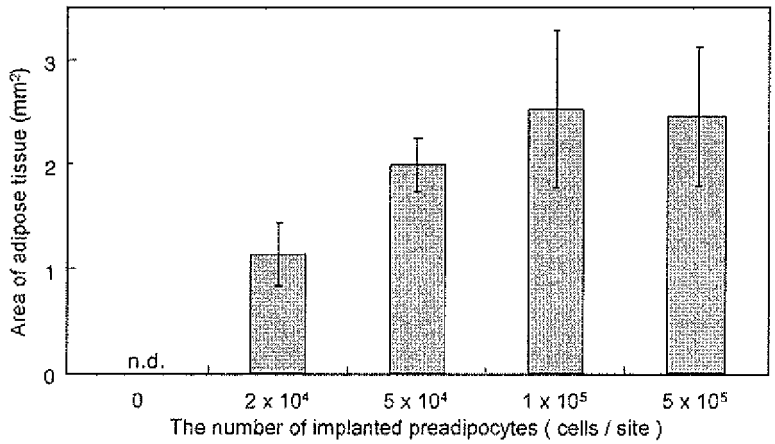

Fig. 4. Effect of preadipocytes number on the area of adipose tissue newly formed 6 weeks after subcutaneous implantation of collagen sponge incorporating human preadipocytes and gelatin microspheres containing 1 μg of bFGF into the back of mice (n.d.: not detected).

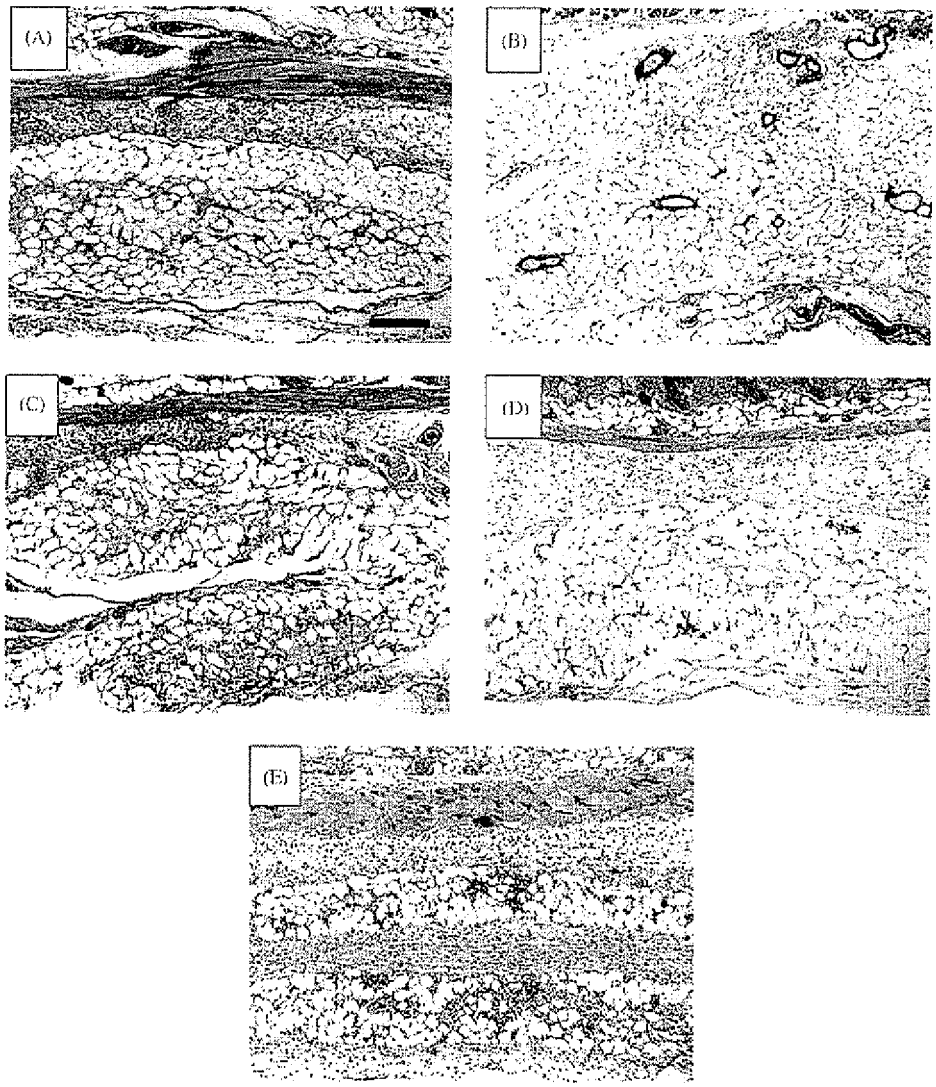

Fig. 5. Effect of the bFGF dose on the adipogenesis 6 weeks after subcutaneous implantation of collagen sponge incorporating human preadipocytes and gelatin microspheres containing bFGF into the back of mice: (A) 0.5, (B) 1, (C) 5, (D) 10, and (E) 50 μg bFGF/site (1×10^5 preadipocytes/site) (magnification × 100, HE staining, Bar = 200 μm).

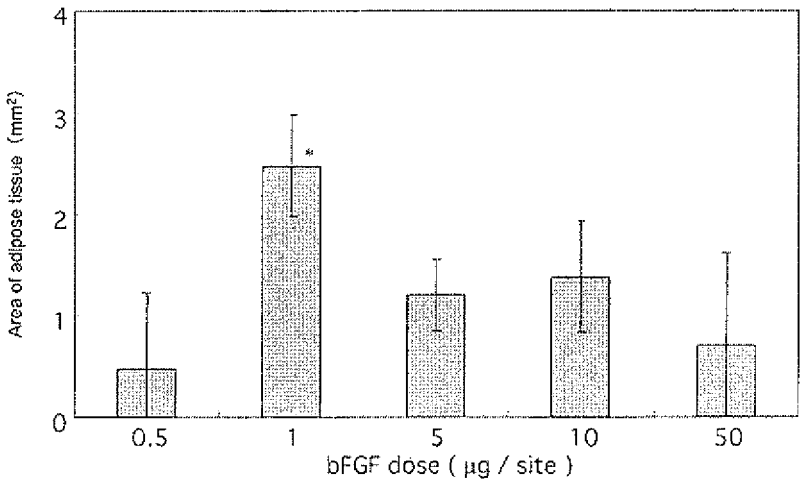

Fig. 6. Effect of the bFGF dose on the area of adipose tissue newly formed 6 weeks after subcutaneous implantation of collagen sponge incorporating human preadipocytes and gelatin microspheres containing 1 μg of bFGF into the back of mice (1×10^5 preadipocytes/site).

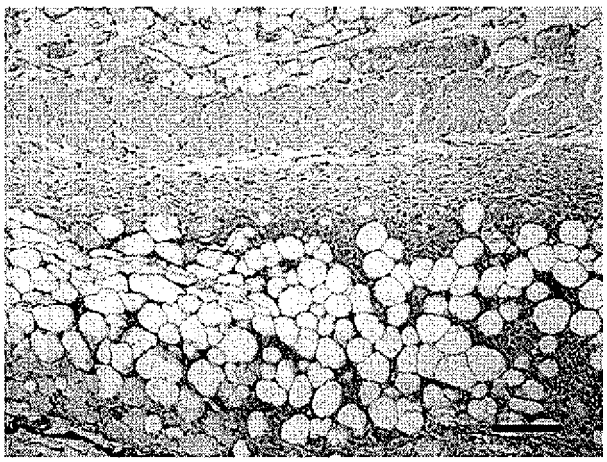

Fig. 7. Immunohistological section of adipose tissue newly formed 6 weeks after implantation of a collagen sponge incorporating human preadipocytes and gelatin microspheres containing 1 μg of bFGF (1×10^5 preadipocytes/site) (magnification × 200, Bar = 100 μm).

proliferation or other growth factors which are given by the bFGF-induced vasculature enables the cells to proliferate. It is conceivable that the collagen sponge plus the preadipocytes without the bFGF release system did not induce angiogenesis enough to maintain the survival of cells transplanted, resulting in no formation of fat tissue. The collagen sponge dose not have a function as the carrier of bFGF release [26], which will cause poor angiogenesis in the collagen sponge combined with preadipocytes and free bFGF. As a result, it is possible that the scaffold-cell-free bFGF combination results in poor adipogenesis compared with the scaffold-cell-released bFGF one. Secondly, we cannot rule out the possibility that bFGF has a direct adipogenic effect. Sheep preadipocytes have been reported to differentiate in a culture medium containing bFGF [35]. It is conceivable that the controlled release of bFGF increases the number of preadipocytes and the rate of adipocyte differentiation, resulting in totally enhanced adipogenesis.

One promising way to effectively induce in vivo angiogenesis is to achieve the controlled release of bFGF over an extended period of time. We have demonstrated that significant angiogenesis was induced through the controlled release of biologically active bFGF from gelatin hydrogel microspheres, in marked contrast to bFGF administered in the solution form [19–22]. Histological observation revealed that co-implantation of the gelatin microspheres containing bFGF-induced angiogenesis in the collagen scaffold to a greater extent than that of free bFGF. We can be fairly certain that such promoted angiogenesis was one of the key contributing factors to significantly pronounced formation of adipose tissue. In addition, the adipogenic effect of bFGF should be considered. The bFGF dose dependence indicates that there is an optimal concentration range of bFGF for adipogenesis. Probably, a low dose of bFGF is not enough to exert its angiogenetic or adipogenic effect even though the bioactive bFGF is released from the gelatin microspheres. On the other hand, when the bFGF dose is too high, in addition to the two effects of bFGF, the activity to accelerate infiltration of fibrous tissues into the collagen scaffold would become pronounced. A high dose of bFGF caused the inflammatory response at the collagen sponge implanted (Fig. 5). It is possible that the inflammation occurrence is so severe that prevents the tissue from tissue regeneration.

Fig. 7 clearly indicates that the adipose tissue newly formed throughout the inside of implanted collagen was prepared based on human-derived cells. The tissue engineering strategy based on combination of cells, the

scaffold, and growth factor was effective in inducing the regeneration of adipose tissue. However, the size of tissue formed was still too small to apply this technology to human therapy. Investigation about the scale-up of preadipocytes culture and technological design of enlarged tissue regeneration is underway at present.

References

[1] Billings Jr E, May Jr JW. Historical review and present status of free fat graft autotransplantation in plastic and reconstructive surgery. Plast Reconstr Surg 1989;83:368–81.

[2] Hartrampf CR, Scheflan M, Black PW. Breast reconstruction with a transverse abdominal island flap. Plast Reconstr Surg 1982;69:216–25.

[3] Ellenbogen R. Free autogenous pearl fat grafts in the face—a preliminary report of a rediscovered technique. Ann Plast Surg 1986;16:179–94.

[4] Smahel J. Failure of adipose tissue to heal in the capsule preformed by a silicone implant. Chir Plast 1985;8:109–15.

[5] Smahel J. Experimental implantation of adipose tissue fragments. Br J Plast Surg 1989;42:207–11.

[6] Ersek RA. Transplantation of purified autologous fat: a 3-year follow-up is disappointing. Plast Reconstr Surg 1991;87:219–27.

[7] Fagrell D, Eneström S, Berggren A, Kniola B. Fat clinder transplantation: an experimental comparative study of three different kinds of fat transplants. Plast Reconstr Surg 1996;98: 90–6.

[8] Tabata Y. The importance of drug delivery system in tissue engineering. Pharm Sci Tech Today 2000;3:80–9.

[9] Patrick Jr CW, Mikos AG, McIntire LV, editors. Frontiers in tissue engineering. Oxford: Pergamon, 1998.

[10] Patrick Jr CW. Adipose tissue engineering: the future of breast and soft tissue reconstruction following tumor resection. Semin Sur Oncol 2000;19:302–11.

[11] Brey EM, Patrick Jr CW. Tissue engineering applied to reconstructive surgery. IEEE Eng Med Biol Mag 2001;19:122–5.

[12] Zuk PA, Zhu M, Mizuno H, Huang J, Futrell JW, Katz AJ, Benhaim P, Lorenz HP, Hedrick MH. Multilineage cells from human adipose tissue: implications for cell-based therapies. Tissue Eng 2001;7:211–28.

[13] Green H, Kehinde O. Formation of normally differentiated subcutaneous fat pads by an established preadipose cell line. J Cell Physiol 1979;101:169–71.

[14] Patrick Jr CW, Chauvin PB, Hobley J, Reece GP. Preadipocytes seeded PLGA scaffolds for adipose tissue engineering. Tissue Eng 1999;5:139–51.

[15] von Heimburg D, Zachariah S, Heschel I, Kühling H, Schoof H, Hafemann B, Pallua N. Human preadipocytes seeded on freeze-dried collagen scaffolds investigated in vitro and in vivo. Biomaterials 2001;22:429–38.

[16] von Heimburg D, Zachariah S, Low A, Pallua N. Influence of different biodegradable carriers on the in vivo behavior of human adipose precursor cells. Plast Reconstr Surg 2001;108:411–20.

[17] Kawaguchi N, Toriyama K, Nicodemou-Lena E, Inou K, Torii S, Kitagawa Y. De novo adipogenesis in mice at the site of injection of basement membrane and basic fibroblast growth factor. Proc Natl Acad Sci USA 1998;95:1062–6.

[18] Passaniti A, Taylor RM, Pili R, Guo Y, Long PV, Haney JA, Pauly RR, Grant DS, Martin GR. A simple, quantitative method for assessing angiogenesis and antiangiogenetic agents using reconstituted basement membrane, heparin, and fibroblast growth factor. Lab Invest 1992;67:519–28.

[19] Tabata Y, Hijikata S, Ikada Y. Enhanced vascularization and tissue granulation by fibroblast growth factor impregnated in gelatin hydrogels. J Control Release 1994;31:189–99.

[20] Tabata Y, Ikada Y. Potentiated in vivo biological activity of basic fibroblast growth factor by incorporation into polymer hydrogel microsphere. Fourth Japan International SAMPE Symposium, vol. 4, Tokyo, Japan, 1995. p. 577.

[21] Tabata Y, Ikada Y. Protein release from gelatin matrices. Adv Drug Deliv Rev 1998;31:287–301.

[22] Tabata Y, Hijikata S, Muniruzzaman Md, Ikada Y. Neovascularizton effect of biodegradable gelatin microspheres incorporating basic fibroblast growth factor. J Biomater Sci Polym Ed 1999;10:79–94.

[23] Tabata Y, Nagano A, Ikada Y. Biodegradation of hydrogel carrier containing fibroblast growth factor. Tissue Eng 1999;5:127–38.

[24] Tabata Y, Miyao M, Ishii T, Hirano Y, Yamaoki Y, Ikada Y. De novo formation of adipose tissue by controlled release of basic fibroblast growth factor. Tissue Eng 2000;6:279–89.

[25] Kimura Y, Ozeki M, Inamoto T, Tabata Y. Time course of de novo adipogenesis in Matrigel by gelatin microspheres incorporating basic fibroblast growth factor. Tissue Eng 2002;8:603–13.

[26] Tabata Y, Nagano A, Muniruzzaman M, Ikada Y. In vitro sorption and desorption of basic fibroblast growth factor from biodegradable hydrogels. Biomaterials 1998;19:1781–9.

[27] Muniruzzaman M, Tabata Y, Ikada Y. Physicochemical properties of basic fibroblast growth factor–gelatin complex. J Bioact Compat Polym 2000;15:365–75.

[28] Tabata Y, Morimoto K, Katsumata H, Yabuta T, Iwanaga K, Kakemi M, Ikada Y. Surfactant-free preparation of biodegradable hydrogel microspheres for protein release. J Bioact Compat Polym 1999;14:371–84.

[29] Tabata Y, Ikada Y. Vascularization effect of basic fibroblast growth factor released from gelatin hydrogels with different biodegradabilities. Biomaterials 1999;20:2169–75.

[30] Caplan AI. Mesenchymal stem cells. J Orthop Res 1991;9: 641–50.

[31] Hauner H, Entenmann G, Wabitsch M, Gaillard D, Ailhaud G, Negrel R, Preiffer EF. Promoting effect of glucocorticoids on the differentiation of human adipocytes precursor cells cultured in a chemically defined medium. J Clin Invest 1989;84:1663–70.

[32] Wabitsch M, Brenner RE, Melzner I, Braun M, Moller P, Heinze E, Debatin KM, Hauner H. Characterization of a human preadipocyte cell strain with high capacity for adipose differentiation. Int J Obes 2001;25:8–15.

[33] Ailhaud G, Grimaldi P, Negrel R. Cellular and molecular aspects of adipose tissue development. Annu Rev Nutr 1992;12:207–33.

[34] Yuksel E, Weinfeld AB, Cleek R, Waugh JM, Jensen J, Boutros S, Shenaq SM, Spira M. De novo adipose tissue generation through long-term, local delivery of insulin and insulin-like growth factor-1 by PLGA/PEG microspheres in an in vivo rat model: a novel concept and capability. Plast Reconstr Surg 2000;105:1721–9.

[35] Broad TE, Ham RG. Growth and adipose differentiation of sheep preadipocyte fibroblasts in serum-free medium. Eur J Biochem 1983;135:33–9.

Available online at www.sciencedirect.com
SCIENCE DIRECT®
Biomaterials 26 (2005) 7025–7037
Biomaterials
www.elsevier.com/locate/biomaterials

Implantation of preadipocyte-loaded hyaluronic acid-based scaffolds into nude mice to evaluate potential for soft tissue engineering

Karsten Hemmrich[a,1], Dennis von Heimburg[a,1], Raoul Rendchen[a], Chiara Di Bartolo[b], Eva Milella[c], Norbert Pallua[a,*]

[a]*Department of Plastic Surgery and Hand Surgery, Burn Centre, University Hospital of the Aachen University of Technology, Pauwelsstr. 30, D-52057 Aachen, Germany*
[b]*Fidia Advanced Biopolymers S.r.l., via Ponte della Fabbrica 3/B, 35031 Abano Terme (PD), Italy*
[c]*PASTIS-CNRSM, Biomaterials Unit, S.S. 7 Appia, Km 714, 72100, Brindisi, Italy*

Received 4 November 2004; accepted 24 April 2005
Available online 17 June 2005

Abstract

The reconstruction of soft tissue defects following extensive deep burns or tumor resections remains an unresolved problem in plastic and reconstructive surgery since adequate implant materials are still not available. Preadipocytes, immature precursor cells found between mature adipocytes in adipose tissue, are a potential material for soft tissue engineering since they can proliferate and differentiate into adipose tissue after transplantation. In previous studies, we identified hyaluronan benzyl ester (HYAFF®11) sponges to be promising carrier matrices. This study now evaluates, in vitro and in vivo, a new sponge architecture with pores of 400 μm either made of plain HYAFF®11 or HYAFF®11 coated with the extracellular matrix glycosaminoglycan hyaluronic acid. Human preadipocytes were isolated, seeded onto carriers and implanted into nude athymic mice. Explants harvested after 3, 8, and 12 weeks were examined for macroscopical appearance, thickness, weight, pore structure, histology, and immunohistochemistry. Compared to previous studies, we found better penetration of cells into both types of scaffolds, with more extensive formation of new vessels throughout the construct but with only minor adipose tissue. Our encouraging results contribute towards a better seeded and vascularised scaffold but also show that the enhancement of adipogenic conversion of preadipocytes remains a major task for further in vivo experiments.
© 2005 Elsevier Ltd. All rights reserved.

Keywords: Adipose tissue engineering; Hyaluronic acid; Progenitor cell

1. Introduction

Preadipocytes, stem-cell derived precursor cells which are located between mature adipocytes in adipose tissue [1], are a promising material for tissue engineering of bones, cartilage, muscle, fat, and other mesenchymal tissue types since these cells are capable of differentiating into a variety of cell types, including osteoblasts, chondrocytes, myoblasts, neuron-like cells, and adipocytes [2,3]. We here focus on the application of preadipocytes for soft-tissue defect reconstruction since successful long-term treatment of these defects remains an unresolved problem in plastic and reconstructive surgery. Disfiguring soft-tissue defects are caused by trauma (e.g. extensive deep burns, avulsions, post-surgical defects), tumors (e.g. breast cancer), or congenital deformities like Romberg's disease [4] or Poland syndrome [5]. In most cases, dissatisfaction is caused by the absence or the loss of subcutaneous adipose tissue. Since soft tissue plays a major role in maintaining contours and also serves as a mechanical cushion for muscles, tendons, and bones, a restoration of this protecting tissue is necessary. Possible approaches are

*Corresponding author. Tel.: +49 0 241 8089701; fax: +49 0 241 8082448.
E-mail address: npallua@ukaachen.de (N. Pallua).
[1]Both authors are first authors.

0142-9612/$ - see front matter © 2005 Elsevier Ltd. All rights reserved.
doi:10.1016/j.biomaterials.2005.04.065

local and free flaps, dermal fat grafts, collagen injections, synthetic materials, and the transfer of free adipose tissue grafts. Unfortunately, all of these methods include serious disadvantages: while synthetic materials always cause foreign body reactions, biologically derived materials shrink to an unpredictable extent [6]. Many studies show that free adipose tissue grafts are largely absorbed or replaced by fibrous tissue and oil cysts [7] although some reports also demonstrate increasing survival of the transplanted tissue by careful handling [8,9].

Preadipocytes have a high proliferation and differentiation capacity whereas fully differentiated adipocytes have lost the capacity to divide [10]. Furthermore, adipogenic progenitors have a lower oxygen consumption than mature fat cells [11]. This tolerance of ischemia is helpful for survival of the time period until grafts are sufficiently vascularised. In order to use preadipocytes for tissue engineering purposes, cells are isolated from adult human adipose tissue, cultured and seeded onto carriers to avoid that they are washed away from the site of transplantation. The use of carriers also allows a better determination of cell survival, differentiation, and newly formed extracellular matrix. Beside chemical composition and mechanical stability, an adequate porous structure of the matrix is very important to allow cellular penetration into the construct and full differentiation inside after transplantation. During differentiation, adipocytes store lipids in cellular vacuoles thereby gaining volume up to 20-fold. Hence, appropriate porous structures are required not to inhibit the growth process and differentiation of the seeded and subsequently growing (pre)adipocytes. Earlier experiments of our group with collagen-based scaffolds, one of the first biodegradable carriers, have shown that a pore diameter of 45 μm is too small for preadipocytes since the cells increase in size when undergoing differentiation [12]. Hyaluronic acid, present in the extracellular matrix of many tissues, is a newer material in tissue engineering and is assumed to have a supportive effect on progenitor cell development thereby facilitating tissue repair [13]. Therefore, we next compared collagen sponges with hyaluronan benzyl ester (HYAFF®11) scaffolds and found that hyaluronan carriers showed better results in terms of weight, homogenous distribution of precursor cells, and amount of differentiated adipose tissue [14]. Pore diameter in these HYAFF®11 sponges varied between 50 and 340 μm. Disadvantages of these constructs were that scaffold penetration was insufficient and seeding of the matrix with cells was very time consuming due to the slow uptake of the preadipocyte suspension by the porous system. Therefore, this study now evaluates HYAFF®11 scaffolds with a totally new architecture, a unique pore diameter of 400 μm, in vitro and in vivo, to improve scaffold penetration. Furthermore, to facilitate and accelerate the seeding process, we compared unmodified HYAFF®11 carriers (HYAFF®11-LP, HS) to HYAFF®11 sponges additionally coated with the extracellular matrix glycosaminoglycan (GAG) hyaluronic acid (HYAFF®11-LP-coated, HB). Human preadipocytes of adults from 15 to 72 years of age were isolated, cultured in two different types of sera (fetal calf serum (FCS), serum poor platelet plasma (SPPP)), and seeded onto carriers. In vitro analyses were performed to analyse fluid uptake of the construct, cell adherence to surfaces and serum-dependent proliferation on sponges. Afterwards, cell-loaded scaffolds were implanted into nude athymic mice and explanted after 3, 8, and 12 weeks. All samples were examined for macroscopical appearance, thickness, weight, pore structure, and histology to find out whether the new pore architecture and/or additional hyaluronic acid coating of carriers have a beneficial effect on cell distribution and proliferation, vascularisation, and adipose tissue formation in sponges.

2. Materials and methods

2.1. Materials

Sponges made of HYAFF®11, a linear derivative of hyaluronic acid, in which the carboxylic function of the monomer glucuronic acid in the hyaluronic acid chain is totally esterified with benzyl groups [15], were supplied by Fidia Advanced Biopolymers (Abano Terme/Italy). The structure of these sponges shows open interconnecting pores (compare Fig. 1). Two types of sponges were used, one plain (HYAFF®11-LP, HS) and one coated with hyaluronic acid (HYAFF®11-LP-coated, HB) (Fig. 1). Sponges were provided as cylinders ($\varnothing$ 14 mm, $h = 4$ mm; $V = 616\,\text{mm}^3$). Coated sponges (HB) were obtained by submersion in a hyaluronic acid solution, followed by freeze-drying. Weight of hyaluronic acid/weight of HYAFF®11 scaffold was 15%. All carriers were sterilised by γ-irradiation before use.

Collagenase solution type I, M199, Dulbecco's modified Eagle medium (DMEM), Ham's F12 (F12), and FCS were from Biochrom, Berlin/Germany. Trypsin/EDTA was purchased from PAA Laboratories, Cölbe/Germany. Serum of platelet poor plasma (SPPP) was from Sigma, München/Germany, basic fibroblast growth factor (bFGF) from Tebu, Frankfurt/Germany. The 250 μm nylon sieve was from Verseidag Techfab GmbH, Geldern/Germany. DAB (LSAB-kit) and all antibodies used here were from DAKO, Hamburg/Germany. All other materials were of best quality and purchased from diverse conventional suppliers.

2.2. Isolation, culturing, and seeding of preadipocytes

Preadipocytes were isolated out of fragments (38–90 g per fragment) freshly obtained from human subcutaneous adipose tissue of healthy donors between 15 and 72 years of age who had undergone elective operations (e.g. breast reduction) at the Department of Plastic Surgery and Hand Surgery—Burn

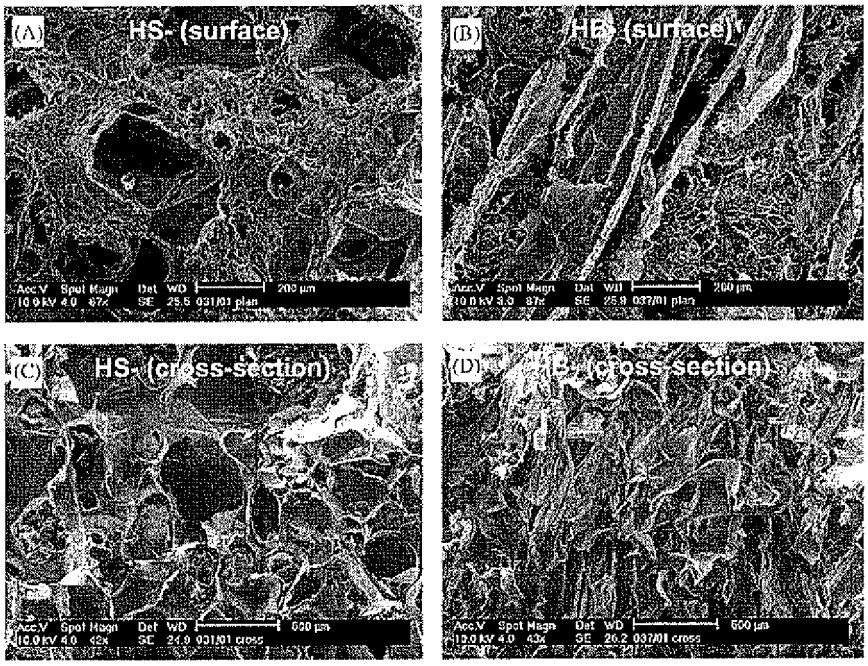

Fig. 1. Analyses of HYAFF®11-biohybrids by electron microscopy. Two different kinds of hyaluronic acid-based sponges, HYAFF®11-LP (HS) and HYAFF®11-LP-coated (HB), with a unique pore size of 400 μm were analysed by electron microscopy. Shown here are surface (Fig. 1A and B) and cross-section (Fig. 1C and D) of the unloaded sponges.

Centre. After removal of fibrous tissue, adipose tissue was chopped into pieces and digested by collagenase (0.1 U ml^{-1}/ dispase 0.8 U ml^{-1}, Boehringer Mannheim, Germany) under permanent shaking in a water bath at 37 °C for 60 min. Digestion was stopped by adding DMEM containing 10% FCS or 10% SPPP, respectively, followed by an incubation in erythrocyte lysis buffer (154 mmol l^{-1} NH_4Cl, 10 mmol l^{-1} $KHCO_3$, 1 mmol l^{-1} EDTA) for 10 min. This cell suspension was centrifuged (200*g* for 10 min at 17 °C) and the pellet was used for culture. For this purpose, cells were seeded on tissue culture dishes (63.6 cm^2, Greiner, Solingen, Germany) with M199 plus 10% FCS or 10% SPPP (supplemented with 1 nM bFGF, 100 U ml^{-1} Penicillin, and 100 μg ml^{-1} Streptomycin) with a seeding density of 3×10^4 cells cm^{-2}. After 24 h, medium was changed to DMEM/F12 (1:1) plus the additives as used before. Preadipocytes of the second passage were trypsinised at confluence and used for seeding of sponges. For all experiments, preadipocytes from three different donors were pooled by mixing one frozen and re-thawed and two freshly obtained cell samples. All trials involving the use of human preadipocytes had been approved by the Ethical Committee of the Aachen University of Technology.

2.3. Preparation of hyaluronic acid-based sponges for in vitro analyses and for implantation

Uncoated scaffolds (HS) were precoated 24 h before seeding with 1000 μl FCS or SPPP (800 μl at the bottom side and 200 μl on top) at 37 °C. Hyaluronic acid-coated sponges were used withouth pretreatment. Each scaffold was inoculated with 1×10^6 pooled preadipocytes/600 μl culture medium. After 4 h, 2 ml culture medium were added. For in vitro examinations of cell adherence and proliferation on carriers, sponges were analysed after 3, 7, and 14 days (d), and histologically evaluated. Cell adherence was determined by counting non-attached cells, which adhered on the bottom of the seeding dish and in the supernatant instead of the scaffold, in a Neubauer's chamber. Cell viability was routinely checked by trypan blue exclusion assays and was always below 8%. For in vivo studies, HS and HB samples were left undisturbed in DMEM/F12 (1:1) plus Penstrep/Streptomycin in the incubator for 24 h until implantation.

2.4. Determination of three-dimensional growth of preadipocytes in various sera

To monitor preadipocyte proliferation and viability on HYAFF®11 sponges, the MTT assay was chosen. Preadipocytes from three donors were pooled and expanded. Sponges were inoculated with 1 million cells each. Formazan formation by the composites was analysed 3, 7, and 14 d after seeding. As control, one scaffold for each time point and material was cultured without cells. To measure formazan formation, biohybrids were transferred to a 24-well plate and washed twice with PBS^{2-}. Each composite was then treated with 5 mg ml^{-1} MTT in a cell incubator for 45 min at 37 °C. Thereafter, all probes were washed again prior to extraction with isopropanol/0.04 M HCl for 3 h. Extraction was completed by vortexing and centrifugation for 5 min at 13500 rpm. Supernatant was used in a 1:4 dilution with isopropanol/0.04 M HCl and extinction was analysed in a microtiterplate (570 nm).

2.5. Histological and immunhistological examination of developed biohybrids

Scaffolds from in vitro and in vivo trials were fixed overnight in Lidi's 4% formalin. After removal of formalin by exhaustive washes with water, the probes were dehydrated by increasing concentrations of isopropanol, embedded into paraplast, and cut into 2 and 8 μm sections. Paraplast was removed from sections with xylol followed by staining with Hematoxylin and human vimentin according to histological standard procedures. Immunocytochemical staining of human vimentin was performed with a mouse anti-human vimentin antibody (1:50 and 1:75, mahv, clone V9, Code Nr. M 0725 Lot 057). Detection of the primary antibody was achieved with a biotinylated secondary antibody and peroxidase-conjugated streptavidin and DAB as substrate.

2.6. In vivo experimental model: nude mouse

The fabricated preadipocyte/sponge matrix constructs (total 120: 60 HS: 30 seeded constructs (HS+), 30 controls (HS−); 60 HB: 30 seeded constructs (HB+), 30 controls (HB−)) were transplanted subcutaneously to the right and left scapular area of 60 athymic, 8-week-old nude mice. Mice were operated under aseptic conditions and inhalation anesthesia (Enflurane®). The bottom of the constructs was placed on the muscle fascia. In each of these animals, the cell-loaded sample was transplanted to the right and the control scaffold (HS-/HB-, without cells, 24 h, soaked with DMEM) to the left scapular area through separate incisions. All animal experiments were performed according to the animal protection laws and were officially permitted.

After 3 weeks (group A), 8 weeks (group B), and 12 weeks (group C), 10 animals of the HS and 10 animals of the HB group were killed by an overdose of gaseous anesthetic and the grafts were explanted. These three groups were formed randomly. The macroscopic (colour, ingrowth and formation of vessels, weight, thickness) and microscopic (pore size, specific and unspecific cellularity, vascularity) aspects of the grafts were documented after excision.

2.7. Examination of the grafts after explantation

The weight of each scaffold was assessed 24 h after the cells had been seeded onto the sponge (before implantation), and after explantation (3, 8, 12 weeks—groups A, B, and C).

Two blinded examiners (D.v.H., R.R.) independently assessed the histological sections. When there were differences between the assessments, the mean value was calculated.

The thickness of the grafts was evaluated by measuring the thickness of the cross-sectional cut of the hyaluronic acid scaffolds at three different sites using intraocular micrometer (Zeiss, Germany). A mean value for each graft was calculated.

For analyzing specific and unspecific cellularity of the grafts, microscopical fields of the cross-sectional cuts were examined at 200× magnification. Overall cellularity was assessed by counting of all stained cells in histological sections of bottom, centre, and surface areas. Cellularity of seeded preadipocytes was analysed by counting all human-vimentin positive cells.

2.8. Statistical evaluation

Data of thickness and weight of the grafts, pore size as well as overall cellularity in the grafts were expressed as mean value ± SD. The significance of differences was evaluated by the t-test for in vitro analyses of scaffolds and by the Mann–Whitney U-test for in vivo experiments. Differences at $p < 0.05$ were considered significant.

3. Results

3.1. Structural and hydrophilic properties of the hyaluronan sponges HYAFF®11-LP and HYAFF®11-LP-coated

Two different kinds of hyaluronic acid-based sponges, HYAFF®11-LP (HS) and HYAFF®11-LP-coated (HB), with a unique pore size of 400 μm were analysed by electron microscopy (EM). Shown in Fig. 1 are pictures from surface and the inner architecture of unloaded sponges.

EM pictures of HS sponges reveal an open porous structure with a rather unique pore size of about 400 μm. Apart from a few ruptured pores, most cavities have approximately equal diameters with an elliptical form. HB carriers, in contrast, contain many compressed or ruptured pores and the network of pores has a rather linear orientation. The pore diameter appears smaller than in the HS sponge, approximately 350 μm.

Hydrophilic or hydrophobic properties of HYAFF® 11-biohybrids were analysed by dropping 600 μl of a bromphenol blue solution on the surface of the contructs and measuring the absorption by the sponge after 1 h (Fig. 2B), 4 h (Fig. 2C), and 7 h (Fig. 2D). In Fig. 2A, the HYAFF®11 sponges are shown before addition of the solution. Our findings clearly demonstrate that the coating with hyaluronic acid significantly accelerates the uptake of fluid by the sponge. Already after 1 h, the fluid has almost completely penetrated the coated construct whereas in HS, surface properties still prevent the droplet from soaking into the material. Not even after 7 h, the HS sponge is completely penetrated by the fluid.

3.2. Attachment and growth of preadipocytes on hyaluronic acid-based sponges under different culture conditions

HS and HB sponges were prewetted with FCS or SPPP. Each scaffold was then inoculated with 1×10^6 pooled preadipocytes, placed in the incubator for 4 h and analysed afterwards for preadipocyte attachment. As shown in Table 1, the range of non-attached cells was approximately 1.5–3.5% in all sponges. Adherence of preadipocytes to sponges was higher in HS than in HB.

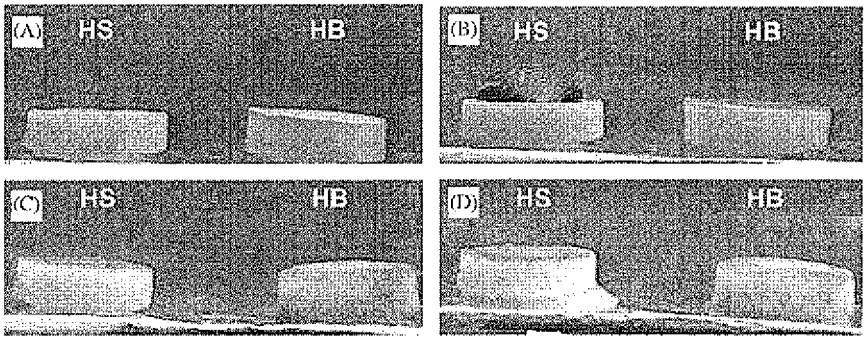

Fig. 2. Analyses of hydrophilic properties of HYAFF®11-biohybrids. A bromphenol blue solution (600 µl) was given on HYAFF®11-LP (HS) and HYAFF®11-LP-coated (HB) and absorption by the sponge was analysed after 1 (Fig. 2B), 4 h (Fig. 2C), and 7 h (Fig. 2D). Fig. 2A shows the sponges before addition of the solution.

Table 1
Comparison of cell attachment in cell-loaded HYAFF®11-LP and HYAFF®11-LP-coated sponges under different culture conditions

Sponge	Cells not attached to the matrix (%)
HYAFF®11-LP-coated (HB) with FCS (no pretreatment)	2.69±0.59*
HYAFF®11-LP-coated (HB) with SPPP (no pretreatment)	2.92±0.51
HYAFF®11-LP (HS) with FCS (precoating FCS)	1.78±0.26
HYAFF®11-LP (HS) with SPPP (precoating SPPP)	2.67±0.81

24 h before seeding, uncoated scaffolds were precoated with 1000 µl FCS or SPPP (800 µl at the bottom side and 200 µl on top) at 37 °C. According to the medium supplementation, FCS or SPPP were used for precoating of HS sponges. Coated sponges (HB) were used without pretreatment. Each scaffold was then inoculated with 1×10^6 pooled preadipocytes/600 µl culture medium supplemented with FCS or SPPP, respectively. After 4 h, sponges were removed and uninoculated cells left in the supernatant and on the culture dishes were counted. Shown here are data from three independent experiments. Cell counts are given in percentage±SD relative to the amount of initially seeded cells, i.e. 1×10^6 cells.
*$p < 0.01$ compared to Hyaff®11-LP (HS) with FCS.

However, this difference was only significant for FCS-cultured cells (Table 1). Furthermore, preadipocyte attachment was generally higher if FCS and not SPPP was used in the culture medium. For cell proliferation analyses on carriers, serum-supplemented (FCS or SPPP) medium was added and sponges were histologically analysed for preadipocyte proliferation after 7 and 14 d. Both carriers, HS+ and HB+, showed good spreading and distribution of preadipocytes (Fig. 3). However, matrices with FCS-supplemented medium revealed significantly higher cell numbers than SPPP-cultivated scaffolds, as confirmed by formazan formation in the MTT assay (Table 2, Fig. 3). Comparing HS and HB sponges in terms of preadipocyte proliferation after 7 and 14 d, we found no significant differences.

3.3. *In vivo experiments: nude mouse study*

All 120 grafts were included in the evaluation since there had been no infections and no animal had died during the operation or during the observation period.

3.4. *Vascularisation and texture of explanted scaffolds*

Unseeded and seeded HS and HB carriers were implanted in nude mice and explanted after 3, 8, and 12 weeks. Grafts could easily be identified in all animals, even after 12 weeks. Cell-loaded transplants revealed very thin but tightly integrated vessels in almost all layers of the sponge thereby presenting a more intense vascularisation than controls (see also Table 3). This was most obvious in 8-week explants (group B: Fig. 4B and E). The contrast in vessel formation between seeded and unseeded sponges was macroscopically a little more evident in HB (Fig. 4D–F) than in HS (Fig. 4A–C). Microscopical analyses confirmed the differences between HS+/HB+ and HS−/HB−, however, they did not reveal a superiority of hyaluronic acid-coated sponges in new vessel formation as predicted from the macroscopical impression.

The texture of the scaffolds from group A had changed during the 3-week-implantation period to the same extent in cell-loaded as in unloaded sponges from a soft to a more tough kind. Both, HS+ and HB+ carriers, were slightly bigger than the matching controls.

In group C (12 weeks after implantation), the surfaces of explanted HS+ and HB+ sponges showed macroscopically only a weak vascularisation. Microscopically, however, these explants revealed the best overall vessel formation of all samples (Table 3). Compared to groups A and B, degradation of scaffolds was more obvious in the sponges explanted after 12 weeks (Fig. 4).

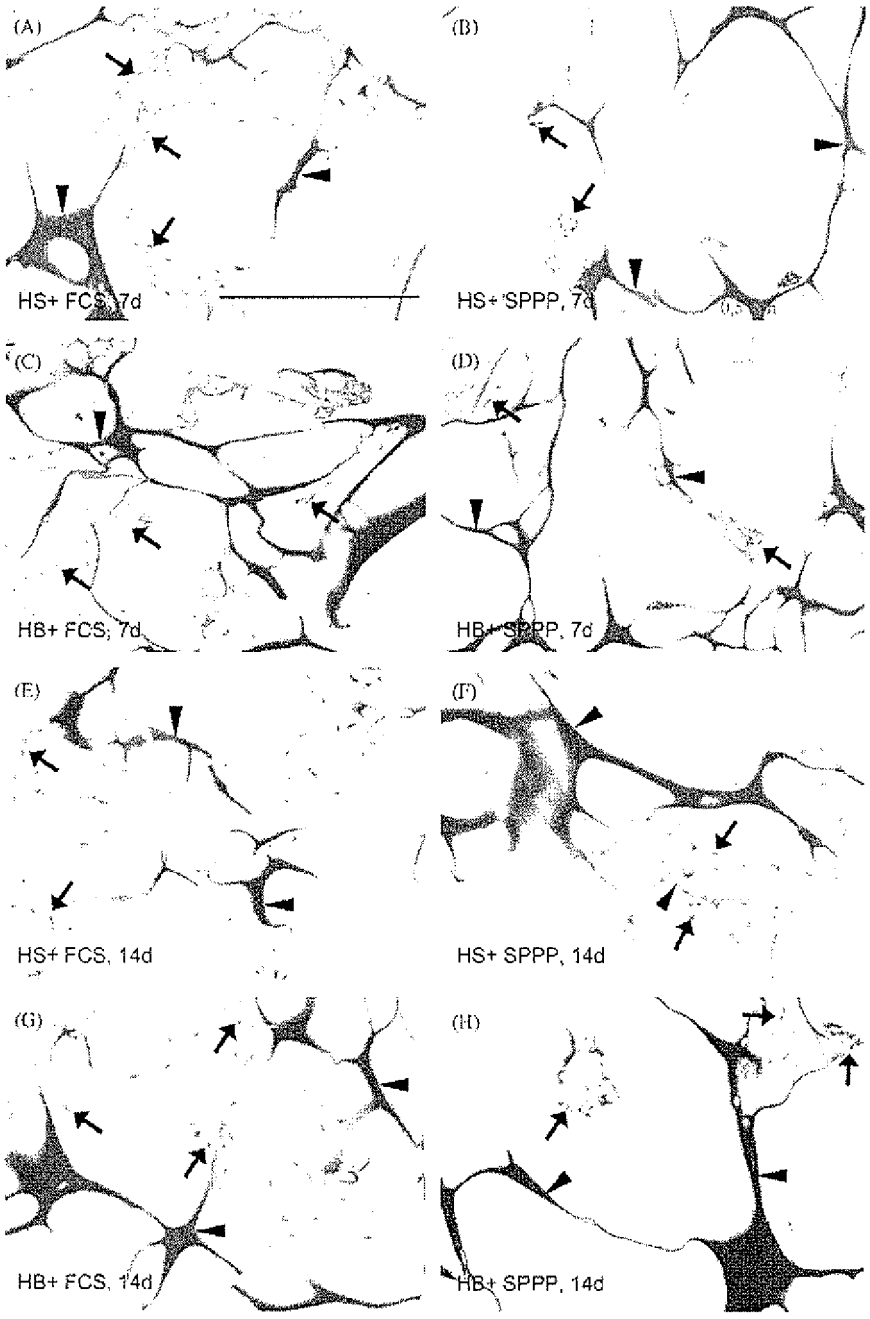

Fig. 3. In vitro preadipocyte growth in cell-loaded HYAFF®11-biohybrids under FCS- versus SPPP-treatment. Human preadipocytes of the second passage at confluence were trypsinised and resuspended. A suspension of 600 µl, containing 1×10^6 cells, was seeded on both types of HYAFF®11-sponges. The uncoated carriers had been prewetted with 1000 µl FCS or SPPP (800 µl at the bottom side and 200 µl on top) whereas coated sponges did not receive any pretreatment. Scaffolds were then left in the incubator for cell proliferation. After 7 and 14 d, sponges were histologically analysed for preadipocyte proliferation. Shown are Giemsa-stained histological samples of HYAFF®11-LP (HS) (Fig. 3A, B, E, F) and HYAFF®11-LP-coated (HB) (Fig. 3C, D, G, H) after 7 d (Fig. 3A–D) and 14 d (3E–H). Magnification × 50. Bar in Fig. 3A represents 0.5 mm. ➡, preadipocytes; ▶, HYAFF®11-sponge material.

3.5. *Thickness and weight of preadipocyte-loaded and control grafts*

Thickness and weight of preadipocyte-loaded and control grafts were measured on explants after 3, 8, and 12 weeks. Even though thickness in both sponges after 3 weeks was identical to the original measurements before implantation, both scaffold types showed a slight decrease in thickness with time. This was more obvious in HB+ (Fig. 5A). Controls were always 0.2–0.5 mm

Table 2
Preadipocyte growth in HYAFF®11-biohybrids under FCS- versus SPPP-treatment *in vitro*

	Formation of formazan [$E_{570\,nm}$]			
	After seeding	3 days	7 days	14 days
HS+, FCS	0.125±0.024*	0.145±0.016	0.305±0.022*	0.408±0.055*
HS+, SPPP	0.098±0.012	0.120±0.022	0.181±0.037	0.322±0.039
HB+, FCS	0.087±0.021	0.187±0.029*	0.263±0.018*	0.468±0.038*
HB+, SPPP	0.097±0.011	0.122±0.014	0.198±0.021	0.365±0.033

To monitor preadipocyte proliferation and viability on hyaluronic acid-based sponges under different medium conditions, the MTT assay was chosen. Sponges were inoculated with 1×10^6 preadipocytes each. Formazan formation by the composites was analysed after 3, 7, and 14 d after seeding. As control, one scaffold for each time point and material was cultured without cells. Extinction of formazan is given as means±SD related to control. Results are from three independent experiments.
*$p < 0.001$ compared to equivalent sponges under SPPP-treatment.

Table 3
Quality of vascularisation in the hyaluronic acid-based scaffolds HYAFF®11-LP and HYAFF®11-LP-coated

Vascularisation	3 weeks	3 weeks	8 weeks	8 weeks	12 weeks	12 weeks
HYAFF®11-LP scaffold (HS)						
	HS−[a]	HS+	HS−	HS+	HS−	HS+
−	1	2	0	0	0	0
+	5	3	0	0	1	0
+ +	0	1	6	2	5	2
+ + +	0	0	0	4	0	4
Total	+	+	+ +	+ + +	+ +	+ + +
HYAFF®11-LP-coated scaffold (HB)						
	HB−[a]	HB+	HB−	HB+	HB−	HB+
−	2	0	0	0	0	0
+	2	5	3	0	0	0
+ +	2	1	2	5	5	3
+ + +	0	0	1	1	1	3
Total	+	+	+ +	+ +/+ + +	+ +/+ + +	+ + +

Vascularisation in HS and HB was analysed in explants after 3, 8, and 12 weeks in the nude mouse and estimated by microscopical analyses in the cross-sections. No visualisation of vessels was defined as "−", visualisation of vessels in one or more surface regions was rated as "+", in the central region "+ +" and a homogenous distribution of vessels within the graft was rated "+ + +".
We observe a significant increase in vessel formation from 3 to 12 weeks in both types of sponges.
[a]HS+/HB+: sponges initially seeded with preadipocytes, HS−/HB−: control scaffolds without cell seeding

smaller than cell-loaded constructs. They also showed a decrease in size in the course of time parallel to their cell-loaded counterparts. HB− sponges were initially thicker than the corresponding HS− carriers but subsequently revealed a more progressive reduction in thickness at 8 and 12 weeks.

Weight analyses showed that preadipocyte-loaded constructs were always heavier than the control grafts (Fig. 5B). This finding was very prominent at 3 weeks after implantation and especially for HS sponges, since weights of these cell-seeded scaffolds were significantly increased at this point of explantation. Besides, our results show that highest weights were found after 3 weeks in cell-loaded constructs with a constant decrease in weight from that point on for both types of scaffolds. This change was especially obvious between 3-week and 8-week explants. Comparing both types of sponges, coated and uncoated structures, individually, we found that HS+ scaffolds were significantly heavier than HB+ carriers at 3 weeks. Explants from 8 and 12 weeks did not show this difference.

3.6. Changes in pore size and specific/unspecific cellularity

Changes in pore size in hyaluronic acid-based constructs were examined by microscopy on explanted grafts after 3, 8, and 12 weeks. We found that the pore size of preadipocyte-loaded scaffolds was always 0.12–0.25 mm higher than in the controls but decreased

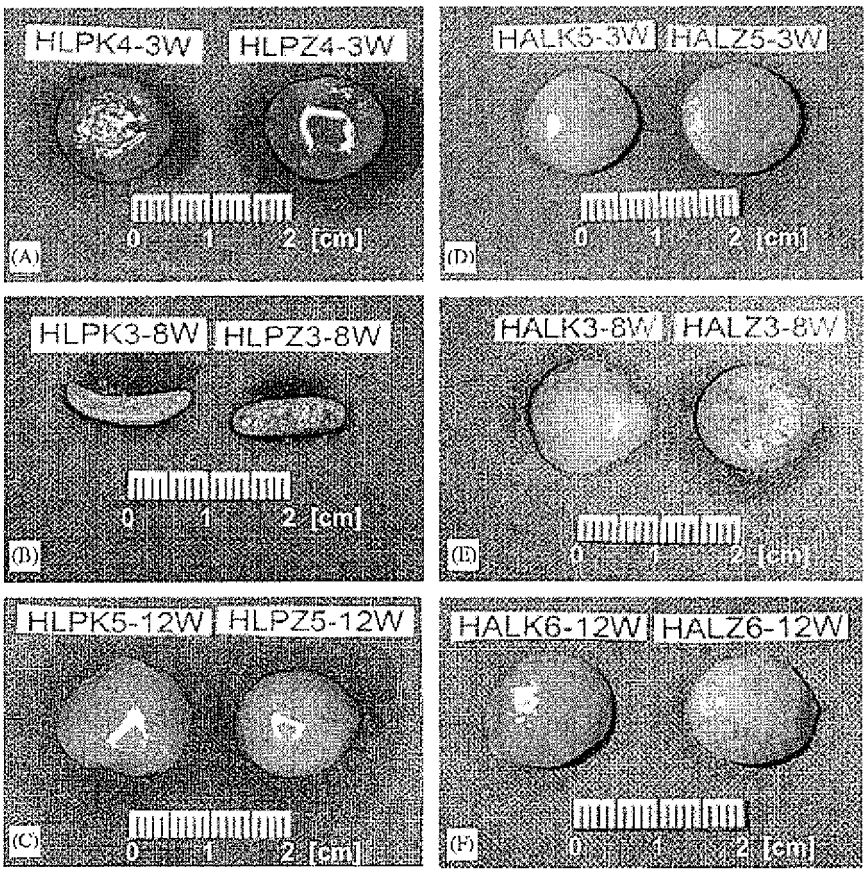

Fig. 4. Macroscopical examination of scaffolds. Preadipocytes were grown to confluence, trypsinised, resuspended and 1×10^6 cells were seeded on prewetted scaffolds in a suspension of 300 µl. Sponges were then implanted in nude mice, and explanted after 3, 8, and 12 weeks. Control groups without cells are located on the left side and preadipocyte-loaded scaffolds are on the right side in every photo. (A)–(C) Shown are explanted HS scaffolds. (D)–(F) Results from explanted HB scaffolds. HLPK: HYAFF®11-LP unseeded; HLPZ: HYAFF®11-LP seeded; HALK: HYAFF®11-LP-coated unseeded; HALZ: HYAFF®11-LP-coated seeded; 3W, 6W, 12W: weeks of implantation.

constantly from 3 to 12 weeks (Fig. 6A). This continuous reduction in pore diameter was especially prominent in HB+. While there was hardly any difference in pore size between HS+ and HB+ at 3 weeks (difference: 0.011 mm), pore diameters differed dramatically after 12 weeks of implantation (difference of 0.117 mm). The pore size in unloaded HS− controls after 3 weeks of implantation exactly matched the original measurements of the pore structure whereas HB− carriers at 3 weeks already showed a slight reduction in pore size. In the course of time, we observe a significant and continuous decrease in pore size which was more prominent in HB− than in HS− sponges (Fig. 6A).

Examining specific cellularity of human preadipocytes versus unspecific cellularity of other cells (Fig. 6B), we found that in all samples, cellularity was higher in preadipocyte-loaded scaffolds than in controls. However, this difference between loaded and unloaded samples was only significant for HB at 12 weeks. Highest numbers of cells were detected in 8-week explants.

3.7. Histological and immunohistochemical examination of scaffolds

Hematoxylin plus human vimentin/peroxidase stained HS+ and HB+ sponges were histologically compared to controls after 3, 8, and 12 weeks (Fig. 7). After 3 weeks, a good spreading and distribution of preadipocytes over the whole cross-section was visible. There are clearly more cells detectable in the preadipocyte-loaded biohybrids than in the control sponges. Examining 8- and 12-week explants, we found that control-scaffolds were more degraded than cell-loaded sponges. This decomposition was especially prominent in unseeded HB sponges (compare Fig. 7K and L). Immunohistological characterisation of the explants with human vimentin/peroxidase staining confirmed a good distribution of preadipocytes over the whole cross-section (Fig. 7). Human preadipocytes were well distinguishable from cells of mouse origin. Adipose tissue formation was only observed in Fig. 7I, however, this tissue is likely to be a part of the subcutaneous adipose tissue layer since a layer of fibrous tissue separates it from the

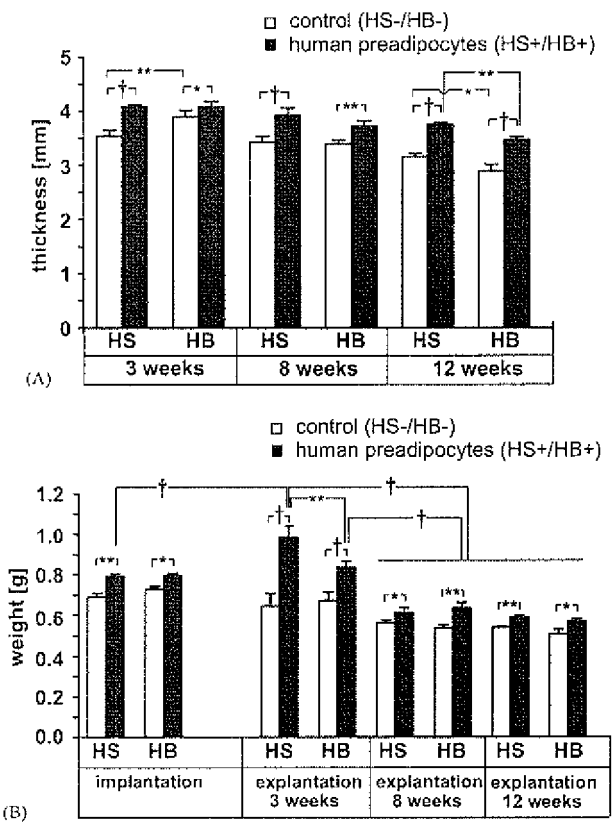

Fig. 5. Thickness and weight of preadipocyte-loaded and control grafts. Sponges were treated as described in Fig. 3, explanted after 3, 8, and 12 weeks and analysed for thickness and weight. (A) A general decrease in thickness in the course of time appears for both types of sponges, especially for HB. Cell-loaded scaffolds were always thicker than unloaded controls. (B) Weight analyses showed a decrease in the course of time for both types of scaffolds. Preadipocyte in hyaluronic acid-based constructs were always heavier than the control grafts. $^{*}p<0.05$; $^{**}p<0.01$; $^{\dagger}p<0.001$

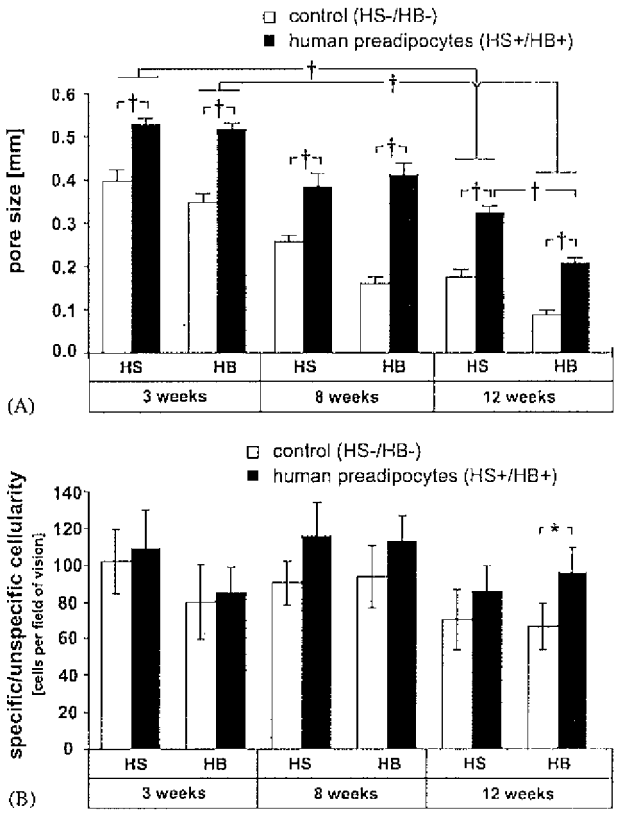

Fig. 6. Changes in pore size and specific/unspecific cellularity. Changes in pore size in HYAFF$^{®}$11 constructs were examined by microscopy on explanted grafts after 3, 8, and 12 weeks. Specific cellularity of human preadipocytes versus unspecific cellularity of other cells were determined by histological analyses. (A) The pore size of preadipocyte-loaded scaffolds was always higher than in the controls. There is a continuous and significant decrease in pore size from 3 to 12 weeks. (B) In all samples, cellularity is higher in the preadipocyte-loaded scaffolds than in the controls. $^{*}p<0.05$; $^{\dagger}p<0.001$

sponge material. Besides this one incidence of adipose tissue, all other pictures present predominantly fibrous tissue, separating and surrounding the sponge material.

4. Discussion

Before the beneficial role of preadipocytes was discovered, trials did not focus on progenitor cells but on the use of mature adipose tissue which is widely available and therefore seemed to represent an optimal donor tissue for filling or reconstructing tissue defects. However, transplantation of mature adipocytes resulted in the shrinkage or complete resorption of the grafts [16]. Rodbell [17] was the first to use collagenase treatment in order to separate preadipocytes from mature adipocytes out of adipose tissue. As has been shown in previous studies, this fraction of adipogenic progenitors in fat tissue has high potency for tissue engineering purposes [12,18,19]. In this present trial, human preadipocytes were expanded in cell culture, seeded on hyaluronic acid-based scaffolds (HYAFF$^{®}$11 sponges) with an innovative architecture consisting of large unique pores of 400 μm, and implanted in immunodeficient mice. The aim of the study was to find out whether the new pore structure and coating of sponges with hyaluronic acid has a beneficial effect on cell distribution, proliferation, vascularisation, and adipose tissue formation in scaffolds. Our findings clearly reveal a beneficial role of hyaluronic acid-derived carriers with large unique pores to enable preadipocytes to survive transplantation and perform good spreading, substantial proliferation and extensive induction of vascularisation at the recipient site. Satisfactory differentiation of preadipocytes, however, was not observed with this porous construct, neither in coated nor in uncoated sponges.

Scaffold architecture is assumed to have a strong influence on the in vivo differentiation of transplanted preadipocytes. Earlier in vivo experiments of our group

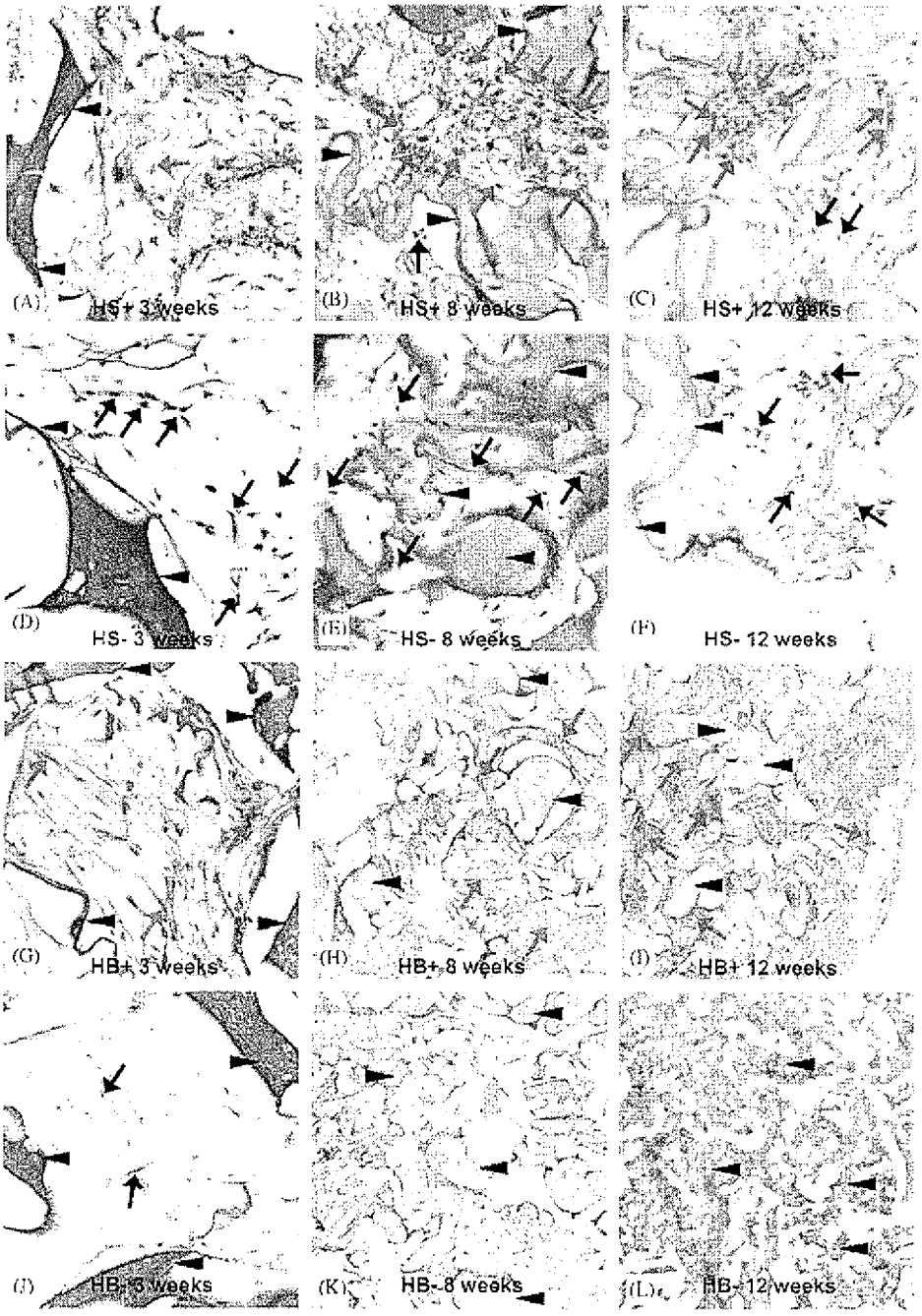

Fig. 7. Immunohistological characterisation of the explants stained by human vimentin/peroxidase. Seeded and unseeded HS and HB implants were analysed from explants at 3, 8, and 12 weeks. Samples were histologically prepared by Hematoxilin and human vimentin/peroxidase staining. Magnification of ×200 in all samples, except in H, I, K, and L (×50). (A)–(F). HS sponges with (A)–(C) and without (D)–(F) cells. (G)–(L) HB sponges with (G)–(I) and without (J)–(M) cells. ►, HYAFF®11-sponge material; ➡(black), cells of mouse origin; ➡(brown), human preadipocytes; ➡(yellow), adipose tissue.

with collagen sponges showed that human preadipocytes penetrate scaffolds with a pore size of 40 μm insufficiently, most probably due to the pore structures being too small. Growth and differentiation appeared to be restricted and limited to outer parts of the construct [14]. We therefore assumed that scaffold structures have to be designed for mature adipocytes which reach much larger dimensions up to a diameter of about 400 μm when undergoing differentiation. Since bovine products bear the risk of prior disease transmission which is not ideal for tissue engineering and implantation in humans, we focussed on hyaluronic acid-based scaffolds as

preadipocyte carriers in following in vivo studies since hyaluronic acid has been stated to support the growth and development of progenitor cells [13,20]. Pore diameter in the first hyaluronan sponges varied from 50 to 340 μm. Results were very promising since they clearly demonstrated the supremacy of the scaffold structure in contrast to previous constructs [14]. Cellular penetration of sponges was better and preadipocyte differentiation was not restricted to outer parts. A new generation of HYAFF®11 sponges with a unique pore size of 400 μm had shown good characteristics in in vitro examinations so far [21]. Therefore, we here now analysed the applicability of these innovative scaffold structures to allow cell ingrowth, proliferation, vascularisation, and adipose tissue formation. Two types of HYAFF®11 sponges were compared, one plain (HS) and one coated with hyaluronic acid (HB). The reason why HB sponges were designed is that despite HS sponges had been proved to allow good cell adhesion, the cell loading process was time consuming due to the hydrophobic nature of the polymer. The modification of the scaffold structure was intended to ameliorate this cell loading procedure without altering the optimal adhesion properties.

Our results indeed show that coating of hyaluronan sponges with hyaluronic acid significantly reduces the hydrophobic nature of the construct (Fig. 2). While HS sponges required prewetting with FCS or SPPP to allow a quick and satisfying uptake of the cell suspension, HB sponges were successfully seeded directly with cells without pretreatment. Both types of sponges revealed a spontaneous uptake of the cell-loaded medium.

Evaluating the attachment and growth of preadipocytes on HYAFF®11 sponges, we found the amount of attached cells to be very high in both carriers, HS and HB (Table 1). This proves that the material HYAFF®11 allows good adherence of cells to the matrix which is an important prerequisite for cell-loaded implants. Analysing preadipocyte attachment and growth on HYAFF®11 sponges in SPPP- versus FCS-supplemented media, we found that cells adhere better and proliferate more quickly with the latter medium (Fig. 3, Table 2). Although our results with higher cell numbers in FCS-treated matrices confirm the high potency of FCS [22], recent moral and ethical concerns about the gain of FCS from newborn calves have called the use of this bovine product into question [23]. Lot-to-lot variability, high production costs, limited availability of FCS [24–27], and finally the activation of immunological processes after transplantation of FCS-cultured cells [28–31] are further arguments supporting the search for FCS alternatives. SPPP contains much lower concentrations of growth factors than FCS but is of human origin which is necessary in the context of human preadipocyte tissue engineering. However, the optimal solution would be an autologous system with human serum used for prewetting of scaffolds and culturing of preadipocytes. We found that human serum is highly beneficial for human preadipocyte cultivation since it allows good in vitro expansion of adipogenic progenitor cells and a much better conversion to mature adipocytes than the conventionally used FCS, especially after long-term proliferation [32].

Our results of explanted cell-loaded transplants reveal very thin but tightly integrated vessels in almost all layers of the sponge thereby presenting a more intense vascularisation than controls (Fig. 4). The finding that preadipocyte-seeded transplants show a more intense vascularisation of the surface than controls may be due to preadipocyte-mediated induction of vascularisation. Adipogenic progenitors do not only influence vessel formation but also have a positive influence on scaffold stability. The organisation of the vessels in the scaffolds proceeds during implantation as confirmed by microscopy after 12 weeks revealing the best results for vessel formation compared to 3- and 8-week explants. Furthermore, we observe that preadipocytes stabilise the hyaluronan matrix by filling the gaps in the sponge thereby maintaining the thickness of the graft which is otherwise compressed in the subcutaneous location. Unloaded scaffolds were always more compressed and degraded (Fig. 5A). Macroscopically, degradation of sponges after 12 weeks in vivo is more obvious in HS than in HB scaffolds. However, this difference between HS and HB constructs is most likely due to explantation since microscopical data clearly prove the contrary (Fig. 5A). In terms of weight, we found that cell-loaded explants were always heavier than controls. At 3 weeks after implantation, this difference was particularly obvious evidencing that the porous structure HYAFF®11 well supports attachment and growth of preadipocytes. In contrast to the present findings in HYAFF®11 constructs, previous studies with collagen sponges of 65 and 100 μm pore diameter showed a highly significant weight loss between the point of implantation and explantation after 3 weeks, losing 50% of the initial weight. Furthermore, these collagen scaffolds decreased in thickness by more than 25% during implantation. Since it is hoped that preadipocyte-seeded scaffolds will one day offer a solution for the reconstruction of soft-tissue defects, maintaining the thickness and weight of the construct is a very important parameter [19]. The HYAFF®11 constructs presented here show better results in this context than previously tested collagen sponges.

Our results reveal good spreading and distribution of preadipocytes over the whole cross-section. As confirmed by histological analyses, the pore size of 400 μm allows an optimal distribution of preadipocytes over the whole carrier which has not been reached in previous experiments with smaller pores [14,19]. Analyses of 8-week and 12-week explants show a protective effect of

the inoculation with human preadipocytes for the three-dimensional structure. However, it is of note that the pore size generally decreased during the implantation period. This is in accordance with the absence of adipose tissue formation in the construct. In experiments with collagen sponges, in which conversion of preadipocytes to mature fat cells was found after explantation, pore diameter was shown to increase over time [19], most likely due to the size increase of converting preadipocytes. These results could unfortunately not be reproduced with HYAFF®11 sponges with a unique pore size of 400 μm. One possible explanation could be that 400 μm is too high a diameter to present an adequate stimulus for preadipocytes to undergo adipogenic conversion. Contact inhibition by neighbouring cells is a key stimulus for adipose tissue progenitors to perform differentiation [33,34]. This might not be guaranteed by such big pores. A solution for achieving the necessary cellular contact inhibition could be to increase the number of cells seeded per sponge or to generate three-dimensional structures where the pore diameter varies between 100 and 400 μm. Initially tested hyaluronan sponges with pore diameters varying from 50 to 340 μm within one construct showed successful preadipocyte differentiation but mainly in outer parts of the scaffold [14].

Analysing penetration of the scaffolds by preadipocytes, we used human vimentin peroxidase staining since vimentin is a typical marker for preadipocytes [35] as it allows for the distinction between human preadipocytes and cells of mouse origin. Our findings reveal that preadipocytes show good spreading and penetration in HYAFF®11 matrices (Fig. 7). This again confirms the optimal applicability of HYAFF®11 sponges to enable satisfactory seeding with preadipocytes, good cellular penetration of the construct, and proliferation. We therefore consider our results as being encouraging for the use of preadipocytes in combination with a three-dimensional hyaluronic acid-based matrix for further in vivo adipose tissue engineering trials.

5. Conclusion

Our results demonstrate that the innovative architecture of HYAFF®11 sponges with a unique pore size of 400 μm allows good cell spreading, proliferation, and stability of the three-dimensional construct. Coating with hyaluronic acid significantly reduces the hydrophobic nature of this scaffold type, thereby allowing a quick and satisfying uptake of cell suspensions without any pretreatment. Compared to previous studies, we found better penetration of cells into both coated and uncoated scaffolds with more extensive formation of new, tightly integrated vessels throughout the whole construct but hardly any adipose tissue. The fact that no mature adipocytes were found in the sponges after explantation proves that some complex problems remain; besides the development of an optimised autologous medium, formation of adipose tissue in vivo by full differentiation of preadipocytes is an aim which requires additional efforts and analyses. Fibronectin coating as well as the induction of differentiation on sponges before implantation or seeding of carriers with predifferentiated preadipocytes are approaches which have shown promising results in vitro so far [32,36]. These findings will have to be implemented and verified in new in vivo experiments to further improve adipose tissue formation in tissue engineering models.

Acknowledgements

We wish to acknowledge the technical assistance of Ms. T. Oepen.

This research work is part of a project funded by the European Community under the "Competitive and Sustainable Growth" Programme (5th framework programme), contract number G5RD-CT-1999-00111, project number GRD1-1999-11159.

References

[1] Smahel J. Experimental implantation of adipose tissue fragments. Br J Plast Surg 1989;42:207–11.
[2] Zuk PA, Zhu M, Ashjian P, De Ugarte DA, Huang JI, Mizuno H, et al. Human adipose tissue is a source of multipotent stem cells. Mol Biol Cell 2002;13(12):4279–95.
[3] Zuk PA, Zhu M, Mizuno H, Huang J, Futrell JW, Katz AJ, et al. Multilineage cells from human adipose tissue: implications for cell-based therapies. Tissue Eng 2001;7(2):211–28.
[4] Finch GD, Dawe CJ. Hemiatrophy. J Pediatr Orthop 2003;23(1):99–101.
[5] Fokin AA, Robicsek F. Poland's syndrome revisited. Ann Thorac Surg 2002;74(6):2218–25.
[6] Dzubow L, Goldman G. Introduction to soft tissue augmentation: a historical perspective. In: Klein A, editor. Tissue augmentation in clinical practice. Basel: Marcel Dekker; 1998. p. 1–22.
[7] Ersek R. Transplantation of purified autologous fat: a 3-year follow-up is disappointing. Plast Reconstr Surg 1991;87:219–27.
[8] Ersek R, Chang P, Salisbury M. Lipo layering of autologous fat: an improved technique with promising results. Plast Reconstr Surg 1998;101:820–6.
[9] Jackson IT, Simman R, Tholen R, DiNick VD. A successful long-term method of fat grafting: recontouring of a large subcutaneous postradiation thigh defect with autologous fat transplantation. Aesthetic Plast Surg 2001;25(3):165–9.
[10] Ailhaud G, Grimaldi P, Négrel R. Cellular and molecular aspects of adipose tissue development. Annu Rev Nutr 1992;12:207–33.
[11] von Heimburg D, Hemmrich K, Zachariah S, Staiger H, Pallua N. In vitro oxygen consumption in mesenchymal precursor cells of the adipogenic lineage in undifferentiated versus differentiated state. Resp Physiol Neurobiol 2005;46(2-3):107–16.
[12] von Heimburg D, Zachariah S, Heschel I, Kuhling H, Schoof H, Hafemann B, et al. Human preadipocytes seeded on freeze-dried

collagen scaffolds investigated in vitro and in vivo. Biomaterials 2001;22(5):429–38.
[13] Solchaga LA, Dennis JE, Goldberg VM, Caplan AI. Hyaluronic acid-based polymers as cell carriers for tissue-engineered repair of bone and cartilage. J Orthop Res 1999;17(2):205–13.
[14] von Heimburg D, Zachariah S, Low A, Pallua N. Influence of different biodegradable carriers on the in vivo behavior of human adipose precursor cells. Plast Reconstr Surg 2001;108:411–20.
[15] Rastrelli A, Beccaro M, Biviano F, Calderini G, Pastorello A. Hyaluronic acid esters, a new class of semisynthetic biopolymers: chemical and physico-chemical properties. Clin Implant Mater 1990;9:199–205.
[16] Billings Jr E, May Jr JW. Historical review and present status of free fat graft autotransplantation in plastic and reconstructive surgery. Plast Reconstr Surg 1989;83(2):368–81.
[17] Rodbell M. Metabolism of isolated fat cells. J Biol Chem 1964; 239:375–80.
[18] von Heimburg D, Ulrich D, Hemmrich K, Pallua N. Soft tissue engineering by implantation of autologous adipose precursor cells into the rabbit ear-pathophysiology in adipose tissue transplantation. Clin. Exp. Plast. Sur. 2001;33:127–32.
[19] von Heimburg D, Kuberka M, Rendchen R, Hemmrich K, Rau G, Pallua N. Preadipocyte-loaded collagen scaffolds with enlarged pore size for improved soft tissue engineering. Int J Artif Organs 2003;26(12):1064–76.
[20] Brun P, Cortivo R, Zavan B, Vecchiato N, Abatangelo G. In vitro reconstructed tissues on hyluronan-based temporary scaffolding. J Mater Sci 1999;10:683–8.
[21] Milella E, Brescia E, Massaro C, Ramires PA. Chemico-physical properties of hyaluronan-based sponges. J Biomed Mater Res 2000;52(4):695–700.
[22] Freshney RI. Culture of animal cells: A manual of basic technique. 2nd ed. New York: Alan, R. Liss Inc.; 1987.
[23] Jochems CE, van der Valk JB, Stafleu FR, Baumans V. The use of fetal bovine serum: ethical or scientific problem? Altern Lab Anim 2002;30(2):219–27.
[24] Barnes D, Sato G. Serum-free cell culture: a unifying approach. Cell 1980;22(3):649–55.
[25] Barnes D, Sato G. Methods for growth of cultured cells in serum-free medium. Anal Biochem 1980;102(2):255–70.
[26] Jayme DW, Blackman KE. Culture media for propagation of mammalian cells, viruses, and other biologicals. Adv Biotechnol Process 1985;5:1–30.
[27] Jayme DW, Epstein DA, Conrad DR. Fetal bovine serum alternatives. Nature 1988;334(6182):547–8.
[28] Johnson MC, Meyer AA, deSerres S, Herzog S, Peterson HD. Persistence of fetal bovine serum proteins in human keratinocytes. J Burn Care Rehab 1990;11(6):504–9.
[29] Johnson LF, deSerres S, Herzog SR, Peterson HD, Meyer AA. Antigenic cross-reactivity between media supplements for cultured keratinocyte grafts. J Burn Care Rehab 1991;12(4):306–12.
[30] Mizushima Y, Cohen EP. A study on an artifact introduced by fetal bovine serum-supplemented medium. Hokkaido Igaku Zasshi 1985;60(3):321–6.
[31] Toldbod HE, Agger R, Bolund L, Hokland M. Potent influence of bovine serum proteins in experimental dendritic cell-based vaccination protocols. Scand J Immunol 2003;58(1):43–50.
[32] Hemmrich K, von Heimburg D, Cierpka K, Haydarlioglu S, Pallua N. Optimization of the differentiation of human preadipocytes in vitro. Differentiation 2005;73:17–24.
[33] Smas CM, Sul SH. Control of adipocyte differentiation. Biochem J 1995;309:697–710.
[34] Gregoire FM, Smas CM, Sul HS. Understanding adipocyte differentiation. Physiol Rev 1998;78(3):783–809.
[35] Greenberg AS, Egan JJ, Wek SA, Garty NB, Blanchette-Mackie EJ, Londos C. Perilipin, a major hormonally regulated adipocyte-specific phosphoprotein associated with the periphery of lipid storage droplets. J Biol Chem 1991;15:11341–6.
[36] Halbleib M, Skurk T, de Luca C, von Heimburg D, Hauner H. Tissue engineering of white adipose tissue using hyaluronic acid-based scaffolds. I: in vitro differentiation of human adipocyte precursor cells on scaffolds. Biomaterials 2003;24(18):3125–32.

ELSEVIER

Biomaterials 22 (2001) 429–438

Biomaterials

Human preadipocytes seeded on freeze-dried collagen scaffolds investigated in vitro and in vivo

Dennis von Heimburg[a,*], Sascha Zachariah[a], Ingo Heschel[b], Hendrik Kühling[a], Heike Schoof[b], Bernd Hafemann[a], Norbert Pallua[a]

[a]*Department of Plastic Surgery and Hand Surgery—Burn Centre University Hospital, Aachen University of Technology, Pauwelsstrasse 30, D-52057, Aachen, Germany*

[b]*Helmholtz-Institute for Biomedical Engineering, Aachen University of Technology, Pauwelsstrasse 20, D-52074, Aachen, Germany*

Received 8 November 1999; accepted 8 May 2000

Abstract

Currently, there is no adequate implant material for the correction of soft tissue defects such as after extensive deep burns, after tumor resection and in hereditary and congenital defects (e.g. Romberg's disease, Poland syndrome). The autologous transplantation of mature adipose tissue has poor results. In this study human preadipocytes of young adults were isolated and cultured. 10^6 preadipocytes were seeded onto collagen sponges with uniform 40 μm pore size and regular lamellar structure and implanted into immunodeficient mice. Collagen sponges without preadipocytes were used in the controls. Macroscopical impression, weight, thickness, histology, immunohistochemistry (scaffold structure, cellularity, penetration depth of the seeded cells) and ultrastructure were assessed after 24 h in vitro and after explantation at 3 and 8 weeks. Preadipocytes penetrated the scaffolds 24 h after seeding at a depth of 299 ± 55 μm before implantation. Macroscopically after 3 and 8 weeks in vivo layers of adipose tissue accompanied by new vessels were found on all preadipocyte/collagen grafts. The control grafts appeared unchanged without vessel ingrowth. There was a significant weight loss of all grafts between 24 h in vitro and 3 weeks in vivo ($p < 0.05$), whereas there was only a slight weight reduction from week 3 to 8. The thickness decreased in the first 3 weeks ($p < 0.05$) in all grafts. The preadipocyte/collagen grafts were thinner but had a higher weight than the controls at this point in time. The histology showed adipose tissue and a rich vascularisation adherent to the scaffolds under a capsule. The control sponges contained only few cells and a capsule but no adipose tissue. Human-vimentin positive cells were found in all preadipocyte/collagen grafts but not in the controls, penetrating 1188 ± 498 μm (3 weeks) and 1433 ± 685 μm (8 weeks). Ultrastructural analysis showed complete in vivo differentiation of viable adipocytes in the sponge seeded with preadipocytes. Formation of extracellular matrix was more pronounced in the preadipocyte/collagen grafts. The transplantation of isolated and cultured preadipocytes within a standardised collagen matrix resulted in well-vascularised adipose-like tissue. It is assumed that a pore size greater than 40 μm is required, as preadipocytes enlarge during differentiation due to incorporation of lipids. © 2001 Elsevier Science Ltd. All rights reserved.

Keywords: Human preadipocytes; Adipose tissue engineering; Collagen matrices; Pore structure; Scaffold

1. Introduction

The reconstruction of soft tissue defects remains a challenge in plastic and reconstructive surgery. Examples for considerable loss of soft connective tissue especially adipose tissue are extensive deep burns, defects after tumor resection, hereditary defects and congenital defects such as Romberg's disease and Poland syndrome. Soft tissue plays a major role in maintaining contours and also serves as a mechanical cushion for muscles, tendons and bones. Among the various approaches are local and free flaps, dermal fat grafts, collagen injections, the use of synthetic materials and free adipose tissue grafts. Every method shows considerable disadvantages: Synthetic materials always cause foreign body reactions and biologically derived materials shrink to an unpredictable extent [1]. Autologous adipose tissue should be an ideal material, as there usually is sufficent supply for grafting but the results are generally poor and unpredictable. Studies using free adipose tissue grafts showed that most of it was absorbed and replaced by

* Corresponding author.
E-mail address: d.v.heimburg@plastchir.rwth-aachen.de (D. von Heimburg).

0142-9612/01/$ - see front matter © 2001 Elsevier Science Ltd. All rights reserved.
PII: S0142-9612(00)00186-1

fibrous tissue and oil cysts [2,3]. These inferior results are thought to be due to the slow rate of revascularisation of the graft and the low tolerance of ischemia of fat cells [4]. Even the revived technique of injecting aspirated fat fragments has unsatisfactory results, ranging from 50% shrinkage of the graft to complete resorption [5–8].

Preadipocytes, which are located between mature adipocytes in adipose tissue, are a potential material for soft tissue engineering [5]. The proliferative activity is high in preadipocytes, whereas fully differentiated adipocytes have lost their capacity to divide [9]. Isolation of adipocyte precursor cells from stroma of adult adipose tissue and their differentiation in culture were achieved in the last two decades [10]. We continued this work by transferring the previous in vitro studies on human preadipocytes to an in vivo model.

To protect the preadipocytes from being washed from the site of transplantation they were seeded into collagen sponges. This also enabled a better determination of cell survival, differentiation and newly formed ECM (extracellular matrix). The scaffold had to have a suitable chemical composition and pore structure to allow the cells to enter and differentiate after transplantation. Furthermore the scaffold had to be mechanically stable enough to be implanted and had not to be absorbed too quickly after transplantation.

The aim of this study was to:

1. isolate and culture preadipocytes from adult human adipose tissue,
2. study the penetration of these in vitro cultured cells into directionally solidified collagen sponges,
3. observe the macroscopical and microscopical in vivo changes within these scaffolds after implantation into immunodeficient mice, and
4. study the potential of the grafted preadipocytes to differentiate in vivo (to adipocytes).

2. Materials and methods

2.1. Collagen sponge

The collagen sponge scaffolds were produced by a directional solidification method and subsequent freeze-drying. The method has been described in detail in [11,12], therefore only a brief description is given here. After the addition of 3.8% acetic acid to the basic collagen suspension (1.8 wt% bovine collagen type I, Dr. Otto Suwelack, Germany) the collagen suspension is frozen under uniform conditions with a temperature gradient of 50°C/cm and an ice front velocity of 30 μm/s. These parameters lead to a homogeneous plate-like ice crystal morphology with the smallest distance between the ice crystal layers of 55 μm. During the subsequent vacuum-drying step the ice crystals are removed by sublimation and the collagen fibres cross-link without the need for additives. This leads to a porous structure of the sponge that corresponds to the previous ice crystal structure (Fig. 1). The average distance between the collagen layers after vacuum-drying is 40 μm. The pore volume fraction is approximately 95%. For the studies we used sponges measuring 7.5 × 7.5 × 5 mm. The sponges were sterilized by ethylene oxide before use in the study. The antigenicity of the basic collagen suspension that was used to produce the sponges was investigated in an independent study. The results showed that no antibodies against the bovine collagen suspension were found in sera of dogs having the material implanted for a period of 2 and 3 weeks. Furthermore the provided collagen fulfills the required EN 12442, Part 2, i.e. in relation to the origin of the material, as well as the certifications according to EN 12442; Part 3, relating to the degradation process (unpublished data). Thus, the application safety concerning the BSE risk is guaranteed with considerable safety margins.

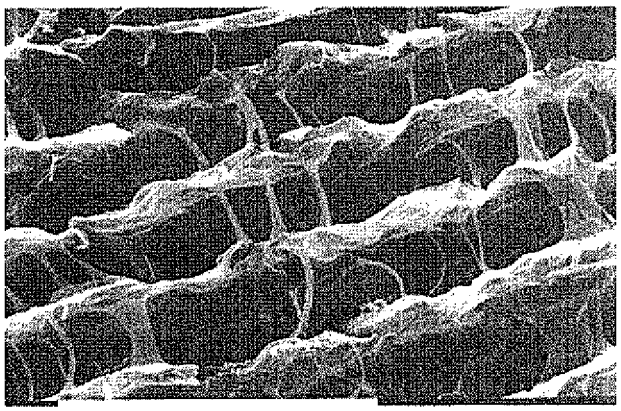

Fig. 1. SEM of a collagen scaffold produced by directional solidification and subsequent vacuum-drying showing a regular structure. The white scale bar is equivalent to 0.1 mm. In this sponge the average distance between the collagen layers is 40 μm. Open porous architecture is assumed to allow a better vascularisation of the matrix.

2.2. In vitro tissue culture (preadipocyte isolation, culture and seeding)

2.2.1. Isolation

Preadipocytes were isolated out of fragments (0.4–0.7 g) of freshly obtained human subcutaneous adipose tissue of young adults (age: 18–29 yr) who had undergone elective operations (e.g. reduction mammaplasty) at the Department of Plastic Surgery and Hand Surgery—Burn Centre. After removing fibrous tissue, the adipose tissue was chopped into pieces digested by collagenase 0.1 U ml^{-1}/dispase 0.8 U ml^{-1} (Boehringer Mannheim, Germany) in a water bath at 37°C for 60 min under permanent shaking. The digestion was stopped by

adding DMEM (Dulbecco's modified Eagle's medium) containing 15% FCS (Fetal calf serum, Biochrom, Berlin, Germany) followed by an incubation in erythrocyte lysis buffer (154 mmol l^{-1} NH_4Cl, 10 mmol l^{-1} $KHCO_3$, 1 mmol l^{-1} EDTA, 10 min). This cell suspension was centrifuged ($200 \times g$ for 10 min at 17°C) and the pellet was used for culture. For this purpose the cells were seeded on tissue culture dishes (63.6 cm^2, Greiner, Solingen, Germany) with DMEM + 15% FCS (supplemented with 100 U ml^{-1} Penicillin, 100 μg ml^{-1} Streptomycin) with a seeding density of 3×10^4 cells/cm^2.

2.2.2. Culture and preparation of human preadipocytes/collagen scaffold grafts

The cells were then cultured at 37°C at 10% CO_2. The following day medium was changed and supplemented with EGF (epidermal growth factor, 10 ng ml^{-1}, Sigma). Preadipocytes of the second passage at confluence (Fig. 2) were trypsinised. The cells were resuspended in 0.5 ml of DMEM 15% FCS and counted in a haemocytometer. A suspension of 100 μl, containing $1 \times 10^6 \pm 5 \times 10^4$ cells, was seeded on the upper surface by gentle dropping on the pre-wetted scaffolds. The direction of the pores was perpendicular to the surface (Fig. 1), so that the medium and the accompanying cells could be soaked in the sponges. The sponges were left undisturbed in the incubator for 24 h to allow the cells to attach.

In order to assess the ratio of preadipocytes to all cultured cells, differentiation was induced by adding dexamethasone 250 nmol ml^{-1} and insulin 5 μg ml^{-1} to the control dishes. The percentage of preadipocytes was calculated by direct counting using the phase-contrast microscope (Zeiss, Germany). Seven preadipocyte/collagen constructs were not grafted and microscopically and ultrastructurally assessed after 24 h in vitro (see Section 2.4.1).

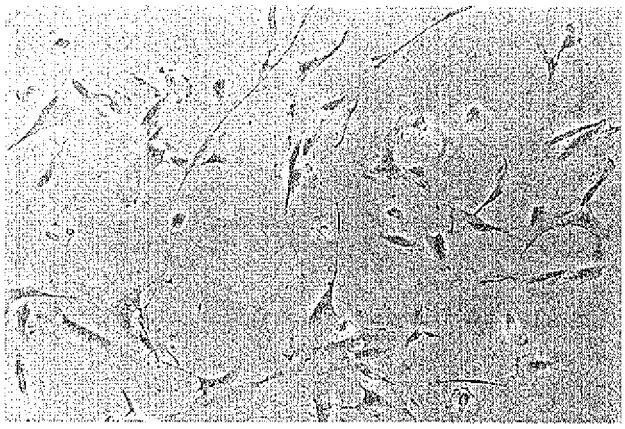

Fig. 2. Human preadipocytes (first passage) in monolayer culture at day 10 after isolation. The differentiation is suppressed by added EGF (epidermal growth factor).

2.3. In vivo experiments

2.3.1. Transplantation

Twenty-four hours after seeding of the cells to the scaffolds (Fig. 3), 14 fabricated preadipocyte/sponge (S+) constructs were transplanted subcutaneously to the right scapular area of 14 athymic, 8-week-old, nude mice (nmri, nu/nu, Charles River, Germany). The base of the constructs was placed on the muscle fascia. In each of these animals a control scaffold (S−, without cells, 24 h soaked with DMEM) was transplanted to the left scapular area through a separate incision. All animal experiments had been performed according to the animal protection laws and were officially permitted.

2.3.2. Explantation

After 3 weeks (group A, $n = 7$) and 8 weeks (group B, $n = 7$) the mice were killed and the grafts were explanted. These two groups were formed randomly. The macroscopic aspects (colour, vessels, ingrowth) of the grafts after excision were documented.

2.3.3. Weight

The weight of each sponge was assessed dry (before wetting), 24 h after the cells were seeded onto the sponge (before transplantation) and after explantation (3 weeks—group A—or 8 weeks—group B—after transplantation). The weights of the scaffolds were averaged by using data from all mice at each examination date (dry, 24 h in vitro, 3 weeks (group A) and 8 weeks (group B) in vivo).

2.4. Histology/immunohistochemistry

The explanted material was divided. One half was fixed in 4% buffered formaldehyde solution, embedded, vertically sectioned, and stained. The other half was cryofixed.

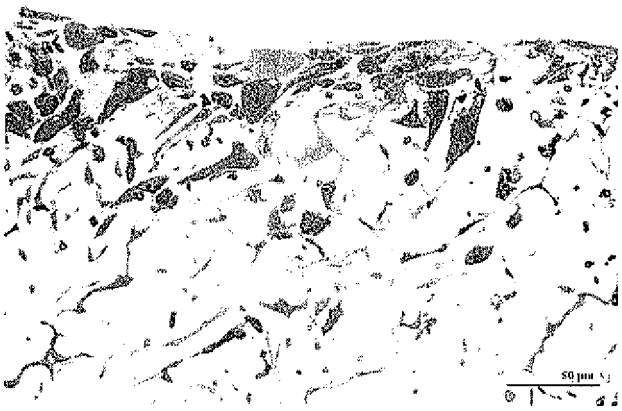

Fig. 3. Human preadipocytes 24 h after being seeded on collagen sponges. Good adherence of viable cells can be observed but the penetration to the scaffold center is not sufficient. 299 μm shows the best penetration into the collagen sponge. Note the collagen sponge lamellar structure (semi-thin, ×400, toluidine-blue).

Ultrastructural images were obtained from two in vitro and eight in vivo specimens.

2.4.1. Microscopy and immunohistochemistry

The formalin fixed fragments were dehydrated in ascending series of alcohols and embedded in paraffin. Tissue slices of 2 μm were prepared and stained with hematoxylin–eosin and Giemsa. The cryofixed fragments were also stained with oil-red in order to identify lipid vacuoles.

2.4.2. Immunohistochemistry

Paraffin cuts of S+ and S− grafts were stained by monoclonal antibodies specific for human vimentin (mahv, clone V9, Code Nr. M 0725 Lot 057, DAKO, Denmark). The antibody was used at a dilution of 1 : 10.

Three blinded examiners (D.v.H., H.K., S.Z.) independently assessed the histological sections. When there were differences between the assessments, the mean value was calculated.

2.4.3. Thickness of the grafts

The thickness of the graft was assessed by measuring the thickness of the cross-sectional cut of the collagen sponge at three different sites using intraocular micrometer (Zeiss) and a mean value for each graft was calculated.

2.4.4. Cellularity

Microscopic fields of the cross-sectional cuts (Fig. 4a) were examined at 200× magnification. The overall cellularity was assessed by counting all Giemsa stained cells in these fields. For base, centre and surface areas the numbers were obtained and a mean value for the cellularity of each cut was calculated.

2.4.5. Cellularity of seeded preadipocytes

Microscopic fields of the human-vimentin stained cross-section (Fig. 4a) were examined under 200× magnification. The cellularity was assessed by counting all human-vimentin positive cells in these fields.

2.4.6. Penetration of seeded preadipocytes

In representative areas of the cross-section (Fig. 4b) the penetration depth of human-vimentin positive cells was measured at 200× magnification by using intraocular micrometer (Zeiss, Germany).

2.4.7. Ultrastructural appearance

After fixation (1% osmium tetroxide) the microdissected samples were dehydrated and embedded in Epon-Araldite. Semi thin sections (1 μm) were stained with 1% toluidine blue and areas of interest selected for electron microscopy. Ultrathin sections (0.1 μm) were collected on copper grids and stained with uranyl acetate and lead citrate. Sections were viewed by a Philips EM 400 electron microscope.

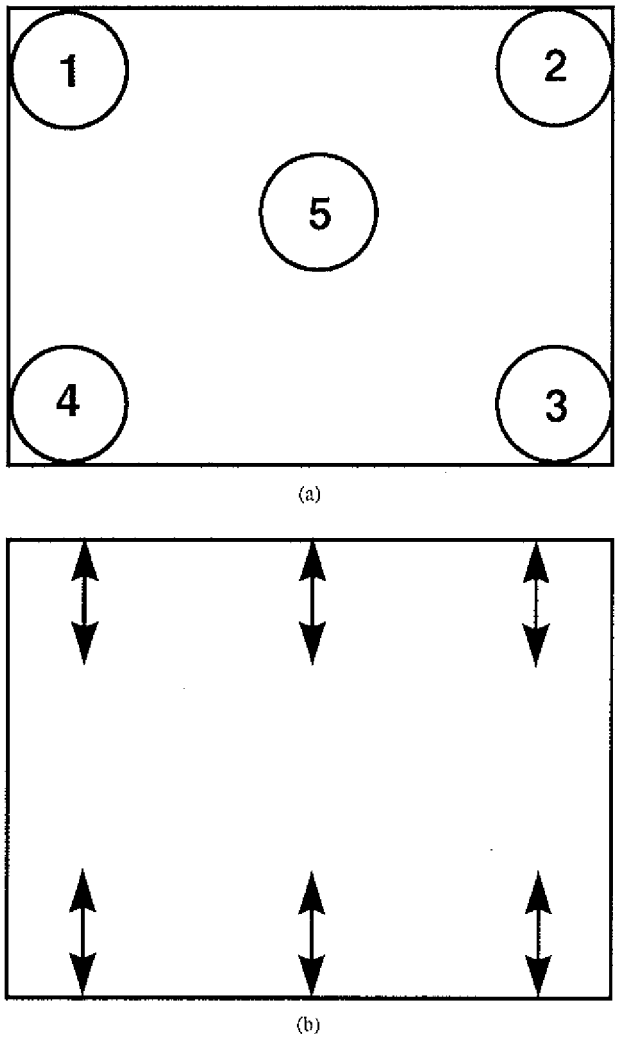

Fig. 4. Scheme of the microscopical fields to assess of the cross-sectional cut of the constructs: (a) for assessment of cellularity (Giemsa stain, mah-vimentin stain), (b) assessment of the penetration depth (Giemsa stain).

2.4.8. Statistical evaluation

Data of weight and thickness of the grafts, the overall cellularity in the grafts and the penetration depth of the seeded human preadipocytes were expressed as mean value ± standard deviation. The significance of differences at different time points and between the preadipocyte/collagen constructs and the control grafts was evaluated by the Mann–Whitney *U*-test. Differences at $p < 0.05$ were regarded to be significant.

3. Results

3.1. In vitro

The preadipocytes adhered well to the plates. The attached cells uniformly presented elongated fibroblast-like

morphology. By adding EGF enriched medium after 24 h a differentiation of the preadipocytes to mature adipocytes by accumulating lipid could be suppressed completely. Confluence was achieved after 10 days. There was no initiation of adipocyte differentiation (Fig. 2) which is usually observed at preadipocyte confluence. An 8-fold increase in cell number was observed.

Twenty-four hours after the seeding to the collagen scaffolds individual cells filled the spaces of the sponge porous system (Fig. 3). Seven S+ grafts were assessed for microscopical appearance and thickness measurements after 24 h. At that time penetration of the cells was only observed into the scaffold surface areas. The maximum penetration of the cells into the scaffold (surface to cells) was 299 ± 55 μm. At the time of transplantation preadipocytes were round shaped but showed no signs of differentiation to mature adipocytes (Fig. 3).

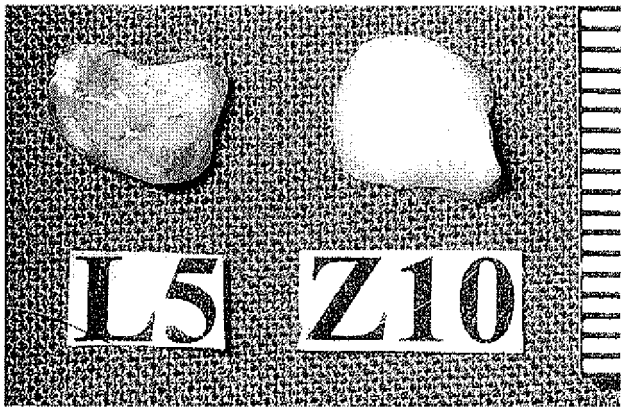

Fig. 6. Macroscopic appearance of the grafts after 8 weeks in the nude mouse. The yellow tissue presented on all preadipocyte grafts (left) while the contralateral control sponge out of the same animal revealed a different structure (right).

3.2. In vivo

No animal died during the operation or during the observation period. There were no infections. Therefore, all 28 grafts (14 collagen sponges with preadipocytes and 14 collagen sponges without cells) could be included in the evaluation.

3.2.1. Macroscopical examinations

Transplants (group A, 3 weeks): In all animals the grafts could easily be identified. The gross shape of the scaffolds was almost unchanged. All collagen sponges with preadipocytes showed a thin layer of macroscopically yellow tissue and new vessels on the top (Fig. 5). This layer could not be removed and was tightly connected to the sponge. The control grafts appeared white and almost avascular. The sponge tissue was easily dissected and the slight adhesions to the surrounding tissue were carefully separated. There were fine ligamentous contacts to the surrounding mouse tissue, while the sponges without cells did not show these connections.

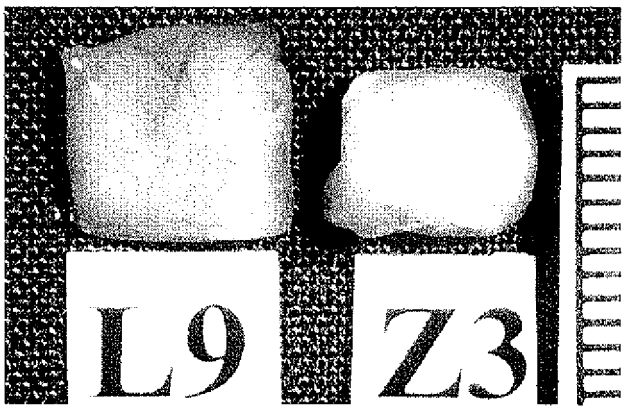

Fig. 5. Macroscopic appearance of the grafts after 3 weeks in the nude mouse. A thin yellow tissue presented on the preadipocyte grafts with new vessel formation (left). The contralateral control sponge out of the same animal revealed almost no change to the sponge before transplantation and no vessels (right).

Transplants (group B, 8 weeks): In all animals the grafts could be easily identified. The sponge volume had decreased and macroscopically the grafts appeared irregular with rounded edges (Fig. 6). All sponges with preadipocytes presented yellow tissue on the surface. The control sponges also showed the signs of degradation, but no vessels and they still appeared white.

3.2.2. Weights

The course of the weights is shown in Fig. 7. There was remarkable weight reduction at the time of explantation compared to the weights after 24 h in vitro. The weight loss was proven to be significant for both graft types ($p < 0.05$). The higher weight of the S+ grafts compared to the S− grafts was also significant ($p < 0.05$).

3.2.3. Histomorphologic chronology of the grafts

Group A, 3 weeks: All grafts presented a thin capsule layer of fibro–vascular tissue. No neutrophils were found. The scaffold itself appeared almost unchanged and the homogenous pore structure was still present. The mean pore size was measured 40 ± 5 μm. At the edges of the sponges minimal signs of degradation (curling) were observed.

Microscopical examination of the S+ grafts demonstrated viable adipose tissue located on the surfaces of the scaffolds under the capsule. The adipose tissue was composed of up to 10 layers of adipocytes. Mature adipocytes were found in the areas just beneath the surface (Fig. 8). No differentiated adipocytes were observed in the central region of the sponges. Many vessels presented in this new formed adipose tissue. In the S− grafts no adipocytes were found at all.

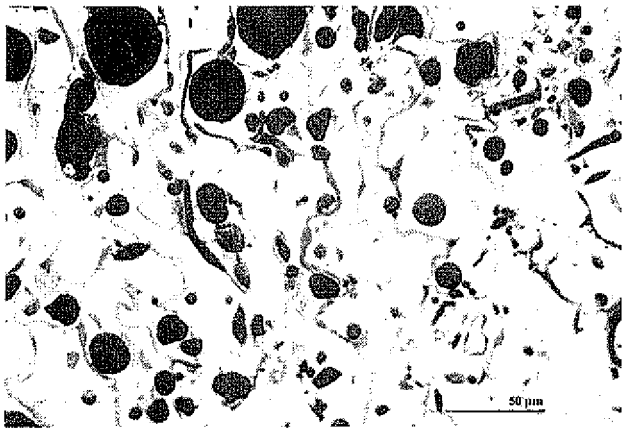

Fig. 7. Microscopical view of the scaffold after 3 weeks in the nude mouse. Differentiated adipocytes are more numerous in the upper layers of the collagen matrix. In the deeper sponge areas adipocytes appear smaller and 'constricted' by the collagen material (semi-thin, ×200, toluidine-blue).

Group B, 8 weeks: After 8 weeks all grafts were encapsulated by a thin layer of fibro-vascular tissue comparable to that seen after 3 weeks. There was a slightly higher number of macrophages and few giant cells. The scaffolds were more degraded and the structure had changed to a more irregular structure (shrinkage and curling). The pores appeared to have collapsed and only in some areas the homogenous structure of the scaffold was observed. Viable adipose tissue was found unchanged in layers on the top of the S+ grafts. The S− grafts did not show adipose tissue attached to the scaffolds.

Thickness of the grafts could be easily assessed and the course is shown in Fig. 9. There was a decrease compared to the thickness after 24 h in vitro. The decrease in the first 3 weeks was greater for the S+ grafts than for the S− grafts, the decrease was significant for both graft types. There was only a slight decrease between 3 and 8 week values. Variation of the thickness in each group was more obvious in the S− grafts while there were no statistical differences between the S+ and the S− grafts.

The overall cellularity was higher in the S+ grafts. The S+ grafts showed higher cell number on the upper side of the sponge compared to the S− grafts in vivo after 3 weeks. Assessment of cell density revealed 97 ± 49 (cells/field) in the S+ grafts compared to 80 ± 45 (cells/field) in the S− grafts after 3 weeks. After 8 weeks in the S+ grafts cellularity was 77 ± 56 (cells/field) while the S− grafts showed 66 ± 44 (cells/field).

3.2.4. Immunohistochemistry

Staining for human-vimentin indicated that cells within the S+ grafts were strongly positive and human origin. There was no staining in the S− grafts. This specific cellularity slightly decreased between 3 weeks 60 ± 52 (cells/field) and 8 weeks 40 ± 26 (cells/field).

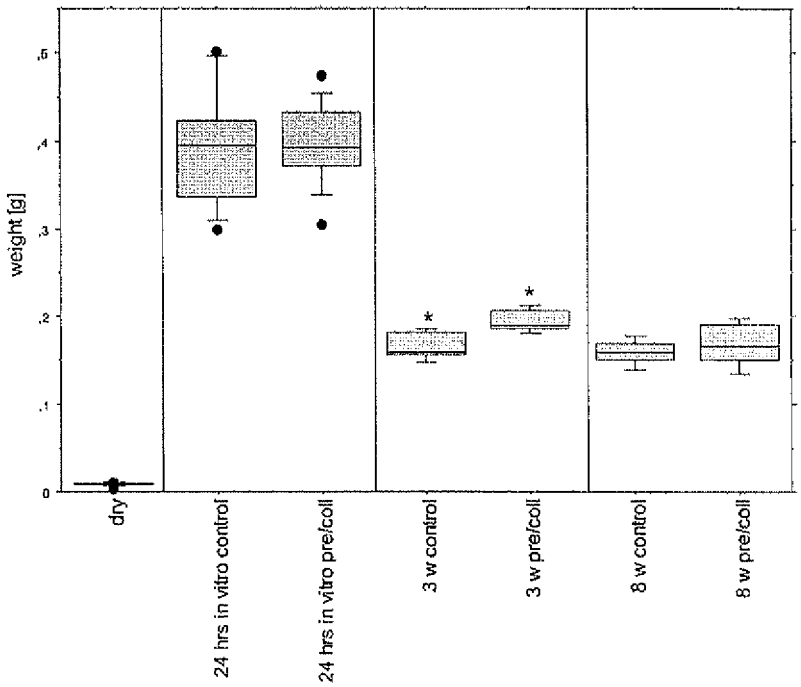

Fig. 8. Weight of preadipocyte/collagen and control grafts. As assumed there was significant increase after the wetting and seeding of the collagen scaffolds. The decrease of the weight was significant after 3 weeks in vivo for preadipocyte/collagen grafts and the control grafts ($*p < 0.05$). There were significant differences between the type of grafts after 3 weeks (unnotched box plot with outliers represented by data points).

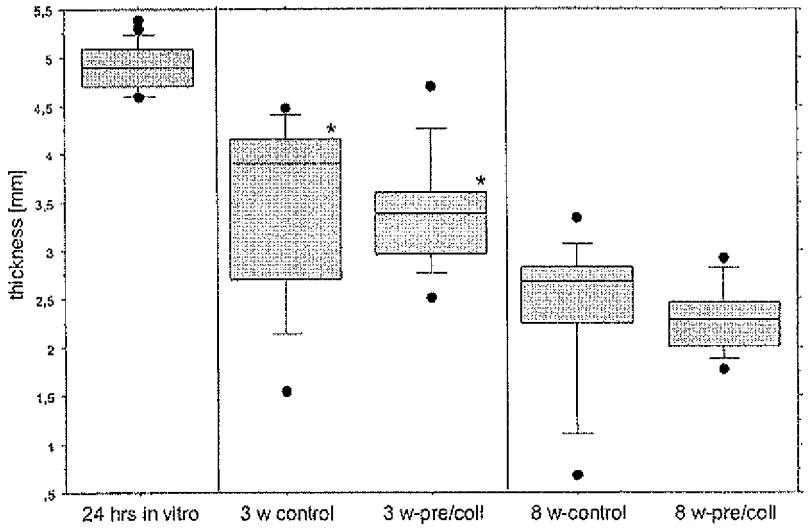

Fig. 9. Thickness showed significant decrease in the first 3 weeks of implantation ($*p < 0.05$). No statistical difference could be seen between preadipocyte/collagen grafts and control grafts while the thickness in the pre preadipocyte/collagen grafts was more constant.

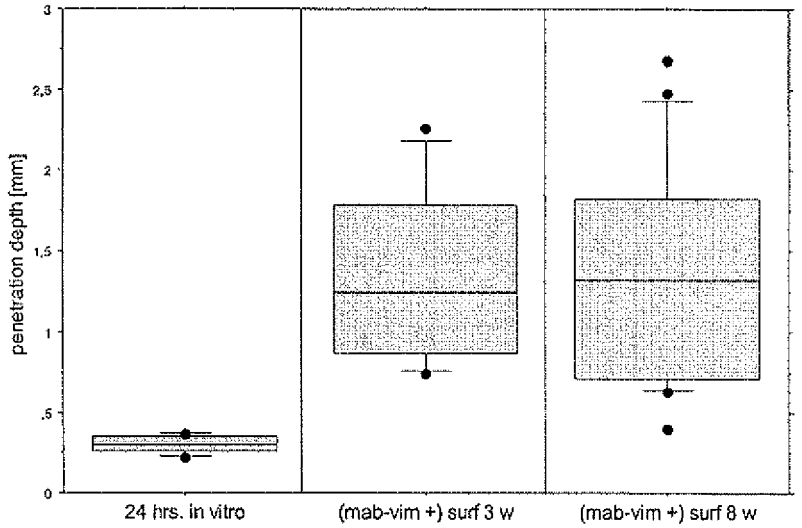

Fig. 10. Average maximum penetration depth of human preadipocytes in collagen constructs in vitro (after 24 h) and of mah-vimentin stained cells on cross-sectional areas in vivo (3 and 8 weeks in the nude mouse). There was significant increase in penetration depth between in vitro and 3 weeks and 8 weeks in vivo. After 8 weeks in some scaffolds human cells could be found in the centre (2.5 mm depth).

Penetration depth of the human preadipocytes is shown in Figs. 10 and 11. There was a significant increase compared to the penetration depth after 24 h. After 8 weeks the mean penetration depth of human preadipocytes in the grafts was higher.

3.2.5. *Ultrastructure of the grafts*

Twenty-four hours in vitro (Fig. 12): The cytoplasm showed few small fat droplets, which identified them as preadipocytes. The typical preadipocytes showed numerous organelles and most of these were located in the paranuclear area. The preadipocytes presented elongated contour and tight contact to the scaffold.

Three weeks in vivo (Fig. 13): The lipid droplets were larger. Cells with single large lipid droplets were seen. There were multiple capillaries located near the preadipocytes and adipocytes. New collagen fibrils were found in close vicinity to the collagen of the scaffold. Viable adipocytes (with minimal in the narrow pores) were found only to a depth of 350 μm (Fig. 8). Adipocytes were closely attached to the scaffold collagen and bundles of new collagen fibrils were found inbetween.

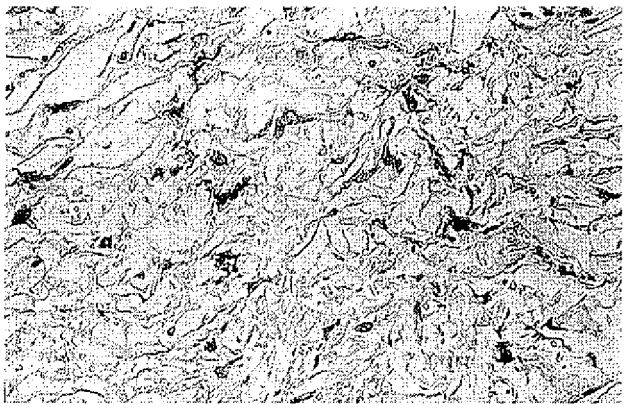

Fig. 11. Invaded human cells in a preadipocyte/collagen graft in group A (3 weeks in vivo). Note good and homogenous distribution of human cells in the scaffold and the attached mature adipocytes which are not stained (×200, mah-vim stain).

Fig. 13. Ultrastructure of human preadipocyte-seeded collagen sponges after 3 weeks in nude mouse. The 'old' collagen with the adhered mature adipocyte beside the 'new' collagen matrix.

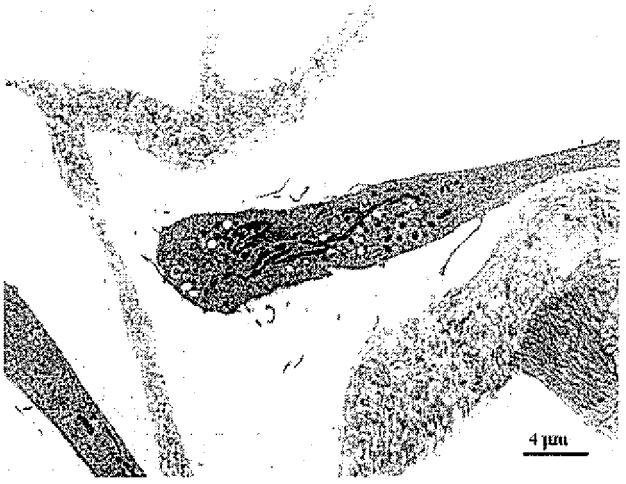

Fig. 12. Ultrastructure of human preadipocyte attached to a collagen sponge after 24 h in vitro. The cells are closely adhered to the scaffold collagen material. Note the small lipid droplets which identifies the cell as a preadipocyte.

Undifferentiated preadipocytes presented deep inside the sponge in narrow pores and were closely attached to the scaffold material.

Eight weeks in vivo: Morphology of the adipocytes was unchanged. The scaffold showed a more irregular structure and obstructed pores by collapsed collagen remnants. There were some giant cells and newly formed ECM mainly composed of collagen fibres.

4. Discussion

This study presents an efficient method of adipose tissue transplantation for the reconstruction of soft tissue defects. Human preadipocytes were isolated, cultured and attached to collagen sponges of specific pore structure. The preadipocytes survived transplantation into the immunodeficient mouse and fully differentiated at the recipient site after vascularisation.

The first transplantation of adipose tissue was performed over a century ago in an attempt to find an optimal material for autologous soft tissue replacement. In general, the results were unsatisfactory because of shrinkage up to complete resorption of the grafts [13]. Hausberger was the first to achieve a successful take of fat grafts by using immature adipose tissue in a new born rat model. The immature adipose tissue was transplanted 'empty', some days before fat deposition began. Hausberger observed fat deposition in the free transferred adipocytes at the recipient site. The volume of the grafts reached 83% of the non-transplanted controls [14]. This amount of surviving adipose tissue after free transplantation could never be reached by other techniques [7,15,16].

Hausberger's results prompted a further investigation of preadipocyte transplantation instead of the transplantation of mature adipocytes. In previous experiments we achieved a delipidation of mature adipose tissue by mechanical compression in vivo. The adipocytes changed their signet ring-like appearance to an elongated contour. After free grafting of this compressed adipose tissue the storage of lipid in the cells reoccured similar to the differentiation of preadipocytes to adipocytes. The revascularisation and the take of these compressed grafts was better than with non-compressed adipose tissue [17]. This procedure proved to be too elaborate for clinical application. Therefore an alternative method to obtain non-differentiated cells out of adults was used as described by Rodbell [18]. Rodbell was the first who

separated preadipocytes from mature adipocytes out of adipose tissue by collagenase treatment. The fraction of preadipocytes in adipose tissue has a great variability depending on the species and its age. In rats 50% of the stromal-vascular cells are preadipocytes, whereas in humans the fraction is between 1% in children and less than 0.1% in adults [19,20].

In contrast to previous studies, e.g. Patrick et al. who used rat preadipocytes [21], we cultured and transplanted precursor cells of human origin in the study presented.

For a good outcome we found it important to transplant a high number of preadipocytes. For this reason culture medium was enriched by EGF to support proliferation and suppress differentiation of preadipocytes. By using this medium an 8-fold increase in cell number in monolayer was reached before seeding the cells onto the sponges. After the implantation the preadipocytes differentiated to mature adipocytes in vivo. EGF reversibly suppressed the differentiation of preadipocytes during the in vitro period. This observation supports the use of EGF as opposed to other cytokines which cause irreversible inhibition of differentiation [22].

In our study preadipocytes were identified after induced differentiation to adipocytes by the enrichment of the medium with dexamethasone and insulin. This method proved to be reliable and detected that more than 80% of the cells for grafting were preadipocytes. The direct distinction between preadipocytes and possible fibroblasts in the monolayer culture is currently not possible [23]. Stored lipid droplets in the cytoplasm have specific microscopical features during differentiation but markers of preadipocytes at earlier stages are not very specific. Vimentin and also ADRP (Perilipin) were first introduced as typical markers for preadipocytes [24]. However these proteins were also found in other cells, i.e. vimentin occurs in almost all mesenchymal cells [25] and ADRP also in Schwann cells [26].

The optimal matrix for preadipocyte transplantation is not yet known. Collagen is a widely used material in tissue regeneration and porous collagen matrix supports cellular ingrowth and new matrix synthesis [27–29].

To this date bovine collagen was not the optimal choice because it could not be manufactured with a high degree of reproducibility [30]. Freed et al. found many pores to be 'closed' and not open for the ingrowth of cells. In preliminary work we could show that commercially available collagen scaffolds have an irregular pore size distribution and therefore in vitro results based on these matrices vary greatly (unpublished data). The used collagen scaffolds produced by a directional solidification method [11] and subsequent freeze-drying [12] provided a regular architecture and therefore more reproducible results than scaffolds with an irregular pore structure.

We found that the in vivo differentiation of the transplanted preadipocytes also depends on the scaffold architecture. The human preadipocytes penetrated the scaffold in vivo to a depth of more than 1400 μm, whereas mature adipocytes were only found to a depth of 350 μm. Developing adipocytes grow to a diameter of up to 100 μm and their further growth and differentiation appeared to be restricted due to the narrow pore size of the scaffold. As seen in previous studies mechanical compression of adipose tissue leads to delipidation [17]. We conclude that preadipocytes need enough porous space to differentiate to mature adipocytes. In case of preadipocytes which enlarge significantly during differentiation due to incorporation of lipids it is assumed that pore sizes are required that are larger than 40 μm.

The transplantation of isolated and cultured preadipocytes within a standardised collagen matrix resulted in well vascularised adipose-like tissue. The results support the use of directionally solidified collagen sponges as preadipocyte delivery matrix in adipose tissue engineering. Currently, we cannot compare our results to other studies because to our knowledge no other investigations on the transplantation of human preadipocytes have been published yet. Other matrices and larger pore sizes have to be tested in order to define the optimal delivery matrix.

Acknowledgements

This work was supported by a grant from the Medical Faculty of Aachen University of Technology RWTH (START-03/97) and IZKF 'BIOMAT' (BMBF-01KS9503/9). The development of the collagen scaffolds was supported by the Deutsche Forschungsgemeinschaft (DFG), grant: Ra 335/22-1,2. The ultrastructural examination was done by Dr. Hollweg of the Institute of Pathology of the RWTH Aachen, Germany. We wish to acknowledge the technical assistance of Mrs. B. Kowol and Mrs. D. Benner and of Mrs. M. Geiser-Letzel for her excellent assistance in immunohistochemistry.

References

[1] Dzubow LM, Goldman G. Introduction to soft tissue augmentation: a historical perspective. In: Klein A, editor. Tissue augmentation in clinical practice. Basel: Marcel Dekker, 1998. p. 1–22.
[2] Peer L. The neclected free fat graft. Am J Surg 1956;18:233–50.
[3] Rossatti B. Revascularisation and phagocytosis in free fat autografts: an experimental study. Br J Plast Surg 1960;13:35–41.
[4] Smahel J, Meyer VE, Schütz K. Vascular augmentation of free adipose tissue grafts. Eur J Plast Surg 1990;13:163–8.
[5] Smahel J. Experimental implantation of adipose tissue fragments. Br J Plast Surg 1989;42:207–11.
[6] Ersek R. Transplantation of purified autologous fat: a 3-year follow-up is disappointing. Plast Reconstr Surg 1991;87:219–27.
[7] Kononas TC, Bucky LP, Hurley C, May JW. The fate of suctioned and surgically removed fat after reimplantation for soft-tissue augmentation: a volumetric and histologic study in the rabbit. Plast Reconstr Surg 1993;91:763–8.

[8] Niechajev I, Sevcuk O. Long-term results of fat transplantation: clinical and histologic studies. Plast Reconstr Surg 1994;94: 496–506.
[9] Ailhaud G, Grimaldi P, Négrel R. Cellular and molecular aspects of adipose tissue development. Annu Rev Nutr 1992;12:207–33.
[10] Green H, Kehinde O. Formation of normally differentiated subcutaneous fat pads by an established preadipose cell line. J Cell Physiol 1979;101:169–72.
[11] Heschel I, Lückge C, Rödder M, Garbering C, Rau G. Possible applications of directional solidification techniques in cryobiology. In: Kittel P, editor. Advances of cryogenic engineering. New York: Plenum Press, 1996. p. 13–9.
[12] Heschel I, Rau G. Method for producing porous structures. International Patent Application PCT/DE 98/03403, November 19, 1997.
[13] Billings E, May JW. Historical review and present status of free fat graft autotransplantation in plastic and reconstructive surgery. Plast Reconstr Surg 1989;83:368–81.
[14] Hausberger FX. Quantitative studies on the development of autotransplants of immature adipose tissue of rats. Anat Rec 1955; 122:507–15.
[15] Eppley BL, Sidner RA, Platis JM, Sadove AM. Bioactivation of free-fat transfers: a potential new approach to improving graft survival. Plast Reconstr Surg 1992;90:1022–30.
[16] Ullmann Y, Hyams M, Ramon Y, Beach D, Peled IJ, Lindenbaum ES. Enhancing the survival of aspirated human fat injected into nude mice. Plast Reconstr Surg 1998:1940–4.
[17] von Heimburg D, Lemperle G, Dippe B, Kruger S. Free transplantation of fat autografts expanded by tissue expanders in rats. Br J Plast Surg 1994;47:470–6.
[18] Rodbell M. Metabolism of isolated fat cells. J Biol Chem 1964; 239:375–80.
[19] Pettersson P, Cigolini M, Sjostrom L, Smith U, Bjorntorp P. Cells in human adipose tissue developing into adipocytes. Acta Med Scand 1984;215:447–51.
[20] Loeffler G, Hauner H. Adipose tissue development: the role of precursor cells and adipogenic factors. Part II: the regulation of the adipogenic conversion by hormones and serum factors. Klin Wochenschr 1987;65:812–7.
[21] Patrick CW, Chauvin PB, Hobley J, Reece GP. Preadipocyte seeded PLGA scaffolds for adipose tissue engineering. Tissue Eng 1999;5:139–51.
[22] Petruschke T, Rohrig K, Hauner H. Transforming growth factor beta (TGF-β) inhibits the differentiation of human adipocyte precursor cells in primary culture. Int J Obes Relat Metab Disord 1994;18:532–6.
[23] Hauner H, Loeffler G. Adipose tissue development: the role of precursor cells and adipogenic factors. Part I: adipose tissue development and the role of precursor cells. Klin Wochenschr 1987;65:803–11.
[24] Greenberg AS, Egan JJ, Wek SA, Garty NB, Blanchette-Mackie EJ, Londos C. Perilipin, a major hormonally regulated adipocyte-specific phosphoprotein associated with the periphery of lipid storage droplets. J Biol Chem 1991;15:11341–6.
[25] Franke WW, Hergt M, Grund C. Rearrangement of the vimentin cytoskeleton during adipose conversion: formation of an intermediate filament cage around lipid globules. Cell 1987;10: 131–41.
[26] Brasaemle DL, Barber T, Wolins NE, Serrero R, Blanchette-Mackie EJ, Londos C. Adipose differentiation-related protein is an ubiquitously expressed lipid storage droplet-associated protein. J Lipid Res 1997;38:2249–63.
[27] Li ST, Archibald SJ, Krarup C, Madison R. Semipermeable collagen nerve conduits for peripheral nerve regeneration. Polym Mater Sci Engng 1990;62:575–82.
[28] Stone KR, Steadman JR, Rodkey WG, Li ST. Regeneration of meniscal cartilage with use of a collagen scaffold. Analysis of preliminary data. J Bone Jt Surg Am 1997;79:1770–7.
[29] Silver FH, Pins G. Cell growth on collagen: a review of tissue engineering using scaffolds containing extracellular matrix. J Long Term Effects Med Implants 1992;2:67–80.
[30] Freed LE, Vunjak-Novakovic G, Biron RJ, Eagles DB, Lesnoy DC, Barlow SK, et al. Biodegradable polymer scaffolds for tissue engineering. Biotechnology 1995;12:689–93.

TISSUE ENGINEERING
Volume 10, Number 3/4, 2004
© Mary Ann Liebert, Inc.

Photocured, Styrenated Gelatin-Based Microspheres for *de Novo* Adipogenesis through Corelease of Basic Fibroblast Growth Factor, Insulin, and Insulin-Like Growth Factor I

TEIICHI MASUDA, M.D.,[1,2] MASUTAKA FURUE, M.D., Ph.D.,[2] and TAKEHISA MATSUDA, Ph.D.[1]

ABSTRACT

***De novo* adipose tissue formation appears to proceed via two different biological events: neovascularization and spontaneous accumulation of preadipocytes and subsequent differentiation to mature adipocytes. In this article, we perform accelerated *de novo* adipose tissue engineering using photocured, styrenated, gelatin-based microspheres (SGMs) with different drug release rates of immobilized angiogenic and adipogenic factors. The concept of this system is to induce neovascularization and migration of endogenous preadipocytes by the rapid delivery of the angiogenic factor basic fibroblast growth factor (bFGF), followed by the proliferation and differentiation of preadipocytes into adipocytes by the prolonged delivery of the adipogenic factors, insulin and insulin-like growth factor I (IGF-I). Bioactive substance-immobilized SGMs with different drug release rates were prepared with different gelatin concentrations. An *in vitro* study showed the prolonged release of an immobilized model protein and the dependence of drug release rate on gelatin concentration. After the subcutaneous injections of SGMs immobilized with these bioactive substances in different combinations, the formation of masses or clusters of adipocytes was observed in rats. Triglyceride content in the injection site for the group that received bFGF-, insulin-, and IGF-I-immobilized SGMs was significantly higher than that for the group that received insulin- and IGF-I-immobilized SGMs 4 weeks after the injection of microspheres. These results suggest that the system developed here is effective for the *de novo* formation of adipose tissue as it enables the induction of the two-step biological reaction by single injection.**

INTRODUCTION

SOFT TISSUE AUGMENTATION is still an ongoing challenge in the field of plastic and reconstructive surgery. The use of adipose tissue equivalents is required for the treatment of soft tissue defects such as congenital malformations (e.g., hemifacial microsomia and Poland's syndrome) and posttraumatic or postoperative wounds. The available clinical approaches to overcoming these issues include local–regional or free microvascular flaps, dermal fat graft, collagen injection, the use of synthetic materials, and autologous fat transplantation. Each of these methods, however, is associated with certain drawbacks such as operative risk to some degree, donor site morbidity, resorption of implanted grafts, and foreign body reaction to the implanted synthetic materials.[1–4]

The tissue-engineering approach to forming adipose

[1]Department of Biomedical Engineering, Graduate School of Medicine, Kyushu University, Fukuoka, Japan.
[2]Department of Dermatology, Graduate School of Medicine, Kyushu University, Fukuoka, Japan.

tissue can be realized via two methods: one method is to transplant preadipocytes with or without a scaffold into the site in which soft tissue repair is required, followed by the spontaneous differentiation of preadipocytes or adipocyte progenitor cells to mature adipocytes,[5–10] and the other method is *de novo* adipogenesis, which proceeds via a two-step biological process. First, the enhanced migration of preadipocytes is accompanied by induced local neovascularization, followed by the subsequent adipogenic differentiation of preadipocytes to mature adipocytes.[11–14] Regardless of the type of approach, neovascularization appears to be essentially required to avoid necrosis and possibly to secrete unknown differentiation factors. These two different biological events of angiogenesis and adipogenesis have been proven to be promoted by the addition of basic fibroblast growth factor (bFGF) for the former process and insulin and insulin-like growth factor I (IGF-I) for the latter process.[11–16]

For example, *de novo* adipogenesis was realized by injecting a mixed solution of an extract of a basement membrane (Matrigel) and bFGF[11] or gelatin microspheres immobilized with bFGF,[12,13] or by injecting poly(lactic-co-glycolic-acid)-polyethylene glycol (PLGA/PEG) microspheres coimmobilized with insulin and IGF-I into the subcutaneous lesion.[14] However, an attempt at long-term simultaneous delivery of both angiogenic and adipogenic factors to generate adipose tissues has not yet been reported.

Our approach toward *de novo* adipose tissue formation aims at the construction of a long-term simultaneous delivery system for angiogenic (bFGF) and adipogenic (insulin and IGF-I) factors, both of which are separately immobilized in photocured, styrenated gelatin microspheres (SGMs). Our previous study showed that a photocured SG matrix can serve as a drug delivery system with the following features: (1) the desired amount of drug in a photocured matrix can be easily loaded and (2) the drug release rate can be controlled.[17]

Our strategy by which *de novo* adipose tissue formation is accelerated involves coinjection of three different types of photocured SGMs, each of which is immobilized with protein drugs of different biological activities. Because an ideal scenario of *de novo* adipogenesis involves a sequential or simultaneous process of capillary formation and accumulation and differentiation of preadipocytes to adipocytes, co-use of SGMs with the fast release characteristic of bFGF and SGMs and the relatively slow release characteristic of both insulin and IGF-I may be beneficial. In this study, the preparation of SGMs, and their *in vitro* drug release characteristics, are described and the adipogenic effects on implantation of these microspheres into subcutaneous lesions of rats are examined.

MATERIALS AND METHODS

Materials

Gelatin (from bovine bone; MW, 9.5×10^4 g/mol) was purchased from Wako Pure Chemical Industries (Osaka, Japan). Water-soluble carboxylated camphorquinone (CQ), (1S)-7,7-dimethyl-2,3-dioxobicyclo[2.2.1]hepatane-1-carboxylic acid, was prepared according to the method described previously.[18] Rhodamine–lactalbumin, fluorescein isothiocyanate (FITC)–insulin, and 3,3-diaminobenzidine were purchased from Sigma (St. Louis, MO). Recombinant human basic fibroblast growth factor (bFGF) was purchased from R&D Systems (Minneapolis, MN). Recombinant human IGF-I was purchased from Genzyme (Cambridge, MA). Anti-human von Willebrand factor antibody and peroxidase-conjugated anti-rabbit IgG antibody were purchased from DakoCytomation (Carpinteria, CA). Cryostat specimen matrix (Tissue-Tek O.C.T. compound) was purchased from Sakura Finetek Japan (Tokyo). All other reagents were purchased from Wako Pure Chemical Industries.

Preparation of styrenated gelatin microspheres

The synthesis of photocurable, styrenated gelatins (styrene content, approximately 27.6 per gelatin molecule) and preparation of aqueous styrenated gelatin solutions were carried out according to procedures reported previously.[17] Briefly, styrenated gelatin was synthesized by condensation reaction of gelatin with 4-vinylbenzoic acid. The reaction mixture was dialyzed and then lyophilized, using a freeze-drier. One gram of aqueous styrenated gelatin solution was poured into 20 mL of liquid paraffin with 0.2% Span 85 and stirred at 120–150 rpm under visible light irradiation, using an 80-W halogen lamp (Tokusou Power Lite; Tokuyama, Tokuyama, Japan; wavelength, 400 nm $< \lambda <$ 520 nm; irradiation intensity, 1.3×10^6 lux) for 20 min. After the addition of 20 mL of hexane, the gelatin microspheres formed were collected by filtration through a glass fiber filter (pore size, 0.6 μm). The microspheres were then washed three times with 40-mL aliquots of hexane to remove residual paraffin, and dried for 1 h at room temperature. SGMs were used in further *in vitro* or *in vivo* experiments immediately after preparation.

Morphological analysis of microspheres

SGM morphology was determined by scanning electron microscopy (SEM) (JSM-6301F; UEOL, Tokyo, Japan). Particle size was determined on the basis of randomly selected 500 microspheres from 5 fields of view, using an optical microscope (TE300; Nikon, Tokyo, Japan) fitted with a micrometer scale.

In vitro *drug release*

Two hundred milligrams of aqueous gelatin solution containing 0.1 wt% CQ and 0.2 wt% rhodamine–lactalbumin or FITC–insulin as model drugs, was poured into the bottom of a well of a 48-well dish, and then irradiated with 1.3×10^6 lux of visible light for 3 min to form a gel. Disk-type gels were dispensed into a 12-well dish. Two milliliters of phosphate buffer solution (PBS, pH 7.4) supplemented with penicillin and streptomycin was added to each well and liquid samples were withdrawn from the wells at regular intervals at 37°C. The amount of model drug released from the gel was determined spectrophotometrically at 558 nm for rhodamine–lactalbumin and at 493 nm for FITC–insulin, respectively (DU 530; Beckman Coulter, Fullerton, CA).

In vivo *experiments*

Animal experiments were reviewed by the Committee on the Ethics of Animal Experiments (Faculty of Medicine, Kyushu University, Fukuoka, Japan) and carried out in accordance with the *Guidelines for Animal Experiments* of the Faculty of Medicine, Kyushu University and the law (no. 105) and notification (no. 6) of the Japanese government. Six-week-old male Wistar rats (Kyudou, Saga, Japan) were anesthetized by intraperitoneal injection of pentobarbital (40 mg/kg). Either bFGF, insulin, or IGF-I was premixed with aqueous styrenated gelatin solution, and SGMs were prepared according to the procedure described previously. The gelatin concentrations were 20% for bFGF-immobilized SGMs and 30% for insulin- or IGF-I-immobilized SGMs. One hundred milligrams of bioactive substance-immobilized SGMs was injected subcutaneously into the dorsal area bilaterally. Table 1 details the SGMs used in these experiments, with their various contents of bioactive substances. For group IV, two different SGMs, each immobilized with insulin (2 IU/100 mg of SGM) or IGF-I (2 μg/100 mg of SGM), were prepared separately, and mixed in equal amounts and injected at each site. For group V, three types of SGMs immobilized with either bFGF (3 μg/100 mg of SGM), insulin (3 IU/100 mg of SGM), or IGF-I (3 μg/100 mg of SGM) were prepared and mixed in equal amounts for injection. SGMs without any bioactive substances were used as control. The amount of immobilized insulin was determined approximately from our preliminary animal experiments. That is, a single subcutaneous injection of a quantity 10-fold higher than the total immobilized amount (10 IU of insulin for injected SGMs used for this study) in the backs of rats resulted in death within 1 day of injection, whereas injection of one-tenth the total immobilized amount resulted in no adipose tissue formation. The amount of total immobilized IGF-I was determined from those in previous papers.[14–16] Four rats for each experimental group were used and samples were harvested for further studies.

TABLE 1. EXPERIMENTAL GROUPS[a] AND INGREDIENTS FORMULATION

	Active ingredient (per 100 mg of SG)		
Group no.	*bFGF (μg)*	*Insulin (IU)*	*IGF-I (μg)*
I (0.01)	0.01	—	—
I (0.01)	0.1	—	—
I (1)	1	—	—
I (10)	10	—	—
II	—	1	—
III	—	—	1
IV	—	1	1
V	1	1	1
VI (control)	—	—	—

[a] *Group I:* SGMs immobilized with bFGF at four different concentrations (μg per 100 mg of photocured SG) (group I [0.01 μg], group I [0.1]; group I [1], and group I [10]). *Group II:* SGMs immobilized with 1 IU of insulin per 100 mg of photocured SG. *Group III:* SGMs immobilized with 1 μg of IGF-I per 100 mg of photocured SG. *Group IV:* SGMs immobilized with 1 IU of insulin and 1 μg of IGF-I per 100 mg of photocured SG. *Group V:* SGMs immobilized with 1 μg of bFGF, 1 IU of insulin, and 1 μg of IGF-I per 100 mg of photocured SG. *Group VI:* SGMs immobilized with no ingredient.

Histological studies

Skin paddles with underlying subcutaneous tissue (2×2 cm^2), including the site of injection, were harvested and fixed in 10% formalin. For groups I (0.01) (0.01 μg of bFGF per 100 mg of SGM), I (0.1), I (1), I (10), and VI, the specimens were embedded in paraffin and sectioned, followed by staining with hematoxylin and eosin (H&E) or immunostaining with an antibody to human von Willebrand factor at a dilution of 1:1600 at 4°C for 16 h. After further incubation with the peroxidase-conjugated anti-rabbit IgG antibody, peroxidase activity was visualized with 3,3-diaminobenzidine. The immunostained sections were counterstained with hematoxylin. Twenty different fields were selected from fibrous tissue surrounding residual injected SGMs for determining the number of capillaries (×200 magnification). For groups I (1), II, III, IV, V, and VI, the specimens were divided into two pieces. One-half of each specimen was embedded in paraffin for H&E and von Willebrand factor staining, and the remaining half was embedded in O.C.T. compound, cryosectioned, and stained with Sudan IV.

Lipid analysis

Fibrous tissue (2×2 cm^2), which lies in between the cutaneous muscle of the trunk and the superficial mus-

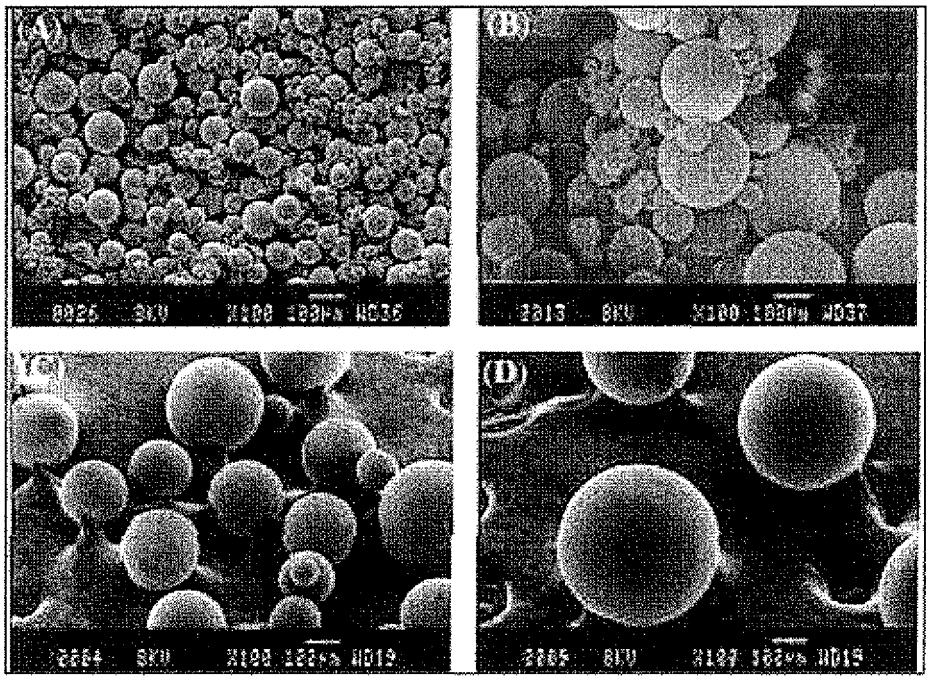

FIG. 1. Scanning electron micrographs of SGMs. SG concentration: (A) 20%, (B) 30%, (C) 40%, (D) 50%.

cles of the back, including the site of SGM injection, was harvested. The specimens were minced and homogenized in distilled water. Total lipid was extracted with chloroform–methanol (2:1, v/v) and centrifuged for 5 min at 1.2×10^4 rpm. The mixed organic solution layer containing triacylglycerol was extracted and placed under vacuum to evaporate the chloroform and methanol. Triacylglycerol content was measured with a triglyceride E-test kit (Wako Pure Chemical Industries) according to the manufacturer's instructions.

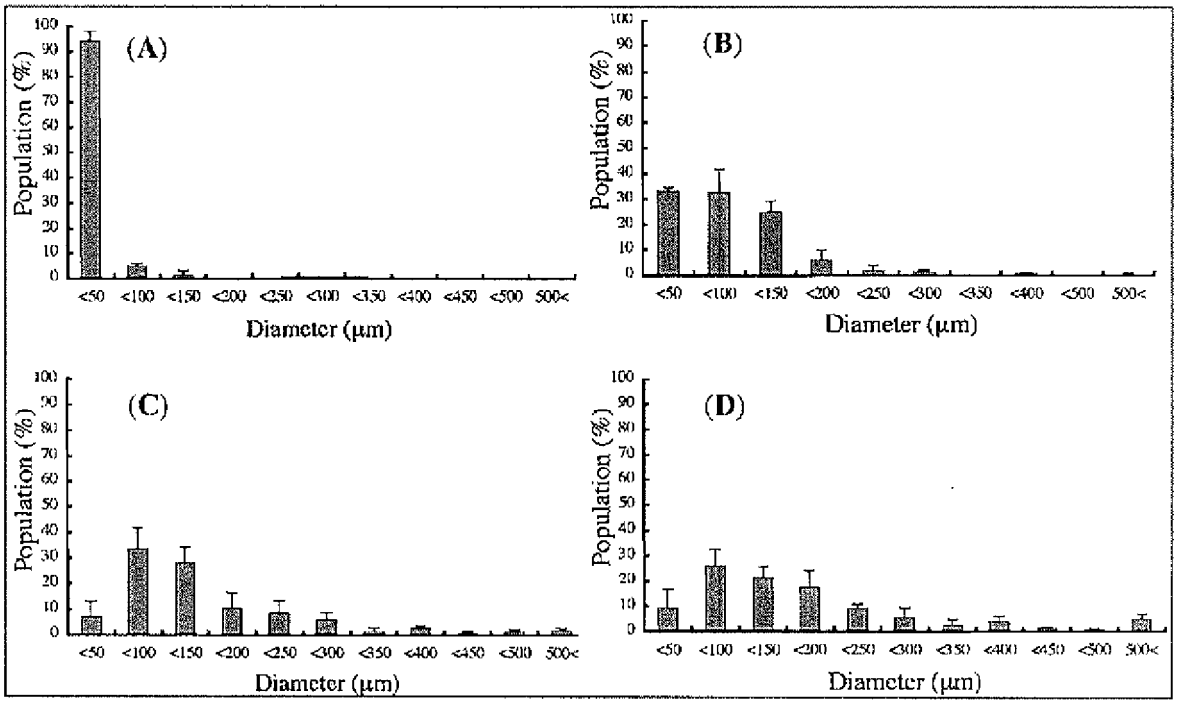

FIG. 2. Particle size distribution of SGMs. SG concentration: (A) 20%, (B) 30%, (C) 40%, (D) 50%.

TABLE 2. MEAN PARTICLE DIAMETER OF SGMs AS FUNCTION OF SG CONCENTRATION

SG concentration (wt %)	*Mean diameter (μm ± SD)*[a]
20	25.4 ± 18.6
30	85.9 ± 69.9
40	145.8 ± 113.4
50	187.1 ± 234.5

Abbreviations: SG, styrenated gelatin; SGMs, styrenated gelatin-based microspheres.

[a]The data were statistically determined on the basis of 500 particles randomly selected from 5 fields of view, using an optical microscope.

Statistical analysis

Experimental results were expressed as means ± standard deviation (SD). The data were subjected to statistical analysis (analysis of variance, ANOVA). Statistical analysis was carried out by ANOVA with a Tukey–Kramer post hoc test; $p < 0.05$ was considered statistically significant. All statistical analyses were performed with StatView 5.0 (Abacus, Berkley, Calif., USA).

RESULTS

Preparation and morphological analysis of photocured gelatin microspheres

Styrenated gelatin (SG)-based microspheres (SGMs) were prepared by dispersing an aqueous solution containing SG and carboxylated camphorquinone as a photocleavable radical generator in liquid paraffin under stirring at room temperature and subsequently subjecting it to visible light irradiation. SEM observations revealed that the SGMs obtained by filtration are fairly round particles with a smooth surface (Fig. 1A–D). Qualitatively, at higher SG concentration, larger microspheres with a broader diameter distribution were obtained. In a quantitative study to determine population size, the obtained histograms show that, at the lowest SG concentration (20%), the size of the majority of microspheres was below 50 μm, and that an increase in SG concentration resulted in a heterogeneous size distribution (Fig. 2A–D). The mean particle diameter of SGMs ranged from approximately 25 to 187 μm, depending on SG concentration (Table 2).

In vitro *drug release*

The SG concentration-dependent release characteristics of model drugs, as shown below, were determined as follows: the photocured SG disks (diameter, 12 mm; thickness, 1.8 mm) were prepared from a premixed solution of SG with a model protein, rhodamine–lactalbumin, the molecular weight of which (1.4×10^4) is almost identical to that of bFGF (1.6×10^4), and FITC–insulin, the molecular weight of which (6.1×10^3) is almost identical to those of insulin (5.7×10^3) and IGF-I (7.6×10^3), at various SG concentrations in the wells of culture dishes. The time course of the release of the model protein into a buffer solution was determined spectrophotometrically. Figure 3A and B shows the time-dependent fractional change in the amount of released rhodamine–lactalbumin and FITC–insulin from SG disks prepared at different SG concentrations, respectively. Irrespective of SG concentration, the release profiles are characterized by an initial burst of protein release during the first day, followed by prolonged release at a lower rate for up to 21 days (length of observation period). The fractional releases of both rhodamine–lactalbumin and FITC–insulin were dependent on SG concentration: the higher the SG concentration, the lower the release rate. Significant differences in release rate were not observed

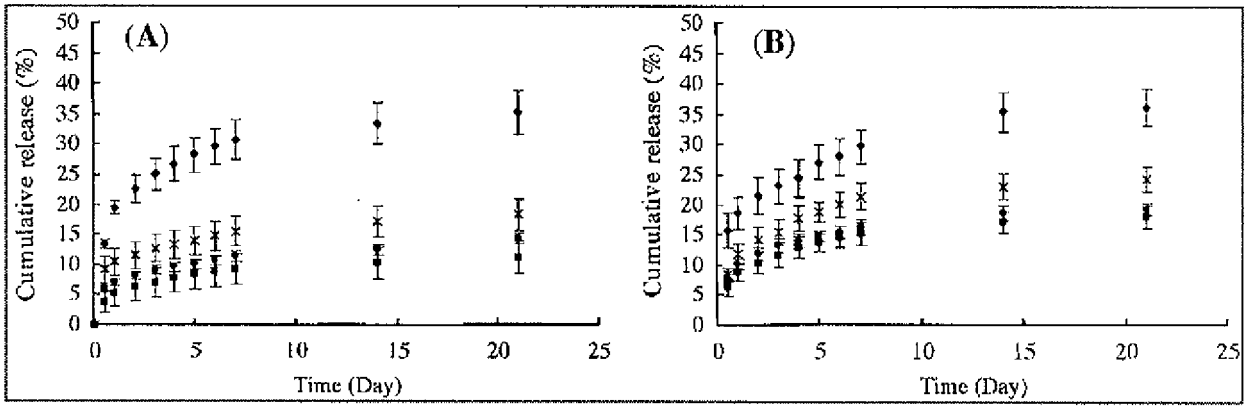

FIG. 3. Fractional release of (A) rhodamine–lactalbumin and (B) FITC–insulin from SG disks ($n = 4$). SG concentration: 20 wt% (◆), 30 wt% (×), 40 wt% (●), and 50 wt% (■). CQ concentration: 0.1 wt% of SG. Visible light irradiation: 3 min at a photointensity of 1.3×10^6 lux. Values are expressed as means ± SD.

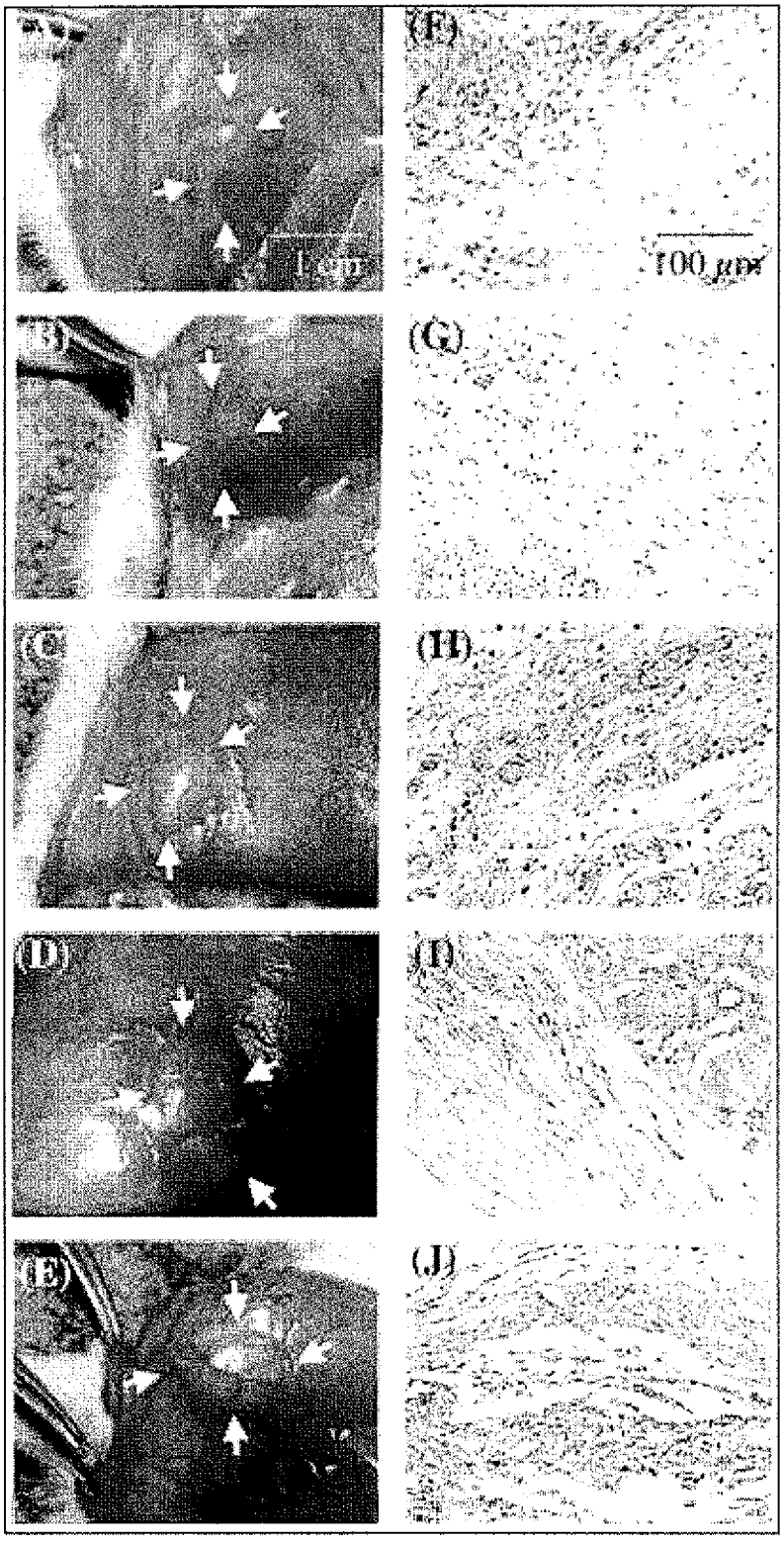

FIG. 4. Tissue appearance (A–E, surrounded by arrows) and von Willebrand factor-staining sections (F–J) of injection site, 2 weeks after injection of SGMs immobilized with 0.01 [A and F: group I (0.01)], 0.1 [B and G: group I (0.1)], 1 [C and H: group I (1)], 10 [D and I: group I (10)], and 0 (E and J: group VI) μg of bFGF.

at a fixed SG concentration, probably because of small difference in the molecular weight of model proteins.

De novo *adipose tissue generation*

Various SGMs immobilized with or without bioactive substances including bFGF, insulin, and IGF-I were prepared at a fixed SG concentration: the SG concentrations used were 20 wt% for bFGF-immobilized SGMs and 30 wt% for insulin- or IGF-I-immobilized SGMs. One hundred milligrams of SGMs was injected into the subcutaneous tissues of Wistar rats. An implantation study was conducted with six different groups as follows. Group I consisted of SGMs immobilized with only bFGF at four different concentrations (μg) per 100 mg of photocured SG, designated Group I (0.01), Group I (0.1), Group I (1), and Group I (10). Group II consisted of SGMs immobilized only with insulin (1 IU per 100 mg of photocured SG), group III consisted of SGMs immobilized only with IGF-I (1 μg per 100 mg of photocured SG), group IV consisted of SGMs immobilized with insulin (1 IU) and IGF-I (1 μg) per 100 mg of photocured SG, and group V consisted of SGMs immobilized with three ingredients (bFGF [1 μg], insulin [1 IU], and IGF-I [1 μg] per 100 mg of photocured SG). Group VI consisted of SGMs immobilized with no bioactive substances.

Effect of bFGF-immobilized microspheres on neovascularization. Figure 4A–E shows macroscopic views of tissues 2 weeks after subcutaneous injection of SGMs with or without bFGF. For Group I, vascularization around the injection site of bFGF-immobilized SGMs became apparent as the amount of bFGF immobilized in SGMs increased. The highest degree of neovascularization was observed for SGMs immobilized with bFGF at a concentration of 1 μg/100 mg of photocured SG, whereas the lowest degree was found for group VI (without bFGF). Figure 4F–J shows results of the histochemical vWF staining of sections of the surrounding tissues in the injection site 2 weeks after the subcutaneous injection of SGMs with or without bFGF. The number of capillaries around the injection site increased as the amount of bFGF immobilized in SGMs increased. The capillary densities of the surrounding tissues 2, 4, and 6 weeks after injection of bFGF-immobilized SGMs, in comparison with those of SGMs without any bioactive substance, are shown in Fig. 5. The highest capillary density was observed for group I (1) 2 weeks after injection, and it was about twice that of the control group (group VI) during the same period; little difference in capillary density was observed 4 and 6 weeks after injection regardless of the group. In comparison with other groups (groups II, III, IV, and V), at 4 weeks postimplantation, there is no significant difference in capillary density between groups, although the mean capillary density of the bioactive substance-immobilized groups, except for the group with the least bFGF, is higher than that of the control (group VI).

Gross observations. Figure 6A–F shows macroscopic views of subcutaneous lesions of groups I (1), II, III, IV, V, and VI, 4 weeks after injection of SGMs immobilized

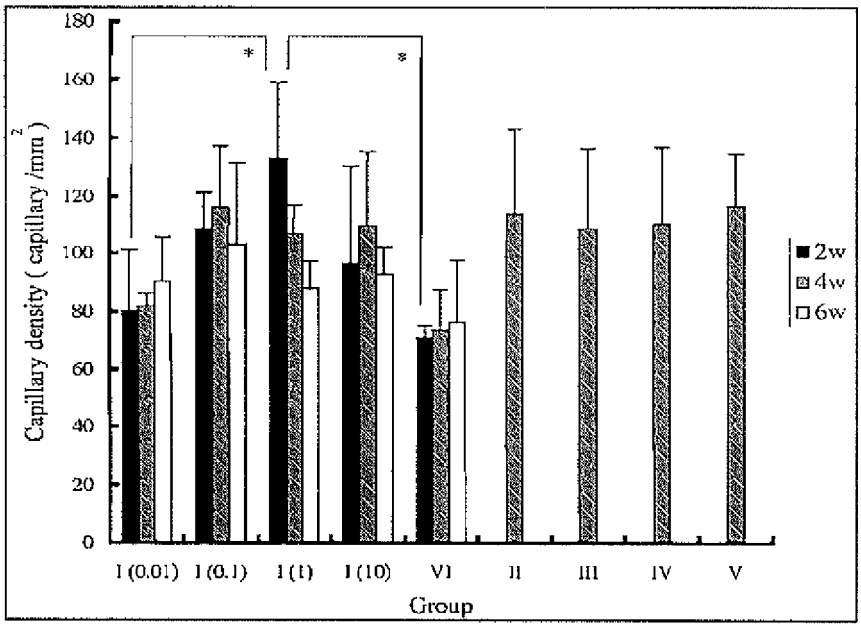

FIG. 5. Capillary density of tissue of the injection site, 2, 4, and 6 weeks after injection of bFGF-immobilized or blank SGMs. Data represent means ± SD. $^*p < 0.05$.

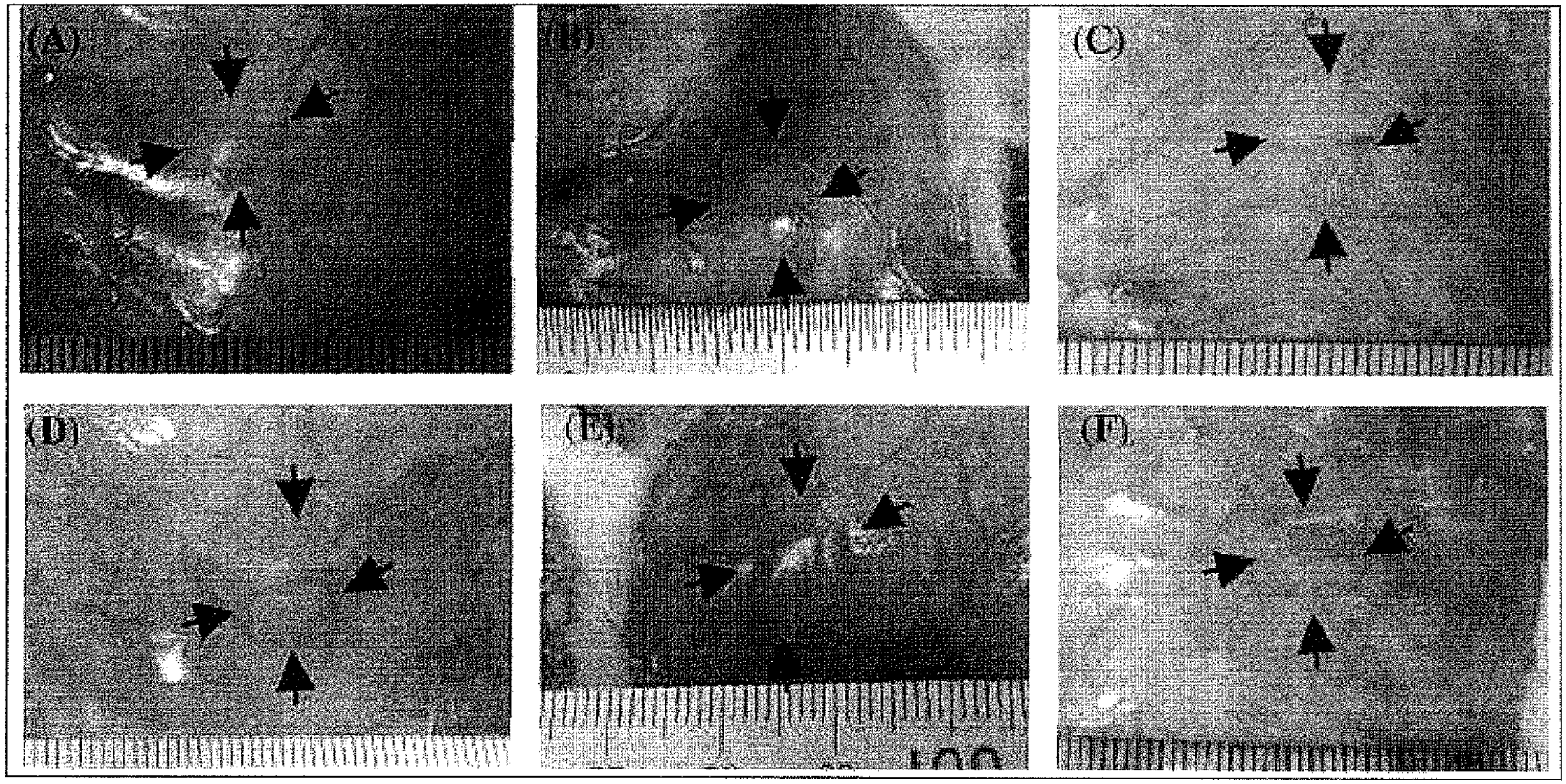

FIG. 6. Tissue appearance of injection site (surrounded by arrows), 4 weeks after injection of SGMs immobilized with various bioactive substances. (**A**) Group I (1) (SGMs immobilized with 1 μg of bFGF per 100 mg of SG); (**B**) group II (SGMs immobilized with 1 IU of insulin per 100 mg of SG); (**C**) group III (SGMs immobilized with 1 μg of IGF-I per 100 mg of SG); (**D**) group IV (SGMs immobilized with 1 IU of insulin and 1 μg of IGF-I per 100 mg of SG); (**E**) group V (SGMs immobilized with 1 μg of bFGF, 1 IU of insulin, and 1 μg of IGF-I per 100 mg of SG); (**F**) group VI (no bioactive substances).

with various bioactive substances. Slightly elevated plaques (approximately 1 × 1 cm^2) were observed at the injection sites of rats in groups I (1), II, III, IV, V, and VI; the most prominent are those of group V (Fig. 6E).

Histology. Figure 7A–L shows the H&E-stained sections of rat subcutaneous lesions of Group I (1), II, III, IV, V, and VI samples 4 weeks after injection of SGMs with or without various bioactive agents. Although partial biodegradation and biosorption occur, residual SGMs remained in all the groups at the injection sites, which were surrounded by tissue composed mainly of collagen fibers and fibroblasts. In groups II–V, masses or clusters of adipocytes were observed between the layers of fibrous tissue. These adipocytes existed in greater number in deeper lesions than in superficial lesions of the residual SGMs. Among these groups, a larger amount of adipose tissue was observed in groups IV and V compared with groups II, III, and VI. In group V, a layer of adipose tissue approximately 1 mm thick was observed adjacent to residual SGMs in deeper lesions. In group VI, however, the injection site was surrounded by a thick layer of connective tissue with few adipocytes interspersed between the layers of fibrous tissue. Sudan IV staining enabled clear visualization of the presence of lipid-containing adipocytes: Sudan IV-positive cells were observed mainly in clusters between the fibrous layers surrounding the residual SGMs, and some cells were also observed among cells that infiltrated residual SGMs (Fig. 8).

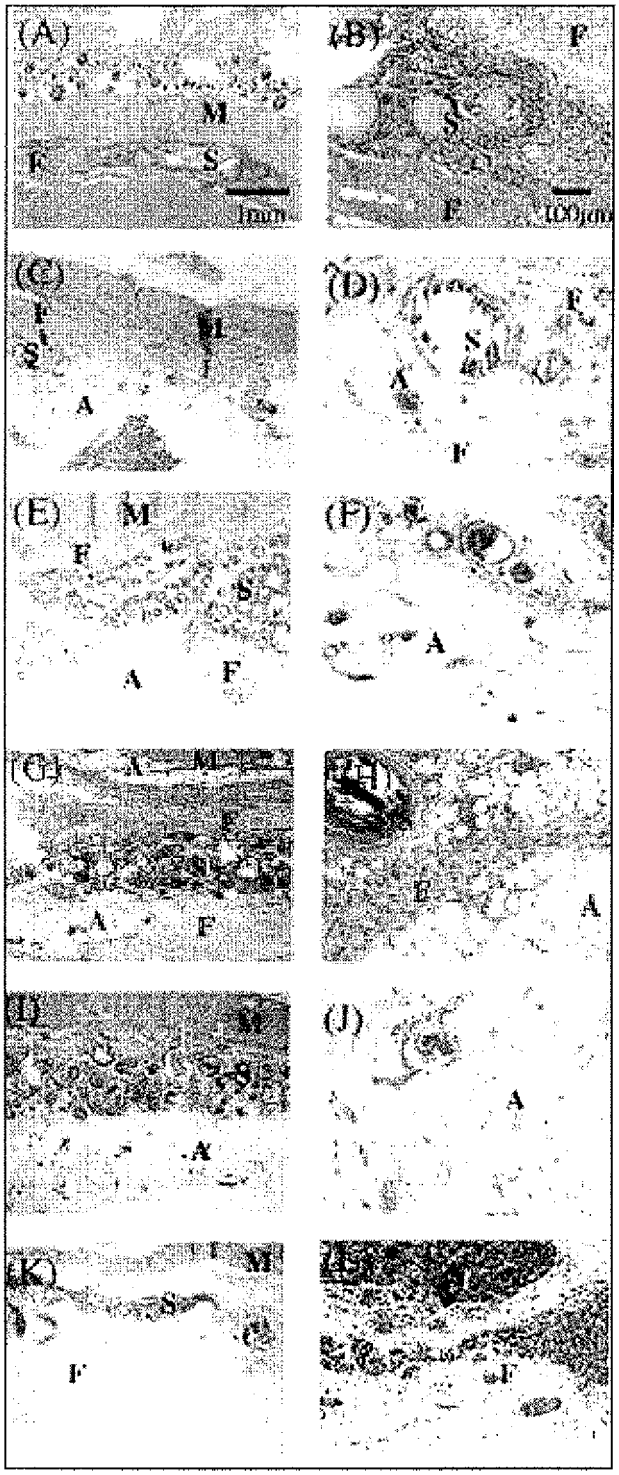

Triacylglycerol content. Total lipid at the injection site and surrounding tissue was extracted with chloroform–methanol (2:1, v/v) and triacylglycerol content was determined. In groups IV and V, triacylglycerol content in the surrounding tissues of the injection site were significantly higher than those in groups I (1), III, and VI. Triacylglycerol content in group V was significantly (almost 1.5-fold) higher than that in group IV (Fig. 9).

DISCUSSION

Several studies on the *de novo* formation of adipose tissue by the sustained release of bioactive substances with or without matrixes have been reported. Possible explanations for this adipogenic phenomenon are the migration of endogenous preadipocytes or mesenchymal stem cells into the treated site followed by their pro-

FIG. 7. H&E-stained sections of injection sites, 4 weeks after injection of SGMs immobilized with various bioactive substances. (**A** and **B**) Group I (1) (SGMs immobilized with 1 μg of bFGF per 100 mg of SG); (**C** and **D**) group II (SGMs immobilized with 1 IU of insulin per 100 mg of SG); (**E** and **F**) group III (SGMs immobilized with 1 μg of IGF-I per 100 mg of SG); (**G** and **H**) group IV (SGMs immobilized with 1 IU of insulin and 1 μg of IGF-I per 100 mg of SG); (**I** and **J**) group V (SGMs immobilized with 1 μg of bFGF, 1 IU of insulin, and 1 μg of IGF-I per 100 mg of SG); (**K** and **L**) group VI (no bioactive substances). Original magnifications: (**A**, **C**, **E**, **G**, and **I**) ×20; (**B**, **D**, **F**, **H**, and **J**) ×100. A, Adipose tissue; F, fibrous layer; M, cutaneous muscle of the trunk; S, residual SGMs.

FIG. 8. Representative Sudan IV-stained sections of lipid-containing adipocytes in group V. (A) Adipocytes were observed mainly in clusters between the fibrous layers surrounding the injection site of bioactive substance-immobilized SGMs. (B). Some Sudan IV-positive cells were also observed among cells that infiltrated around residual SGMs.

liferation and differentiation to mature adipocytes.[11–14] Various hormones, cytokines, and growth factors modulate adipocyte differentiation. Among them, insulin and IGF-I separately stimulate adipocyte proliferation and the adipogenic differentiation of nonadipocyte cells to mature adipocytes.[19,20] Angiogenic factors (e.g., bFGF) play a critical role in neovascularization for blood supply and oxygenation, and for recruitment and proliferation of preadipocytes.[11–13,21] For example, the amount of newly formed adipose tissue increased with an increase in the concentration of bFGF, which was immobilized in Matrigel.[11] On the other hand, there appeared to be an optimal dose of bFGF immobilized in gelatin microspheres for adipose tissue formation.[12]

The major issue in adipose tissue regeneration technology is how to accelerate adipose tissue formation and how to regenerate a large amount of adipose tissue in the site of soft tissue defects. One possible means of accelerating adipose tissue formation is to realize the concerted actions of neovascularization and accumulation of preadipocytes, which are driven by the gradual release of angiogenic factors (e.g., bFGF),[11,12,22,23] which should operate in the early phase of implantation, followed by the differentiation of preadipocytes to mature adipocytes as induced by the sustained release of adipogenic factors[14–16] in the later stage. If these two different biological events synchronously or sequentially occur, adipose tissue formation would be accelerated. On the basis of the above-mentioned working principle, we attempted to devise a local drug delivery system that simultaneously releases these biological substances with different release rates. To this end, microspheres made of photocurable, styrenated gelatin were employed as a drug-immobilizing and -releasing matrix.[17] The study on the release characteristics of rhodamine–lactalbumin and FITC–insulin from gel into PBS revealed that the release rate is dependent on SG concentration, independent of the type of model drugs used within the range of the molecular weight tested (approximately 6×10^3–1.4×10^4) (Fig. 3A and B). The release rate was highest for the gel prepared with the lowest gelatin concentration (20%), which was employed for immobilization of bFGF for the rapid release of an angiogenic factor. Denser SGMs, prepared at 30% gelatin concentration, were employed for immobilization of insulin and IGF-I, aiming at a slower release of adipogenic factors than the former version. These microspheres, which were not mechanically fragile, withstood the mechanical stress applied during injection and implantation.

However, it is of importance to verify and discuss how the *in vitro* releasing profile of a protein can correlate with the *in vivo* releasing profile. We did not conduct any such experiment in this study. It is noteworthy to cite briefly a series of studies by Tabata *et al.*[24,25] They used glutaraldehyde-cross-linked "acidic" gelatin (isoelectric point [IEP], 5.0) as a drug carrier, in which bFGF is sorbed from an aqueous solution. *In vitro* releasing from cross-linked gelatin was inhibited because of ionic interaction between bFGF (IEP, 9.6) and acidic gelatin, except for the burst release within the first day of immersion into buffer solution. However, in animal experiments, radioisotope-labeled bFGF was continuously released with implantation time because of proteolytic biodegradation of gelatin. This indicates that *in vitro* releasing characteristics did not reflect *in vivo* releasing characteristics. This must also have occurred in this experiment. Although the IEP of gelatin used in this study was not determined, the *in vitro* releasing profile in Fig. 3A must be due to the

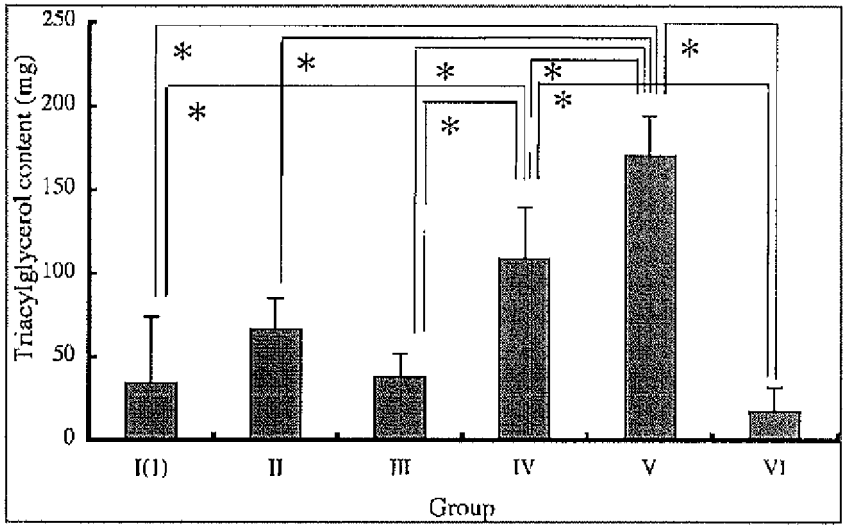

FIG. 9. Total lipid was extracted from SGM injection site tissue and triacylglycerol content was measured as described in Materials and Methods. Data represent means ± SD. $^*p < 0.05$.

combined contribution of size effects of the protein used and some ionic interaction between proteins and gelatin under no proteolytic biodegradation, as mentioned above. Therefore, it is highly anticipated that such a releasing profile does not necessarily correlate with the *in vivo* releasing profile. If biodegradation is a major determinant for release, the time course of released bioactive substances must depend on the degree of photocuring and gelatin concentration, which are principal determinants for biodegradiation as previously reported by us.[17]

A high angiogenesis potential of bFGF-immobilized SGMs was noted (Fig. 4F–J). The capillary densities at the sites treated with bFGF-immobilized SGMs were higher compared with those at the sites treated with SGMs without bFGF (Fig. 5). The capillary density appears to be dependent on bFGF concentration as well as implantation period. At the earlier stage after injection (2 weeks), the highest capillary density was observed at the site treated with group I (1) (1 μg of bFGF immobilized per 100 mg of SG): the capillary density was almost 2-fold higher than that of the site treated with SGMs without bFGF. However, such dependency appears to diminish at a prolonged period after injection (6 weeks). The observed tendency is in good agreement with those previously reported.[26,27] These findings suggest that bFGF released from SGMs induces rapid neovascularization at an early stage after injection.

The study on subcutaneous injection of SGMs immobilized with either an adipogenic factor or combined angiogenic and adipogenic factors clearly showed the possibility of adipose tissue formation (Figs. 7 and 8). Among the groups studied, the largest amount of adipose tissue was observed for the group that received a mixture of three different SGMs, each of which was immobilized with respective bioactive substances (group V). Triacylglycerol content at the site of SGM injection in group V was about 1.5-fold higher than in the group that received a combination of SGMs immobilized with insulin and IGF-I (group IV). This *de novo* adipogenesis is achieved by creating a microenvironment for recruiting endogenous preadipocytes, which subsequently undergo proliferation and differentiation. A single injection of two types of SGMs with two different drug release rates enabled induction of the two-step biological events.

The advantageous features of photocurable gelatin as a drug-immobilized matrix include (1) a controlled degree of cross-linking, which can achieved by the degree of derivatized styrene group in a gelatin molecule, the concentration of styrenated gelatin, and the photocuring time, which is a determinant for the drug-releasing rate as well as the biodegradation rate, and (2) simultaneous photocuring of SG and highly effective immobilization of protein (the amount of protein immobilized can be determined from the formulation during microsphere preparation, due to expected high immobilization efficacy). Water-soluble SG and protein, both of which are not soluble in paraffin, should exist in water phase during microsphere preparation. Therefore, high immobilization efficacy is expected in principle. As for biological activity in immobilized proteins, minor loss of biological activity during photocuring process may not be ruled out. SGMs did not induce substantial damage at cell and tissue levels after the injection of SGMs without any bioactive substances into rat subcutaneous tissue (Fig. 7I and J). Therefore, SGMs can serve as a nontoxic local drug delivery system with easy control of drug immobilization and drug release characteristics.[17]

Although the application of this two-step method for pharmacologically stimulated *de novo* adipose tissue formation is effective, further improvements are required before clinical application of this system. One is to sufficiently increase the amount of newly formed adipose tissue to meet the requirement of soft tissue augmentation and the other is to reduce local fibrosis around injection sites, which occurs with *de novo* adipogenesis. Further studies need to be conducted not only to minimize side effects, but also to maximize the amount of newly formed adipose tissue for soft tissue augmentation. These include optimization of the amount of angiogenic and adipogenic factor, drug release rate, and local inflammation control.

ACKNOWLEDGMENTS

This study was financially supported in part by the Promotion of Fundamental Studies in Health Science of the Organization for Pharmaceutical Safety and Research (OPSR), grant 97-15, and in part by a Grant-in-Aid for Scientific Research (A2-12358017 and B2-12470277) and by a Grant-in-Aid for the Creation of Innovations through Business-Academic-Public Sector Cooperation from the MEXT of Japan. The authors thank Mr. Takaaki Kanemaru (Morphology Core, Graduate School of Medical Sciences, Kyushu University) for SEM observation.

REFERENCES

1. Katz, A.J., Llull, R., Hedrick, M.H., and Futrell, J.W. Emerging approaches to the tissue engineering of fat. Clin. Plast. Surg. **26,** 587, 1999.
2. Billings, E., Jr., and May, J.W., Jr. Historical review and present status of free fat graft autotransplantation in plastic and reconstructive surgery. Plast. Reconstr. Surg. **83,** 368, 1989.
3. Chajchir, A. Fat injection: Long-term follow-up. Aesthetic Plast. Surg. **20,** 291, 1996.
4. Kononas, T.C., Bucky, L.P., Hurley, C., and May, J.W., Jr. The fate of suctioned and surgically removed fat after reimplantation for soft-tissue augmentation: A volumetric and

histologic study in the rabbit. Plast. Reconstr. Surg. **91,** 763, 1993.
5. Green, H., and Kehinde, O. Formation of normally differentiated subcutaneous fat pads by an established preadipose cell line. J. Cell. Physiol. **101,** 169, 1979.
6. Patrick, C.W., Jr., Chauvin, P.B., Hobley, J., and Reece, G.P. Preadipocyte seeded PLGA scaffolds for adipose tissue engineering. Tissue Eng. **5,** 139, 1999.
7. Schoeller, T., Lille, S., Wechselberger, G., Otto, A., Mowlawi, A., and Piza-Katzer, H. Histomorphologic and volumetric analysis of implanted autologous preadipocyte cultures suspended in fibrin glue: A potential new source for tissue augmentation. Aesthetic Plast. Surg. **25,** 57, 2001.
8. von Heimburg, D., Zachariah, S., Heschel, I., Kuhling, H., Schoof, H., Hafemann, B., and Pallua, N. Human preadipocytes seeded on freeze-dried collagen scaffolds investigated in vitro and in vivo. Biomaterials **22,** 429, 2001.
9. Patrick, C.W., Jr., Zheng, B., Johnston, C., and Reece, G.P. Long-term implantation of preadipocyte-seeded PLGA scaffolds. Tissue Eng. **8,** 283, 2002.
10. Halberstadt, C., Austin, C., Rowley, J., Culberson, C., Loebsack, A., Wyatt, S., Coleman, S., Blacksten, L., Burg, K., Mooney, D., and Holder, W., Jr. A hydrogel material for plastic and reconstructive applications injected into the subcutaneous space of a sheep. Tissue Eng. **8,** 309, 2002.
11. Kawaguchi, N., Toriyama, K., Nicodemou-Lena, E., Inou, K., Torii, S., and Kitagawa, Y. *De novo* adipogenesis in mice at the site of injection of basement membrane and basic fibroblast growth factor. Proc. Natl. Acad. Sci. U.S.A. **95,** 1062, 1998.
12. Tabata, Y., Miyao, M., Inamoto, T., Ishii, T., Hirano, Y., Yamaoki, Y., and Ikada, Y. De novo formation of adipose tissue by controlled release of basic fibroblast growth factor. Tissue Eng. **6,** 279, 2000.
13. Kimura, Y., Ozeki, M., Inamoto, T., and Tabata, Y. Time course of de novo adipogenesis in matrigel by gelatin microspheres incorporating basic fibroblast growth factor. Tissue Eng. **8,** 603, 2002.
14. Yuksel, E., Weinfeld, A.B., Cleek, R., Waugh, J.M., Jensen, J., Boutros, S., Shenaq, S.M., and Spira, M. De novo adipose tissue generation through long-term, local delivery of insulin and insulin-like growth factor-1 by PLGA/PEG microspheres in an in vivo rat model: A novel concept and capability. Plast. Reconstr. Surg. **105,** 1721, 2000.
15. Yuksel, E., Weinfeld, A.B., Cleek, R., Jensen, J., Wamsley, S., Waugh, J.M., Spira, M., and Shenaq, S. Augmentation of adipofascial flaps using the long-term local delivery of insulin and insulin-like growth factor-1. Plast. Reconstr. Surg. **106,** 373, 2000.
16. Yuksel, E., Weinfeld, A.B., Cleek, R., Wamsley, S., Jensen, J., Boutros, S., Waugh, J.M., Shenaq, S.M., and Spira, M. Increased free fat-graft survival with the long-term, local delivery of insulin, insulin-like growth factor-1, and basic fibroblast growth factor by PLGA/PEG microspheres. Plast. Reconstr. Surg. **105,** 1712, 2000.
17. Okino, H., Nakayama, Y., Tanaka, M., and Matsuda, T. In situ hydrogelation of photocurable gelatin and drug release. J. Biomed. Mater. Res. **59,** 233, 2002.
18. Matsuda, T., and Magoshi, T. Preparation of vinylated polysaccharides and photofabrication of tubular scaffolds as potential use in tissue engineering. Biomacromolecules **3,** 942, 2002.
19. Caplan, A.I. The mesengenic process. Clin. Plast. Surg. **21,** 429, 1994.
20. Gregoire, F.M., Smas, C.M., and Sul, H.S. Understanding adipocyte differentiation. Physiol. Rev. **78,** 783, 1998.
21. Eppley, B., Sidner, R., Platis, J., and Sadove, M. Bioactivation of free-fat transfers: A potential new approach to improving graft survival. Plast. Reconstr. Surg. **90,** 1022, 1992.
22. Rupnick, M.A., Panigrahy, D., Zhang, C.Y., Dallabrida, S.M., Lowell, B.B., Langer, R., and Folkman, M.J. Adipose tissue mass can be regulated through the vasculature. Proc. Natl. Acad. Sci. U.S.A. **99,** 10730, 2002.
23. Babensee, J.E., McIntire, L.V., and Mikos, A.G. Growth factor delivery for tissue engineering. Pharm. Res. **17,** 497, 2000.
24. Tabata, Y., and Ikada, Y. Protein release from gelatin matrices. Adv. Drug Deliv. Rev. **31,** 287, 1998.
25. Yamamoto, M., Ikada, Y., and Tabata, Y. Controlled release of growth factors based on biodegradation of gelatin hydrogel. J. Biomater. Sci. Polym. Ed. **12,** 77, 2001.
26. Tabata, Y., Hijikata, S., Muniruzzaman, M., and Ikada, Y. Neovascularization effect of biodegradable gelatin microspheres incorporation basic fibroblast growth factor. J. Biomater. Sci. Polymer Ed. **10,** 79, 1999.
27. Tanihara, M., Suzuki, Y., Yamamoto, E., Noguchi, A., and Mizushima, Y. Sustained release of basic fibroblast growth factor and angiogenesis in a novel covalently crosslinked gel of heparin and alginate. J. Biomed. Mater. Res. **56,** 216, 2001.

Address reprint requests to:
Takehisa Matsuda, Ph.D.
Department of Biomedical Engineering
Graduate School of Medicine
Kyushu University
3-1-1 Maidashi, Higashiku
Fukuoka 812-8582, Japan

E-mail: matsuda@med.kyushu-u.ac.jp

This article has been cited by:

1. Jamie L. Ifkovits , Jason A. Burdick . 2007. Review: Photopolymerizable and Degradable Biomaterials for Tissue Engineering Applications. *Tissue Engineering* 13:10, 2369-2385. [Abstract] [PDF] [PDF Plus]
2. Yosuke Hiraoka , Hiroyasu Yamashiro , Kaori Yasuda , Yu Kimura , Takashi Inamoto , Yasuhiko Tabata . 2006. In Situ Regeneration of Adipose Tissue in Rat Fat Pad by Combining a Collagen Scaffold with Gelatin Microspheres Containing Basic Fibroblast Growth Factor. *Tissue Engineering* 12:6, 1475-1487. [Abstract] [PDF] [PDF Plus]
3. Karsten Hemmrich, Dennis von Heimburg. 2006. Biomaterials for adipose tissue engineering. *Expert Review of Medical Devices* 3:5, 635. [CrossRef]
4. Liu Hong, Ioana Peptan, Paul Clark, Jeremy J. Mao. 2005. Ex Vivo Adipose Tissue Engineering by Human Marrow Stromal Cell Seeded Gelatin Sponge. *Annals of Biomedical Engineering* 33:4, 511. [CrossRef]
5. Teiichi Masuda , Masutaka Furue , Takehisa Matsuda . 2004. Novel Strategy for Soft Tissue Augmentation Based on Transplantation of Fragmented Omentum and Preadipocytes. *Tissue Engineering* 10:11-12, 1672-1683. [Abstract] [PDF] [PDF Plus]

DE NOVO ADIPOSE FORMATION IN A VASCULARIZED ENGINEERED CONSTRUCT

ROBERT L. WALTON, M.D., F.A.C.S.,[1] ELISABETH K. BEAHM, M.D.,[2*] and LIZA WU, M.D.[1]

While the field of tissue engineering is a burgeoning one, progress with fat engineering has lagged, due in large part to problems associated with nurturing and sustaining this unique tissue in vivo. In a pilot study using an experimental rat model, we induced liponeogenesis with a combination of Matrigel and basic fibroblast growth factor in an fibrovascular scaffold, isolating the construct to a pedicled blood supply (the superficial inferior epigastric vessels) via a silicone housing, creating an engineered three-dimensional adipose tissue construct. Adipose tissue and vascular ingrowth were assessed histologically and followed by serial study at 4-week intervals for 16 weeks. We demonstrated persistence of shaped adipose tissue constructs over time, and postulate that incorporating a vascular supply may enhance the durability of experimentally induced fat constructs and potentially provide a means for microsurgical transfer of the construct. © 2004 Wiley-Liss, Inc. Microsurgery 24:378–384, 2004.

The transfer of autologous fat alone would seem to be an ideal reconstructive solution for defects characterized by loss of soft-tissue volume. Unfortunately, experience with free fat grafting to date has been largely disappointing. The grafts become progressively absorbed over time, fibrous tissue replaces the original fat cells, and there is limited proliferation of the graft.[1,2] This is not surprising when one considers the critical role that blood supply plays in the survival of transplanted fat. The amount of free fat that can be transferred to fill a defect is limited because of the lack of sufficient blood supply to nourish the graft during the critical period immediately following transfer. In this context, vascularized autologous fat grafts have considerable advantage over conventional fat grafts for reconstruction of large defects, because the blood supply is intrinsic to the graft. Unfortunately, large vascularized fat grafts have limited donor sites, and harvest may produce considerable donor-site deformity and morbidity.

An engineered fat construct having its own blood supply could potentially circumvent many of the current pitfalls of large-volume fat grafting. Precisely, scaffolds and/or molds could render size and shape of the construct, an intrinsic blood supply isolated to an identifiable vascular pedicle would provide sustenance, and the donor-site deformity would be minimal. This technology would have widespread clinical application, particularly in the area of breast reconstruction and the reconstruction of other soft-tissue deformities.

[1]Section of Plastic Surgery, Department of Surgery, University of Chicago, Chicago, IL

[2]Department of Plastic Surgery, M.D. Anderson Cancer Center, Houston, TX

*Correspondence to: Elisabeth K. Beahm, M.D., Department of Plastic Surgery, M.D. Anderson Cancer Center, 1515 Holcombe Blvd., Houston, TX 77030. E-mail: ebeahm@mdanderson.org

Received 21 January 2002; Accepted 4 January 2004

Published online 25 June 2004 in Wiley InterScience (www.interscience.wiley.com). DOI: 10.1002/micr.20056

© 2004 Wiley-Liss, Inc.

Current strategies for in vivo tissue engineering of fat have pursued two general pathways: cultured or isolated adipose cells or precursors are transferred to tissue sites, or de novo fat formation is induced by altering the tissue microenvironment.[3–29] In previous studies, we demonstrated the feasibility of engineering a fibrovascular stroma to an alloplast scaffold in vivo, and successfully transferred this construct microsurgically (Fig. 1).[10–12] In the current study, we sought to induce liponeogenesis in an engineered fibrovascular scaffold, therefore isolating the construct to its own pedicled blood supply. We postulate that this approach will enhance the durability and growth of the experimentally induced fat and also provide a means for its transfer.

MATERIALS AND METHODS

Athymic rats were used in the experimental model, so that the cellular and humoral responses to the allogeneic inducer agents could be minimized. All animal procedures were conducted under the guidelines and approval of the University of Chicago Institutional Animal Care and Use Committee. Anesthesia was induced with ketamine/acepromazine (0.001 ml/g) by intraperitoneal injection for all experimental operative procedures. The procedures were performed under strict sterile surgical conditions.

The superficial inferior epigastric vessels of each animal were exposed through bilateral groin incisions and atraumatically dissected. A standardized weight (0.02 g) of teased polyglycolic acid suture fibers (Dexon®) was placed adjacent to the vessels to serve as a biodegradable scaffold. The fiber/vessel composite was then isolated between leaves of flat silicone sheeting (1.2 × 1.2 cm^2) and secured with surgical clips (Fig. 2). In a separate group, dome-shaped molds (1.7 × 1.7 cm^2) carved from block silicone were utilized to engineer constructs of greater volume (Fig. 3). Control animals

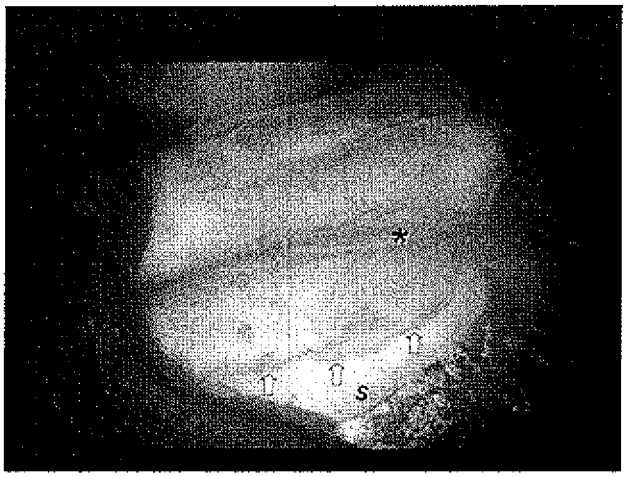

Figure 1. Vascularized alloplast construct. Fibrovascular integration of expanded polytetrafluoroethylene scaffold at 3 weeks. Advancing edge of fibrovascular growth (arrows) is seen arising from inferior epigastric pedicle (asterisk) on porous polytetrafluoroethylene scaffold (S) (after Walton and Brown[10]).

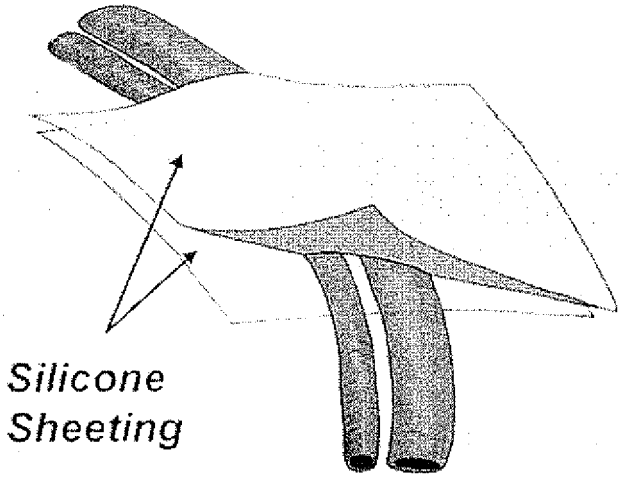

Figure 2. Flat construct (diagramatic representation). In six experimental constructs, composite was isolated between two leaves of flat silicone sheeting.

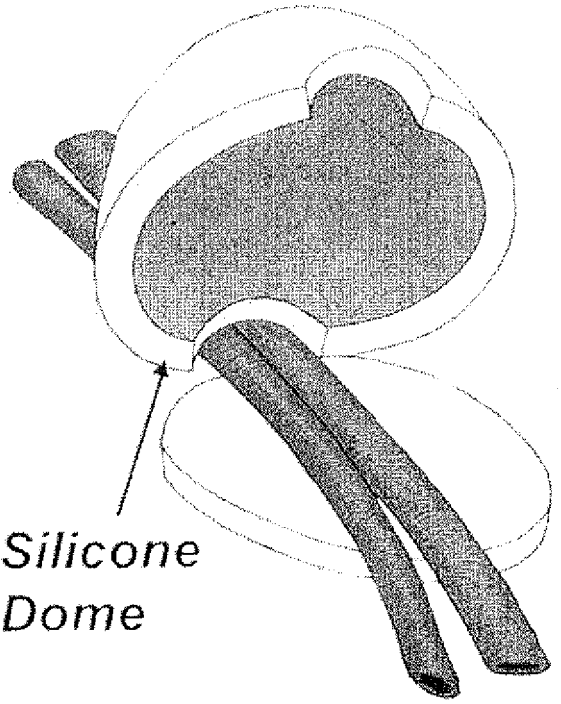

Figure 3. Dome construct (diagramatic representation). In 12 experimental constructs, the composite was isolated in a larger volume, dome-shaped carved silicone housing (1.7 × 1.7 cm^2).

Table 1. Fibrovascular Proliferation*

Time (weeks)	4	8	12	16	20
Control	+	+	+	-	-
Matrigel	++	++	++	+	-
Matrigel/BFGF	++	+++	+++	+++	+++

**All early specimens revealed some fibrovascular ingrowth, which was far greater in the Matrigel/bFGF constructs.*

received no further treatment. A total of 12 animals was utilized for the study, with two experimental preparations per animal (one for each set of superficial inferior epigastric vessels), for a total of 24 preparations. Eighteen preparations were experimental with 6 flat (sheet preparations) and 12 (dome constructs), and the remaining 6 (4 dome, 2 flat) were controls.

In the experimental group, two combinations of drugs were injected into the scaffold/vessel complex housed within the silicone barriers as follows: Matrigel (10 mg/ml, 0.2 ml volume; Becton Dickinson Labware, Bedford, MA) alone, or Matrigel and bFGF (100 ng/100 μl, 0.1 ml volume; R&D Systems) combined, utilizing the ratio found successful in prior studies.[27,29] Following injections, the groin incisions were closed with 4-0 nylon monofilament sutures and dressed with antibiotic ointment.

The animals were housed separately, fed normal chow and water ad libitum, and weighed weekly. The constructs were reexamined at 4-week intervals for a total of 16 weeks. Selected specimens were harvested at each interval, weighed, and subjected to hematoxylin and eosin (H&E) staining, and Oil red O (ORO) staining. Adipose growth and vascular ingrowth were assessed photographically and graded qualitatively. The qualitative 0–3 scale for vascular ingrowth was determined by the total number of vascular structures on three randomly selected areas of slides per low power field (LPF) by a blinded histologist.

Table 2. Fat Proliferation*

Time (weeks)	4	8	12	16	20
Control	–	–	–	–	–
Matrigel	+	+	+	+	+
Matrigel/BFGF	++	+++	+++	+++	+++

No fat growth was noted in the controls, and only minimal fat growth was noted with the Matrigel-alone preparation, while significant fat was noted in the Matrigel/bFGF constructs.

Table 3. Percentage of adipocytes*[a]

Matrigel/bFGF (N = 6)	Matrigel (N = 6)	Control (N = 4)
66.43–79.42% (72.93%)	2.34–7.02% (4.68%)	0–0.56% (0.26%)

*Three images per sample were utilized, sections centrally through and on either side of the vascular pedicle to express adipose content of constructs as percentage of adipocytes as function of area (in microns).
[a]Dome-shaped constructs, 3 images per sample, 200x magnification.

Table 4. Adipose tissue area*[a]

	Area of fat (μm^2)	Total tissue area (μm^2)	% fat
Matrigal/bFGF, N = 6	2.67–2.81E + 06 (2.74E + 06)	4.28–7.07E ± 06 (5.28E + 06)	52% (38–66%)
Matrigel, N = 6	0.10.46E + 06 (0.15E + 06)	1.28–3.26E + 06 (1.84E + 06)	8% (4–11%)
Control, N = 4	0	0	0

*Areas of adipose tissue relative to total cross-sectional are of construct tissue
[a]Exclusive of vascular pedicle, dome, constructs, 4x objective; 1 pixel = 1.85 (μm^2).

As we were specifically looking at adipose tissue ingrowth, histology and histomorphology may be considered more accurate than weight (fibrous tissue is often objectively heavier than fat per given volume), and as such, these measures were used to address adipose ingrowth. The percentage of adipose tissue in each construct as a function of total tissue area was calculated by examination of the central cross-sectional area of each construct (exclusive of the pedicle, calculated in μm^2) (Table 3). The percentage of adipocytes from each preparation was addressed by calculating adipose cell counts from digital images of magnified histologic sections (Nixon IX70 microscope and Hammamatsu camera c5810, image size of 640 × 483). Three histologic sections images per construct (one centrally, and two adjacent measures equidistant from the central cross section were examined; Table 4 and Fig. 9).

RESULTS

Fibrovascular Growth

All week 4 specimens revealed fibrovascular ingrowth that stabilized at 8 weeks. There appeared to be no difference in degree of fibrovascular ingrowth between the Matrigel-only preparations and controls. The degree of fibrovascular growth was qualitatively greater in the Matrigel/bFGF constructs (Table 1). Residual Dexon fibers were observed in controls, but none were apparent upon serial sectioning of the more vascularized Matrigel/bFGF constructs (Figs. 4, 5).

Liponeogenesis

No fat was observed in the control group at any interval (Table 2 and Fig. 6A). Minimal fat proliferation was noted with the Matrigel-alone preparation (Fig. 6B). Significant fat was noted in the Matrigel/bFGF constructs. These findings were consistent in both the flat and the dome constructs (Fig. 6C,D). Fat durability and fat growth were demonstrated early in the Matrigel/bFGF and persisted. This appeared to be independent of the age of the animals. Comparable fat growth was seen in the 6-week, as well as the 16-week experimentals. Qualitatively it appeared that fat volume related directly to the configuration of the silicone housing. The dome-shaped molds resulted in larger, qualitatively more voluminous, three-dimensional fat constructs (Fig. 6C,D).

H&E staining demonstrated that the fat proliferation noted in the constructs was histologically mature vascularized fat with normal architecture (Fig. 7). Oil red O staining of the construct demonstrated cytoplasmic lipid deposition characteristic of mature fat cells, and this was noted to be strongly positive on higher magnification (Fig. 8). No residual Dexon fibers were noted. The percentage of adipose tissue in each construct was marked greater in the matrigel bFGF preparations (Table 3), as was the percentage of adipocytes (Table 4 and Fig. 9).

DISCUSSION

Over the past 10 years, tissue engineering has emerged as a multidisciplinary field focused on the development of functional constructs of living tissue. Prototypes of skin, cartilage, bone, blood vessels, and other organs have illuminated the biomedical landscape, and some have even made their way to the bedside.[13–16] While the field of tissue engineering is a burgeoning one, progress with fat engineering has lagged, due in large

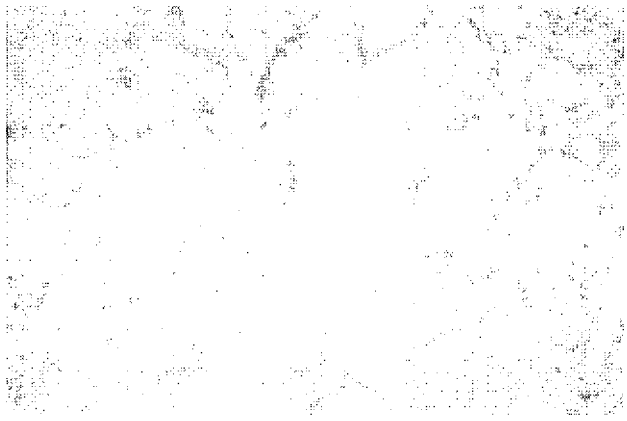

Figure 4. Control construct with residual Dexon fibers. Fibroblasts are seen throughout. There is no evidence of fat growth (H&E, ×50).

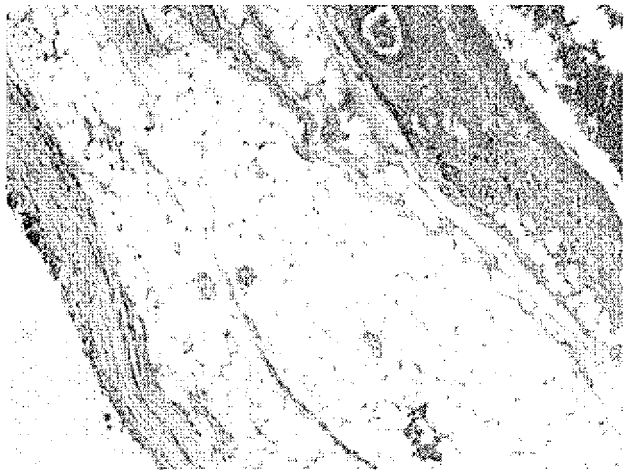

Figure 5. Matrigel/bFGF construct. Vascular ingrowth and mature fat are seen (H&E, ×10).

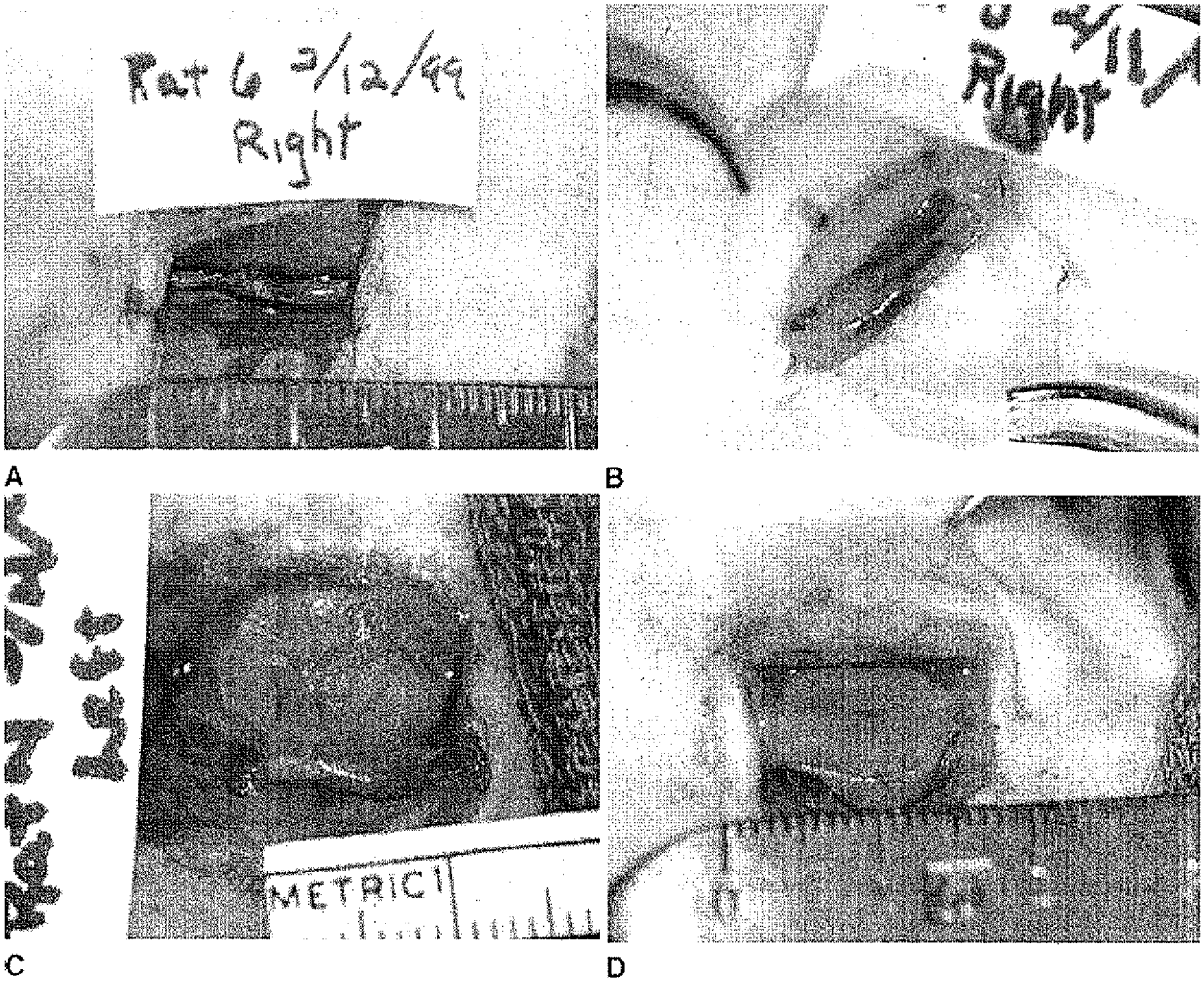

*Figure 6. Evidence of fat proliferation. **A:** Control. In vivo preparation reveals absence of fat growth. **B:** Matrigel-only preparation. Minimal fat proliferation is noted. **C, D:** Matrigel/bFGF preparation. Significant fat growth is noted in both flat and dome housing. Qualitatively it appeared that fat volume related directly to configuration of silicone housing. Dome-shaped molds resulted in larger, qualitatively more voluminous three-dimensional fat constructs than flat constructs.*

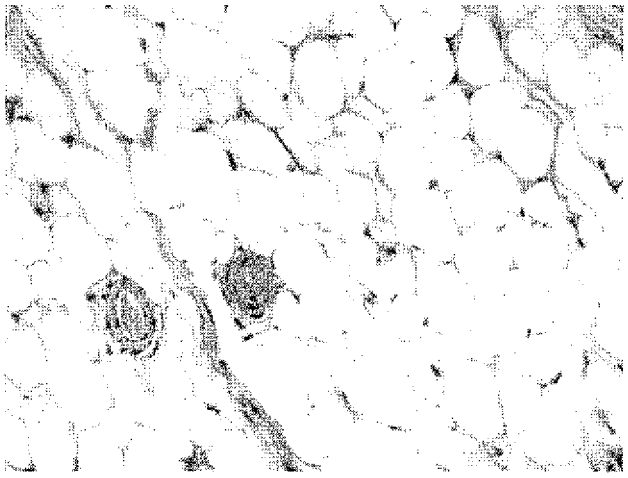

Figure 7. Fat analysis I. H&E staining demonstrates that fat proliferation noted in this Matrigel/bFGF construct is histologically mature vascularized fat with normal architecture (×50).

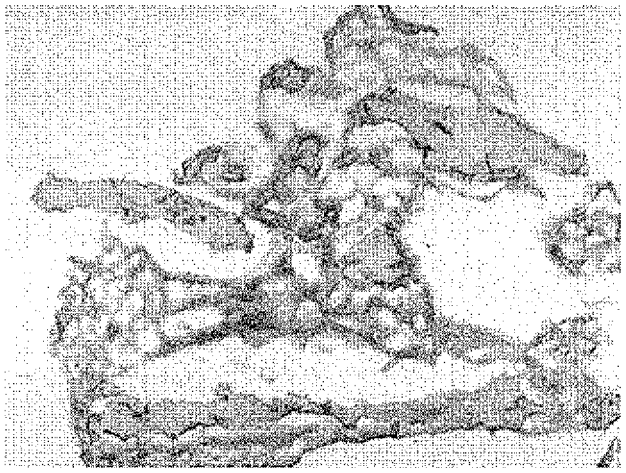

Figure 8. Fat analysis II. Oil red O staining of this Matrigel/bFGF construct demonstrates cytoplasmic lipid deposition characteristic of mature fat (×50).

part to problems associated with nurturing and sustaining this unique tissue in vivo.

A traditional method of tissue engineering relies on harvesting a small amount of tissue, multiplying the cells in culture, and transplanting the new cells to a target site where they will perform the desired functions. To date, investigations that applied this approach to fat have largely focused on manipulating adipocyte growth and differentiation, and were conducted on dedicated cell lines derived from cell culture.[17–20] Technically, mature fat cells with large amounts of cytoplasmic lipid are notoriously fragile, and do not withstand manipulation or transfer well. The fat precursor cells (preadipocytes) are more resilient and have been the preferred cell type for study. Preadipocytes synthesize collagen early in their differentiation, and this may be an autocrine signal for terminal differentiation. Mature fat cells can undergo de novo lipogenesis and lipolysis as a result of the influence of a number of different regulatory enzymes and proteins related to energy metabolism. The regulation of preadipocyte differentiation may be similarly influenced, suggesting that multiple hormonal pathways exist for the induction of adipocyte differentiation.[4–8] It was shown that cultured preadipocytes, implanted in a well-vascularized environment and under precisely controlled conditions, will expand and differentiate in vivo.[17,21,22] Unfortunately, the translation of this in vitro technology to the animal model (the next logical step in the engineering of a fat construct) is quite problematic and does not always follow a direct line of expectation. For example, while preadipocytes were successfully seeded onto a biodegradable polymer (PLGA) scaffold and noted to differentiate, the fat disappeared when the scaffold dissipated.[9]

Our current understanding of the mechanisms regulating adipogenesis is still relatively limited, but suggests a complex series of interactions involving growth factors related to angiogenesis. Embyologically, the development of fat is codependent on the development of blood vessels, closely linking the two processes. The extracellular matrix (ECM) appears to play a critical role in many aspects of both vascular and adipose development.[23] A known mitogen and angiogenic growth factor, basic fibroblast growth factor (bFGF), was implicated as a key factor in adipogenesis and adipose-related angiogenesis and differentiation.[24,25] When bFGF is contained within a gel, to optimize its biologic activity, and injected into tissues, adipogenesis was induced in vivo.[26–28] The adipogenesis in these instances was thought to derive from endogenous connective-tissue stem cells. Basement membrane components secreted by endothelial cells were shown to stimulate preadipocyte differentiation in vitro. When reconstituted basement membrane (Matrigel) is combined with bFGF, de novo lipogenesis also occurs, but to a greater degree than that observed with either bFGF or Matrigel alone.[23,29] It thus appears that basement membrane (Matrigel), which is comprised of type IV collagen, perlecan, and laminin, not only functions to prevent degradation of bFGF, but is also an effective cofactor in de novo adipogenesis.[29,30]

The degree of in vivo fat growth and thus the size of the fat constructs generated in the above studies were relatively modest. This may relate to the shear and compressive forces in the surrounding tissues that limit three-dimensional growth. Larger injected volumes of Matrigel/bFGF result in wider, but not volumetrically larger fat deposits. Additionally, experimental observations in the referenced studies were made early

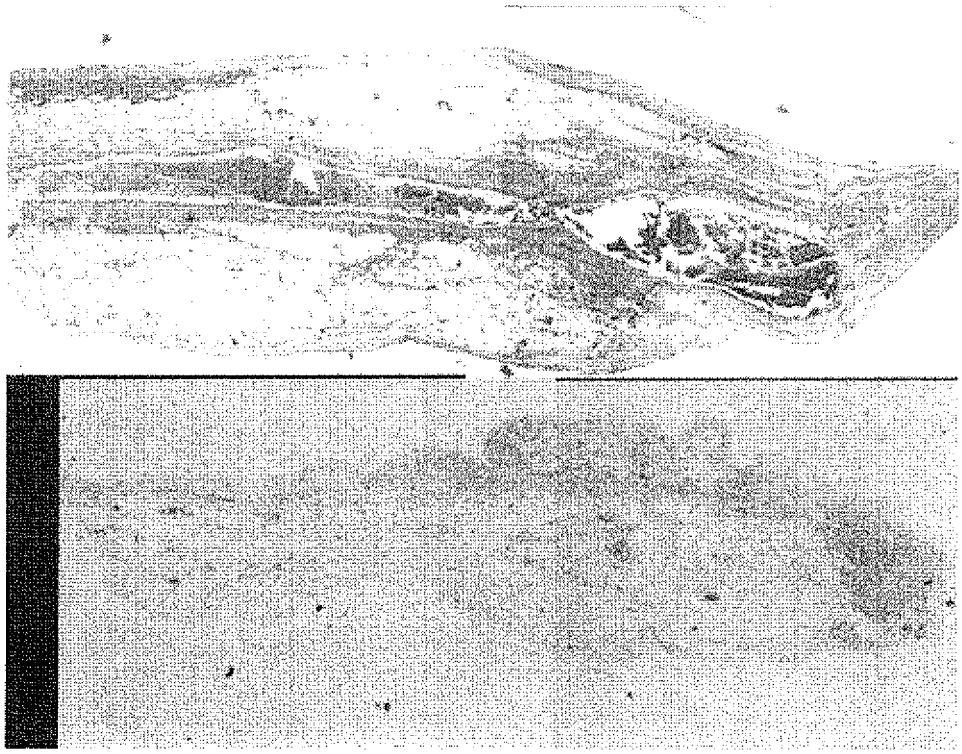

Figure 9. Percentage of adipocytes. Three representative longitudinal cross sections (centrally through and on either side of vascular pedicle) in dome-shaped constructs were utilized to express adipose content of constructs as percentage of adipocytes. Data are presented in Table 3 (H&E preparations at ×20 magnification).

(6 weeks), and therefore the extent of fat growth may not have been fully realized.[27,29]

These limitations formed the basis of our study design in which we utilized a soft, flat silicone construct, subject to the surrounding tissue forces, and a more rigid higher-profile, volumetric construct that could resist these potentially deforming forces. Our results comport with those demonstrating that adipose tissue can be induced, de novo, in tissue with the combined injection of bFGF and reconstituted basement membrane (Matrigel).[27,29] The greater growth observed in the bFGF/Matrigel constructs compared to the Matrigel-alone constructs underscores the interdependence of these two components in lipogenesis. Our findings also suggest that the size and shape of the fibrovascular scaffolds (as determined by the silicone molds) may influence the resultant degree of fat formation. While this may seem intuitively obvious, it was not previously demonstrated experimentally with engineered fat.

Unique to this study was the observation that adipogenesis was induced on an engineered fibrovascular stroma that also provided a means for sustained, intrinsic nourishment of the construct. While vascular ingrowth was noted in prior studies, none exhibited the degree of vascularization demonstrated here. Moreover, isolation of the construct to its own pedicled blood supply offers a basis for its independent manipulation and transfer. This concept of engineering a blood supply to a construct is relatively new in tissue engineering. In our model, the source of revascularization was an intact, flow-through vascular pedicle. Others demonstrated neoangiogenesis using an arteriovenous shunt preparation.[31] The degree of vascularization in the flow-through preparation compared to the arteriovenous shunt preparation remains to be determined.

The animals in this study were followed for a longer period of time compared to previous studies. Observations at 16 weeks showed no substantive changes in histologic appearance or construct size up to that point. Additionally, the induction of de novo adipogenesis was achieved in rats of varying degrees of maturity, underscoring the notion that certain stem cells, at least, retain their plasticity over time, therefore allowing the applicability of this technology to all age groups. This is in contradistinction to observations of engineered cartilage constructs where embryologic chondrocytes were required for cartilage neogenesis.[13]

The qualitative nature of the current study limits any far-reaching conclusions. Ongoing investigations will evaluate larger constructs, in larger animals, over longer periods of time, and will quantify fat growth. An engineered fat construct must be as reliable as the currently available reconstructive options. It must be biocompatible and sufficiently stable to maintain its three-dimensional shape and volume over time. Concerns should focus on whether the fat produced is normal (although histological studies of engineered fat to date indicate this to be the case). The induced construct must

establish equilibrium and mature at the recipient site. Control of adipose differentiation, determination, and growth will need to focus on the nuclear underpinnings. The close linkage between angiogenesis and adipogenesis must be carefully investigated, and most importantly, these engineered events must not pose an oncologic risk.

ACKNOWLEDGMENTS

The authors acknowledge the efforts of Drs. Charles Patrick, Eric Brey, and Wendy Recant for their invaluable support and assistance with the histologic preparation and analyses in this study.

REFERENCES

1. Ersek RA. Transplantation of purified autologous fat: a 3-year follow-up is disappointing. Plast Reconstr Surg 1991;87:219–227.
2. Kononas TC, Bucky LP, Hurley C, May JW, Jr. The fate of suctioned and surgically removed fat after reimplantation for soft tissue augmentation: a volumetric and histologic study in the rabbit. Plast Reconstr Surg 1993;91:763–771.
3. Safanova I, Dairmont C, Amri EZ, et al. Retinoids are positive effectors of adipose cell differentiation. Mol Cell Endocrinol 1994; 104:201–211.
4. Hauner H, Schmid P, Pfieffer EF. Glucocorticoids and insulin promote the differentiation of human adipocyte precursor cells into fat cells. J Clin Endorinol Metab 1987;64:832–835.
5. Richardson RL, Hausman GJ, Wright JT. Growth factor regulation of insulin like growth factor (IGF) binding proteins (IGFBP) and preadipocyte differentiation in porcine stromal-vascular cell cultures. Growth Dev Aging 1998;62:3–12.
6. Soret B, Lee HJ, Finley E, et al. Regulation of differentiation of sheep subcutaneous and abdominal preadipocytes in culture. J Endocrinol 1999;161:517–524.
7. Hauner H, Rohrig K, Petruschke T. Effects of epidermal growth factor (EGF), Platelet derived growth factor (PDGF) and fibroblast growth factor (FGF) on human adipocyte development and function. Eur J Clin Invest 1995;25:90–96.
8. Petruschke T, Hauner H. Tumor necrosis factor alpha prevents the differentiation of human adipocyte precursor cells and causes dilapidation of newly developed fat cells. J Clin Endocrinol Metab 1993;76:742–747.
9. Patrick CW, Chauvin PB, Hobley BS, et al. Preadipocyte seeded PLGA scaffolds for adipose tissue engineering. Tissue Eng 1999; 5:139–151.
10. Walton RL, Brown RE. Tissue engineering of biomaterials for composite reconstruction: an experimental model. Ann Plast Surg 1993;30:105–110.
11. Walton RL, Brown RE. Creation of a vascularized alloplast for composite reconstruction. San Francisco: Plastic Surgery Research Council; 1988.
12. Walton RL, Chick LR, Brown RE. Creation of a vascularized alloplast. Plast Surg Forum 1988;9:160–162.
13. Vacanti CA, Langer R, Schloo B, et al. Synthetic polymers seeded for new cartilage formation. Plast Reconstr Surg 1991; 88,753–759.
14. Khouri RK, Koudsi B, Reddi H. Tissue transformation into bone in vivo. A potential application. JAMA 1991;266:1953–1955.
15. Burke JF, Yannas IV, Quinby WC, et al. Successful use of a physiologically acceptable artificial skin in the treatment of extensive burn injury. Ann Surg 1981;194:413–428.
16. Boyce ST. Skin substitute from cultured cell and collagen GAG polymers. Med Biol Eng Comput 1998;36:791–800.
17. Green H, Meuth M. An established pre-adipose cell line and its differentiation in culture. Cell 1974;3:127–133.
18. Katz AJ, Llull R, Hedrick MH, et al. Emerging approaches to the tissue engineering of fat. Clin Plast Surg 1999;26:587–602.
19. Cornelius P, Mac Dougald OA, Lane MD. Regulation of adipocyte development. Ann Rev Nutr 1994;14:99–129.
20. Gregoire FM, Smas CM, Sul HS. Understanding adipocyte differentiation. Physiol Rev 1998;78:783–809.
21. Van RLR, Roncari DAK. Complete differentiation in vivo of implanted cultured adipocyte precursors from adult rats. Cell Tissue Res 1982;225:557–560.
22. Katz AJ, Llull R, Hedrick MH, et al. Emerging approaches to the tissue engineering of fat. Clin Plast Surg 1999;26:587–602.
23. Varzaneh FE, Shillabeer G, Wong KL, et al. Extracellular matrix components secreted by microvascular endothelial cells stimulate preadipocyte differentiation in vitro. Metabolism 1994;43: 906–912.
24. Claffey KP, Wilkison WO, Spiegelman BM. Vascular endothelial growth factor regulation by cell differentiation and activated second messenger pathways. J Biol Chem 1992;267: 16317–16322.
25. Folkman JS. Control of angiogenesis by heparin and other sulfated polysaccharides. Adv Exp Med Biol 1992;313:355–364.
26. Eppley BL, Sidner RA, Platis JM, et al. Bioactivation of free fat transfers: a potential new approach to improving survival. Plast Reconstr Surg 1992;90:1022–1030.
27. Tabata Y, Manabu M, Inamoto T, et al. De novo formation of adipose tissue by controlled release of basic fibroblast growth factor. Tissue Eng 2000;6:279–289.
28. Tabata Y, Ikada Y. Controlled protein release from gelatin matrices. Adv Drug Delivery Rev 1998;31:187.
29. Kawaguchi Toriyama K, Nicodemu-Lena E, et al. Denovo adipogenesis in mice at the site of injection of basement membrane and basic fibroblast growth factor. Proc Natl Acad Sci USA 1998;95: 1062–1066.
30. Folkman J, Klagsbrun M, Sasse J, et al. A heparin-binding angiogenic protein-basic fibroblast growth factor-is stored within basement membrane. Am J Pathol 1988;130:393–400.
31. Tanaka Y, Tsutsumi A, Crowe DM, Tajima S, Morrison WA. Generation of an autologous tissue (matrix) flap by combining an arteriovenous shunt loop with artificial skin in rats: preliminary report. Br J Plast Surg 2000;53:51–57.

Experimental

New Murine Model of Spontaneous Autologous Tissue Engineering, Combining an Arteriovenous Pedicle with Matrix Materials

Kevin J. Cronin, F.R.C.S.I., F.R.C.S.(Plast.), Aurora Messina, Ph.D., Kenneth R. Knight, Ph.D., Justin J. Cooper-White, Ph.D., Geoffrey W. Stevens, Ph.D., Anthony J. Penington, F.R.A.C.S., and Wayne A. Morrison, F.R.A.C.S.

Victoria, Australia

The authors previously described a model of tissue engineering in rats that involves the insertion of a vascular pedicle and matrix material into a semirigid closed chamber, which is buried subcutaneously. The purpose of this study was to develop a comparable model in mice, which could enable genetic mutants to be used to more extensively study the mechanisms of the angiogenesis, matrix production, and cellular migration and differentiation that occur in these models. A model that involves placing a split silicone tube around blood vessels in the mouse groin was developed and was demonstrated to successfully induce the formation of new vascularized tissue. Two vessel configurations, namely, a flow-through pedicle ($n = 18$ for three time points) and a ligated vascular pedicle ($n = 18$), were compared. The suitability of chambers constructed from either polycarbonate or silicone and the effects of incorporating either Matrigel equivalent ($n = 18$) or poly(DL-lactic-co-glycolic acid) ($n = 18$) on angiogenesis and tissue production were also tested. Empty chambers, chambers with vessels only, and chambers with matrix only served as control chambers. The results demonstrated that a flow-through type of vascular pedicle, rather than a ligated pedicle, was more reliable in terms of patency, angiogenesis, and tissue production, as were silicone chambers, compared with polycarbonate chambers. Marked angiogenesis occurred with both types of extracellular matrix scaffolds, and there was evidence that native cells could migrate into and survive within the added matrix, generating a vascularized three-dimensional construct. When Matrigel was used as the matrix, the chambers filled with adipose tissue, creating a highly vascularized fat flap. In some cases, new breast-like acini and duct tissue appeared within the fat. When poly(DL-lactic-co-glycolic acid) was used, the chambers filled with granulation and fibrous tissue but no fat or breast tissue was observed. No significant amount of tissue was generated in the control chambers. Operative times were short (25 minutes), and two chambers could be inserted into each mouse. In summary, the authors have developed an in vivo murine model for studying angiogenesis and tissue-engineering applications that is technically simple and quick to establish, has a high patency rate, and is well tolerated by the animals. (*Plast. Reconstr. Surg.* 113: 260, 2004.)

Tissue engineering has many potential applications in all areas of medical practice.[1] Current experimental and clinical models use autologous cells seeded onto extracellular matrices in vitro to generate tissue constructs, which are then implanted in vivo. These constructs must necessarily be relatively thin and two-dimensional, because after implantation the cells must survive by diffusion until the construct is randomly vascularized from the surrounding native tissues.[2] This technique is useful for engineering thin structures such as cartilage, skin, and heart valves.[3–9] To generate truly three-dimensional tissues such as liver, muscle, or bone, however, a ready-made vascular tree is required, to prevent necrosis of cells that are too far away from the host tissues to survive by diffusion.[10]

Two approaches to overcoming this obstacle have been adopted. The first approach is to generate vascular trees on specialized scaffolds

From the Bernard O'Brien Institute of Microsurgery and the Department of Surgery, University of Melbourne, St. Vincent's Hospital; and the Department of Chemical and Biomolecular Engineering, University of Melbourne. Received for publication April 25, 2002; revised March 10, 2003.

DOI: 10.1097/01.PRS.0000095942.71618.9D

in vitro, for later in vivo transplantation and microvascular anastomosis.[11] The second approach harnesses the intrinsic ability of the body to generate new vessels (angiogenesis) in response to certain stimuli, which can, in theory, be controlled with various bioactive proteins.[12,13]

We previously developed an in vivo model of angiogenesis in rats, based on a microvascular arteriovenous loop encapsulated in a polycarbonate chamber in the groin of the rat,[14] which, when combined with a collagen matrix, spontaneously generated a vascularized, three-dimensional, fibrous tissue construct. The model itself, without added matrix, produced a slightly lesser amount of tissue. We assume that this angiogenic process is associated with an endogenous cascade of growth factors and matrix-producing substances that support endothelial proliferation and attract cells to migrate to this environment. We subsequently demonstrated that, when exogenously cultured fibroblasts[15] or myoblasts (unpublished observations) were seeded into the chamber, they survived and even differentiated within the construct. This model has its limitations, however; it is technically demanding, relatively expensive, and time-consuming.

To investigate the fundamental processes involved in tissue engineering, a similar murine model is desirable. Antibodies and transgene and gene-knockout technologies are much more widely available for mice and would allow us to more extensively probe the influence of a number of factors involved in tissue engineering, including growth promoters and inhibitors. Nude mice and severe combined immunodeficient mice also permit the use of human tissues (notably stem cells) in vascularized tissue-engineering experiments. A wide variety of mouse-derived stem cells, which can be seeded into the murine model for assessment of their potential to develop into specific tissue types in vivo, are available. There are also significant cost benefits with the use of mice, compared with other species.

We hypothesized that a model of angiogenesis similar to that in rats could be developed in mice, based on a vascular pedicle; when combined with matrix contained in a chamber, it could spontaneously generate vascularized three-dimensional tissue. This model would be efficacious for the study of angiogenesis and tissue engineering.

We investigated the efficacy of two types of vascular configurations, which were known to be angiogenic from previous work, in combination with polycarbonate or silicone chambers filled with Matrigel or poly(DL-lactic-co-glycolic acid) (PLGA). The first configuration involved a tied-off arteriovenous pedicle consisting of the femoral artery and vein, as described by Khouri et al.[16] for rats. The second configuration involved a flow-through loop pedicle, as previously described by Y. Tanaka, W. A. Morrison, and others (unpublished data).

Materials and Methods

Anesthesia, Animals, and Chambers

All experiments were performed with the approval of the St. Vincent's Hospital Animal Ethics Committee, under the National Health and Medical Research Council (Australia) guidelines. Wild-type male C57BL6 mice (body weight, 18 to 24 g) were used for this set of experiments. All operations were performed with general anesthesia (chloral hydrate administered intraperitoneally, at 0.4 mg/g body weight). Both types of cylindrical noncollapsible chambers were 6 mm long, with an internal diameter of 3.35 mm and a volume of 50 μl. The polycarbonate chambers were constructed by the Department of Chemical Engineering of the University of Melbourne, and the silicone chambers were produced from lengths of laboratory tubing (Dow-Corning Corp., Midland, Mich.).

Surgical Techniques

The groins and upper legs of the mice were rendered hair-free with a depilatory cream. The skin was then decontaminated with chlorhexidine and alcohol.

Tied-Off Arteriovenous Pedicle Model

The tied-off or ligated arteriovenous pedicle technique requires a vertical incision extending from the groin crease to the knee and just offset from the femoral vessels, which are visible through the skin (Fig. 1). The femoral vessels are tied off at the knee and then dissected free from their accompanying nerve back to the origin of the deep branch of the femoral artery. The vascular pedicle thus developed is fed into the lumen of a cylindrical chamber and anchored in place with a 10-0 nylon microsuture. The chamber is filled with matrix material (either Matrigel or PLGA) and

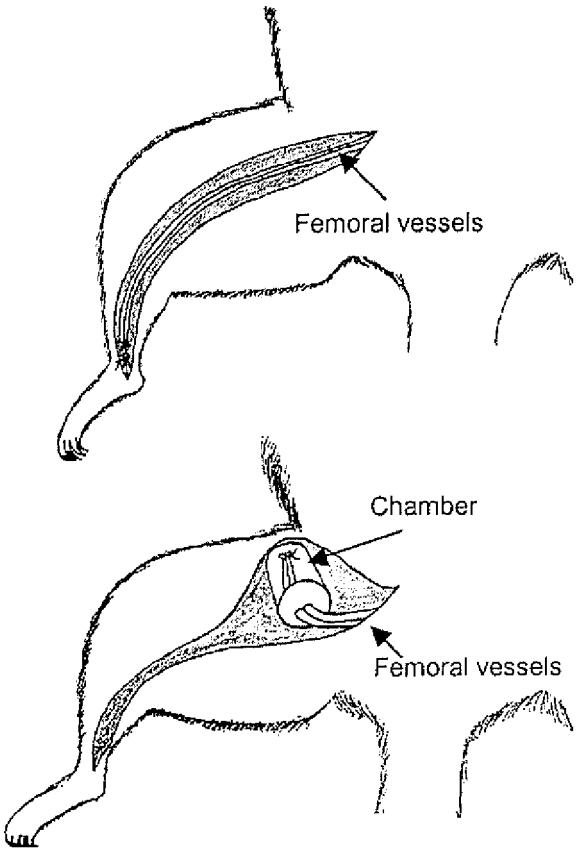

FIG. 1. Diagrammatic representation of the tied-off arteriovenous pedicle model constructed on the femoral vessels.

sealed at both ends with bone wax (Ethicon bone wax, manufactured by Johnson & Johnson International; European Logistics Center, Brussels, Belgium) melted with an ophthalmic cautery, with care not to apply the wax directly to the vessels. The entire construct is then placed in a dissected space in the groin.

Flow-Through Loop Pedicle Model

This method is performed with a transverse groin incision located just above the groin fat pad. The superficial epigastric vessels are dissected free from the surrounding tissue from their origin at the femoral vessels to their point of entry into the groin fat pad (a distance of approximately 1 cm; Fig. 2). There the vessels course through the fat pad, sending nutritional branches to the fat and mammary tissue around them. They then anastomose directly with an ilioinguinal vessel (a direct branch of the infrarenal aorta) that pierces the abdominal wall at the lateral aspect of the inguinal ligament, to enter the fat pad from the lateral side. Therefore, the superficial epigastric vessels have arterial input and venous drainage from both sides, which is likely to increase the long-term patency rates in this model. The entire fat pad is then mobilized from the skin and underlying muscle, creating a space into which the chamber will later be introduced. The first 8 to 10 mm of the superficial epigastric vessels (where they are free from the fat pad) are encased by the cylindrical chamber, which has been opened along one side to allow incorporation of the vessels. The chamber is then filled with the appropriate extracellular matrix (Matrigel or PLGA). The chamber is sealed at the proximal femoral end and along the lateral split with melted bone wax (Ethicon bone wax), with care not to apply the heated wax directly to the vessels. The seal is augmented with two 10-0 nylon microsutures, placed at both ends of the lateral split, and the entire chamber is anchored to the underlying muscle (with 10-0 nylon sutures) near the origin of the superficial epigastric vessels, to prevent the pedicle from being dislodged during postoperative mobilization of the animals. A small amount of fatty tissue surrounding the vessels as they enter the fat pad is allowed to plug the distal or lateral end of the chamber. This plug is augmented with wax sealant and the entire

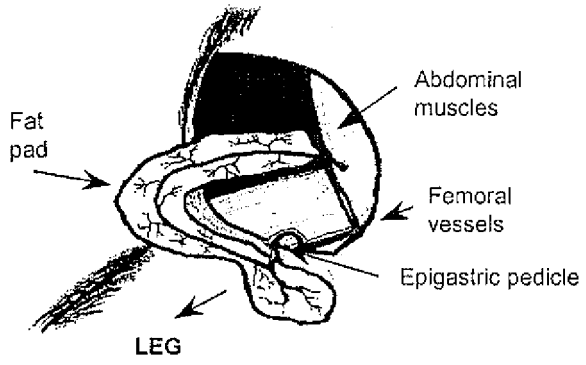

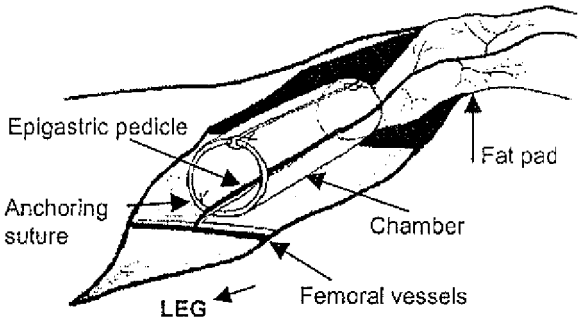

FIG. 2. Diagrammatic representation of the flow-through loop pedicle model constructed on the epigastric vessels.

construct is carefully placed in the groin, so that it lies in the dissected space lateral to the femoral vessels. The wounds are closed with metal clips.

Matrigel

Reconstituted basement membrane (Matrigel equivalent) was prepared directly from the Engelbreth-Holm-Swarm sarcoma that had been grown in the gastrocnemius muscle of wild-type C57BL/6 mice at our institution, with the method described by Kleinman et al.[17] After being prepared, the membrane was sterilized in 10-ml aliquots mixed with Dulbecco's modified Eagle's medium and gentamicin (at an approximate concentration of 12 mg/ml). Matrigel is a liquid at 4°C but gels at room temperature.

PLGA

The PLGA was prepared by the Department of Chemical Engineering of the University of Melbourne, with the particulate leaching method.[18] In essence, PLGA is dissolved in chloroform and mixed with sodium chloride crystals of 300-μm to 400-μm diameter. After evaporation of the chloroform, the resulting scaffold is machined to the desired shape. The salt crystals are then leached from it. The pore size of 50-μm to 400-μm diameter and a porosity of 84 percent were confirmed with scanning electron microscopy and intrusion mercury porosimetry, respectively. The PLGA was sterilized and prewet with an adaptation of the techniques described by Patrick et al.[19] The PLGA was soaked in 100% alcohol for 30 minutes, on a mechanical stirrer, and was subjected to three 30-minute washes in sterile saline solution, also on a mechanical stirrer. The PLGA was then transferred, in a sterile Petri dish, to the surgical suite for implantation.

Experimental Groups

Preliminary experiments. Preliminary experiments were performed to investigate the patency of the two vascular configurations in either polycarbonate or silicone chambers filled with Matrigel. The constructs were examined 2, 4, and 6 weeks after implantation (six mice at each time point).

Experimental groups. The flow-through pedicle/silicone chamber construct configuration was selected for evaluation of the capacity for angiogenesis and tissue generation in this murine model. No-matrix-, Matrigel-, and PLGA-containing constructs were assessed at 2, 4, and 6 weeks (six mice at each time point for each group).

Control groups. In addition to the no-matrix control constructs, control chambers without blood vessels were concurrently implanted in the opposite groin in three animals for each time point. The chambers consisted of an empty silicone chamber, a silicone chamber with Matrigel only, or a silicone chamber with PLGA only. All chambers were sealed with wax in the same way as for the experimental groups.

Assessments

Assessment of vessel patency. Vessel patency was determined during microsurgical exploration and in India ink perfusion studies. If the vessel was extensively thrombosed within the chamber, it was usually possible to determine that with the operating microscope. However, ascertaining definite patency was not always possible. Therefore, India ink perfusion studies were performed with each animal under general anesthesia, before killing. Under the operating microscope, the groin incision was reopened and the chamber was exposed, with care not to damage the pedicle. A laparotomy was performed, and the abdominal aorta was dissected free from the vena cava and cannulated just below the renal vessels, with fine-bore (30-gauge) silicone tubing. The tubing was then gently flushed with heparinized saline solution, to ensure that the cannula was in the correct position. Next, a solution of neat commercial India ink, with 10 international units/ml heparin added, was infused under gentle hand pressure, in a pulsatile manner, until the liver of each animal turned completely black.[20] Patency could be confirmed with direct observation of the transparent chamber, because the India ink could clearly be observed tracking into the chamber along the vascular pedicle. The animals were finally killed with a lethal overdose of Lethobarb (325 mg pentobarbitone sodium per ml, Virbac Australia Pty. Ltd., Peakhurst, Sydney, Australia), and the chambers were carefully removed; the pedicles were cut flush with their entry into the chamber. The tissue was removed from the chamber and weighed, and the volume was estimated on the basis of saline displacement.

Morphometric assessment of angiogenesis. The intact specimens were fixed overnight in neutral buffered formalin and dehydrated through graded alcohol solutions to absolute alcohol.

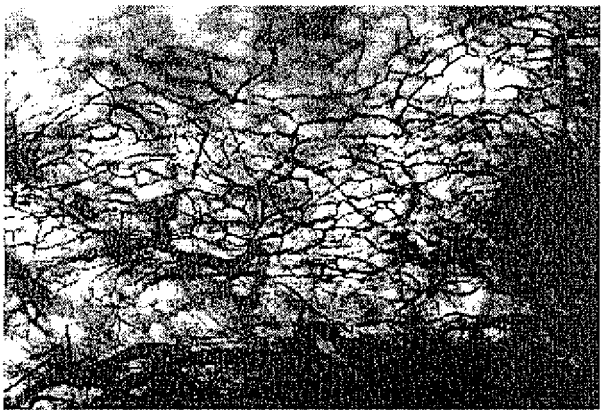

FIG. 3. Microscopic image of a whole-mount preparation of the flow-through chamber contents produced during a period of 6 weeks, showing India ink-perfused vessels (magnification, ×264).

The specimens were then immersed in methylsalicylate and allowed to clear for 72 hours. This whole-mount preparation allowed direct observation of the complete vascular tree, which had been perfused with India ink (Fig. 3). Vessel volume density, which represents the volume fraction of total tissue occupied by the walls and lumina of vessels, reflects the overall number, length, and size of the vessels. Density was estimated stereologically for all new vessels, excluding the large vessels of the primary vascular pedicle. Three randomly selected microscopic fields were sampled at three different depths, 200 μm apart (i.e., nine fields), with an Olympus BH-2 RFCA microscope fitted with a microcator (Heidenhain MT-12; Olympus A/S Denmark, Glostrup, Denmark) and a ×20 objective. Images of ×1500 final magnification were captured on a monitor with a video camera (Panasonic wv-cl700, Olympus Australia, Melbourne, Australia).[21] Care was taken to ensure that none of the fields included the large vessels of the primary vascular pedicle. If such a field was randomly selected, it was rejected and another field was chosen. The monitor images were overlaid with a square lattice grid. The number of times that vessels contacted the intersections of the vertical and horizontal lines of the lattice (the lattice points) was recorded and expressed as a percentage of the total number of lattice points overlying the specimen.

Tissue morphological assessments. The specimens were processed for histological examinations by being embedded in wax. The wax blocks were sectioned at 5-μm thickness and were stained with hematoxylin and eosin in a standard manner. The stained sections were morphologically evaluated in terms of angiogenesis and the cellular characteristics of the newly generated tissue.

Statistical Analyses

When appropriate, results were analyzed with one-way and two-way analyses of variance (SPSS for Windows, version 11.0; SPSS, Inc., Chicago, Ill.). The patency rates (categorical data in 2 × 2 tables) were analyzed with Fisher's exact test (StatXact 4 for Windows; Cytel Software Corp., Cambridge, Mass.).

RESULTS

Operative Times

The operative times were similar for the two vascular configurations. The ligated pedicle group required an average of 23 minutes for completion of the procedure, whereas the flow-through pedicle group required 25 minutes, not including control chambers. If two chambers were constructed for the mouse, then the overall operative time was increased by 5 to 10 minutes. This is substantially less than the average time per procedure in the rat microvascular loop model (approximately 90 minutes).

Patency Rates

Preliminary assessments of the vessel patency rates for the two vascular configurations and the two chamber materials were performed at 2, 4, and 6 weeks. All of those chambers were filled with Matrigel. With polycarbonate chambers, the patency rates were 25 and 77 percent for the tied-off arteriovenous pedicle and the flow-through pedicle, respectively. This difference was statistically significant ($p < 0.005$, Fisher's exact test). Therefore, only the flow-through pedicle was tested in silicone chambers. There the patency rate was 97 percent; the increase in the patency rate, compared with that in polycarbonate chambers, approached but did not achieve statistical significance. It was clear from these preliminary results that the tied-off pedicle design was inappropriate and that silicone chambers were superior to the polycarbonate type. The definitive experiments on tissue mass and volume, vascular density, and histological features were performed with the flow-through vascular pedicle in silicone chambers.

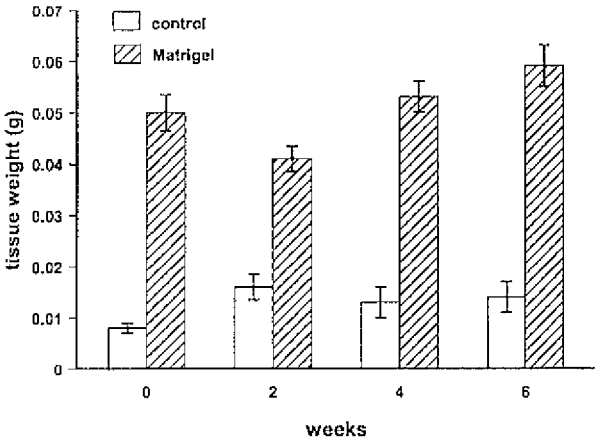

FIG. 4. Weight of the total chamber contents retrieved from flow-through pedicle chambers containing either no matrix or Matrigel, at 0, 2, 4, and 6 weeks (six animals per group). Data are means ± standard errors. In two-way analysis of variance, there was a significant interaction between weight and time for the two groups [$F(2,30) = 12.3$, $p < 0.005$], indicating significantly different growth rates for the Matrigel-filled chambers and the no-matrix chambers. The 0-week time point was excluded from this analysis.

Tissue Mass and Volume

The total weight of tissue present in the chambers containing no matrix with the vessels was minimal. The weight increased between day 0 and day 14 ($p < 0.05$) but remained constant thereafter (Fig. 4). The weight of the contents in the Matrigel-containing chambers decreased during the first 2 weeks, because of resorption of the Matrigel, but increased from 4 to 6 weeks, commensurate with the growth of angiogenic tissue, extracellular matrix, and other cellular infiltrates (Fig. 4). Similarly, the volume decreased at 2 weeks and then increased at 4 and 6 weeks. The mass of contents in the PLGA chambers could not be compared in the same way as in the Matrigel group because, whereas a standard volume of Matrigel could be inserted into the chamber on day 0, the volume of PLGA varied considerably. Because of its hard brittle texture, PLGA needed to be fragmented and variably loosely packed into the chambers, to avoid occlusion of the vascular pedicles.

Qualitative Histological Assessments of Angiogenesis

Assessment of angiogenesis was confined to the flow-through vascular pedicle configuration, because the very low patency rate in the ligated group resulted in minimal delayed angiogenesis. However, in animals in which the pedicle was patent, angiogenesis appeared comparable to that observed in the flow-through group.

In the silicone chamber groups assessed at 2, 4, and 6 weeks, there was marked angiogenesis into both Matrigel and PLGA, which differed qualitatively. With Matrigel, the new vessels penetrated the entire volume of the gel and

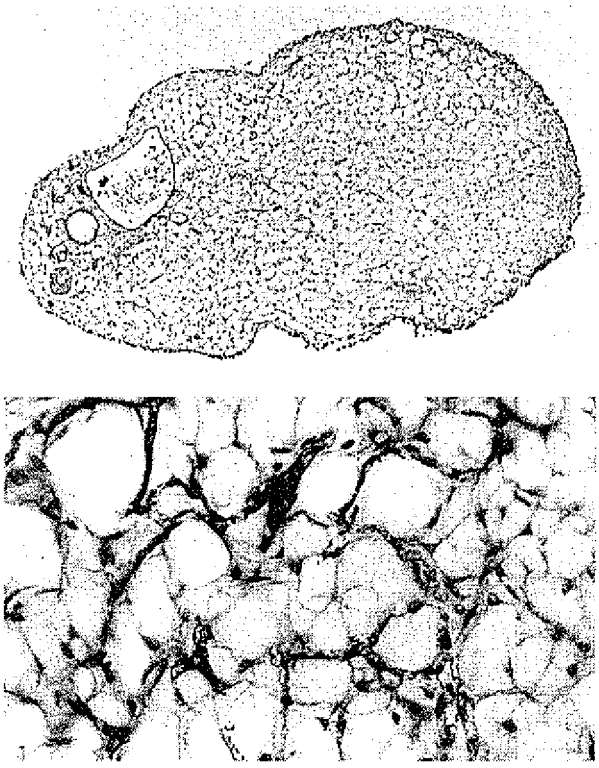

FIG. 5. Hematoxylin/eosin-stained cross-section through a Matrigel-filled chamber at 4 weeks. (*Above*) View of the pedicle (artery, vein, and nerve; magnification, ×26). It should be noted that adipocytes have infiltrated throughout the Matrigel. (*Below*) High-power view of a region of adipocytes, showing a rich plexus of India ink-filled capillaries (magnification, ×660).

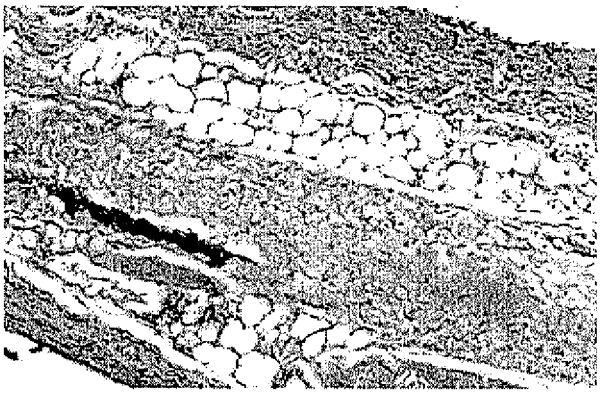

FIG. 6. Hematoxylin/eosin-stained longitudinal section through the pedicle in a control (pedicle-only) chamber. A thin rim of adipose tissue surrounds the vessels (magnification, ×264).

were generally evenly distributed (Figs. 3 and 5). With PLGA, the angiogenesis spread around the periphery of the construct, with fewer vessels (in some cases, no vessels) being observed in the central aspect.

The control chambers containing only the vessels underwent a series of histological changes, presumably in response to the injury caused by dissection (Fig. 6). Angiogenesis and inflammatory cells were noted but with reduced extent and density, compared with findings for the experimental chambers with matrix plus vessels. The amount of angiogenesis was insufficient for quantification using the stereological technique described above.

Quantitative Assessments of Vessel Volume Density

Vessel volume densities in the flow-through chambers were similar at 2, 4, and 6 weeks, measuring approximately 45 percent of total tissue density (Fig. 7). There was no significant difference in vessel volume densities between PLGA and Matrigel when results were analyzed with two-way analysis of variance, although, as stated above, the distribution of vessels differed.

Morphological Features of Total Chamber Contents

Matrigel. In chambers containing the flow-through blood vessel and Matrigel, the majority of the Matrigel was infiltrated with well-vascularized adipocytes at various stages of development. These cells seemed to have migrated through the matrix and survived, presumably nourished by the newly generated vascular tree. A clear border was observed between native fat initially included with the pedicle and newly formed fat. It was evident that the newly formed adipose tissue increased in amount and maturity with time, first appearing in minute amounts at 2 weeks and almost filling the chamber by 6 weeks (Fig. 5). This was not evaluated quantitatively. There was a fibroblastic response at the extracellular matrix-chamber interface.

In some mice, the native fat pads contained mammary ductal tissue. This tissue was occasionally observed in the distal part of the chamber, because part of the fat pad was used as a plug to seal the distal aperture, and could be observed in control chambers containing only the vessels. In some of the animals in the Matrigel group, the ductal tissue seemed to be growing into the Matrigel; in others, there was clear morphological evidence of newly formed acinar/ductal tissue (Fig. 8). Groups of large,

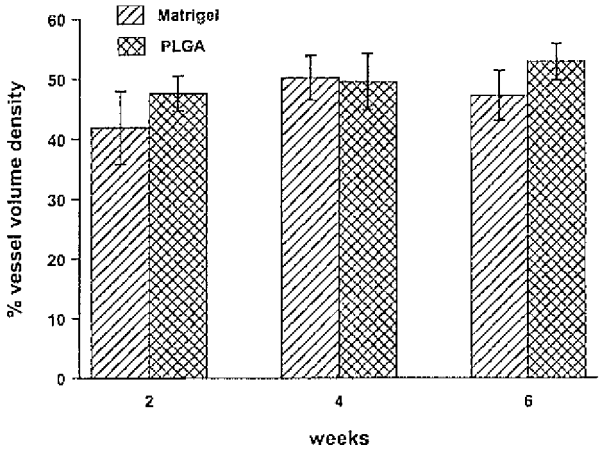

FIG. 7. Vessel volume density of tissue from flow-through pedicle chambers filled with either Matrigel or PLGA. Densities were similar at 2, 4, and 6 weeks. Data are means ± standard errors.

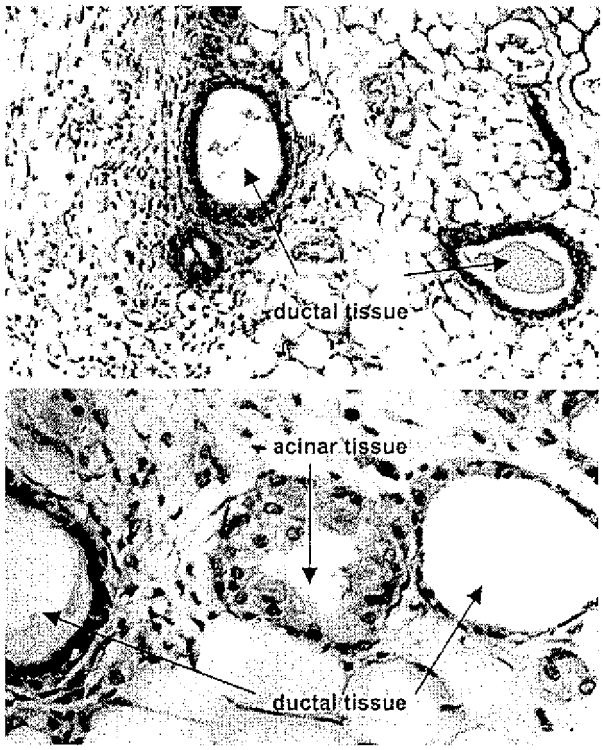

FIG. 8. Hematoxylin/eosin-stained section taken from a Matrigel-filled chamber at 4 weeks. (*Above*) Ductal tissue with flocculent material in the lumen (magnification, ×660). (*Below*) Acinar tissue (magnification, ×1320).

angular, eosinophilic cells resembling acinar tissue could be observed around irregular lumina, which contained flocculent material and were often associated with the accumulation of polymorphonuclear cells. These findings suggest that the Matrigel-filled chambers are capable of supporting the development of epithe-

lial tissue in vivo, as well as fat. To our knowledge, this phenomenon has not been previously reported.

PLGA. PLGA promoted a predominately fibrous foreign-body reaction. At 2 weeks, large areas of the PLGA remained undissolved and with little tissue ingrowth. The relative amounts of PLGA decreased with time as the amounts of tissue ingrowth increased; however, at no time was the PLGA completely dissolved (Fig. 9). Fibroblasts and multinucleated giant cells were the predominant cells observed both peripherally, where the matrix lay against the chamber wall, and centrally, within the substance of the matrix. No adipose tissue or breast ductal tissue was evident.

Control chambers. The morphological appearance of the control chambers with neither matrix nor vessels was unremarkable. The chambers were noted to be filled with fluid, which did not appear to clot. Smears of this fluid were generally devoid of cells, except for occasional dead or dying inflammatory cells. Similarly, the chambers that contained matrix only (Matrigel or PLGA) occasionally contained inflammatory cells but there was no cellular ingrowth or angiogenesis from outside the chamber.

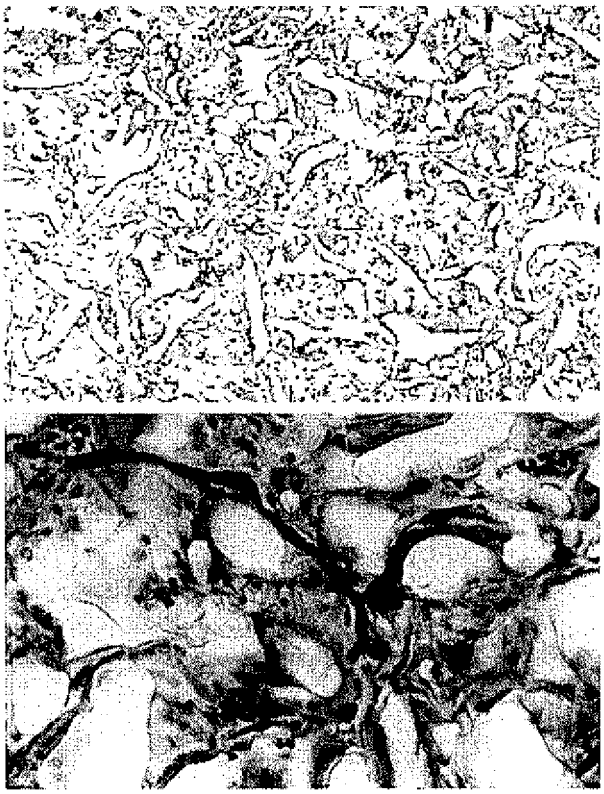

FIG. 9. Hematoxylin/eosin-stained section taken from a PLGA-filled chamber at 6 weeks. (*Above*) Angiogenic and fibrous foreign-body reaction (magnification, ×132). (*Below*) Large, multinucleated, giant cells lining PLGA fragments surrounded by India ink-filled capillaries (magnification, ×1320).

DISCUSSION

In this study, we developed a murine version of the rat model of vascularized tissue generation that was previously developed at our institution.[14,15] In the rat model, the contralateral femoral vein is used as a graft to create an arteriovenous loop in a rigid chamber in the rat groin. This model has been successfully used but is technically demanding and time-consuming. Development of a murine model would allow better access to antibodies and transgenic technologies while reducing experimental costs.

Creating a microvascular loop in mice is impractical because of the tiny size of the femoral vessels (internal diameter, 0.2 to 0.3 mm). Therefore, we explored two vascular configurations, namely, a ligated pedicle model and a flow-through bipedicle model, which were known to be angiogenic on the basis of previous work.[16] It became apparent after a short time that the ligated pedicle configuration had an unacceptable thrombosis rate (25 percent), presumably because of the small internal diameter of the femoral artery. We were able to achieve a much higher patency rate by identifying a second arterial pedicle in the flank, with rich anastomoses with the inferior epigastric artery through the groin fat pad, and dissecting both pedicles in a flow-through model. We observed that the patency rate with this configuration could be further improved with the use of a softer silicone chamber.

We demonstrated that this new model was capable of inducing profound angiogenesis into both Matrigel and PGLA. The India ink studies confirmed the presence of a comprehensive, well-developed, vascular network with an extensive capillary bed, which was noted as early as 2 weeks after implantation. In theory, this should provide a well-vascularized bed in which cells can survive and develop. The vessel volume densities, reflecting the overall number, length, and size of the vessels, were similar at 2, 4, and 6 weeks with both PLGA and Matrigel. This finding suggests not only that the angiogenic process is largely complete by 2 weeks but also that the new vessels are maintained for at least 6 weeks. This should provide

a window for the addition of living cells for the engineering of specific tissues. These observation that the empty control chambers, the matrix-only chambers, and the chambers with thrombosed vascular pedicles remained almost completely inert (except for a few inflammatory cells) suggests that a patent vascular pedicle is critical for angiogenesis and tissue generation. The finding also suggests that the majority of cells that migrate into the matrices do so through the vascular pedicle. These cells may be derived from cells that have physically migrated along the axis of the vessel from either end of the chamber, using the vessel as a conduit, from cells within the vessel wall, or from cells that have migrated transmurally from a systemic source.

Quantitation of the mass and volume of tissue produced in this model was compromised when PLGA was used as the matrix. Solid extracellular matrices such as PLGA and hydroxyapatite must be broken into pieces and placed inside the chamber, with care not to compress the delicate pedicle. Engineering such matrices to be more compatible with the chamber in terms of consistency and shape might be possible, but we wished to confirm the validity of the model before performing such modifications. In the future, it should be possible to cut these matrices exactly to the shape of the chamber, with an appropriate groove cut for the vessels. This would allow standardization of the exact mass and volume inserted in each chamber. Gel-like extracellular matrices such as Matrigel, fibrin, and fibronectin can be inserted preoperatively and allowed to set, facilitating exact quantification of mass and volume. However, these matrices tend to be absorbed or broken down more rapidly when new tissue is formed; therefore, there may be a net loss of mass and volume with time. If the matrix shifts from the periphery of the chamber because of absorption or contraction, then the advancing front of angiogenesis and tissue generation cannot reach the full confines of the chamber; the tissue can become encapsulated within the chamber and be further compromised with respect to exponential growth. We think that a key component of the success of the model in generating tissue is the semirigid nature of the chamber into which the vessels and matrix are implanted. The chamber prevents collapse and encapsulation of the growing tissue bud. If the mature scaffold remains intact and totally fills this space, then new angiogenesis and subsequent tissue production should also completely fill the chamber.

Matrigel is a matrix that is thought to closely mimic the composition of basement membranes. It has been demonstrated to support the migration, differentiation, and growth of adipocytes and their precursors.[22,23] This phenomenon was previously observed with nonencapsulated, basic fibroblast growth factor-impregnated Matrigel injected subcutaneously into mice, using basic fibroblast growth factor with and without added preadipocytes. The presence of mature viable fat in our chambers when Matrigel was used suggests this model is capable of supporting the migration, maturation, and possibly the regeneration of fat cells and their precursors. In serial evaluations of the chambers during the 2-week to 6-week period, it was evident that the fat progressively infiltrated the Matrigel, in a cone-shaped manner, from the distal lateral end of the chamber along the vascular axis, where the fat plug had been used to seal the chamber, until the fat generally filled the chamber by 6 weeks. In our model, unlike the subcutaneous injection model, fat tissue formed without added basic fibroblast growth factor; in the control chambers with Matrigel but no vascular pedicle, no fat grew. This suggests that adipogenesis in Matrigel with basic fibroblast growth factor may be caused by the angiogenesis induced by basic fibroblast growth factor, rather than as a direct effect of basic fibroblast growth factor, although Matrigel itself contains growth factors, including basic fibroblast growth factor.

Several other cell types were able to migrate into and survive within the newly engineered construct, including breast epithelial tissue, fibroblasts, white blood cells, and mast cells. The fact that adipose tissue dominated the Matrigel-filled chambers and fibroblasts/giant cells dominated the PLGA-filled chambers demonstrates that the extracellular matrix and local microenvironment exert significant effects on the types of tissue that form within the chambers. Therefore, it may be possible to alter the phenotype of the tissue produced in the chambers by altering the microenvironment in specific ways, as is performed for tissue culture in vitro. This model can potentially be used to grow specific tissue types "to order," if the correct microenvironment can be created. Other possible uses of the model include studies of angiogenesis and experiments involving the

growth of human tumor cell lines in immunodeficient mice.

CONCLUSIONS

We have developed a valid model of new tissue generation in mice that is comparable to the rat model already being used in our institution. The new model is technically simple and quick to establish, is reliable, is inexpensive, and allows two chambers to be inserted in each animal. It should allow the study of angiogenesis and three-dimensional vascularized tissue engineering and might also have applications in other fields of study.

Wayne A. Morrison, F.R.A.C.S.
Bernard O'Brien Institute of Microsurgery
42 Fitzroy Street
Fitzroy, Victoria 3065, Australia
morriswa@svhm.org.au

ACKNOWLEDGMENTS

Dr. Cronin's fellowship was partly funded by the Microsurgery Foundation, a traveling scholarship awarded jointly by the Royal College of Surgeons of Ireland and the British Association of Plastic Surgeons, and a Melbourne University scholarship. The research was supported by the National Health and Medical Research Council of Australia, Transport Accident Commission, B.H.P. Billiton Community Trust, and L.E.W. Carty Charitable Fund. Histological assistance by Rosalind Romeo-Meeuw and surgical assistance by Sue McKay and Liliana Pepe are gratefully acknowledged.

REFERENCES

1. Langer, R., and Vacanti, J. P. Tissue engineering. *Science* 260: 920, 1993.
2. Eiselt, P., Kim, B. S., Chacko, B., et al. Development of technologies aiding large-tissue engineering. *Biotechnol. Prog.* 14: 134, 1998.
3. Sims, C. D., Butler, P. E., Cao, Y. L., et al. Tissue engineered neocartilage using plasma derived polymer substrates and chondrocytes. *Plast. Reconstr. Surg.* 101: 1580, 1998.
4. Saim, A. B., Cao, Y., Weng, Y., et al. Engineering autogenous cartilage in the shape of a helix using an injectable hydrogel scaffold. *Laryngoscope* 110: 1694, 2000.
5. Arevalo-Silva, C. A., Eavey, R. D., Cao, Y., Vacanti, M., Weng, Y., and Vacanti, C. A. Internal support of tissue-engineered cartilage. *Arch. Otolaryngol. Head Neck Surg.* 126: 1448, 2000.
6. Shum-Tim, D., Stock, U., Hrkach, J., et al. Tissue engineering of autologous aorta using a new biodegradable polymer. *Ann. Thorac. Surg.* 68: 2298, 1999.
7. Shinoka, T., Shum-Tim, D., Ma, P. X., et al. Creation of viable pulmonary artery autografts through tissue engineering. *J. Thorac. Cardiovasc. Surg.* 115: 536, 1998.
8. Shinoka, T., Breuer, C. K., Tanel, R. E., et al. Tissue engineering heart valves: Valve leaflet replacement study in a lamb model. *Ann. Thorac. Surg.* 60 (Suppl.): S513, 1995.
9. Burke, J. F., Yannas, I. V., Quinby, W. C., Jr., Bondoc, C. C., and Jung, W. K. Successful use of a physiologically acceptable artificial skin in the treatment of extensive burn injury. *Ann. Surg.* 194: 413, 1981.
10. Folkman, J., and Hochberg, M. Self-regulation of growth in three dimensions. *J. Exp. Med.* 138: 745, 1973.
11. Kaihara, S., Borenstein, J., Koka, R., et al. Silicon micromachining to tissue engineer branched vascular channels for liver fabrication. *Tissue Eng.* 6: 105, 2000.
12. Risau, W. Mechanisms of angiogenesis. *Nature* 386: 671, 1997.
13. Ferrara, N., and Alitalo, K. Clinical applications of angiogenic growth factors and their inhibitors. *Nat. Med.* 5: 1359, 1999.
14. Tanaka, Y., Tsutsumi, A., Crowe, D. M., Tajima, S., and Morrison, W. A. Generation of an autologous tissue (matrix) flap by combining an arteriovenous shunt loop with artificial skin in rats: Preliminary report. *Br. J. Plast. Surg.* 53: 51, 2000.
15. Mian, R. A., Knight, K. R., Penington, A. J., et al. Stimulating effect of an arteriovenous shunt on the in vivo growth of isografted fibroblasts: A preliminary report. *Tissue Eng.* 7: 73, 2001.
16. Khouri, R. K., Koudsi, B., Deune, E. G., et al. Tissue generation with growth factors. *Surgery* 114: 374, 1993.
17. Kleinman, H. K., McGarvey, M. L., Hassell, J. R., et al. Basement membrane complexes with biological activity. *Biochemistry* 25: 312, 1986.
18. Mikos, A. G., Sarakinos, G., Leite, S. M., Vacanti, J. P., and Langer, R. Laminated three-dimensional biodegradable foams for use in tissue engineering. *Biomaterials* 14: 323, 1993.
19. Patrick, C. W., Jr., Chauvin, P. B., Hobley, J., and Reece, G. P. Preadipocyte seeded PLGA scaffolds for adipose tissue engineering. *Tissue Eng.* 5: 139, 1999.
20. Renkin, E. M., Gray, S. D., and Dodd, L. R. Filling of microcirculation in skeletal muscles during timed India ink perfusion. *Am. J. Physiol.* 241: H174, 1981.
21. Thurston, G., Murphy, T. J., Baluk, P., Lindsey, J. R., and McDonald, D. M. Angiogenesis in mice with chronic airway inflammation: Strain-dependent differences. *Am. J. Pathol.* 153: 1099, 1998.
22. Kawaguchi, N., Toriyama, K., Nicodemou-Lena, E., Inou, K., Torii, S., and Kitagawa, Y. De novo adipogenesis in mice at the site of injection of basement membrane and basic fibroblast growth factor. *Proc. Natl. Acad. Sci. U.S.A.* 95: 1062, 1998.
23. Tabata, Y., Miyao, M., Inamoto, T., et al. De novo formation of adipose tissue by controlled release of basic fibroblast growth factor. *Tissue Eng.* 6: 279, 2000.